



Grant Agreement no. 226967
Seismic Hazard Harmonization in Europe
Project Acronym: SHARE

SP 1-Cooperation

Collaborative project: Small or medium-scale focused research project

THEME 6: Environment

Call: ENV.2008.1.3.1.1 Development of a common methodology and tools to evaluate earthquake hazard in Europe

D4.3 –New site classification scheme and associated site amplification factors

Due date of deliverable: 30.11.2010

Actual submission date: 13.02.2012

Start date of project: 2009-06-01

Duration: 36

Aristotle University of Thessaloniki (AUTH)

Kyriazis PITILAKIS, Anastasios ANASTASIADIS, Evi RIGA

Revision: 1

Dissemination Level

PU	Public	X
PP	Restricted to other program participants (including the Commission Services)	
RE	Restricted to a group specified by the consortium (including the Commission Services)	
CO	Confidential, only for members of the consortium (including the Commission Services)	

Table of Contents

1. Introduction	3
2. Update of the SHARE database	5
3. Validation of EC8	11
3.1 Normalized response spectra	13
3.1.1 SHARE-DS1 (all records)	13
3.1.2 SHARE-DS2 (PGA\geq20cm/sec²)	16
3.1.3 SHARE-DS3 (PGA\geq150cm/sec²)	18
3.2 Soil amplification factors	21
3.2.1 Methodology	21
3.2.2 Results	25
3.2.3 Summary for EC8 soil classes	63
4. New classification system	65
4.1 Proposed soil classes	65
4.2 Normalized acceleration response spectra	68
4.3 Soil amplification factors	73
4.3.1 Approach 1	73
4.3.2 Approach 2	86
4.3.3 Amplification factors for soil class E with Kik-net records	96
4.3.4 Proposed amplification factors	97
4.3.5 Validation with theoretical analyses	98
4.4 Proposed acceleration response spectra and amplification factors for the new soil classes	104
4.5 Comparison of the performance of the proposed classification system and EC8 classification system	107
5. Executive Summary	113
References	115
Appendix I	117
Appendix II	133

1. Introduction

The report presents the work performed by the research group of Aristotle University of Thessaloniki concerning Task 4.3 (Site amplification factors) of SHARE project. The objective of this task, as described in the DoW of the project, is “*to derive appropriate calibrations for the application of generic ground motion prediction equations (GMPE) to specific soil and rock conditions, along two directions: 1. Keeping the EC8 site classification criteria unchanged and proposing the corresponding "optimal" spectral shapes and/or amplification factors and, 2. Exploring new tracks for new site classification, and proposing site amplification factors accordingly*”. AUTH has effectively contributed to both these directions. In particular the work performed and presented herein has as follows:

- Compilation of a strong ground motion database (called hereafter SHARE-AUTH database) with records coming only from very well documented stations regarding the knowledge of the soil conditions.
- Validation and confrontation with EC8 using the whole SHARE database.
- Proposal of improved soil factors S for the EC8 soil classification scheme.
- Proposal of a new soil classification scheme (based on soil type, stratigraphy, depth (T_0) and stiffness (average V_s) as key parameters) for two levels of expected ground shaking. Validation with well constrained records and sites.
- Proposal of soil amplification factors and normalized response spectra for the new classification scheme.

The report is organized in three (3) more chapters and two appendices.

Chapter 2 includes the description of SHARE-AUTH strong motion database, along with the appropriate updates that took place, regarding mainly soil and site documentation.

Chapter 3 describes the methodology that was applied to validate Eurocode 8, regarding the normalized response spectra and the soil amplification factors it proposes. Improved soil factors are estimated for the present EC8 soil classes using the entire SHARE database, incorporating however any changes in the $V_{s,30}$ values and soil classification that resulted from the compilation of the SHARE-AUTH database in Chapter 2.

In Chapter 4, a new soil and site classification scheme is proposed, which is based on one hand on the compilation of the present SHARE-AUTH database and on the other hand on past theoretical analyses (Pitilakis et al. 2004, 2006) on the same subject. Normalized acceleration response spectra and associated soil amplification factors are proposed for the new improved soil classes using the SHARE-AUTH database, enriched with records from other stations worldwide where needed. The proposed new soil classification is validated with theoretical analysis.

In appendix I we present the stations in the SHARE-AUTH database and in appendix II the Kik-Net stations used for the estimation of the soil class E amplification factors.

We would like to thank Professor Ezio Faccioli for his valuable comments in an early version of the report and the constructive discussion we had during the meetings and not only. We are

also grateful to Roberto Paolucci, Francesca Pacor and Chiara Smerzini for checking the velocity profiles of the Italian strong motion stations. We express our appreciation to Fabrice Cotton for successfully leading WP4, Sinan Akkar and Abdullah Sandikkaya for providing the SHARE strong motion database, John Douglas, Julian Bommer, Pierre-Yves Bard and Donat Fäh for their useful comments during the progress of this work and of course all participants of SHARE WP4 for the fruitful discussions that took place in all WP4 meetings. Finally, we would like to thank Professor Theodoros Chatzigogos and Assistant Professor Dimitrios Raptakis for their valuable contribution to this report.

2. Update of the SHARE database

The strong-motion database prepared by METU and presented in D4.1 is a very extensive worldwide database, which covers earthquakes dating back to 1930s and contains a total of 14193 records from 2448 events (Yenier et al. 2010). The version of the database used for this work is v3.1 (March 2010) and contains **13500 records**. The soil and site documentation of the stations included in the database is restricted only to the $V_{s,30}$ values and site classification according to EC8. This was considered as insufficient for the goal of the present work where the new soil classification scheme will not necessarily be based on $V_{s,30}$. It was therefore decided to re-collect data regarding site information and classification for as many stations included in the SHARE database as possible, in order to create a subset of data with **very well known geotechnical information** until the seismic rock basement. The depth of seismic rock basement was defined as the depth with $V_s > 800$ m/s, in order to be consistent with the aim of SHARE, which is to compute seismic hazard for a reference rock with $V_s = 800$ m/s. As a result, independent additional data on the site characteristics of 536 recording stations were obtained from raw data or scratch using several sources of information, which are presented in Table 2.1. The updated database, herein called **SHARE-AUTH database**, contains **3666 strong motion records from 536 stations from Greece, Italy, Turkey, Japan and USA**. Appendix I lists the stations of SHARE-AUTH database. The geographic distribution of the selected stations and records is presented in Figures 2.1 and 2.2 respectively.

Table 2.1: Source of the geotechnical characteristics and V_s profiles of the selected stations

Station Country	V_s profile source	Number of stations
Greece	AUTH Research Unit of Soil Dynamics & Geotechnical Earthquake Engineering	20
Italy	Italian Accelerometric Archive	72
Japan	Kik-Net	100
	K-Net	149
Turkey	Turkish national strong-motion database	131
USA	ROSRINE program	23
	D. Boore's personal webpage	32
	USGS Open-File Report 93-376	2
	USGS Open-File Report 96-740	1
	USGS Open-File Report 92-287	2
	USGS Open-File Report 94-222	1
	Nigbor and Steller Rep#9225-6427 (3/11/1993)	2
Kajima Corporation	1	

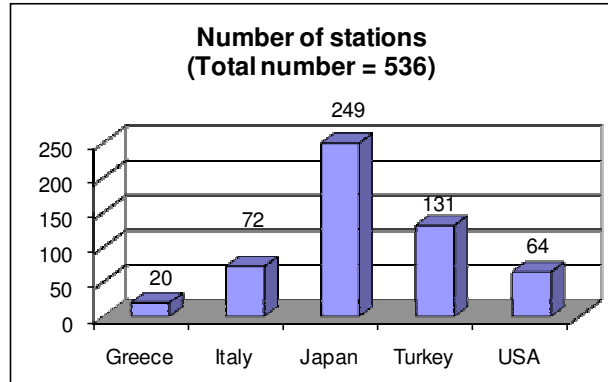


Figure 2.1: Geographic distribution of the well-documented stations included in SHARE-AUTH Strong Motion Database

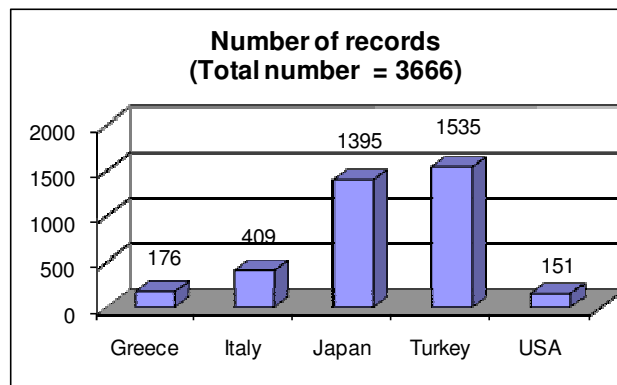


Figure 2.2: Geographic distribution of strong motions recorded only at well-documented sites of SHARE-AUTH Strong Motion Database

The V_s -profiles of the selected stations have been obtained with a variety of surveying methods. For most of the sites (70% of the total sample), V_s -profiles have been obtained from borehole measurements (e.g. cross-hole, down hole). For the rest of the sites, for example the Turkish stations (24% of the total sample), the V_s -profiles have been evaluated using surface surveys.

For all 536 well-documented stations included in SHARE-AUTH database, the $V_{s,30}$ values were re-calculated and the values of the original database were checked for their accuracy, using the available raw data. For those sites, whose V_s models do not extend down to 30m, $V_{s,30}$ values were estimated based on the assumption that the shear wave velocity at the bottom of the existing model extends to the depth of 30m (Boore, 2004).

The $V_{s,30}$ values and the geotechnical description of the sites were used to classify the selected sites according to the classification scheme of Eurocode 8. Figure 2.3 shows the distribution of $V_{s,30}$ values for the stations in SHARE-AUTH database. Most of the sites fall within the range of EC8 soil classes B and C, while there is only a limited number of stations with $V_{s,30} < 180\text{m/s}$ (class D) or $V_{s,30} > 800\text{m/s}$ (class A). The number of stations and sites classified according to EC8 is given in Figure 2.4.

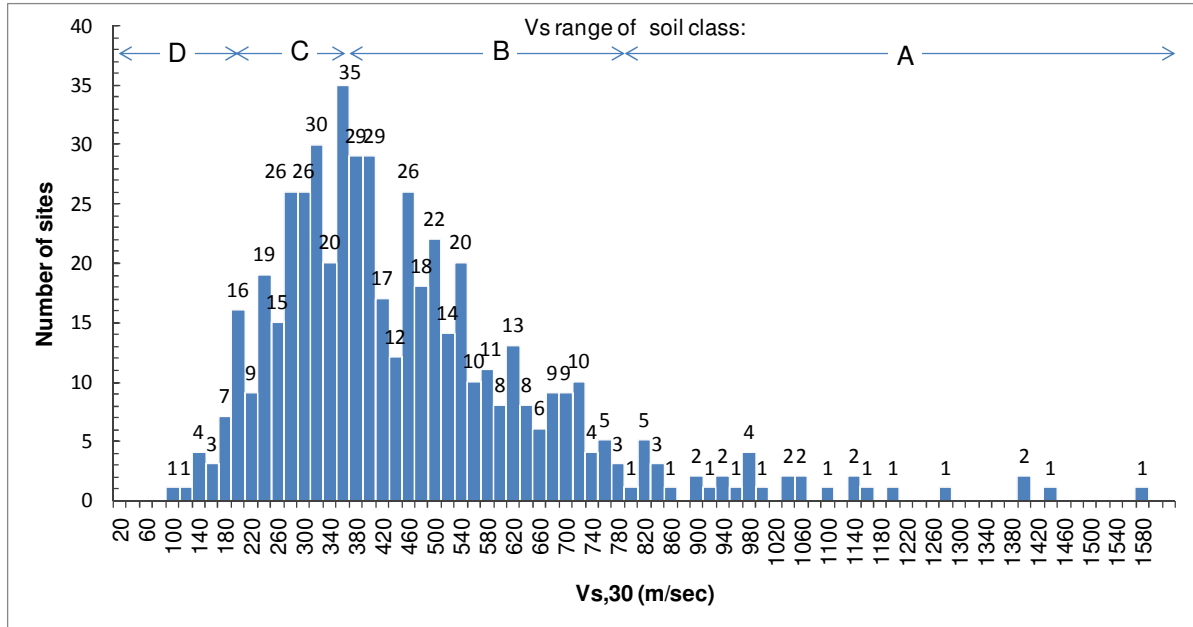


Figure 2.3: Histogram of $V_{s,30}$ values for the sites of SHARE-AUTH database

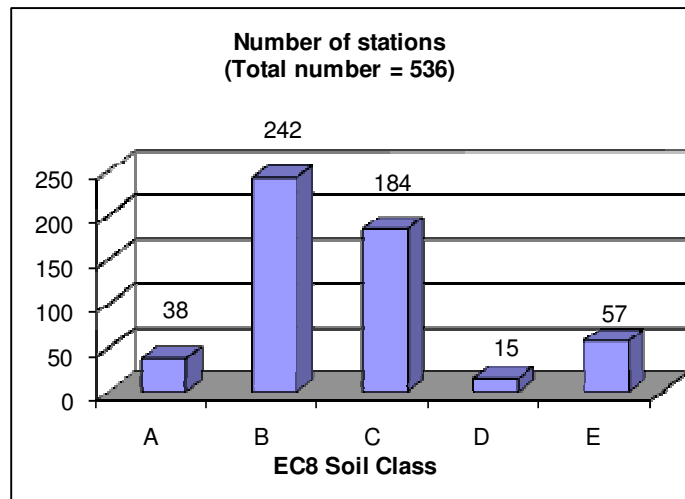


Figure 2.4: Classification of the sites of SHARE-AUTH database according to EC8

Additionally, for all 536 selected stations, new parameters, not included in the original SHARE database, were determined. These include the thickness of the soil deposits (i.e. depth to “seismic” bedrock - $V_s > 800$ m/s), the depth until which the V_s -profile, based on measured data, of the site is known, the average shear wave velocity $V_{s,av}$ of the entire soil deposit and the fundamental period T_0 of the soil deposit. In most cases (344 out of 536 sites or 64% of the sites) the soil thickness and V_s profile until bedrock were well known from in situ measurements. For the rest of the sites (36% of the sites), the extra parameters were implicitly estimated using on one hand the available geotechnical – geological information, and on the other hand the fundamental period of the site evaluated from the horizontal-to-vertical Fourier spectrum ratio (HVSr) of the available records for this specific station (Lermo and Chávez-García, 1993) and statistical analysis. In particular, knowing the fundamental period of the site and the V_s values in the 30 first meters, it is possible to

implicitly estimate the depth of the bedrock and make a reasonable hypothesis of the average shear wave velocity over the whole profile. Figure 2.5 shows the derived distribution of $V_{s,av}$ values for the SHARE-AUTH database sites. T_0 , $V_{s,av}$ and soil description were used to classify the sites according to the new soil classification scheme presented in Chapter 4.

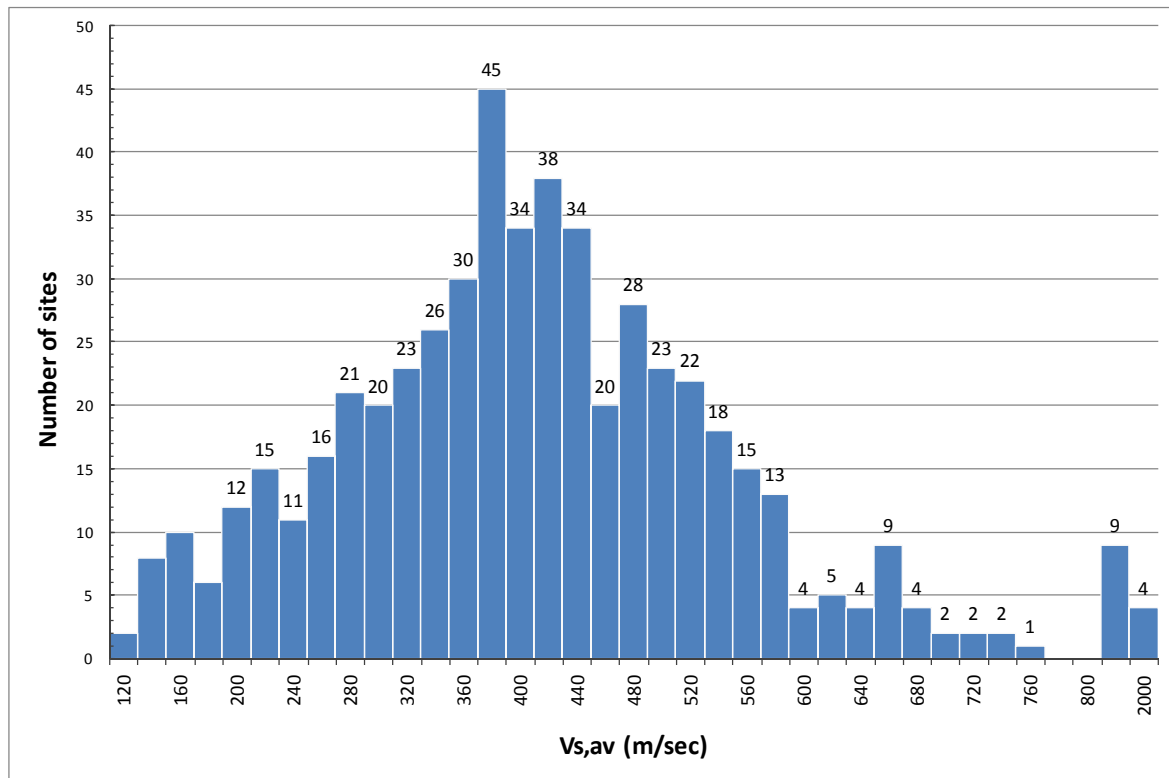


Figure 2.5: Histogram of $V_{s,av}$ values for the sites of SHARE-AUTH database

In total, 7 additional fields were added to the original SHARE database. The names and content of the new fields are described in Table 2.2. No new records (rows in the database) were added.

Table 2.2: New fields added in SHARE-AUTH subset of SHARE Strong Motion Database

Field Name	Description
$H_{bedrock}$ (m)	Thickness of soil deposits (depth to “seismic” bedrock - $V_s > 800$ m/s)
H (m) of known V_s	Depth until which the V_s -profile of the site is known
$V_{s,30,AUTH}$	Updated value of mean shear wave velocity of the upper 30m compiled by AUTH
$V_{s,av}$	Average shear wave velocity of the entire soil deposit
T_0	Fundamental period of the soil deposit (computed as $4 * H_{bedrock} / V_{s,av}$)
EC8 Site Class	EC8 Site Class (based on $V_{s,30,AUTH}$)
New Site Class	New site class (based on T_0 , $V_{s,av}$ and soil description)

Magnitude M_w and peak ground acceleration PGA distributions with the epicentral distance R , of the proposed SHARE-AUTH database are presented in Figures 2.6 and 2.7. The epicentral distance is the same as it has been proposed in the original SHARE database. It is observed that there are significantly fewer records with high PGA values exceeding 200 cm/sec^2 and many weak motion records with values less than 20 cm/sec^2 . For this reason, different datasets were analyzed using the whole dataset or a restrained one with records with PGA greater than 20 cm/sec^2 . It is also important to notice that records with $\text{PGA} > 200 \text{ cm/sec}^2$ are coming from both small ($M_w < 5.5$) and medium to large earthquakes ($M_w > 5.5$) (Figure 2.7).

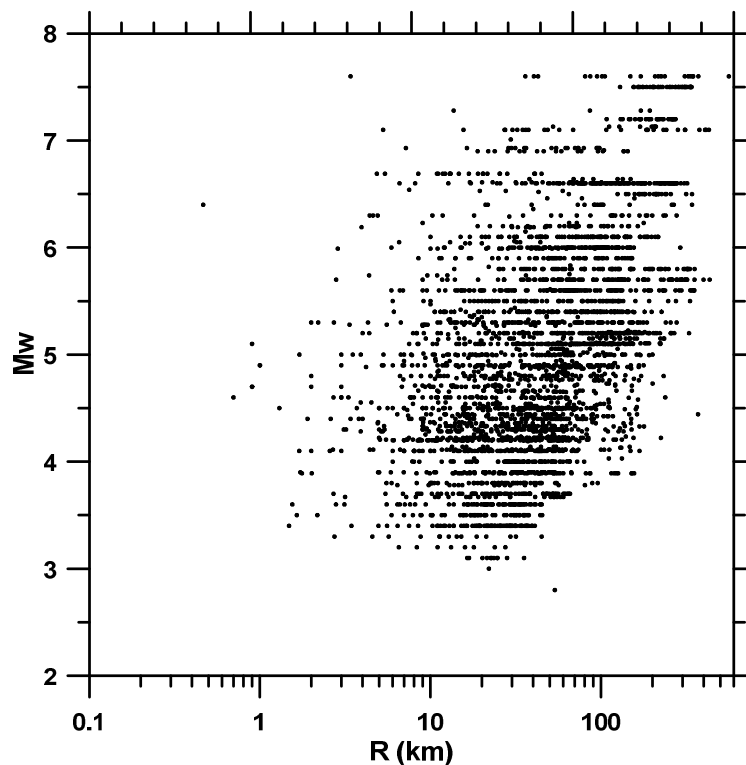


Figure 2.6: SHARE-AUTH database. M_w - R distribution of the selected records

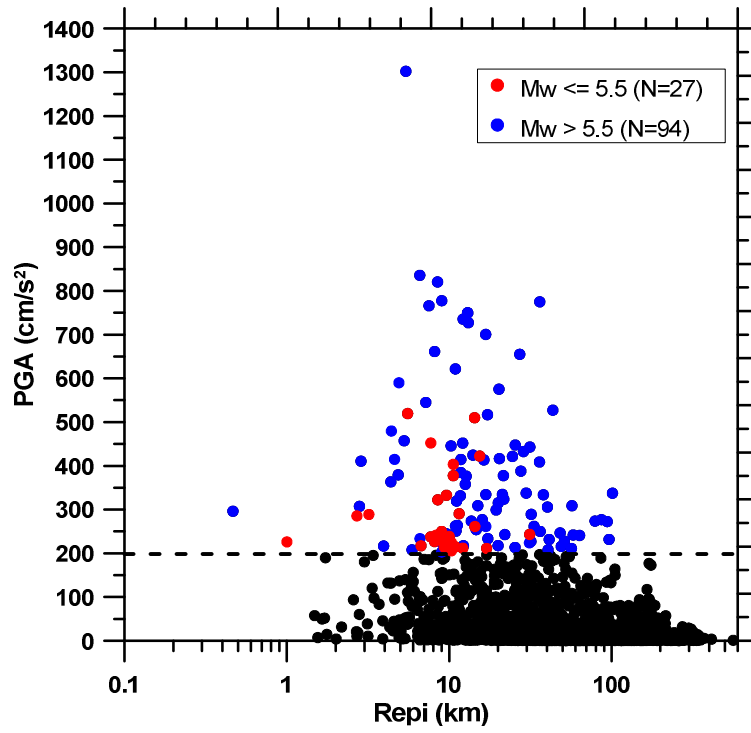


Figure 2.7: SHARE-AUTH database. PGA-R distribution of the selected records

3. Validation of EC8

Data selection

The elastic response spectra proposed in EC8 (CEN, 2004) have been re-evaluated using the entire SHARE database, incorporating however the changes made to the $V_{s,30}$ values and soil classification that resulted from the compilation of the SHARE-AUTH database. The following criteria were applied for the selection of the ground motion records used in this work:

- *Surface wave magnitude $M_s \geq 4$.* For the records for which M_s was not available, it was estimated from M_w using the empirical relation proposed by Scordilis (2006).
- *Available spectral values at least up to 2.5sec.*

Two levels of seismicity proposed by EC8 were adopted: Type 2 spectrum if seismic hazard has been assessed mostly from earthquakes with surface-wave magnitude $M_s \leq 5.5$, otherwise Type 1 spectrum. Magnitude $M > 4.0$ and peak ground acceleration PGA distributions with the epicentral distance R , of the selected records are presented in Figures 3.1 and 3.2.

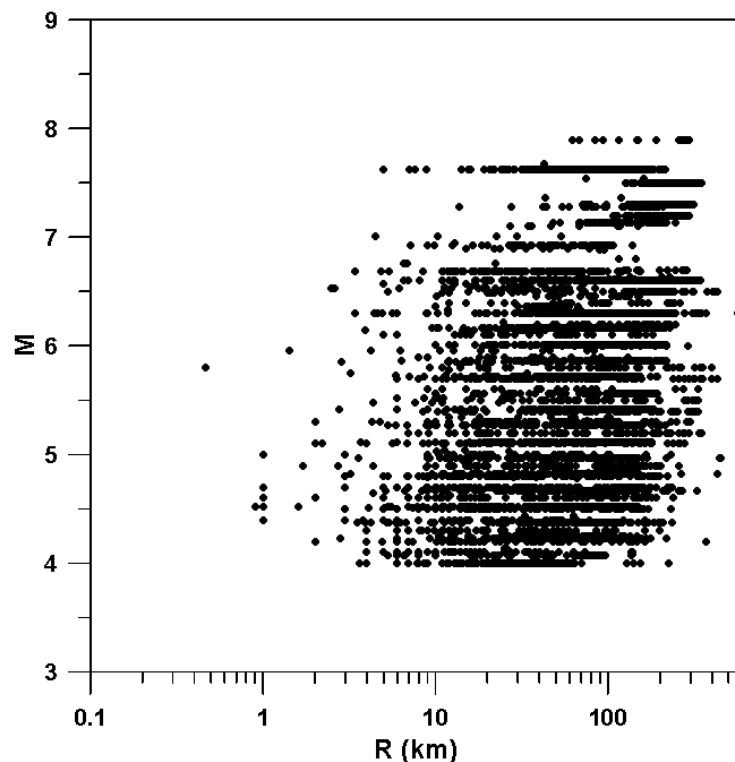


Figure 3.1: *M-R distribution of the selected records ($M > 4.0$)*

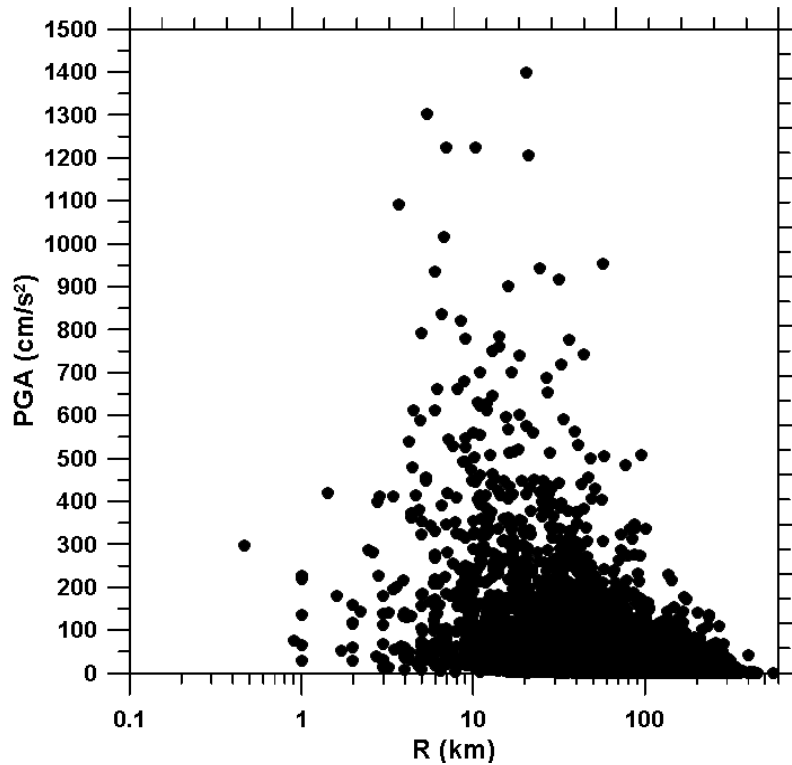


Figure 3.2: PGA-R distribution of the selected records

There are significantly less records with PGA values exceeding 200 cm/sec^2 and many weak motion records with PGA values less than 20 cm/sec^2 . For this reason, and considering the fact that EC8 spectra should be derived basically from records from strong earthquakes, we decided to select three datasets and make the analysis accordingly:

SHARE-DS1: the whole dataset

SHARE-DS2: records with PGA greater or equal to 20 cm/sec^2

SHARE-DS3: records with PGA greater or equal to 150 cm/sec^2

The number of available strong motion records in each dataset is shown in Table 3.1. The records in SHARE-DS3 dataset, although having relatively high PGA values, come not only from Type 1 earthquakes, but also from Type 2 earthquakes.

Moreover and regarding the estimation of soil amplification factors only, it was not feasible to use all records of Table 3.1, since the methodology that was applied sets some extra limitations to the records that can actually be used. In particular, as explained in detail in paragraph 3.2, amplification factors are estimated with two approaches, one of which (Approach 1) uses four GMPEs for the computation of reference spectral acceleration. This requires that reference spectral acceleration at a certain period T can be estimated with all four GMPEs. However, each GMPE requires the knowledge of different parameters and can therefore be implemented for a different subset of data. As a result, the computation of reference spectral acceleration with all four GMPEs, and thus the estimation of amplification factors with Approach 1, was feasible for a limited dataset. These limitations are presented in detail in paragraph 3.2

Table 3.1: Number of strong motion records for each dataset

Soil Class	SHARE-DS1 ⁽¹⁾		SHARE-DS2 ⁽²⁾		SHARE-DS3 ⁽³⁾	
	Type 2	Type 1	Type 2	Type 1	Type 2	Type 1
A	402	264	105	125	9	23
B	1508	1896	419	1151	38	214
C	1133	1775	353	1261	44	219
D	10	4	3	1	-	-
E	73	96	33	49	5	7
Total Records	3126	4035	913	2587	96	463

⁽¹⁾: SHARE-DS1: whole SHARE dataset
⁽²⁾: SHARE-DS2: records having $PGA \geq 20 \text{ cm/s}^2$
⁽³⁾: SHARE-DS3: records having $PGA \geq 150 \text{ cm/s}^2$

3.1 Normalized response spectra

The elastic acceleration response spectra of the records of the SHARE database were first PGA-normalized and then grouped based on the soil class and on the seismicity type. For each soil class and type of seismicity, the median values were calculated, along with the 16th and 84th percentiles. The specific percentiles were selected since, in the case of normal distribution of data, they represent the values of average minus one standard deviation and average plus one standard deviation respectively.

3.1.1 SHARE-DS1 (all records)

Figures 3.3-3.7 illustrate the median spectra derived for each soil class and both types of seismicity, along with the 16th and 84th percentiles, using SHARE-DS1 dataset.

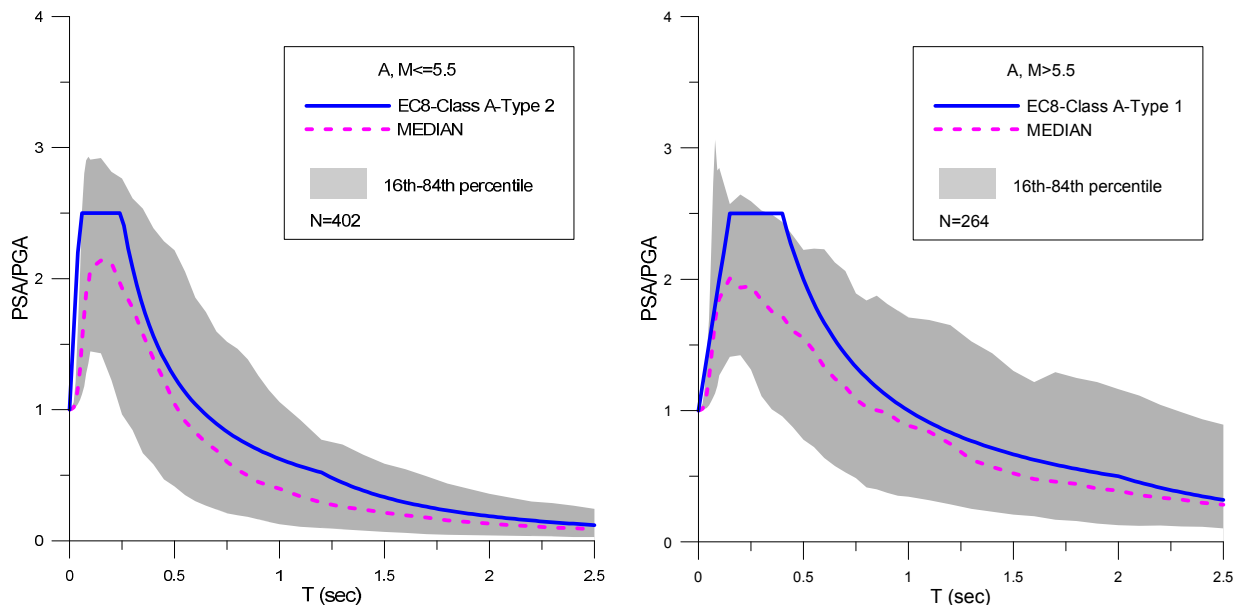


Figure 3.3: SHARE-DS1: Normalized elastic acceleration response spectra for EC8 soil class A for Type 2 seismicity (left) and Type 1 seismicity (right).

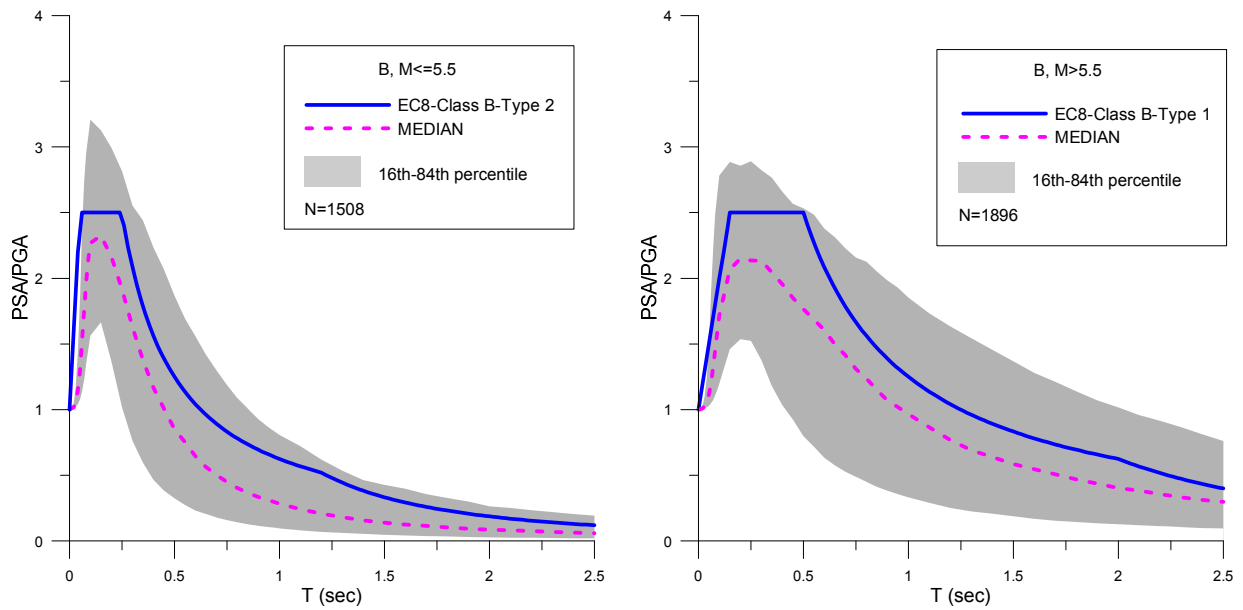


Figure 3.4: SHARE-DS1: Normalized elastic acceleration response spectra for EC8 soil class B for Type 2 seismicity (left) and Type 1 seismicity (right).

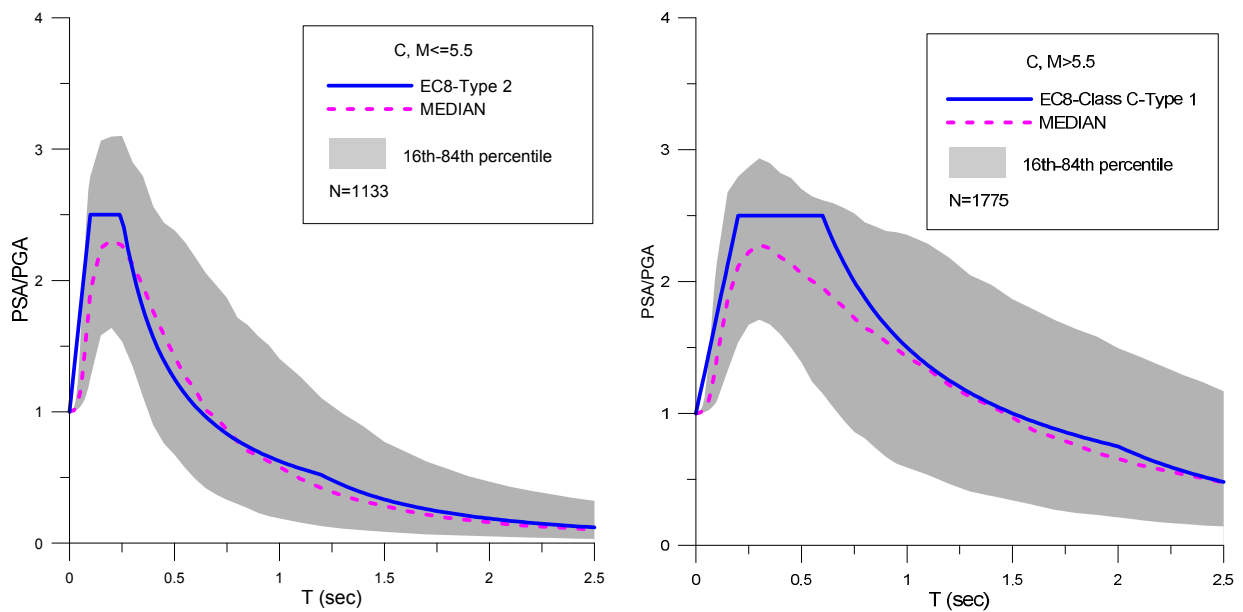


Figure 3.5: SHARE-DS1: Normalized elastic acceleration response spectra for EC8 soil class C for Type 2 seismicity (left) and Type 1 seismicity (right).

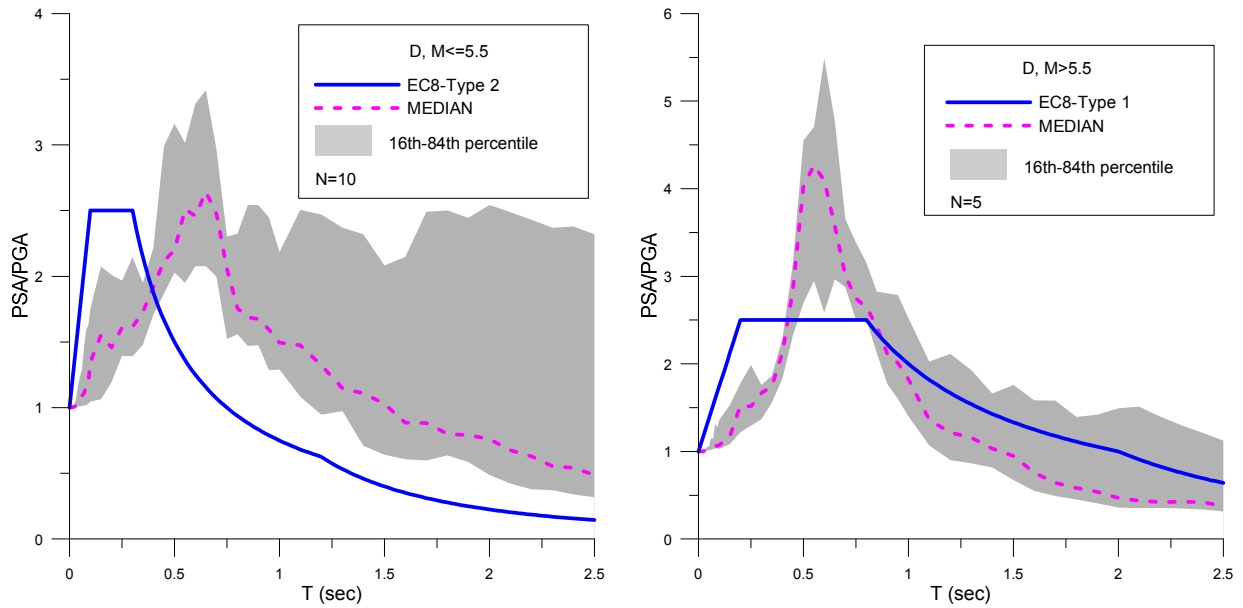


Figure 3.6: SHARE-DS1: Normalized elastic acceleration response spectra for EC8 soil class D for Type 2 seismicity (left) and Type 1 seismicity (right).

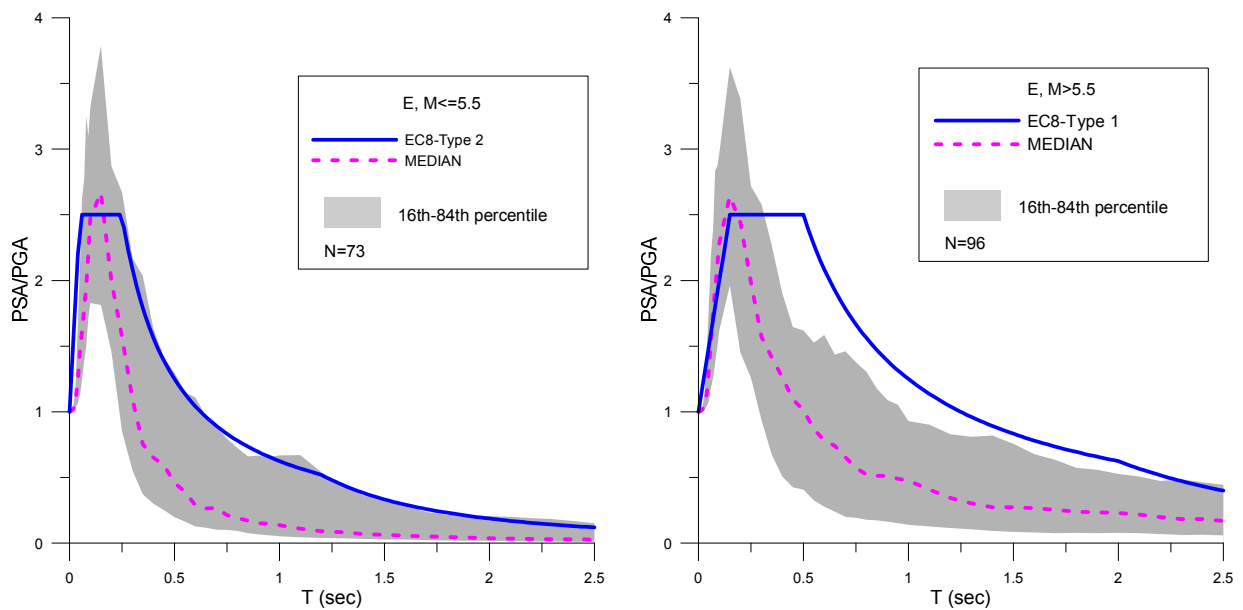


Figure 3.7: SHARE-DS1: Normalized elastic acceleration response spectra for EC8 soil class E for Type 2 seismicity (left) and Type 1 seismicity (right).

Main comments

- EC8 spectra generally match rather well the empirical. The EC8 normalized elastic response spectra are in most cases within the 16% and 84% percentiles. However, they do not seem to have been derived based on a common rationale for all soil classes. For example, in some cases (e.g. soil classes A, B and C) EC8 spectra lie close to the median

normalized curve, while in other cases (e.g. soil class E) EC8 spectra lie closer to or even above the 84th percentile of the empirical normalized spectra.

- EC8 spectra are better representing short periods than long periods. For example for soil class C-Type 1, the proposed spectrum is far below the 84th percentile for spectral periods greater than 0.7s, while it is much closer to the 84th percentile for shorter periods.
- For soil class D, the median normalized spectra have been derived, unfortunately, from a rather poor sample of data. However, the corresponding EC8 spectra fail to capture the empirical data. For Type 2 seismicity, the empirical spectra are shifted towards much longer periods than the proposed ones, while for Type 1 seismicity, the plateau of the empirical spectra reaches much higher values than the spectrum proposed by EC8.
- For soil class E, EC8 spectra are on the conservative side for almost all periods.

3.1.2 SHARE-DS2 (PGA \geq 20cm/sec²)

Figures 3.8-3.12 illustrate the median spectra derived for each soil class and both types of seismicity and the 16th and 84th percentiles using SHARE-DS2 dataset (records having PGA \geq 20cm/s²).

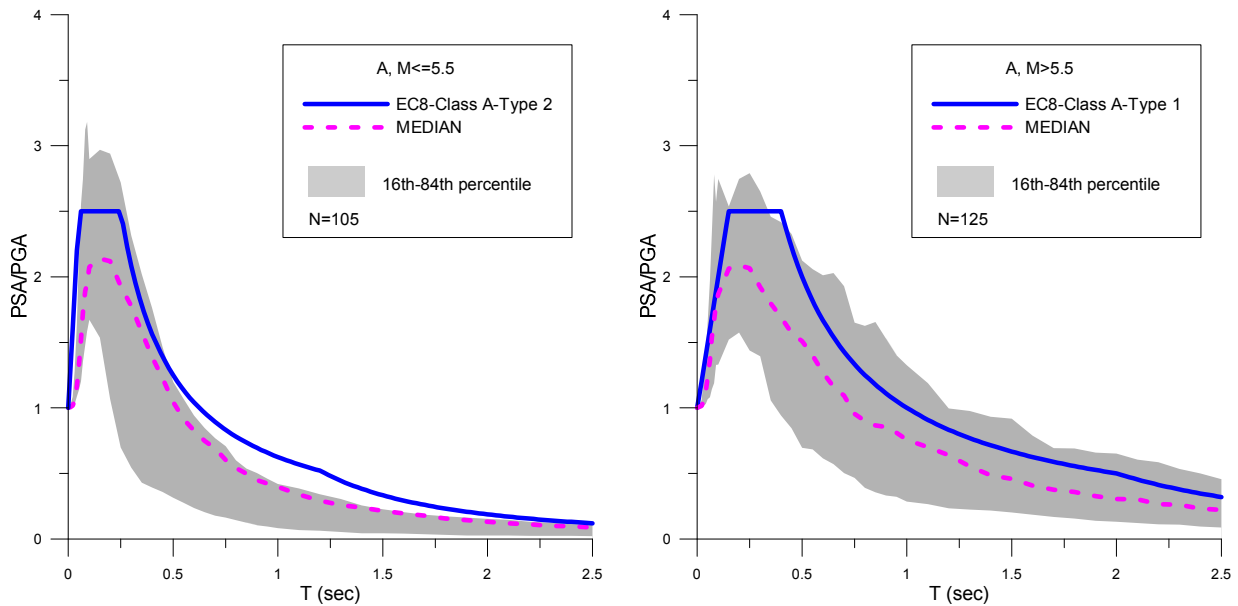


Figure 3.8: SHARE-DS2: Normalized elastic acceleration response spectra for EC8 soil class A for Type 2 seismicity (left) and Type 1 seismicity (right).

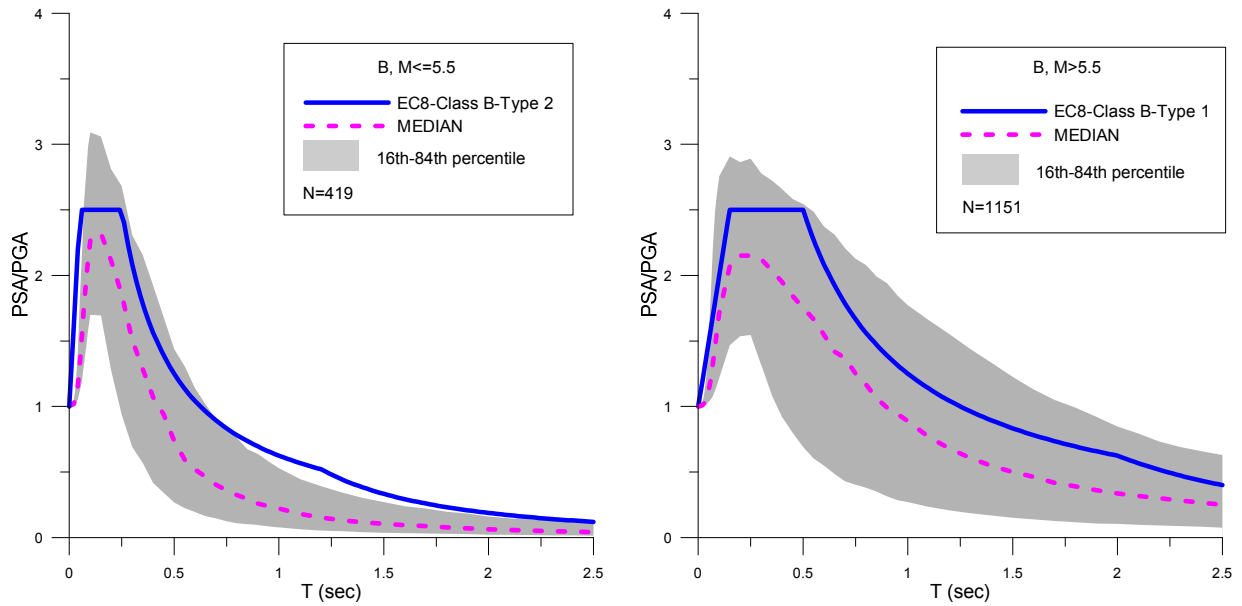


Figure 3.9: SHARE-DS2: Normalized elastic acceleration response spectra for EC8 soil class B for Type 2 seismicity (left) and Type 1 seismicity (right).

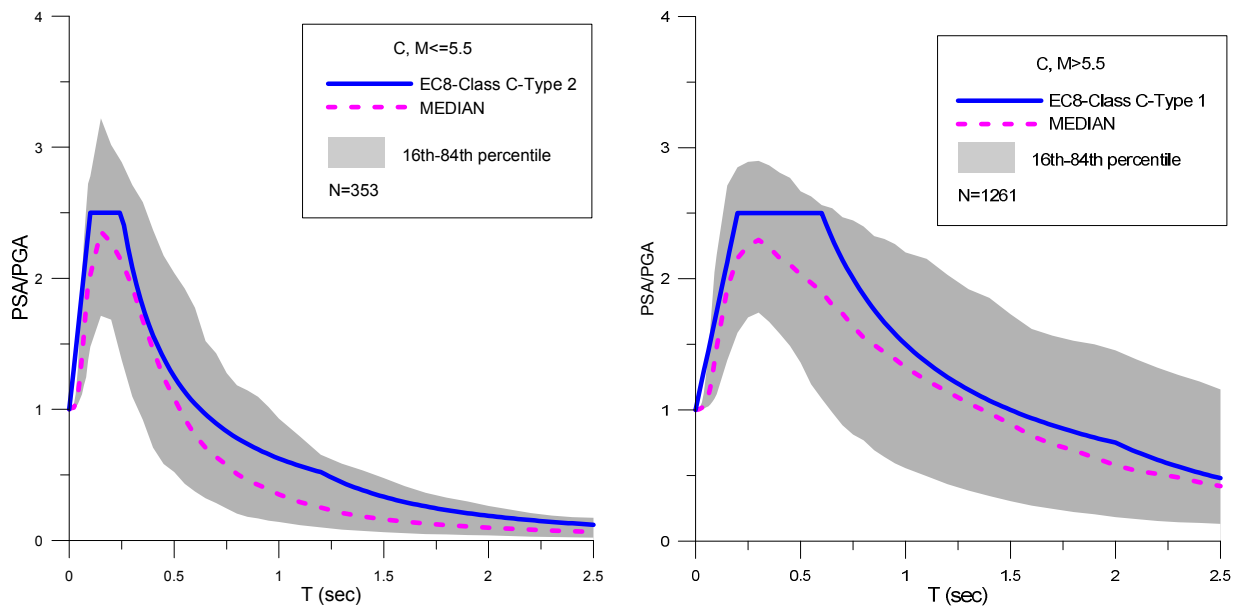


Figure 3.10: SHARE-DS2: Normalized elastic acceleration response spectra for EC8 soil class C for Type 2 seismicity (left) and Type 1 seismicity (right).

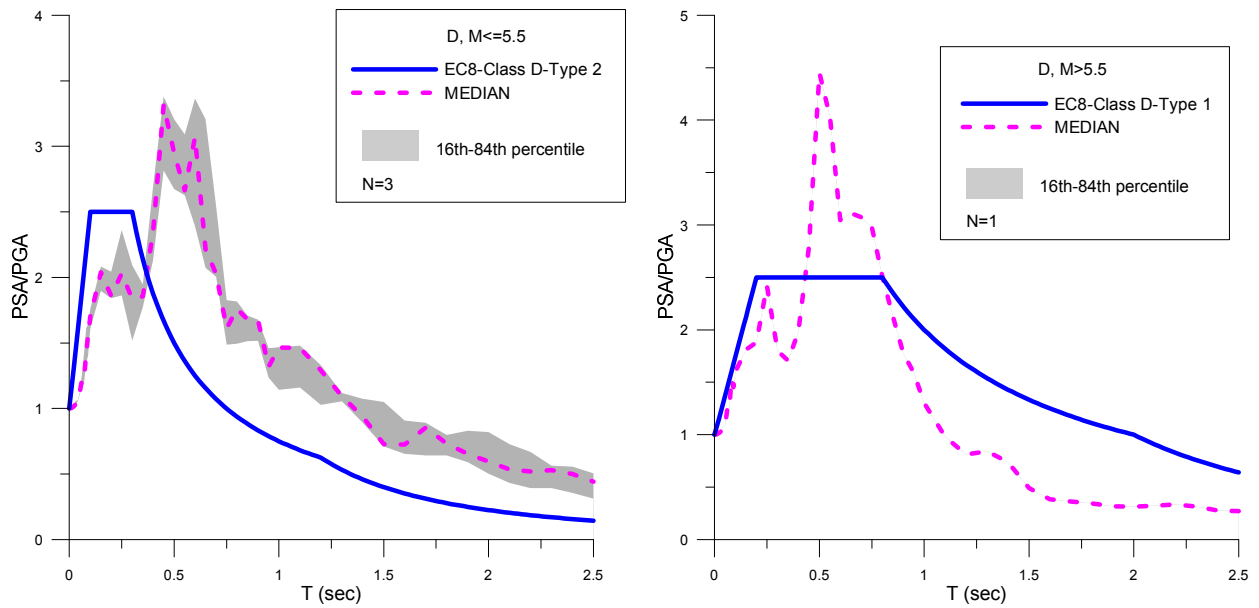


Figure 3.11: SHARE-DS2: Normalized elastic acceleration response spectra for EC8 soil class D for Type 2 seismicity (left) and Type 1 seismicity (right).

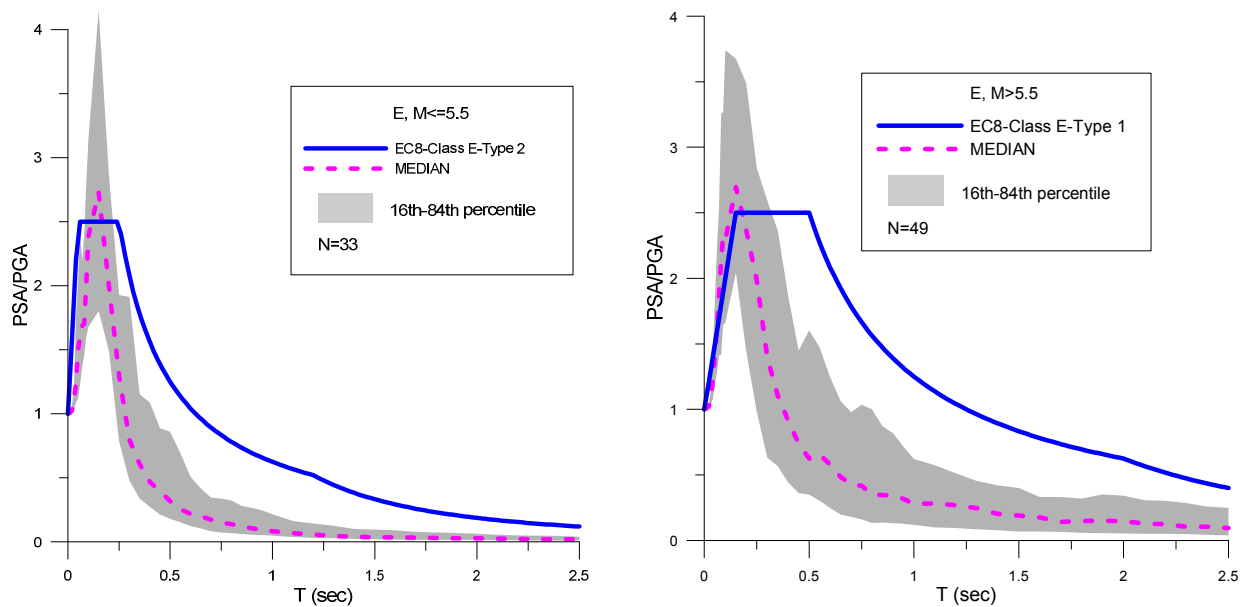


Figure 3.12: SHARE-DS2: Normalized elastic acceleration response spectra for EC8 soil class E for Type 2 seismicity (left) and Type 1 seismicity (right).

Main comments

- More or less the same comments may be made as in the previous case.

3.1.3 SHARE-DS3 (PGA \geq 150cm/sec²)

For SHARE-DS3, the spectra for both Type 2 and Type 1 seismicity are presented in Figures 3.13-3.16 for reasons of completeness, although this dataset was compiled as representative for high seismicity. Type 2 spectra were calculated from those records, which, although

having high PGA values, come from events with $M_s \leq 5.5$. For soil class D there are no available records. The corresponding EC8 spectra are also shown below.

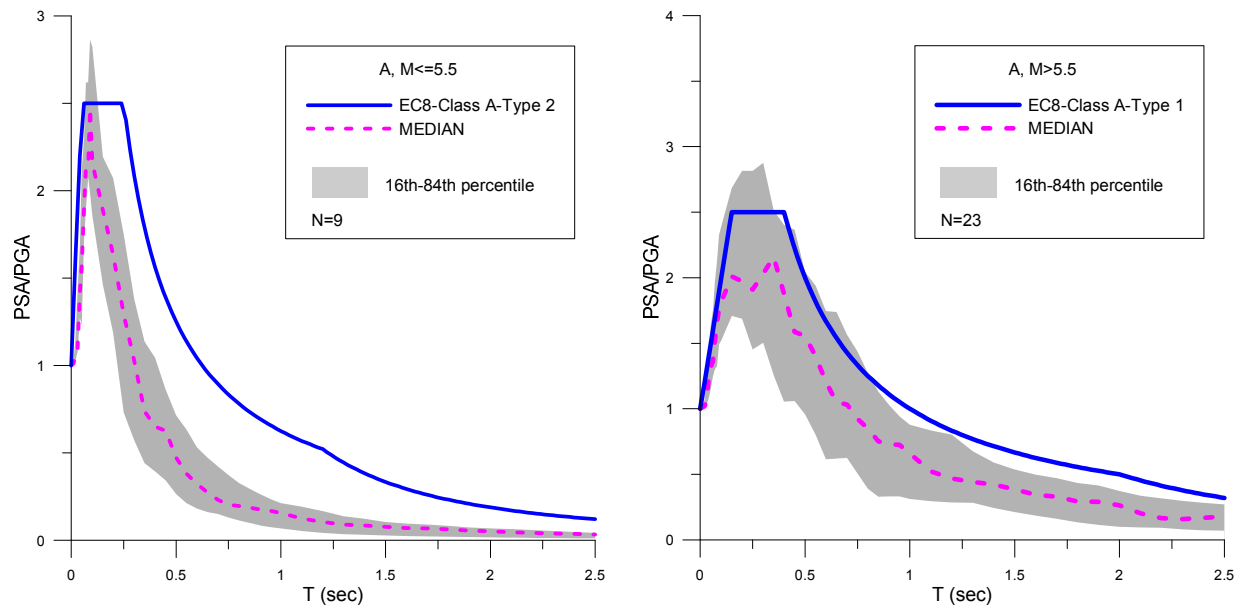


Figure 3.13: SHARE-DS3: Normalized elastic acceleration response spectra for EC8 soil class A for Type 2 seismicity (left) and Type 1 seismicity (right).

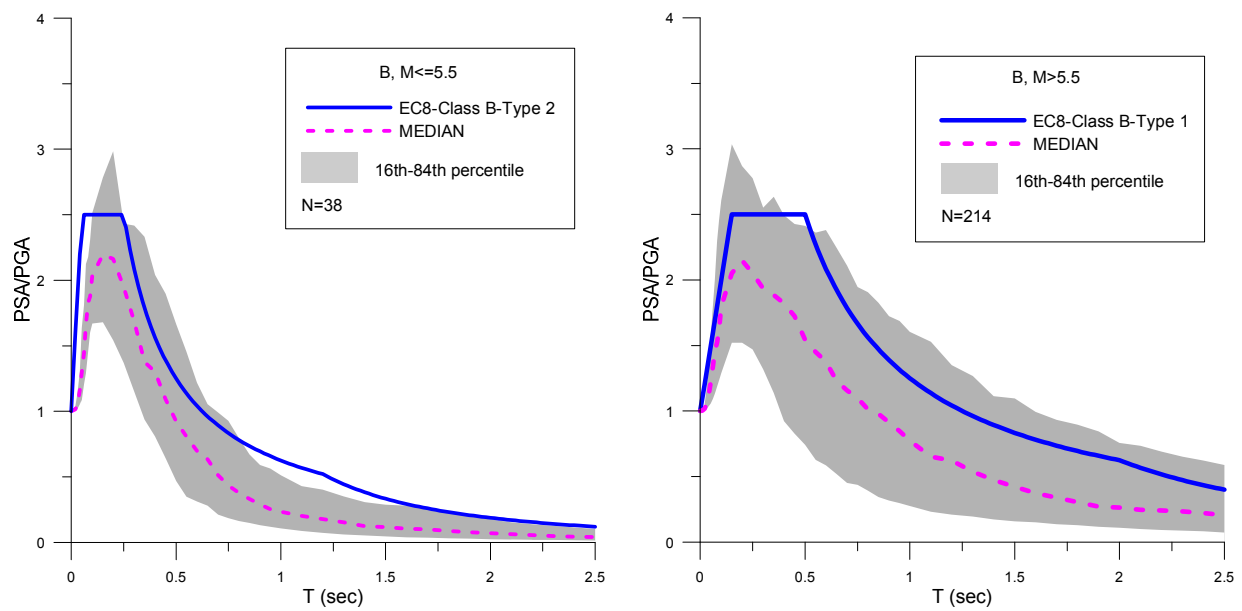


Figure 3.14: SHARE-DS3: Normalized elastic acceleration response spectra for EC8 soil class B for Type 2 seismicity (left) and Type 1 seismicity (right).

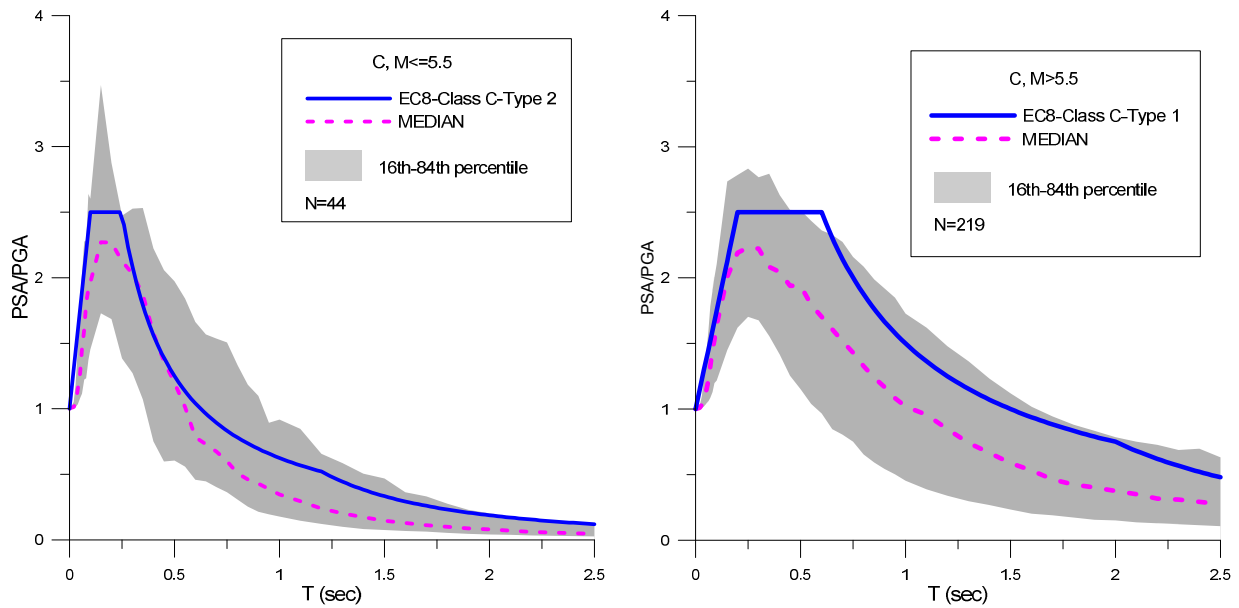


Figure 3.15: SHARE-DS3: Normalized elastic acceleration response spectra for EC8 soil class C for Type 2 seismicity (left) and Type 1 seismicity (right).

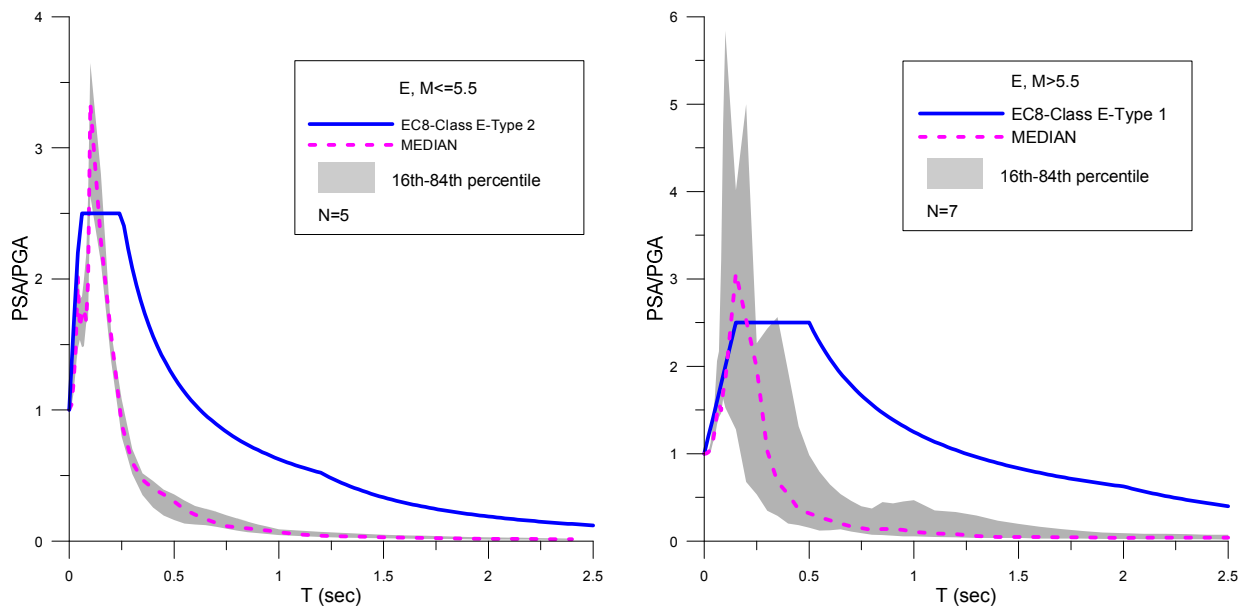


Figure 3.16: SHARE-DS3: Normalized elastic acceleration response spectra for EC8 soil class E for Type 2 seismicity (left) and Type 1 seismicity (right).

Main comments:

SHARE-DS3 dataset is actually representative for Type 1 seismicity according to EC8 independently of the value of the magnitude. Consequently the following comments regard Type 1 spectra.

- For soil classes A, B and C the general picture of the normalized acceleration spectra for SHARE-DS3 dataset as derived from this analysis remains the same with the previous

ones. However we observe that the recorded spectra give somehow lower values compared to the previous two datasets. As a result, EC8 spectra lie closer to the 84th percentile of the empirical spectra.

- For soil class D there are no available records.
- For soil class E, EC8 spectra are even more conservative, compared to the previous two datasets. We remark again the insufficiency of the data for this soil class.

3.2 Soil amplification factors

3.2.1 Methodology

A logic tree approach was used for the estimation of soil amplification factors to the reference rock basement motion for EC8 soil classes. The logic tree approach allows the use of alternative models, each of which is assigned a weighting factor that is interpreted as the relative likelihood of that model being correct. In this way, the epistemic uncertainties associated with the different models can be captured in an efficient way.

The logic tree that was implemented is shown in Figure 3.17. Two state-of-the-art methods were used with equal weights. The first method calculates **period-dependent amplification factors** using Ground Motion Prediction Equations (GMPEs) for the estimation of reference spectral acceleration values (Choi and Stewart, 2005). The GMPEs that are used are the four GMPEs proposed in SHARE (Delavaud et al., 2011 submitted) for ground motion prediction equations for the reference rock sites in active shallow crustal regions. The same weighting factors have been used herein. The second method calculates a **constant period-independent amplification factor for the whole spectrum**, with respect to the “rock sites” of the database (Rey et al., 2002). The second approach has been used for the estimation of the present amplification factors “S” in EC8. Both approaches were used to estimate soil amplification factors for the soil classes of EC8 and for the two seismicity types as suggested in EC8.

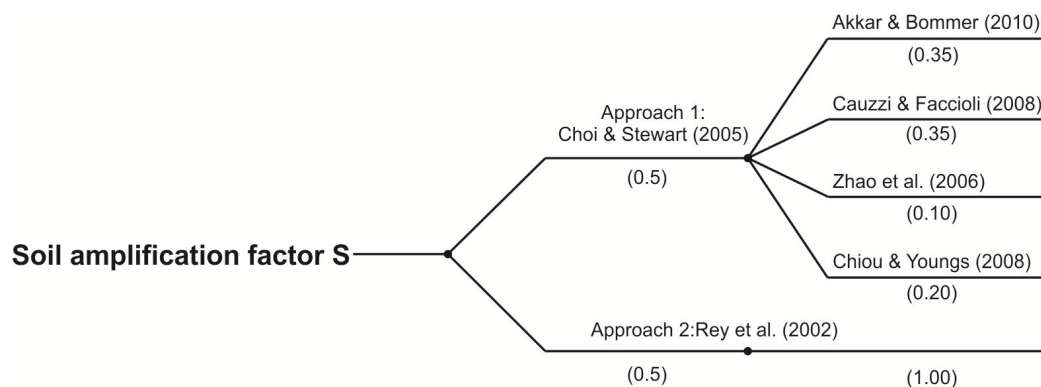


Figure 3.17: Logic tree for estimation of soil amplification factors

Approach 1

In this approach, the amplification factor for ground motion j within site class i , S_{ij} , was evaluated from the geometric mean of 5% damped acceleration response spectra for the two horizontal components of shaking, GM_{ij} , and the reference ground motion for the site, $(GM_r)_{ij}$, as follows (Choi and Stewart, 2005):

$$S_{ij}(T) = GM_{ij} / (GM_r)_{ij} \quad (1)$$

where T is the spectral period. In Equation (1), GM_{ij} and $(GM_r)_{ij}$ are computed at the same spectral period, which is varied from 0 to 2.5 s.

For the calculation of reference motion parameter $(GM_r)_{ij}$, the four Ground Motion Prediction Equations (GMPEs) proposed in SHARE for active shallow crustal regions were used, since the majority of the SHARE database stations are in active regions. The proposed models and corresponding weights are given in Table 3.2. Each GMPE was implemented only for the database records, for which all necessary metadata were either available or could be reliably estimated.

Table 3.2: SHARE logic tree for ground motion prediction for active shallow crustal regions. Selected models and corresponding weights (Delavaud et al., 2011 submitted).

Model	Proposed weight
Akkar and Bommer (2010)	0.35
Cauzzi and Faccioli (2008)	0.35
Zhao et al. (2006)	0.10
Chiou and Youngs (2008)	0.20

The Akkar and Bommer (2010) GMPE, herein called A&B, takes into account the moment magnitude M_w , Joyner-Boore distance r_{jb} , faulting style and soil class (soft, stiff and rock sites are defined based on $V_{s,30}$). Reference spectral accelerations were estimated for all ground motions with available M_w , r_{jb} and faulting style, with the assumption of a rock site with reference $V_{s,30}$ equal to 800m/s.

The Cauzzi and Faccioli (2008) GMPE, herein called C&F, takes into account the moment magnitude M_w , hypocentral distance r_{hyp} , faulting style and soil class (four soil classes A, B, C and D are defined based on $V_{s,30}$). Reference peak ground acceleration PGA and spectral displacements S_d were estimated for all ground motions with available M_w , r_{hyp} and faulting style, with the assumption of a rock site with reference $V_{s,30}$ equal to 800m/s, which corresponds to soil class A. Spectral displacement values were transformed into spectral acceleration values S_a using the following equation:

$$S_a(T) = S_d(T) \cdot 4\pi^2 / T^2 \quad (2)$$

The Zhao et al. (2006) GMPE, herein called Zh, takes into account the moment magnitude M_w , shortest distance to the rupture zone r_{rup} (or hypocentral distance r_{hyp} for earthquakes with no available fault model), focal depth h , source type, faulting style and site class (four site classes I, II, III, IV are defined based on natural period, Molas and Yamazaki, 1995).

Reference spectral accelerations were estimated for all ground motions with available M_w , r_{rup} or r_{hyp} , h and faulting style, with the assumptions of a crustal source type and a rock site with reference $V_{s,30}$ equal to 800m/s, which corresponds to soil class SC I.

The Chiou and Youngs (2008) GMPE, herein called C&Y, takes into account the moment magnitude M_w , shortest distance to the rupture plane r_{rup} , site coordinate R_x , fault dip angle δ , hanging wall effect, depth to top of rupture Z_{TOR} (km), depth to shear wave velocity of 1.0 km/s $Z_{1.0}$ (m), faulting style, $V_{s,30}$ and whether the event is an aftershock or not. Reference spectral accelerations were estimated for all ground motions for which the above parameters were known or could be reliably estimated (mainly using Kaklamanos et al. (2011) approach for estimation of parameters for NGA ground motion prediction models), with the assumption of a rock site with reference $V_{s,30}$ equal to 800m/s. The hanging wall term was omitted due to lack of relative data.

Taking into account all four GMPEs and using the weights of Table 3.2, the reference ground motion $(GM_r)_{ij}$ at a certain period was calculated for each ground motion j within site class i with the following equation:

$$(GM_r)_{ij}(T) = 0.35 \cdot (GM_r)_{ij,AB} + 0.35 \cdot (GM_r)_{ij,CF} + 0.10 \cdot (GM_r)_{ij,Zh} + 0.20 \cdot (GM_r)_{ij,CY} \quad (3)$$

where $(GM_r)_{ij,AB}$, $(GM_r)_{ij,CF}$, $(GM_r)_{ij,Zh}$, $(GM_r)_{ij,CY}$, are the reference spectral accelerations at period T , calculated using the Akkar and Bommer (2010), Cauzzi and Faccioli (2008), Zhao et al. (2006) and Chiou and Youngs (2008) GMPEs respectively.

The computation of reference spectral acceleration using equation (3) requires that reference spectral acceleration at period T can be estimated with all four GMPEs. However, as it has already been explained, each GMPE could be implemented for a different subset of data, since each GMPE requires the knowledge of different parameters. As a result, the computation of reference spectral acceleration with all four GMPEs, and thus the estimation of amplification factors with Approach 1, was feasible for a limited dataset.

Finally, in order to estimate a single period-independent amplification factor for each soil class and each level of magnitude, similar to the soil factor “S” proposed in EC8, the amplification factors were averaged over a range of periods from $T=0$ to $T=2.0s$, since Zhao et al. (2006) and Chiou and Youngs (2008) GMPEs provide no intermediate values between 2.0 and 2.5s. The resulting amplification factors, however, do not represent only the amplification related to the increase of ordinates of soil spectra with respect to rock spectra, but also the amplification due to the change in shape of PGA-normalized response spectra, since average spectra of softer soils tend to have a larger and shifted towards longer periods plateau compared to rock spectra (Rey et al., 2002). In order to assure that the proposed soil factors represent only the amplification related to the increase of ordinates of soil spectra with respect to rock spectra, the period-averaged amplification factors were divided by the spectral shape ratio SR given in Table 3.3, which represents the amplification due to the change in shape of PGA-normalized response spectra.

Table 3.3: Spectral shape ratios SR for EC8 classification scheme.

Soil Class	$M_s \leq 5.5$	$M_s > 5.5$
B	1.00	1.16
C	0.99	1.29
D	1.13	1.53
E	1.00	1.16

Approach 2

In this approach, proposed by Rey et al. (2002), soil amplification for each soil class is calculated with respect to the available rock sites (soil class A) of the database. 5% spectral ordinates $S_a(T)$ for all vibration periods were first distance-normalized (i.e. multiplied by the epicentral distance R). Such distance normalization is supported by the evidence of attenuation relationships, which show that response spectral accelerations are proportional to the distance elevated to an exponent with a value close to -1, which indicates that shapes of spectra do not change with distance (Bommer and Scott, 2000). $R \cdot S_a$ products were then grouped within magnitude intervals (M.I.) of $M_s=0.5$, ranging from $M=4$ to $M=8$. For each soil class and magnitude interval the log average of distance-normalized spectral ordinates $\overline{R \cdot S_a(T)}$ was calculated. Log average curves for softer soils lie consistently above the corresponding curves for soil A, so it makes sense to estimate the average amplification through a single period-independent factor (Rey et al., 2002). The amplification factors S for each soil class and magnitude interval were calculated using the following equation:

$$S = (I_{soil} / I_{rock}) \cdot (1 / SR) \quad (4)$$

In Equation (4) SR is the spectral shape ratio (given in Table 3.3), while I_{soil} and I_{rock} are the spectrum intensities for soil and rock respectively, originally defined by Housner (1952) for spectral velocities and here adapted for spectral accelerations, given by the following equation:

$$I = \int_{0.05}^{2.5} \overline{R \cdot S_a(T)} dt \quad (5)$$

In Equation (5) $\overline{R \cdot S_a(T)}$ denotes the log average of distance-normalized spectral ordinates $R \cdot S_a(T)$ for each soil class and magnitude interval.

3.2.2 Results

3.2.2.1 SHARE-DS1 dataset

Approach 1

Table 3.4 presents the number of strong motion records for which the implementation of all GMPEs was feasible. It is obvious that the restriction of using only those strong motion records, for which all GMPEs can be applied (herein referred to as common dataset), limits the dataset significantly. As a result, while in soil classes B and C there are adequate data, for soil classes D and E there are very few or even no available data. As a result, soil amplification factors using the common dataset could be estimated only for soil classes B and C.

In order to overcome this obstacle, we decided, in addition of estimating amplification factors using only the common dataset, to calculate the median amplification factors using each one of the Akkar and Bommer (2010), Cauzzi and Faccioli (2008), Zhao et al. (2006) and Chiou and Youngs (2008) GMPEs separately for as many records as possible and then to apply the weighting factors of Table 3.2 to the these median values. In this case, **each GMPE is applied to a different dataset** and amplification factors are given by the following equation:

$$S(T) = \frac{1}{\frac{0.35}{S_{AB}} + \frac{0.35}{S_{CF}} + \frac{0.10}{S_{Zh}} + \frac{0.20}{S_{CY}}} \quad (6)$$

where $\overline{S_{AB}}$, $\overline{S_{CF}}$, $\overline{S_{Zh}}$ and $\overline{S_{CY}}$ are the median amplification factors, calculated using solely each one of the Akkar and Bommer (2010), Cauzzi and Faccioli (2008), Zhao et al. (2006) and Chiou and Youngs (2008) GMPEs respectively.

Table 3.5 presents the number of strong motion records for which each one of the four GMPEs could be implemented separately. The available strong motion records for soil class D and soil class E are still very limited, allowing however a first estimate for the corresponding soil factors.

Table 3.4: SHARE-DS1: Number of strong motion records for which reference spectral acceleration could be estimated with all GMPEs. (common dataset)

Soil Class	Type 2 ($4 \leq M_s \leq 5.5$)	Type 1 ($M_s > 5.5$)
B	310	964
C	289	1130
D	-	-
E	-	4

Table 3.5: SHARE-DS1: Number of strong motion records for which each GMPE could be implemented. (different datasets)

Soil Class	A&B		C&F		Zh		C&Y	
	$M_s \leq 5.5$	$M_s > 5.5$						
B	433	1053	774	1586	774	1586	311	1048
C	383	1191	746	1608	746	1608	289	1189
D	7	2	8	4	8	4	-	-
E	10	4	42	58	42	58	-	7

Common dataset for all GMPEs

Figures 3.18 and 3.19 illustrate the amplification factors calculated with equation (1) for soil classes B and C respectively, using the weighted average $(GM_r)_{ij}$ derived from equation (3) as reference spectral acceleration. The median values of the amplification factors for each spectral period, along with the 16th and 84th percentiles are also depicted in Figures 3.18 and 3.19 and given in detail in Table 3.6. The specific percentiles were selected since, in the case of normal distribution of data, they represent the values of average minus one standard deviation and average plus one standard deviation respectively. Figures 3.20 and 3.21 compare the estimated median amplification factors to the corresponding EC8 acceleration response spectra divided by the spectral values for soil class A.

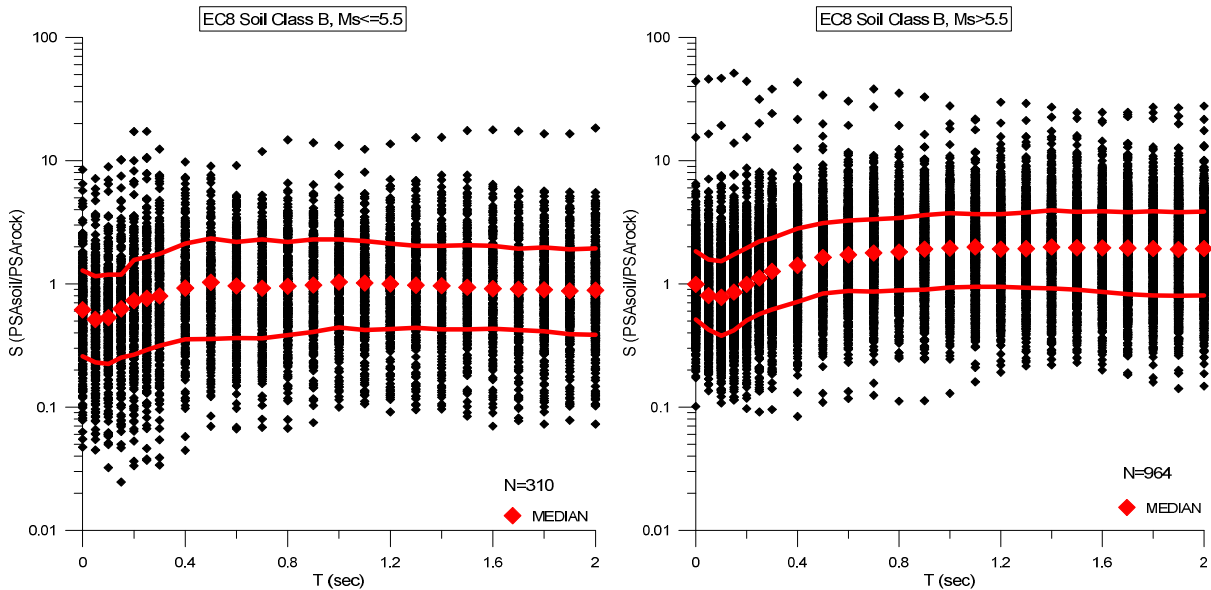


Figure 3.18: SHARE-DS1: Amplification factors estimated with Approach 1 for EC8 soil class B, for Type 2 seismicity (left) and Type 1 seismicity (right). The red lines represent the 16th and 84th percentiles. (common dataset)

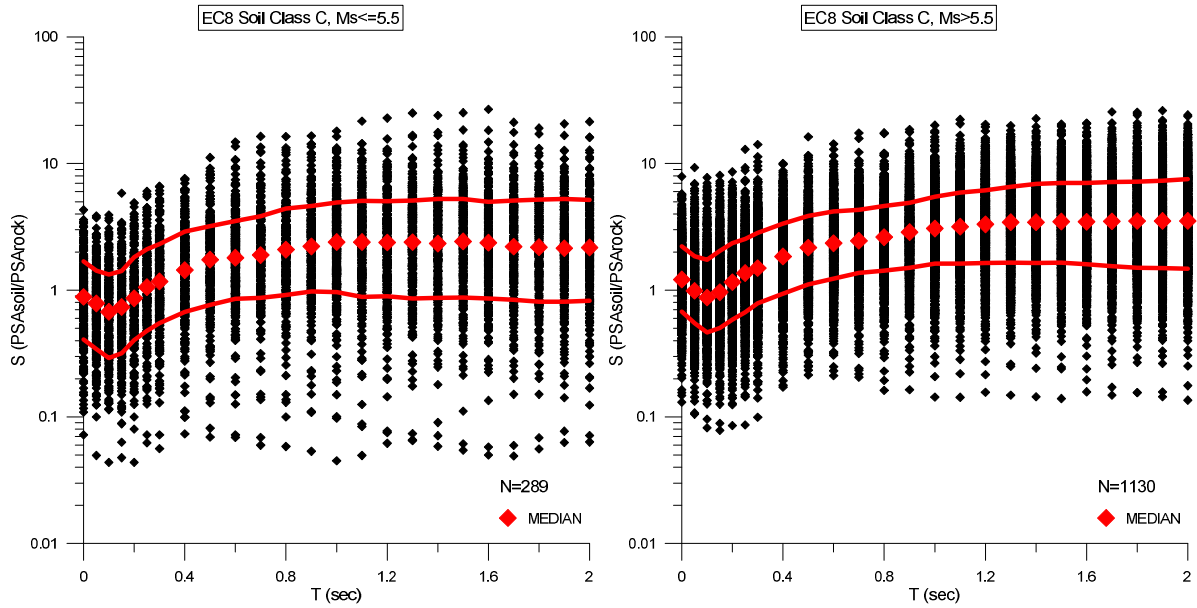


Figure 3.19: SHARE-DS1: Amplification factors estimated with Approach 1 for EC8 soil class C, for Type 2 seismicity (left) and Type 1 seismicity (right). The red lines represent the 16th and 84th percentiles. (common dataset)

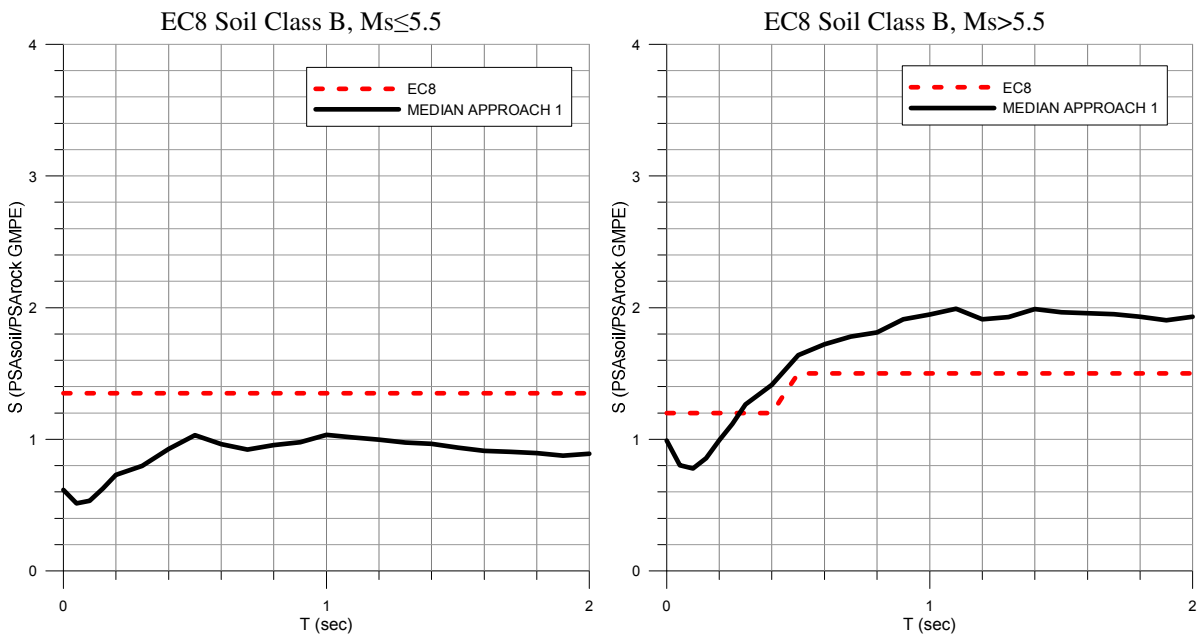


Figure 3.20: SHARE-DS1: Median amplification factors estimated with Approach 1 for EC8 soil class B, for Type 2 seismicity (left) and Type 1 seismicity (right). (common dataset)

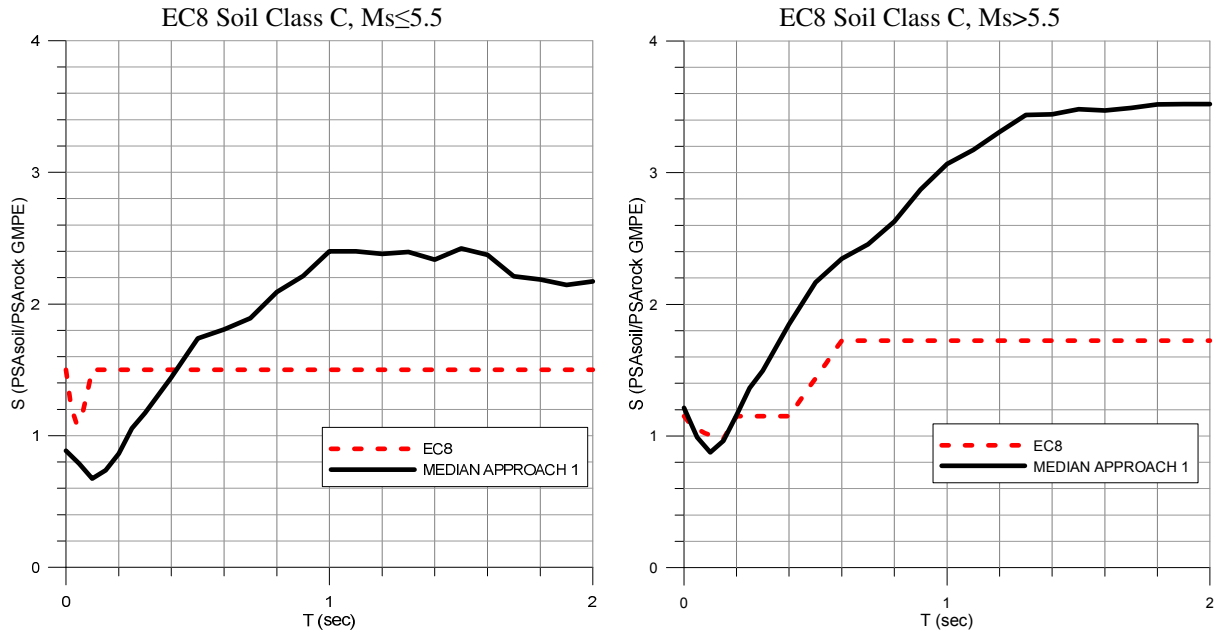


Figure 3.21: SHARE-DS1: Median amplification factors estimated with Approach 1 for EC8 soil class C, for Type 2 seismicity (left) and Type 1 seismicity (right). (common dataset)

Table 3.6: SHARE-DS1: Median amplification factors, 16th and 84th percentiles for EC8 soil classes, estimated with Approach 1. (common dataset)

T	B-Type2			B-Type1			C-Type2			C-Type1		
	Median	16th	84th									
0	0.62	0.26	1.29	0.99	0.51	1.84	0.89	0.41	1.69	1.21	0.68	2.21
0.05	0.51	0.23	1.15	0.80	0.43	1.58	0.79	0.34	1.43	0.99	0.55	1.85
0.1	0.53	0.22	1.19	0.78	0.38	1.53	0.67	0.29	1.33	0.88	0.46	1.74
0.15	0.63	0.25	1.19	0.86	0.42	1.73	0.74	0.32	1.42	0.96	0.50	2.05
0.2	0.73	0.27	1.57	0.99	0.51	1.96	0.86	0.40	1.82	1.16	0.59	2.36
0.25	0.76	0.29	1.65	1.12	0.57	2.22	1.06	0.48	2.11	1.36	0.67	2.54
0.3	0.80	0.32	1.75	1.26	0.62	2.36	1.17	0.55	2.32	1.50	0.79	2.83
0.4	0.93	0.36	2.12	1.41	0.72	2.82	1.44	0.68	2.91	1.85	0.94	3.36
0.5	1.03	0.36	2.34	1.64	0.83	3.12	1.74	0.76	3.20	2.17	1.11	3.86
0.6	0.96	0.36	2.19	1.72	0.87	3.27	1.81	0.86	3.52	2.35	1.24	4.18
0.7	0.92	0.36	2.30	1.78	0.86	3.34	1.89	0.87	3.84	2.45	1.37	4.30
0.8	0.96	0.38	2.19	1.81	0.89	3.41	2.09	0.92	4.40	2.63	1.42	4.62
0.9	0.98	0.41	2.29	1.91	0.89	3.62	2.21	0.98	4.64	2.87	1.51	4.90
1	1.03	0.44	2.29	1.95	0.94	3.74	2.40	0.96	4.93	3.07	1.62	5.48
1.1	1.01	0.42	2.23	1.99	0.95	3.68	2.40	0.88	5.08	3.17	1.62	5.90
1.2	1.00	0.43	2.13	1.91	0.94	3.68	2.38	0.89	5.04	3.31	1.64	6.15
1.3	0.98	0.44	2.03	1.93	0.93	3.78	2.39	0.86	5.10	3.44	1.65	6.54
1.4	0.97	0.43	2.04	1.99	0.92	3.95	2.34	0.87	5.27	3.44	1.64	6.91
1.5	0.94	0.43	2.06	1.97	0.89	3.83	2.42	0.87	5.24	3.48	1.65	7.03
1.6	0.91	0.43	2.04	1.96	0.86	3.89	2.37	0.86	4.98	3.47	1.60	7.05
1.7	0.91	0.42	1.92	1.95	0.82	3.82	2.21	0.84	5.09	3.49	1.55	7.14
1.8	0.89	0.41	1.98	1.93	0.80	3.87	2.19	0.81	5.20	3.52	1.50	7.18
1.9	0.88	0.39	1.91	1.90	0.80	3.82	2.14	0.81	5.24	3.52	1.49	7.33
2	0.89	0.39	1.94	1.93	0.80	3.85	2.17	0.82	5.16	3.52	1.48	7.54

In order to estimate a single period-independent amplification factor for each soil class and each level of magnitude, similar to the S factor proposed in EC8, the median amplification factors were averaged over a range of periods from $T=0$ to $T=2$ s. The resulting amplification factors, divided by the spectral shape ratio SR (which represents the amplification due to the change in shape of PGA-normalized response), are presented in Table 3.7, so that they can be compared to the corresponding EC8 S factors, which are also included in the table.

Table 3.7: *SHARE-DS1: Soil factors for EC8 soil classes with Approach 1 compared to EC8. (common dataset)*

Soil Class	$M_s \leq 5.5$		$M_s > 5.5$	
	Approach 1	EC8	Approach 1	EC8
B	0.90	1.35	1.47	1.20
C	1.93	1.50	2.09	1.15

Different dataset for each GMPE

Figures 3.22 to 3.25 summarize the medians of the amplification factors estimated from the strong motion records of Table 3.5, using the four GMPEs separately, as well as the weighted average amplification factors calculated with equation (6). For the case where the GMPE of Chiou and Youngs (2006) could not be implemented, the weight of this GMPE (equal to 0.20) was equally distributed to the remaining three GMPEs, whose weights were as a result increased by the value of $0.20/3$.

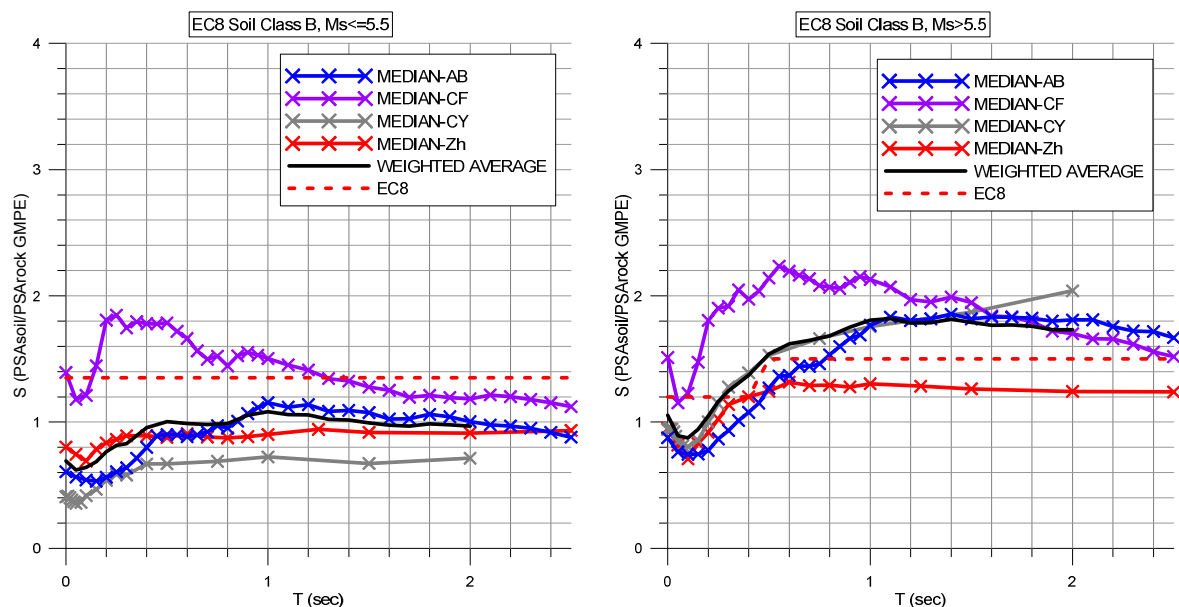


Figure 3.22: *SHARE-DS1: Median amplification factors with Approach 1 for soil class B and PSA_{rock} estimated with all GMPEs, for Type 2 seismicity (left) and Type 1 seismicity (right). (different datasets)*

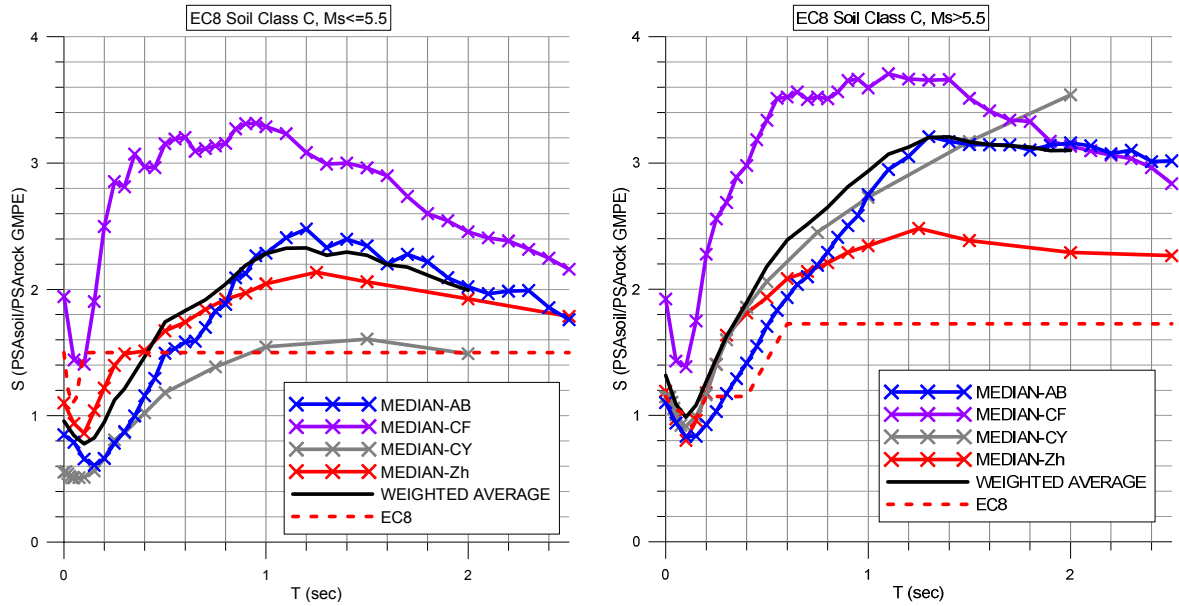


Figure 3.23: SHARE-DS1: Median amplification factors with Approach 1 for soil class C and PSA_{rock} estimated with all GMPEs, for Type 2 seismicity (left) and Type 1 seismicity (right). (different datasets)

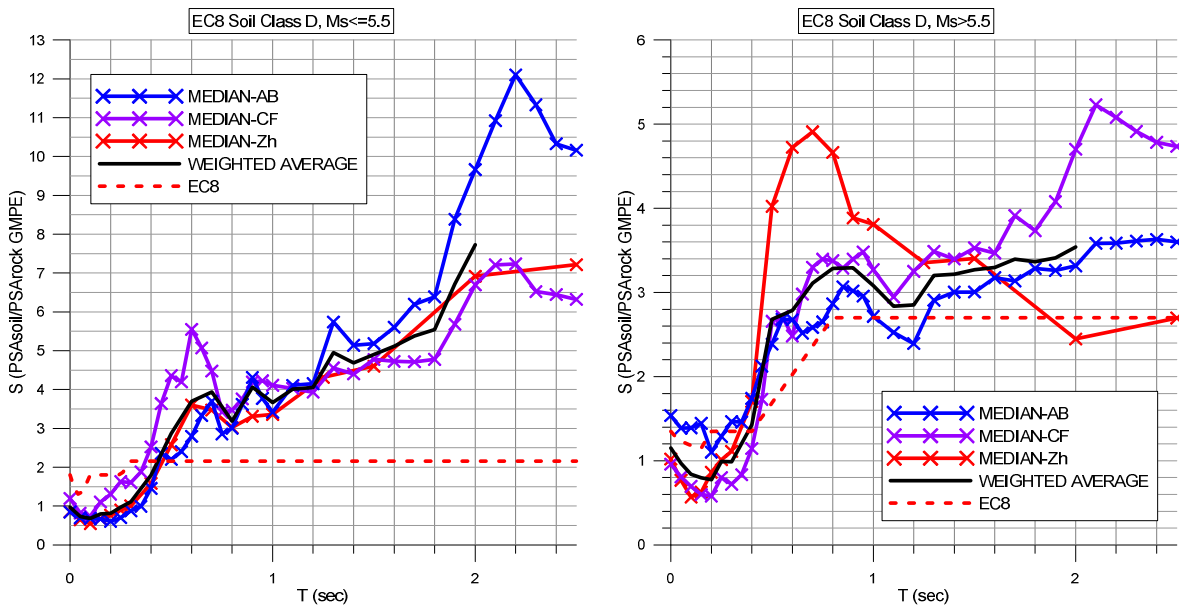


Figure 3.24: SHARE-DS1: Median amplification factors with Approach 1 for soil class D and PSA_{rock} estimated with all GMPEs, for Type 2 seismicity (left) and Type 1 seismicity (right). (different datasets)

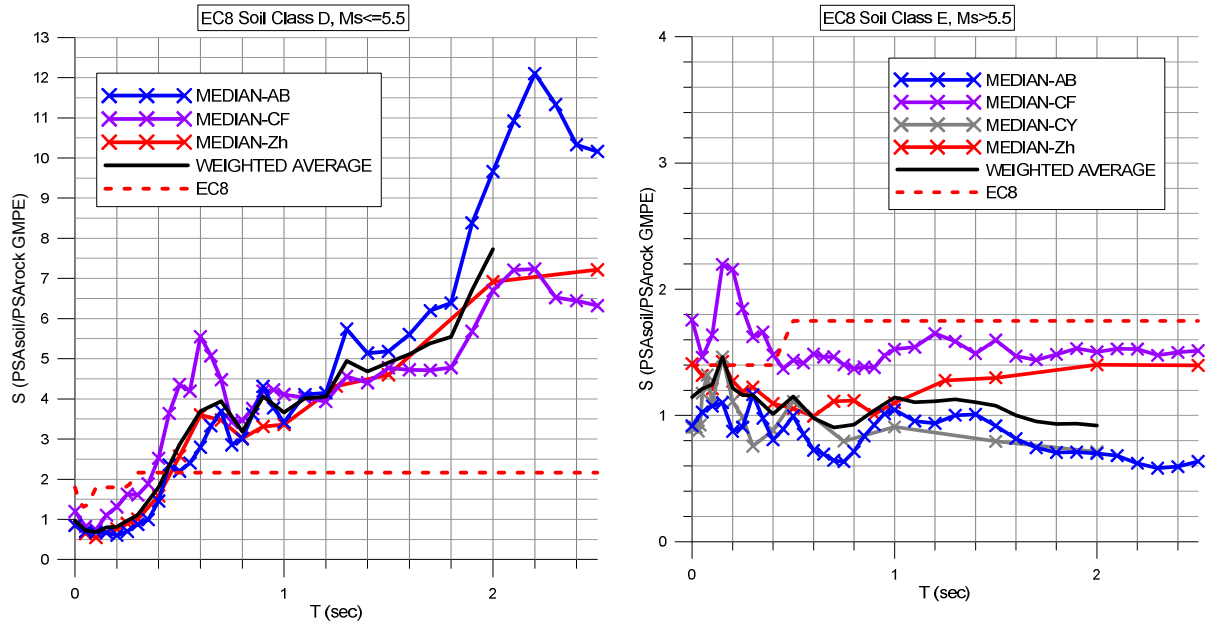


Figure 3.25: SHARE-DS1: Median amplification factors with Approach 1 for soil class E and PSA_{rock} estimated with all GMPEs, for Type 2 seismicity (left) and Type 1 seismicity (right). (different datasets)

In some cases all GMPEs give in general comparable results (soil type D and E for both Type 1 and Type 2 seismicity). For soil classes B and C, where there is a sufficiently large amount of data, there are remarkable differences among GMPEs. The use of C&F GMPE gives in general higher values, while the C&Y results to lower amplification factors, especially for Type 2 earthquakes. One possible reason for these differences is related to the way that C&F or C&Y GMPE estimate the reference spectral acceleration in rock conditions, leading to lower (C&F) or higher (C&Y) values compared to the other two GMPEs.

The second important observation is the period dependency of the amplification factors. In general with few exceptions the larger differences with the constant EC8 values are observed in moderate to long periods ($T > 0.5 \text{ sec}$), while for short periods the comparison is acceptable.

The period-dependent amplification factors calculated from Equation (6) are given in detail in Table 3.8. In order to estimate a single period-independent amplification factor for each soil class and each level of magnitude, similar to the S factor proposed in EC8, the weighted average amplification spectra were averaged over a range of periods from $T=0$ to $T=2 \text{ s}$. The resulting amplification factors, divided by the spectral shape ratio SR are presented in Table 3.9.

Table 3.8: SHARE-DS1: Amplification factors for EC8 soil classes, estimated with Approach 1. (different datasets)

T	B - Type 2	B - Type 1	C - Type 2	C - Type 1	D - Type 2	D - Type 1	E - Type 2	E - Type 1
0	0.69	1.05	0.96	1.32	0.97	1.15	2.21	1.15
0.05	0.62	0.89	0.84	1.09	0.73	0.97	1.96	1.21
0.1	0.64	0.87	0.78	0.99	0.68	0.84	2.12	1.24
0.15	0.69	0.94	0.83	1.08	0.80	0.80	2.60	1.46
0.2	0.77	1.05	0.95	1.27	0.82	0.78	1.98	1.22
0.25	0.82	1.16	1.12	1.45	0.97	0.99	1.46	1.16
0.3	0.83	1.25	1.21	1.63	1.11	0.99	1.06	1.16
0.4	0.96	1.37	1.47	1.90	1.80	1.43	0.83	1.01
0.5	1.00	1.54	1.74	2.18	2.86	2.68	0.85	1.15
0.6	0.99	1.62	1.83	2.39	3.70	2.79	0.70	0.98
0.7	0.98	1.65	1.92	2.51	3.94	3.11	0.68	0.91
0.8	0.99	1.68	2.04	2.65	3.18	3.28	0.69	0.93
0.9	1.05	1.75	2.19	2.81	4.06	3.29	0.69	1.04
1	1.08	1.81	2.28	2.94	3.66	3.08	0.74	1.14
1.1	1.06	1.82	2.33	3.07	4.01	2.84	0.76	1.11
1.2	1.06	1.78	2.33	3.13	4.05	2.85	0.79	1.11
1.3	1.02	1.79	2.27	3.20	4.95	3.20	0.77	1.13
1.4	1.02	1.81	2.30	3.21	4.69	3.22	0.76	1.11
1.5	0.99	1.79	2.27	3.17	4.90	3.27	0.76	1.08
1.6	0.98	1.77	2.20	3.15	5.12	3.30	0.74	1.00
1.7	0.97	1.77	2.18	3.14	5.38	3.40	0.79	0.95
1.8	0.99	1.76	2.11	3.13	5.55	3.36	0.83	0.93
1.9	0.98	1.73	2.05	3.10	6.72	3.41	0.86	0.94
2	0.97	1.73	1.99	3.10	7.73	3.54	0.90	0.92

Table 3.9: SHARE-DS1: Soil factors for EC8 soil classes with Approach 1 compared to EC8. (different datasets)

Soil Class	$M_s \leq 5.5$		$M_s > 5.5$	
	Approach 1	EC8	Approach 1	EC8
B	0.95	1.35	1.37	1.20
C	1.90	1.50	1.99	1.15
D	3.36	1.80	1.74	1.35
E	0.98	1.60	0.91	1.40

Comparing the soil factors obtained for soil classes B and C with Approach 1 using on the one hand the common dataset and on the other hand the different datasets, we observe that the differences are rather insignificant (Table 3.10). This justifies the decision to apply the logic tree weights to the median amplification factors in order to have an estimate for the soil factors for soil classes D and E.

Table 3.10: SHARE-DS1: Soil factors for EC8 soil classes B and C with Approach 1 obtained from common dataset compared to those obtained from the different datasets.

Soil Class	$M_s \leq 5.5$		$M_s > 5.5$	
	Approach 1 (common dataset)	Approach 1 (different datasets)	Approach 1 (common dataset)	Approach 1 (different datasets)
B	0.90	0.95	1.47	1.37
C	1.93	1.90	2.09	1.99

Approach 2

Figures 3.26 to 3.33 illustrate the log average of distance-normalized response spectra for EC8 soil classes B, C, D and E with respect to soil class A, for the different magnitude intervals.

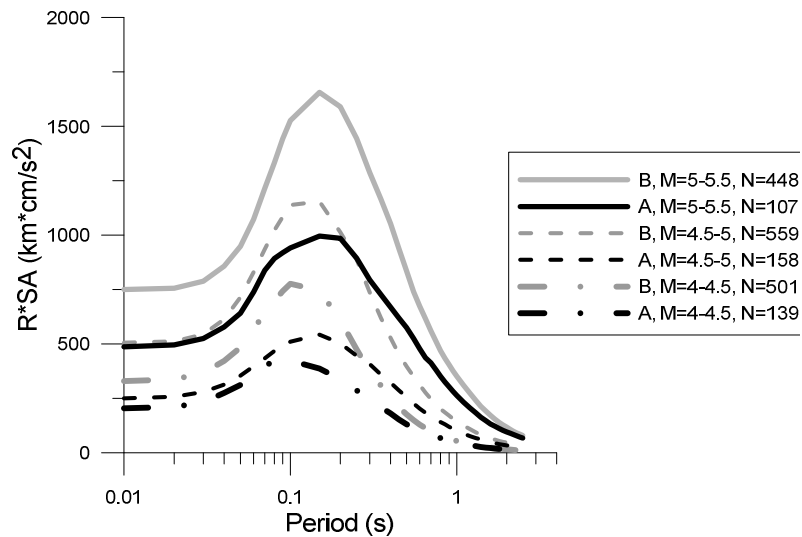


Figure 3.26: SHARE-DS1: Log-average, distance-normalized acceleration response spectra for Type 2 magnitude intervals, for sites of soil class B (grey lines) and rock sites (black lines).

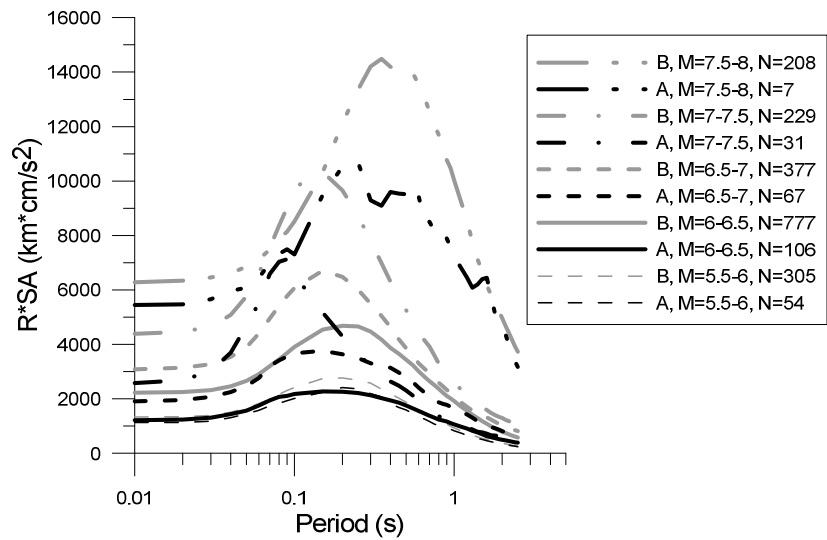


Figure 3.27: SHARE-DS1: Log-average, distance-normalized acceleration response spectra for Type 1 magnitude intervals for sites of soil class B (grey lines) and rock sites (black lines).

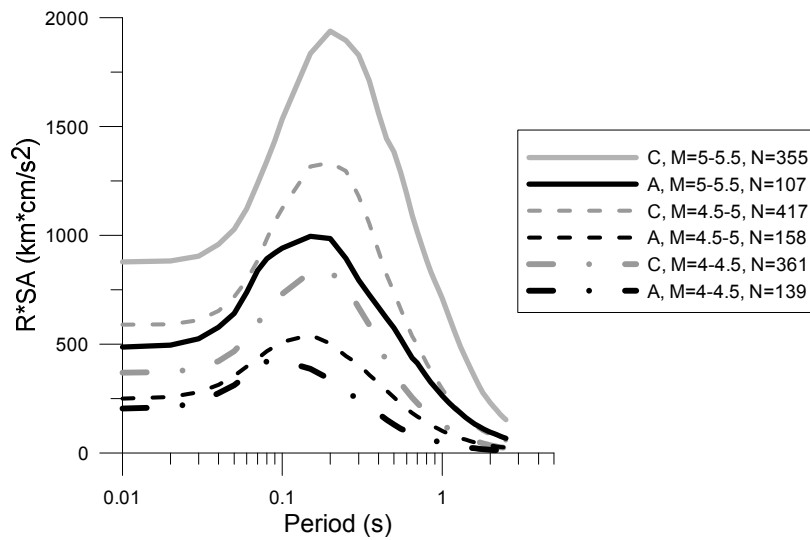


Figure 3.28: SHARE-DS1: Log-average, distance-normalized acceleration response spectra for Type 2 magnitude intervals for sites of soil class C (grey lines) and rock sites (black lines).

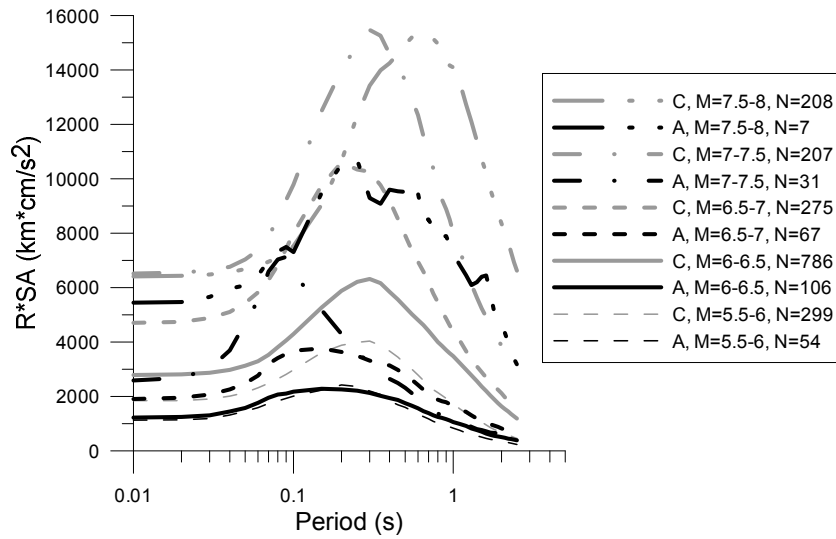


Figure 3.29: SHARE-DS1: Log-average, distance-normalized acceleration response spectra for Type 1 magnitude intervals for sites of soil class C (grey lines) and rock sites (black lines).

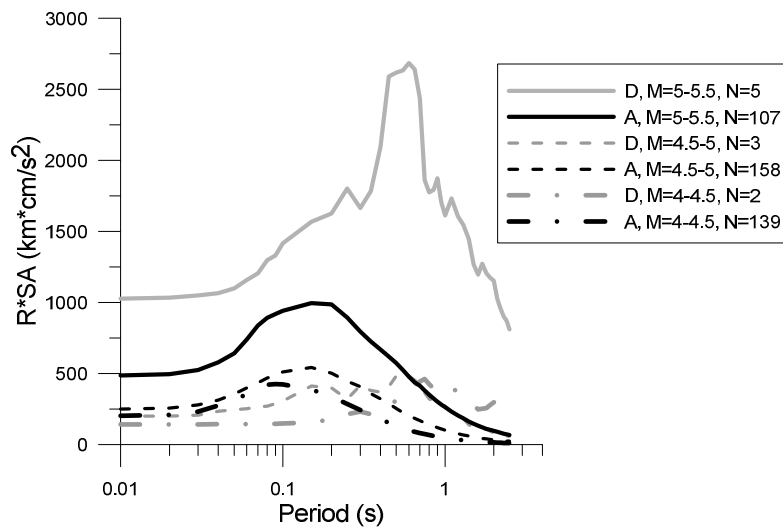


Figure 3.30: SHARE-DS1: Log-average, distance-normalized acceleration response spectra for Type 2 magnitude intervals for sites of soil class D (grey lines) and rock sites (black lines).

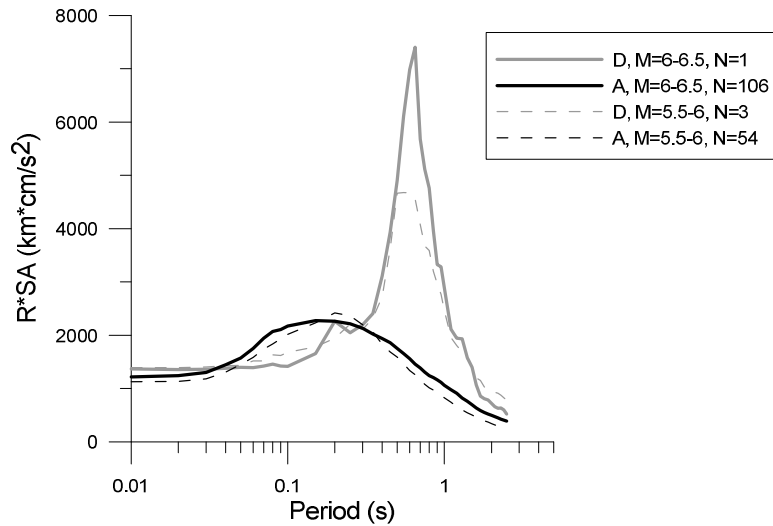


Figure 3.31: SHARE-DS1: Log-average, distance-normalized acceleration response spectra for Type 1 magnitude intervals for sites of soil class D (grey lines) and rock sites (black lines).

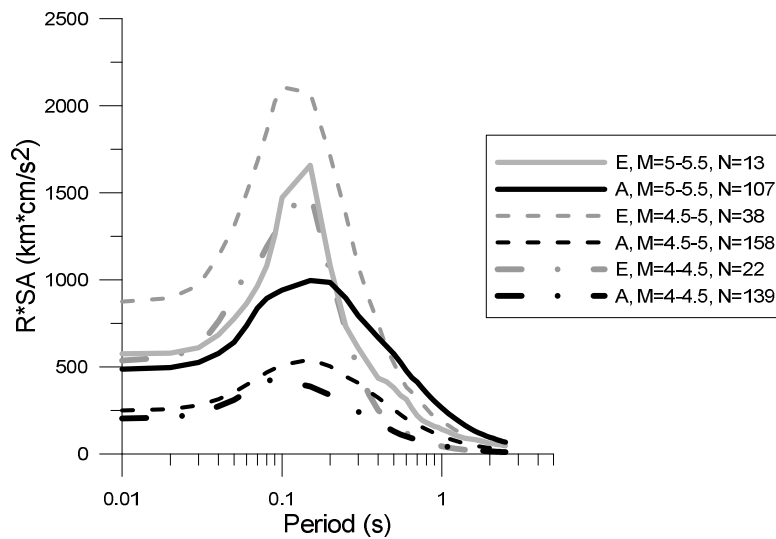


Figure 3.32: SHARE-DS1: Log-average, distance-normalized acceleration response spectra for Type 2 magnitude intervals for sites of soil class E (grey lines) and rock sites (black lines).

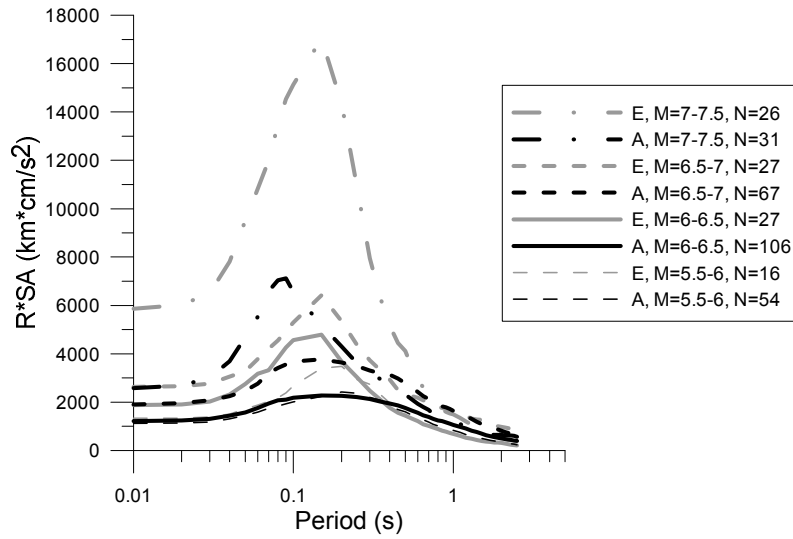


Figure 3.33: SHARE-DS1: Log-average, distance-normalized acceleration response spectra for Type 1 magnitude intervals for sites of soil class E (grey lines) and rock sites (black lines).

I_{soil}/I_A ratios for all magnitude intervals and for soil classes B, C, D and E are presented in Tables 3.11, 3.12, 3.13 and 3.14 respectively. The tables also contain the number of available strong motion records for each case. The PGA range for each soil class and magnitude interval is also provided, with the number in the parenthesis representing the median PGA value for each case.

Table 3.11: SHARE-DS1: I_{soil}/I_A ratios for EC8 soil class B and all magnitude intervals.

$M_s \leq 5.5$				$M_s > 5.5$			
M_s	I_B/I_A	$n(B)/n(A)$	PGA (cm/s^2)	M_s	I_B/I_A	$n(B)/n(A)$	PGA (cm/s^2)
4.0-4.5	1.49	501/139	≤ 269 (8)	5.5-6.0	1.16	305/54	≤ 936 (19)
4.5-5.0	1.71	559/158	≤ 521 (10)	6.0-6.5	1.85	777/106	≤ 953 (26)
5.0-5.5	1.45	448/107	≤ 1091 (10)	6.5-7.0	1.42	377/67	≤ 1207 (46)
				7.0-7.5	2.11	229/31	≤ 1224 (22)
				7.5-8.0	1.28	208/7	≤ 916 (76)

Table 3.12: SHARE-DS1: I_{soil}/I_A ratios for EC8 soil class C and all magnitude intervals.

$M_s \leq 5.5$				$M_s > 5.5$			
M_s	I_C/I_A	$n(C)/n(A)$	PGA (cm/s^2)	M_s	I_C/I_A	$n(C)/n(A)$	PGA (cm/s^2)
4.0-4.5	2.48	361/139	≤ 447 (8)	5.5-6.0	1.92	299/54	≤ 630 (27)
4.5-5.0	2.72	417/158	≤ 347 (9)	6.0-6.5	3.04	786/106	≤ 560 (30)
5.0-5.5	2.31	355/107	≤ 415 (11)	6.5-7.0	2.72	275/67	≤ 1302 (88)
				7.0-7.5	5.06	207/31	≤ 775 (44)
				7.5-8.0	1.69	208/7	≤ 687 (69)

Table 3.13: SHARE-DS1: I_{soil}/I_A ratios for EC8 soil class D and all magnitude intervals.

$M_s \leq 5.5$				$M_s > 5.5$			
M_s	I_D/I_A	$n(D)/n(A)$	PGA (cm/s ²)	M_s	I_D/I_A	$n(D)/n(A)$	PGA (cm/s ²)
4.0-4.5	3.85	2/139	≤9 (6)	5.5-6.0	2.25	3/54	≤74 (16)
4.5-5.0	1.60	3/158	≤11 (4)	6.0-6.5	2.11	1/106	≤14 (14)
5.0-5.5	4.96	5/107	≤44(39)				

Table 3.14: SHARE-DS1: I_{soil}/I_A ratios for EC8 soil class E and all magnitude intervals.

$M_s \leq 5.5$				$M_s > 5.5$			
M_s	I_E/I_A	$n(E)/n(A)$	PGA (cm/s ²)	M_s	I_E/I_A	$n(E)/n(A)$	PGA (cm/s ²)
4.0-4.5	2.03	22/139	≤126 (17)	5.5-6.0	1.04	16/54	≤152 (24)
4.5-5.0	2.55	38/158	≤403 (10)	6.0-6.5	0.92	27/106	≤177 (12)
5.0-5.5	0.79	13/107	≤323 (3)	6.5-7.0	1.12	27/67	≤414 (15)
				7.0-7.5	1.88	26/31	≤177 (28)

Table 3.15 gives the I_{soil}/I_A ratios for soil classes B, C, D and E and for the two different types of seismic actions of EC8. I_{soil}/I_A coefficients of Table 3.15 were calculated as the mean values of the coefficients from all the magnitude intervals belonging to each seismicity Type. For soil classes B, C and E there are sufficient data for both earthquake types, while for soil class D the available records are again very few. The amplification factors S, derived by equation (4), are given in Table 3.16, along with the corresponding soil factors proposed by EC8.

Table 3.15: SHARE-DS1: I_{soil}/I_A ratios for EC8 soil classes and both seismicity contexts

Soil Class	$M_s \leq 5.5$		$M_s > 5.5$	
	Selected M.I.	I_{soil}/I_A	Selected M.I.	I_{soil}/I_A
B	all	1.55	all	1.56
C	all	2.51	all	2.89
D	all	3.47	all	2.18
E	all	1.79	all	1.24

Table 3.16: SHARE-DS1: Soil factors for EC8 soil classes with Approach 2 compared to EC8

Soil Class	$M_s \leq 5.5$		$M_s > 5.5$	
	Approach 2	EC8	Approach 2	EC8
B	1.55	1.35	1.34	1.20
C	2.54	1.50	2.24	1.15
D	3.07	1.80	1.42	1.35
E	1.79	1.60	1.07	1.40

SHARE-DS1 Summary

EC8 soil factors S obtained with the two different approaches using SHARE-DS1 dataset are summarized in Tables 3.17 and 3.18 for Type 2 and Type 1 seismicity respectively.

Table 3.17: SHARE-DS1: Approaches 1, 2 and weighted average soil amplification factors for EC8 soil classes using common and different datasets, for $M_s \leq 5.5$.

Soil Class	$M_s \leq 5.5$					EC8
	Approach 1		Approach 2	Weighted Average		
	Common dataset	Different datasets		Common dataset	Different datasets	
B	0.90	0.95	1.55	1.23	1.25	1.35
C	1.93	1.90	2.54	2.23	2.22	1.50
D	-	3.36	3.07	-	3.22	1.80
E	-	0.98	1.79	-	1.39	1.60

Table 3.18: SHARE-DS1: Approaches 1, 2 and weighted average soil amplification factors for EC8 soil classes using common and different datasets, for $M_s > 5.5$.

Soil Class	$M_s > 5.5$					EC8
	Approach 1		Approach 2	Weighted Average		
	Common dataset	Different datasets		Common dataset	Different datasets	
B	1.47	1.37	1.34	1.41	1.36	1.20
C	2.09	1.99	2.24	2.16	2.12	1.15
D	-	1.74	1.42	-	1.58	1.35
E	-	0.91	1.07	-	0.99	1.40

3.2.2.2 SHARE-DS2 dataset

Approach 1

Table 3.19 presents the number of strong motion records for which the implementation of all GMPEs was feasible. Again, the common dataset can be used to estimate soil amplification factors only for soil classes B and C. For soil classes D and E, following the rationale presented in paragraph 3.2.2.1, Approach 1 was applied to the different datasets for SHARE-DS2 dataset. However, even in this case, the strong motion records for soil classes D and E are limited (Table 3.20).

Table 3.19: SHARE-DS2: Number of strong motion records for which reference spectral acceleration could be estimated with all GMPEs. (common dataset)

Soil Class	Type 2 ($4 \leq M_s \leq 5.5$)	Type 1 ($M_s > 5.5$)
B	51	699
C	50	869
D	-	-
E	-	4

Table 3.20: SHARE-DS2: Number of strong motion records for which each GMPE could be implemented. (different datasets)

Soil Class	A&B		C&F		Zh		C&Y	
	$M_s \leq 5.5$	$M_s > 5.5$						
B	114	755	205	1021	205	1021	52	778
C	100	908	228	1170	228	1170	50	925
D	3	1	3	1	3	1	-	-
E	8	4	21	32	21	32	-	6

Common dataset for all GMPEs

Figures 3.34 and 3.35 illustrate the amplification factors calculated with equation (1) for soil classes B and C respectively, using the weighted average $(GM_r)_{ij}$ derived from equation (3) as reference spectral acceleration. The median values of the amplification factors for each spectral period, along with the 16th and 84th percentiles are also depicted in Figures 3.34 and 3.35 and given in detail in Table 3.21. Figures 3.36 and 3.37 compare the estimated median amplification factors to the corresponding EC8 acceleration response spectra divided by the spectral values for soil class A.

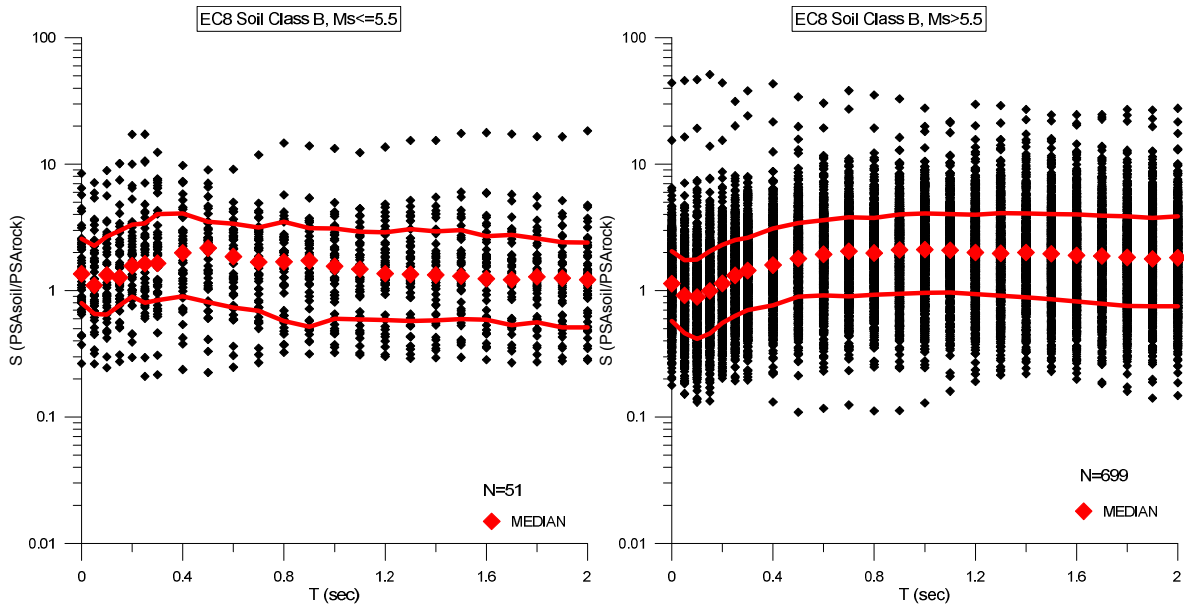


Figure 3.34: SHARE-DS2: Amplification factors estimated with Approach 1 for EC8 soil class B, for Type 2 seismicity (left) and Type 1 seismicity (right). The red lines represent the 16th and 84th percentiles. (common dataset)

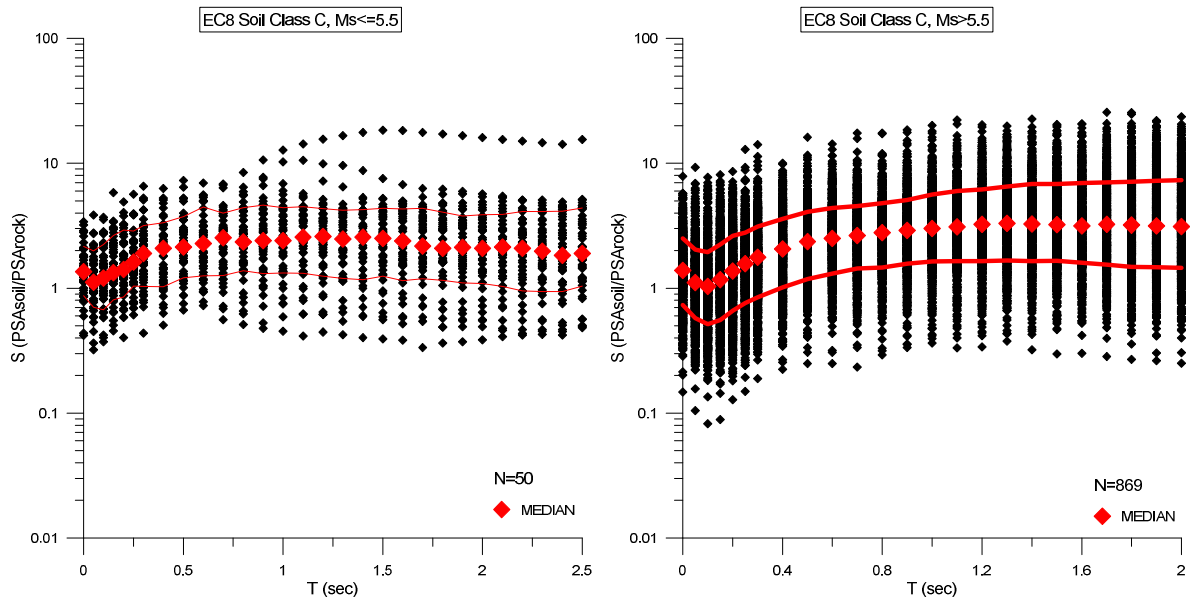


Figure 3.35: SHARE-DS2: Amplification factors estimated with Approach 1 for EC8 soil class C, for Type 2 seismicity (left) and Type 1 seismicity (right). The red lines represent the 16th and 84th percentiles. (common dataset)

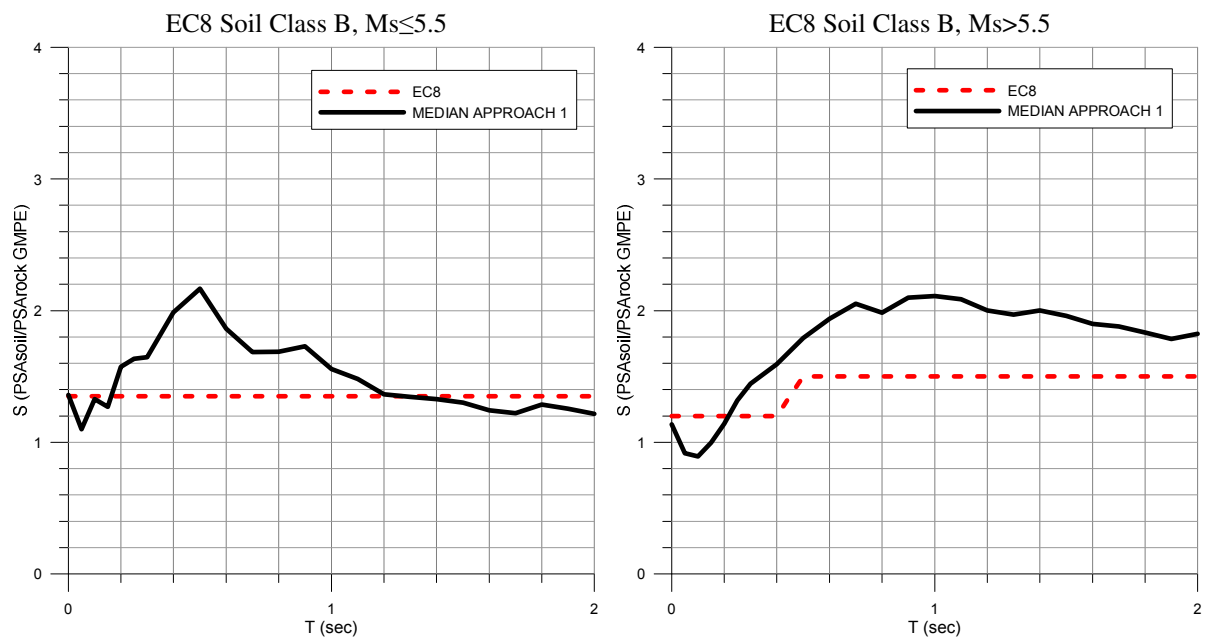


Figure 3.36: SHARE-DS2: Median amplification factors estimated with Approach 1 for EC8 soil class B, for Type 2 seismicity (left) and Type 1 seismicity (right). (common dataset)

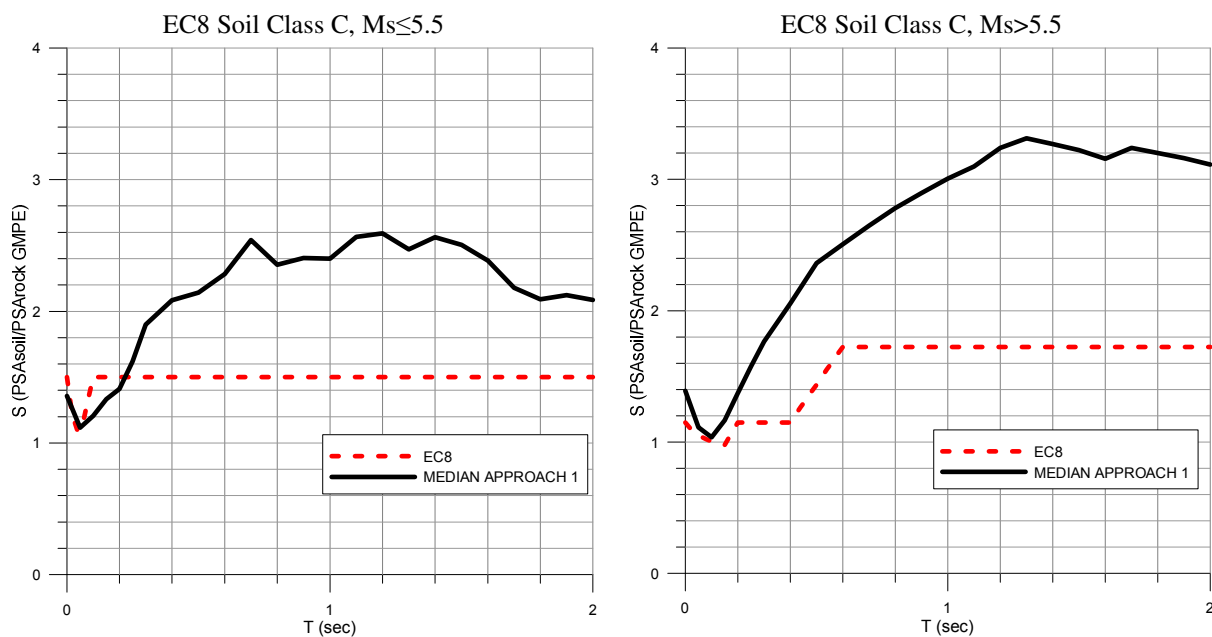


Figure 3.37: SHARE-DS2: Median amplification factors estimated with Approach 1 for EC8 soil class C, for Type 2 seismicity (left) and Type 1 seismicity (right). (common dataset)

Table 3.21: SHARE-DS2: Median amplification factors, 16th and 84th percentiles, estimated with Approach 1. (common dataset)

T	B-Type2			B-Type1			C-Type2			C-Type1		
	Median	16th	84th									
0	1.36	0.80	2.58	1.14	0.58	2.06	1.36	0.87	2.16	1.39	0.73	2.5
0.05	1.10	0.65	2.26	0.92	0.46	1.74	1.12	0.71	1.99	1.11	0.58	2.03
0.1	1.33	0.65	2.69	0.89	0.41	1.76	1.21	0.67	2.24	1.04	0.51	1.94
0.15	1.27	0.76	2.99	1.00	0.46	2.05	1.33	0.81	2.64	1.17	0.56	2.24
0.2	1.57	0.89	3.33	1.14	0.56	2.31	1.41	0.85	2.92	1.37	0.66	2.63
0.25	1.63	0.80	3.40	1.32	0.63	2.51	1.62	1.04	2.86	1.58	0.76	2.78
0.3	1.65	0.84	4.04	1.44	0.70	2.63	1.90	1.03	3.18	1.76	0.85	3.12
0.4	1.99	0.90	4.09	1.59	0.77	3.10	2.09	1.03	3.34	2.06	1.01	3.59
0.5	2.17	0.81	3.50	1.79	0.89	3.44	2.14	1.21	3.74	2.36	1.18	4.10
0.6	1.86	0.73	3.39	1.94	0.92	3.61	2.28	1.26	4.46	2.51	1.31	4.40
0.7	1.69	0.69	3.15	2.05	0.90	3.80	2.54	1.27	4.00	2.65	1.44	4.54
0.8	1.69	0.57	3.50	1.98	0.93	3.76	2.35	1.38	4.42	2.78	1.46	4.79
0.9	1.73	0.52	3.12	2.10	0.95	4.01	2.41	1.31	4.64	2.90	1.57	5.08
1	1.56	0.60	3.10	2.11	0.96	4.08	2.40	1.33	4.41	3.01	1.64	5.64
1.1	1.48	0.59	2.93	2.09	0.97	4.04	2.57	1.31	4.49	3.10	1.65	5.99
1.2	1.36	0.59	2.90	2.00	0.94	3.99	2.59	1.25	4.33	3.24	1.64	6.16
1.3	1.34	0.58	3.06	1.97	0.91	4.11	2.47	1.20	4.20	3.31	1.67	6.50
1.4	1.33	0.58	2.95	2.00	0.89	4.08	2.56	1.17	4.26	3.27	1.65	6.84
1.5	1.30	0.59	3.01	1.96	0.86	4.02	2.51	1.25	4.36	3.22	1.66	6.82
1.6	1.24	0.59	2.70	1.90	0.82	4.01	2.39	1.15	4.32	3.16	1.60	6.97
1.7	1.22	0.53	2.76	1.88	0.79	3.92	2.18	1.19	4.35	3.24	1.55	7.02
1.8	1.29	0.56	2.59	1.83	0.76	3.86	2.09	1.16	4.06	3.20	1.48	7.10
1.9	1.26	0.51	2.42	1.78	0.75	3.76	2.12	1.10	3.79	3.16	1.47	7.26
2	1.22	0.51	2.40	1.82	0.75	3.87	2.09	1.09	3.88	3.11	1.46	7.35

In order to estimate a single period-independent amplification factor for each soil class and each level of magnitude, similar to the S factor proposed in EC8, the median amplification factors were averaged over a range of periods from $T=0$ to $T=2$ s. The resulting amplification factors, divided by the spectral shape ratio SR are presented in Table 3.22, so that they can be compared to the corresponding EC8 S factors, which are also included in the table.

Table 3.22: SHARE-DS2: Soil factors with Approach 1 compared to EC8. (common dataset)

Soil Class	$M_s \leq 5.5$		$M_s > 5.5$	
	Approach 1	EC8	Approach 1	EC8
B	1.51	1.35	1.53	1.20
C	2.19	1.50	2.06	1.15

Different dataset for each GMPE

Figures 3.38 to 3.41 summarize the medians of the amplification factors estimated from the strong motion records of Table 3.20, using the four GMPEs separately, as well as the weighted average amplification factors calculated with equation (6). For the case where the Chiou and Youngs (2006) GMPE could not be implemented, the weight of this GMPE (equal to 0.20) was equally distributed to the remaining three GMPEs, whose weights were as a result increased by the value of $0.20/3$.

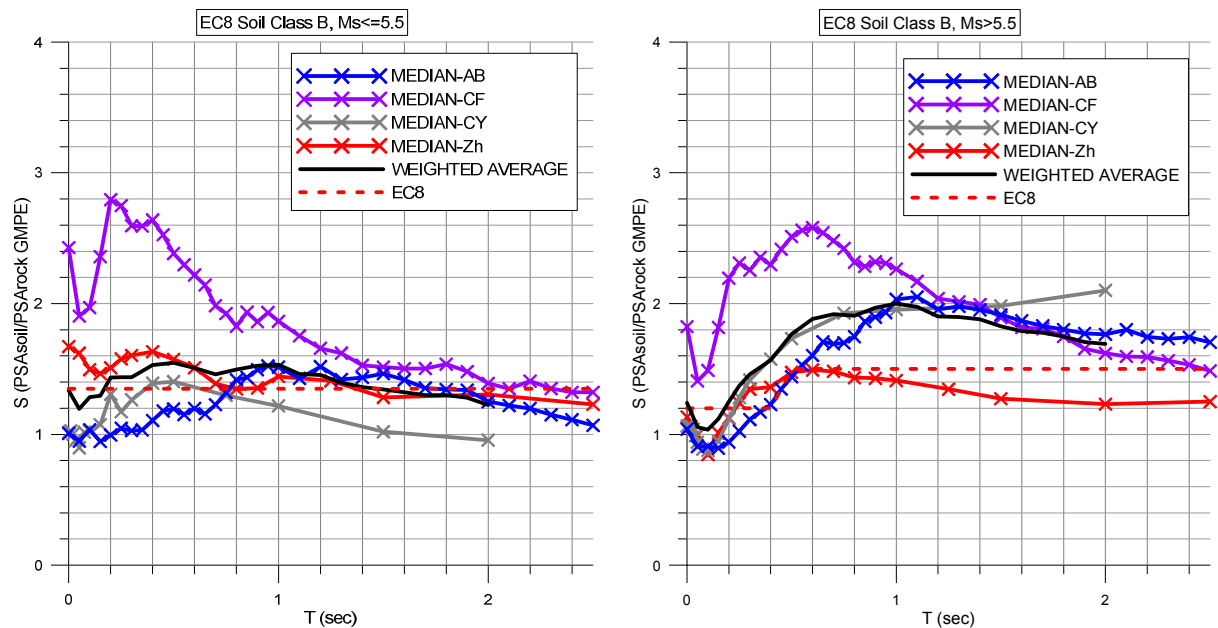


Figure 3.38: SHARE-DS2: Median amplification factors with Approach 1 for soil class B and PSA_{rock} estimated with all GMPEs, for Type 2 seismicity (left) and Type 1 seismicity (right). (different datasets)

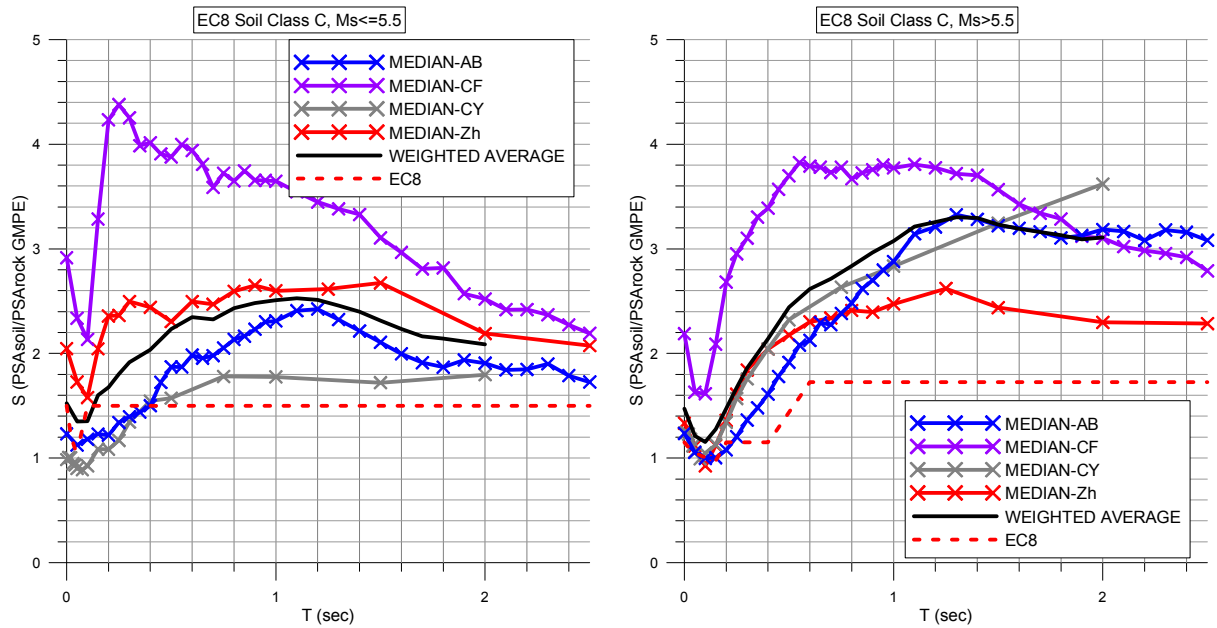


Figure 3.39: SHARE-DS2: Median amplification factors with Approach 1 for soil class C and PSA_{rock} estimated with all GMPEs, for Type 2 seismicity (left) and Type 1 seismicity (right). (different datasets)

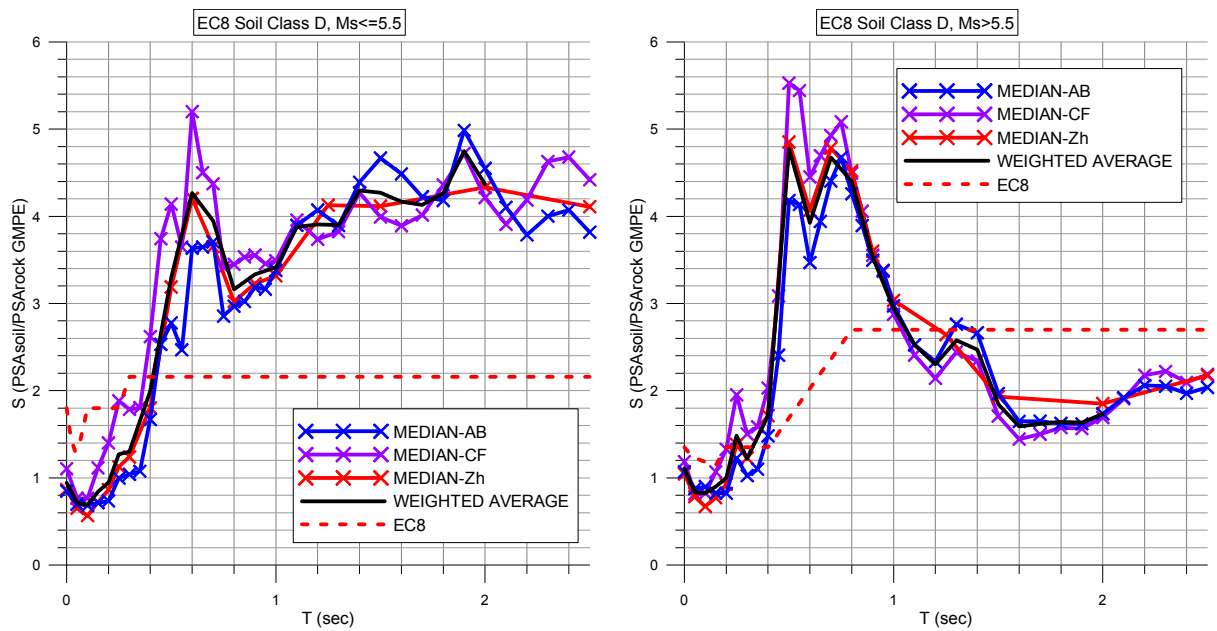


Figure 3.40: SHARE-DS2: Median amplification factors with Approach 1 for soil class D and PSA_{rock} estimated with all GMPEs, for Type 2 seismicity (left) and Type 1 seismicity (right). (different datasets)

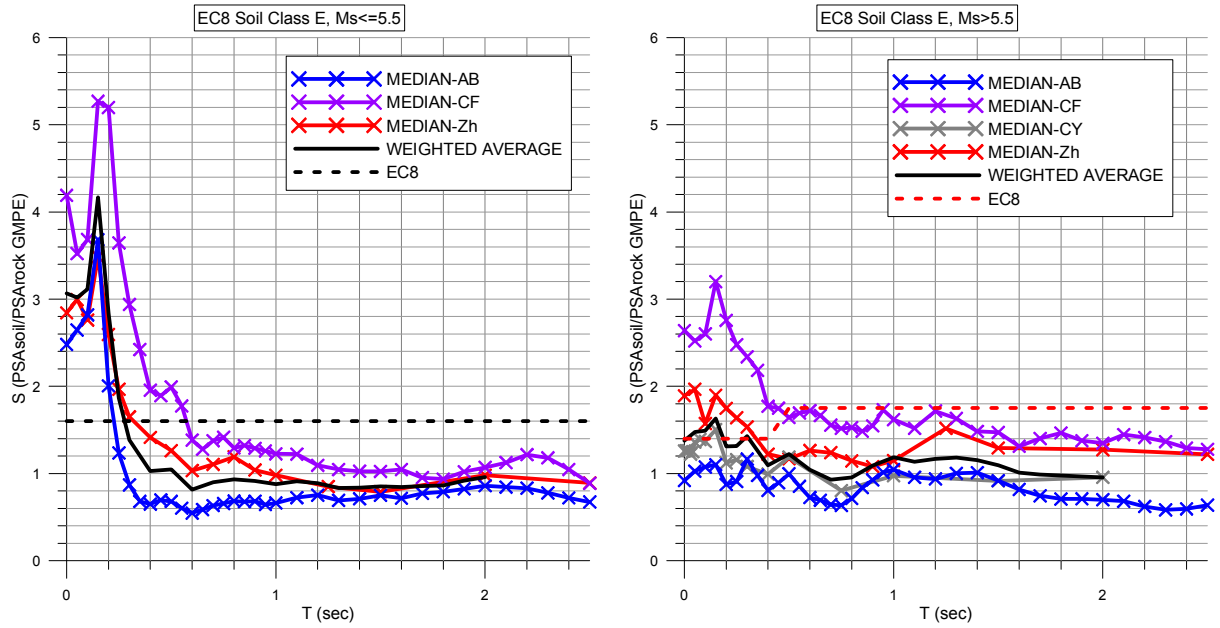


Figure 3.41: SHARE-DS2: Median amplification factors with Approach 1 for soil class E and PSA_{rock} estimated with all GMPEs, for Type 2 seismicity (left) and Type 1 seismicity (right). (different datasets)

The period-dependent amplification factors calculated from Equation (6) are given in detail in Table 3.23. In order to estimate a single period-independent amplification factor for each soil class and each level of magnitude, similar to the S factor proposed in EC8, the weighted average amplification spectra were averaged over a range of periods from $T=0$ to $T=2s$. The resulting amplification factors, divided by the spectral shape ratio SR are presented in Table 3.24.

Table 3.23: SHARE-DS2: Amplification factors for EC8 soil classes, estimated with Approach 1. (different datasets)

T	B - Type 2	B - Type 1	C - Type 2	C - Type 1	D - Type 2	D - Type 1	E - Type 2	E - Type 1
0	1.34	1.24	1.52	1.47	0.94	1.11	3.15	1.38
0.05	1.19	1.06	1.35	1.21	0.72	0.83	3.10	1.48
0.1	1.29	1.03	1.35	1.15	0.69	0.82	3.19	1.49
0.15	1.29	1.12	1.60	1.28	0.84	0.90	4.50	1.63
0.2	1.44	1.25	1.68	1.47	0.95	1.00	2.96	1.31
0.25	1.44	1.37	1.80	1.67	1.27	1.48	2.04	1.31
0.3	1.44	1.46	1.92	1.86	1.30	1.22	1.57	1.43
0.4	1.53	1.57	2.04	2.14	2.00	1.71	1.15	1.09
0.5	1.55	1.77	2.23	2.44	3.30	4.78	1.08	1.22
0.6	1.51	1.88	2.35	2.62	4.27	3.93	0.86	1.04
0.7	1.46	1.92	2.33	2.72	3.95	4.67	0.98	0.93
0.8	1.50	1.91	2.43	2.84	3.16	4.40	0.96	0.96
0.9	1.52	1.97	2.48	2.97	3.34	3.54	0.94	1.09
1	1.53	2.00	2.51	3.07	3.41	2.94	0.94	1.18
1.1	1.46	1.98	2.53	3.21	3.88	2.53	1.02	1.13

1.2	1.45	1.90	2.51	3.26	3.91	2.30	0.97	1.17
1.3	1.40	1.90	2.46	3.30	3.90	2.58	0.91	1.18
1.4	1.36	1.88	2.40	3.29	4.29	2.47	0.92	1.15
1.5	1.34	1.83	2.31	3.23	4.27	1.84	0.94	1.09
1.6	1.32	1.79	2.24	3.19	4.17	1.59	0.95	1.01
1.7	1.30	1.78	2.16	3.16	4.13	1.62	0.92	0.99
1.8	1.30	1.75	2.14	3.13	4.27	1.64	0.93	0.98
1.9	1.28	1.71	2.11	3.09	4.75	1.63	0.96	0.96
2	1.22	1.69	2.09	3.11	4.37	1.73	0.99	0.95

Table 3.24: SHARE-DS2: Soil factors for EC8 soil classes with Approach 1 compared to EC8. (different datasets)

Soil Class	$M_s \leq 5.5$		$M_s > 5.5$	
	Approach 1	EC8	Approach 1	EC8
B	1.41	1.35	1.48	1.20
C	2.20	1.50	2.09	1.15
D	2.92	1.80	1.56	1.35
E	1.30	1.60	0.97	1.40

Comparing the soil factors obtained for soil classes B and C with Approach 1 using on the one hand the common dataset and on the other hand the different datasets, we observe that the differences are rather insignificant (Table 3.25). This justifies the decision to apply the logic tree weights to the median amplification factors in order to have an estimate for the soil factors for soil classes D and E.

Table 3.25: SHARE-DS2: Soil factors for EC8 soil classes B and C with Approach 1 obtained from common dataset compared to those obtained from the different datasets.

Soil Class	$M_s \leq 5.5$		$M_s > 5.5$	
	Approach 1 (common dataset)	Approach 1 (different datasets)	Approach 1 (common dataset)	Approach 1 (different datasets)
B	1.51	1.41	1.53	1.48
C	2.19	2.20	2.06	2.09

Approach 2

Figures 3.42 to 3.49 illustrate the log average of distance-normalized response spectra for EC8 soil classes B, C, D and E with respect to soil class A, for the different magnitude intervals.

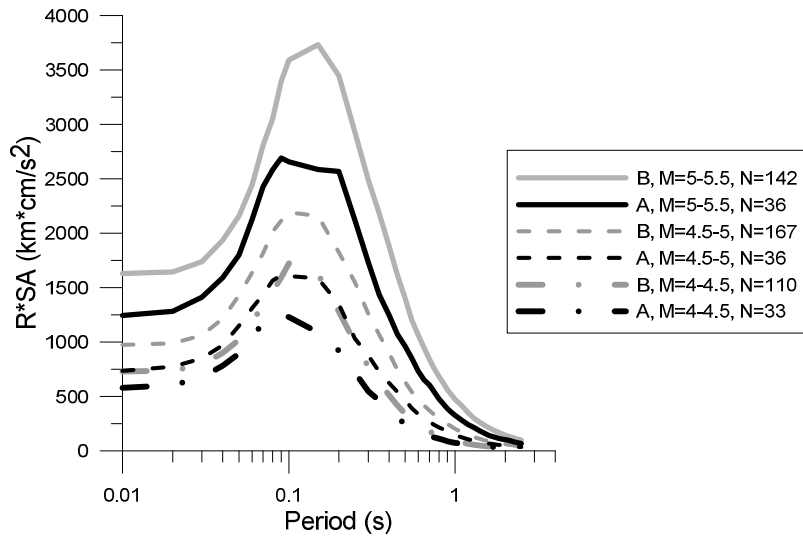


Figure 3.42: SHARE-DS2: Log-average, distance-normalized acceleration response spectra for Type 2 magnitude intervals, for sites of soil class B (grey lines) and rock sites (black lines).

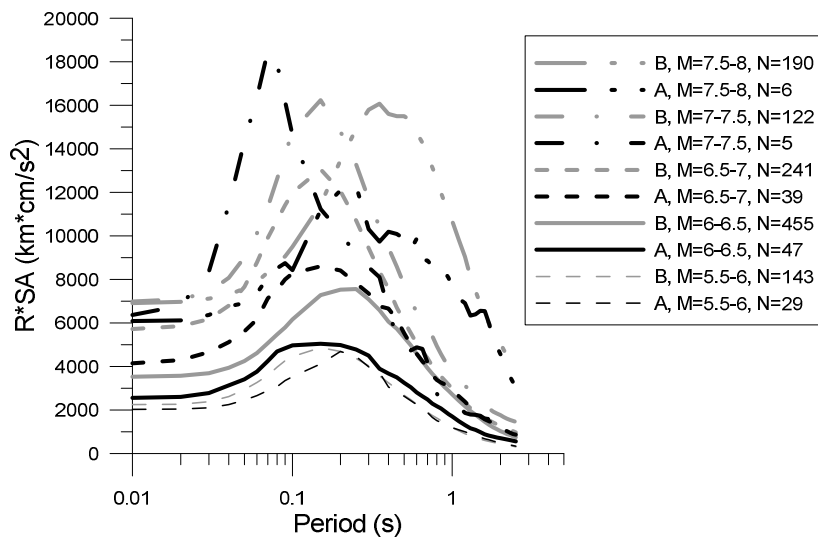


Figure 3.43: SHARE-DS2: Log-average, distance-normalized acceleration response spectra for Type 1 magnitude intervals for sites of soil class B (grey lines) and rock sites (black lines).

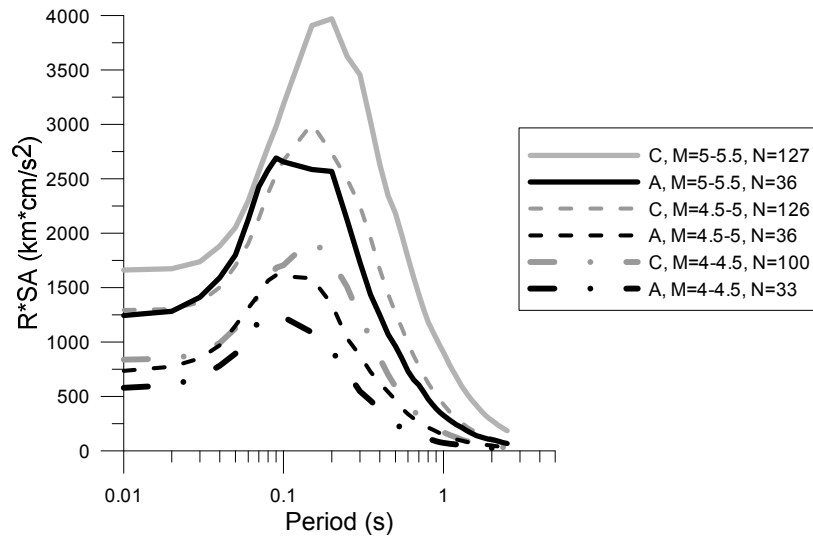


Figure 3.44: SHARE-DS2: Log-average, distance-normalized acceleration response spectra for Type 2 magnitude intervals for sites of soil class C (grey lines) and rock sites (black lines).

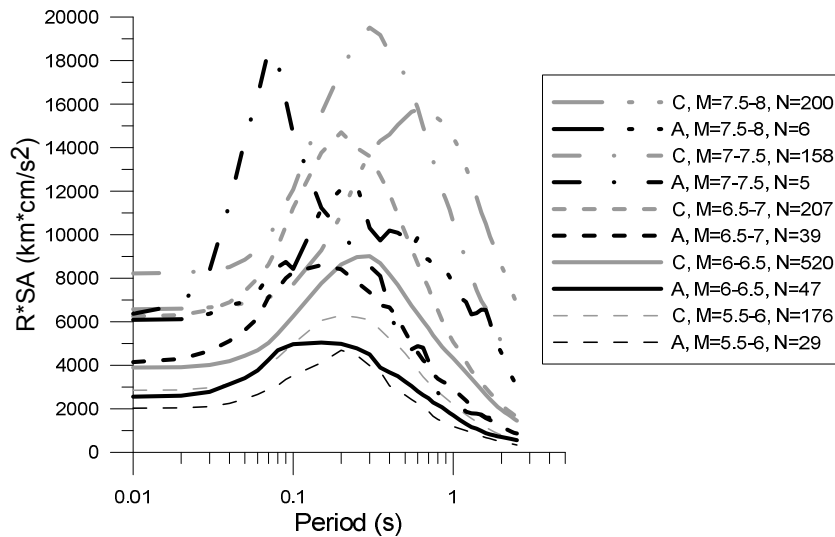


Figure 3.45: SHARE-DS2: Log-average, distance-normalized acceleration response spectra for Type 1 magnitude intervals for sites of soil class C (grey lines) and rock sites (black lines).

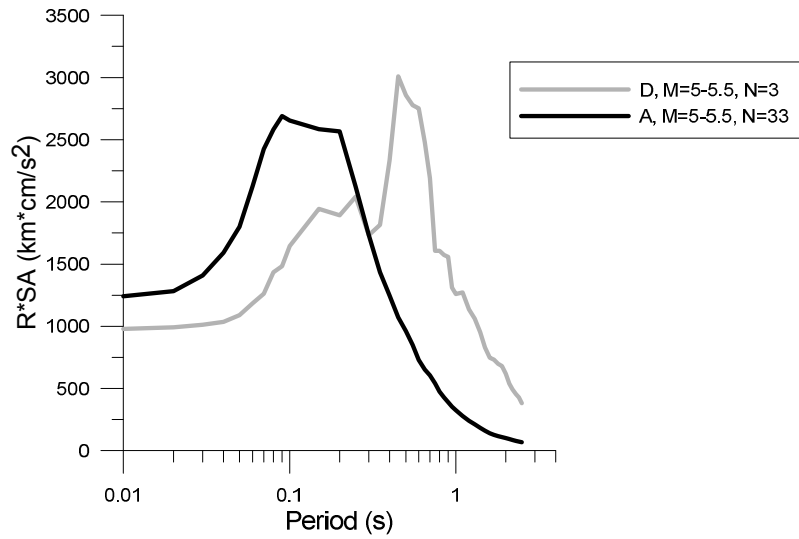


Figure 3.46: SHARE-DS2: Log-average, distance-normalized acceleration response spectra for Type 2 magnitude intervals for sites of soil class D (grey lines) and rock sites (black lines).

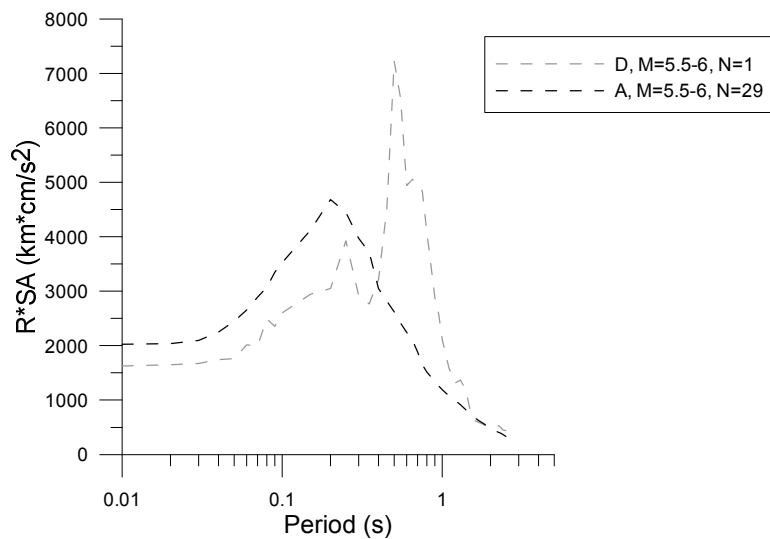


Figure 3.47: SHARE-DS2: Log-average, distance-normalized acceleration response spectra for Type 1 magnitude intervals for sites of soil class D (grey lines) and rock sites (black lines).

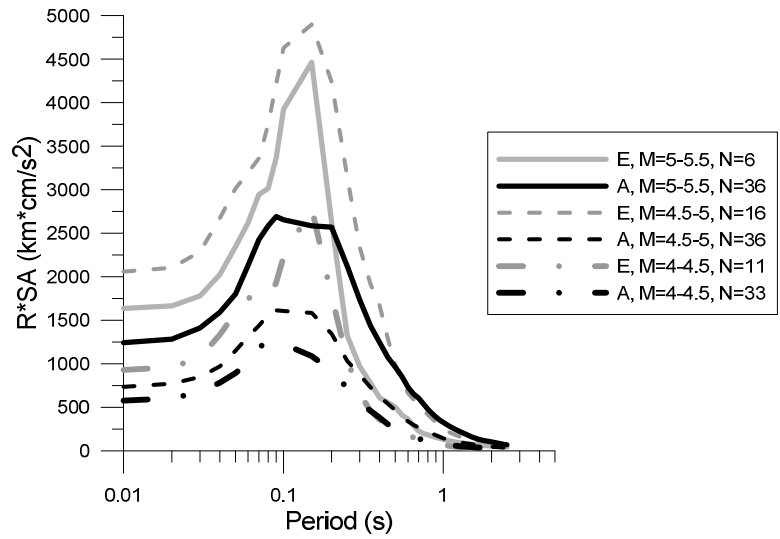


Figure 3.48: SHARE-DS2: Log-average, distance-normalized acceleration response spectra for Type 2 magnitude intervals for sites of soil class E (grey lines) and rock sites (black lines).

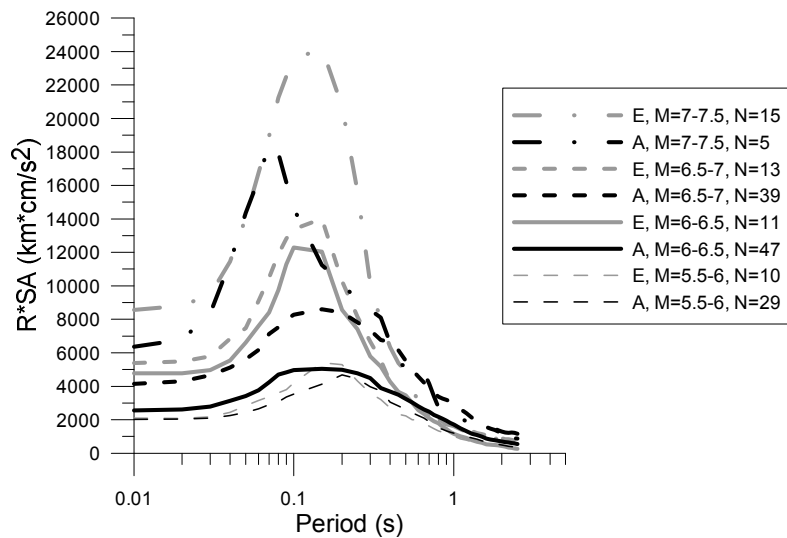


Figure 3.49: SHARE-DS2: Log-average, distance-normalized acceleration response spectra for Type 1 magnitude intervals for sites of soil class E (grey lines) and rock sites (black lines).

I_{soil}/I_A ratios for all magnitude intervals and for soil classes B, C, D and E are presented in Tables 3.26, 3.27, 3.28 and 3.29 respectively. The tables also contain the number of available strong motion records for each case. For certain magnitude intervals the number of available records is not sufficient; consequently for these magnitude intervals the corresponding I_{soil}/I_A ratios cannot be considered very reliable. For example, for soil A there are only five records for $M=7-7.5$ and six records for $M=7.5-8$. The magnitude intervals with a satisfactory number of available strong motion records are depicted in bold. Soil class D data are always very poor. PGA range for each soil class and magnitude interval is also provided, with the number in the parenthesis representing the median PGA value for each case.

Table 3.26: SHARE-DS2: I_{soil}/I_A ratios for EC8 soil class B and all magnitude intervals.

$M_s \leq 5.5$				$M_s > 5.5$			
M_s	I_B/I_A	$n(B)/n(A)$	PGA (cm/s ²)	M_s	I_B/I_A	$n(B)/n(A)$	PGA (cm/s ²)
4.0-4.5	1.32	110/33	≤ 269 (39)	5.5-6.0	1.01	143/29	≤ 936 (43)
4.5-5.0	1.38	167/36	≤ 521 (44)	6.0-6.5	1.56	455/47	≤ 953 (51)
5.0-5.5	1.41	142/36	≤ 1091 (48)	6.5-7.0	1.17	241/39	≤ 1207 (88)
				7.0-7.5	1.36	122/5	≤ 1224 (41)
				7.5-8.0	1.30	190/6	≤ 916 (80)

Table 3.27: SHARE-DS2: I_{soil}/I_A ratios for EC8 soil class C and all magnitude intervals.

$M_s \leq 5.5$				$M_s > 5.5$			
M_s	I_C/I_A	$n(C)/n(A)$	PGA (cm/s ²)	M_s	I_C/I_A	$n(C)/n(A)$	PGA (cm/s ²)
4.0-4.5	1.93	100/33	≤ 447 (41)	5.5-6.0	1.62	176/29	≤ 630 (55)
4.5-5.0	2.35	126/36	≤ 347 (55)	6.0-6.5	2.26	520/47	≤ 560 (50)
5.0-5.5	2.02	127/36	≤ 415 (47)	6.5-7.0	1.78	207/39	≤ 1302 (128)
				7.0-7.5	2.85	158/5	≤ 775 (52)
				7.5-8.0	1.65	200/6	≤ 687 (70)

Table 3.28: SHARE-DS2: I_{soil}/I_A ratios for EC8 soil class D and all magnitude intervals.

$M_s \leq 5.5$				$M_s > 5.5$			
M_s	I_D/I_A	$n(D)/n(A)$	PGA (cm/s ²)	M_s	I_D/I_A	$n(D)/n(A)$	PGA (cm/s ²)
5.0-5.5	2.26	3/36	≤ 44 (42)	5.5-6.0	1.41	1/29	≤ 74 (74)

Table 3.29: SHARE-DS2: I_{soil}/I_A ratios for EC8 soil class E and all magnitude intervals.

$M_s \leq 5.5$				$M_s > 5.5$			
M_s	I_E/I_A	$n(E)/n(A)$	PGA (cm/s ²)	M_s	I_E/I_A	$n(E)/n(A)$	PGA (cm/s ²)
4.0-4.5	1.44	11/33	≤ 126 (42)	5.5-6.0	0.92	10/29	≤ 152 (47)
4.5-5.0	2.48	16/36	≤ 403 (40)	6.0-6.5	1.13	11/47	≤ 177 (64)
5.0-5.5	0.78	6/36	≤ 323 (80)	6.5-7.0	0.83	13/39	≤ 414 (77)
				7.0-7.5	1.06	15/5	≤ 177 (46)

Table 3.30 gives the I_{soil}/I_A ratios for soil classes B, C, D and E and the two seismicity contexts of EC8. I_{soil}/I_A coefficients of Table 3.30 were calculated as the mean values of the coefficients from those magnitude intervals considered as more reliable (in bold). The amplification factors S, derived by equation (4), are given in Table 3.31, along with the corresponding soil factors proposed by EC8.

Table 3.30: SHARE-DS2: I_{soil}/I_A ratios for EC8 soil classes and both seismicity contexts

Soil Class	$M_s \leq 5.5$		$M_s > 5.5$	
	Selected M.I.	I_{soil}/I_A	Selected M.I.	I_{soil}/I_A
B	4.0-4.5, 4.5-5.0, 5.0-5.5	1.37	5.5-6.0, 6.0-6.5, 6.5-7.0	1.25
C	4.0-4.5, 4.5-5.0, 5.0-5.5	2.10	5.5-6.0, 6.0-6.5, 6.5-7.0	1.88
D	5.0-5.5	2.26	5.5-6.0	1.41
E	4.0-4.5, 4.5-5.0	1.96	5.5-6.0, 6.0-6.5, 6.5-7.0	0.96

Table 3.31: SHARE-DS2: Soil factors with Approach 2 compared to EC8

Soil Class	$M_s \leq 5.5$		$M_s > 5.5$	
	Approach 2	EC8	Approach 2	EC8
B	1.37	1.35	1.08	1.20
C	2.12	1.50	1.46	1.15
D	2.00	1.80	0.92	1.35
E	1.96	1.60	0.83	1.40

SHARE-DS2 Summary

EC8 soil factors S obtained with the two different approaches using SHARE-DS2 dataset are summarized in Tables 3.32 and 3.33.

Table 3.32: SHARE-DS2: Approaches 1, 2 and weighted average soil amplification factors for EC8 soil classes using common and different datasets, for $M_s \leq 5.5$

Soil Class	$M_s \leq 5.5$					
	Approach 1		Approach 2	Weighted Average		EC8
	Common dataset	Different datasets		Common dataset	Different datasets	
B	1.51	1.41	1.37	1.44	1.39	1.35
C	2.19	2.20	2.12	2.16	2.16	1.50
D		2.92	2.00	-	2.46	1.80
E		1.30	1.96	-	1.63	1.60

Table 3.33: SHARE-DS2: Approaches 1, 2 and weighted average soil amplification factors for EC8 soil classes using common and different datasets, for $M_s > 5.5$.

Soil Class	$M_s > 5.5$					
	Approach 1		Approach 2	Weighted Average		EC8
	Common dataset	Different datasets		Common dataset	Different datasets	
B	1.53	1.48	1.08	1.31	1.28	1.20
C	2.06	2.09	1.46	1.76	1.78	1.15
D	-	1.56	0.92	-	1.24	1.35
E	-	0.97	0.83	-	0.90	1.40

3.2.2.3 SHARE-DS3 dataset

Approach 1

SHARE-DS3 dataset was used to estimate soil factors only for Type 1 seismicity. Table 3.34 presents the number of strong motion records for which the implementation of all GMPEs was feasible. Again, the common dataset can be used to estimate soil amplification factors only for soil classes B and C; for soil classes D and E, we used different datasets according to the procedure applied previously. However, even in this case, there were no available data for soil class D and only few data for soil class E (Table 3.35).

Table 3.34: SHARE-DS3: Number of strong motion records for which reference spectral acceleration could be estimated with all GMPEs. (common dataset)

Soil Class	Type 2 ($4 \leq M_s \leq 5.5$)	Type 1 ($M_s > 5.5$)
B	6	120
C	6	142
D	-	-
E	-	1

Table 3.35: SHARE-DS3: Number of strong motion records for which each GMPE could be implemented. (different datasets)

Soil Class	A&B		C&F		Zh		C&Y	
	$M_s \leq 5.5$	$M_s > 5.5$						
B	14	145	24	201	24	201	6	152
C	14	145	36	215	36	215	6	169
D	-	-	-	-	-	-	-	-
E	4	1	5	5	5	5	-	2

Common dataset for all GMPEs

Figures 3.50 and 3.51 illustrate the amplification factors calculated by equation (1) for soil classes B and C respectively, using the weighted average $(GM_r)_{ij}$ derived from equation (3) as reference spectral acceleration. The median values of the amplification factors for each spectral period, along with the 16th and 84th percentiles are also depicted in Figures 3.50 and 3.51 and given in detail in Table 3.36. Figures 3.52 and 3.53 compare the estimated median amplification factors to the corresponding EC8 acceleration response spectra divided by the spectral values for soil class A.

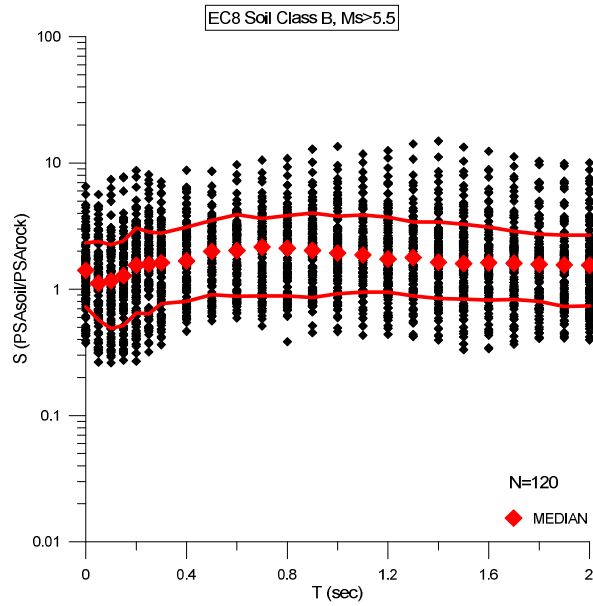


Figure 3.50: SHARE-DS3: Amplification factors estimated with Approach 1 for EC8 soil class B, for Type 1 seismicity. The red lines represent the 16th and 84th percentiles. (common dataset)

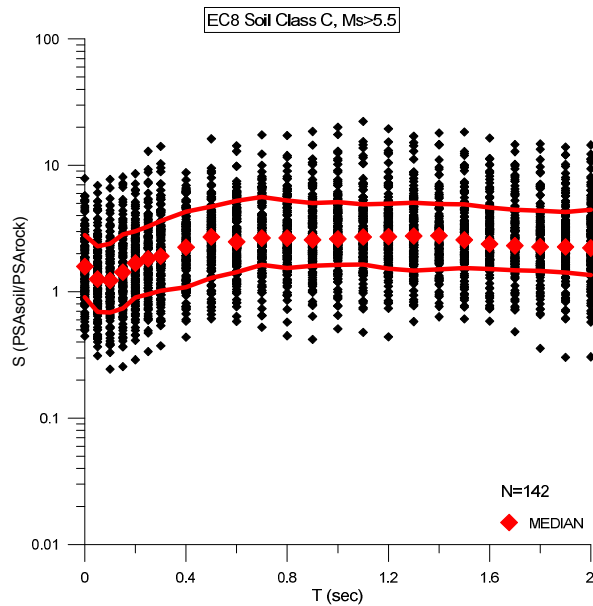


Figure 3.51: SHARE-DS3: Amplification factors estimated with Approach 1 for EC8 soil class C, for Type 1 seismicity. The red lines represent the 16th and 84th percentiles. (common dataset)

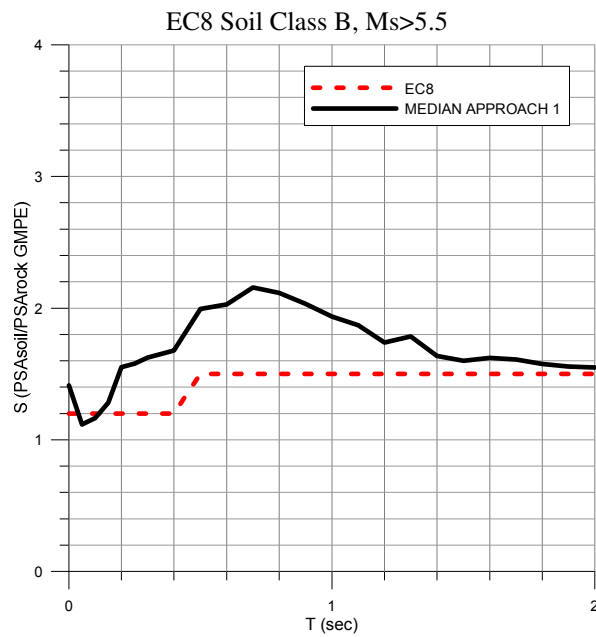


Figure 3.52: SHARE-DS3: Median amplification factors estimated with Approach 1 for EC8 soil class B, for Type 1 seismicity. (common dataset)

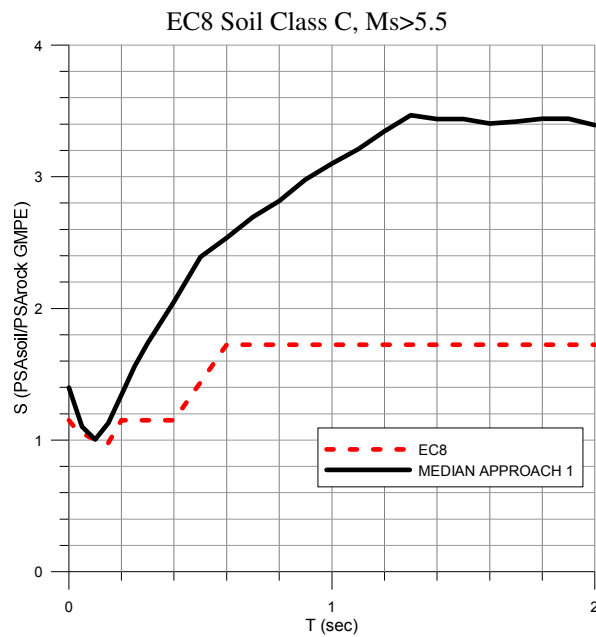


Figure 3.53: SHARE-DS3: Median amplification factors estimated with Approach 1 for EC8 soil class C, for Type 1 seismicity. (common dataset)

Table 3.36: SHARE-DS3: Median amplification factors, 16th and 84th percentiles, estimated with Approach 1. (common dataset)

T	B-Type1			C-Type1		
	Median	16th	84th	Median	16th	84th
0	1.41	0.73	2.33	1.59	0.91	2.81
0.05	1.12	0.57	2.40	1.26	0.69	2.29
0.1	1.16	0.49	2.25	1.23	0.69	2.40
0.15	1.28	0.52	2.41	1.43	0.74	2.84
0.2	1.55	0.65	3.05	1.69	0.90	3.01
0.25	1.58	0.64	2.84	1.83	0.96	3.29
0.3	1.62	0.77	2.77	1.91	1.02	3.63
0.4	1.68	0.80	3.11	2.25	1.09	4.30
0.5	1.99	0.91	3.50	2.72	1.29	4.71
0.6	2.03	0.88	3.89	2.48	1.42	5.24
0.7	2.16	0.88	3.63	2.66	1.64	5.62
0.8	2.12	0.89	3.83	2.66	1.54	5.28
0.9	2.03	0.86	4.01	2.57	1.61	5.04
1	1.93	0.92	3.78	2.61	1.64	5.12
1.1	1.87	0.95	3.87	2.71	1.64	4.92
1.2	1.74	0.95	3.73	2.73	1.52	4.98
1.3	1.78	0.88	3.41	2.76	1.47	5.08
1.4	1.64	0.84	3.41	2.77	1.50	4.96
1.5	1.60	0.84	3.27	2.57	1.54	4.92
1.6	1.62	0.82	3.11	2.39	1.52	4.65
1.7	1.61	0.83	2.88	2.31	1.48	4.46
1.8	1.58	0.80	2.72	2.27	1.46	4.37
1.9	1.56	0.73	2.68	2.27	1.42	4.29
2	1.55	0.74	2.68	2.22	1.36	4.47

In order to estimate a single period-independent amplification factor for each soil class and each level of magnitude, similar to the S factor proposed in EC8, the median amplification factors were averaged over a range of periods from T=0 to T=2s. The resulting amplification factors, divided by the spectral shape ratio SR are presented in Table 3.37, so that they can be compared to the corresponding EC8 S factors, which are also included in the table.

Table 3.37: SHARE-DS3: Soil factors with Approach 1 compared to EC8. (common dataset)

Soil Class	$M_s > 5.5$	
	Approach 1	EC8
B	1.49	1.20
C	1.82	1.15

Different dataset for each GMPE

Figures 3.54 to 3.56 summarize the medians of the amplification factors estimated from the strong motion records of Table 3.35 for Type 1 seismicity, using the four GMPEs separately, as well as the weighted average amplification factors calculated with equation (6).

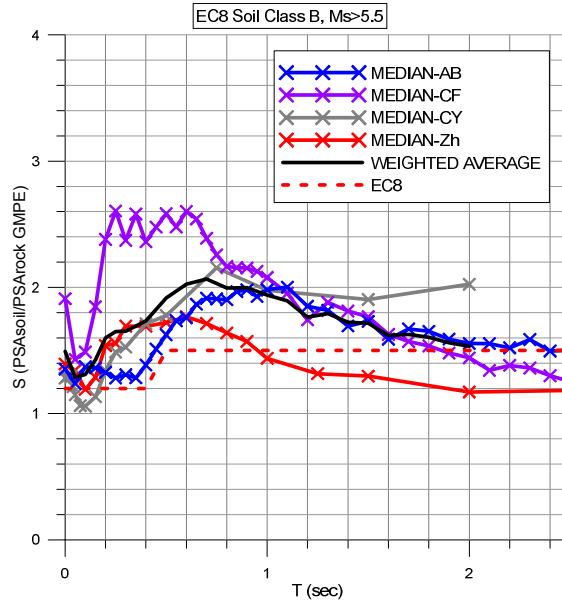


Figure 3.54: SHARE-DS3: Median amplification factors with Approach 1 for soil class B and PSA_{rock} estimated with all GMPEs, for Type 1 seismicity. (different datasets)

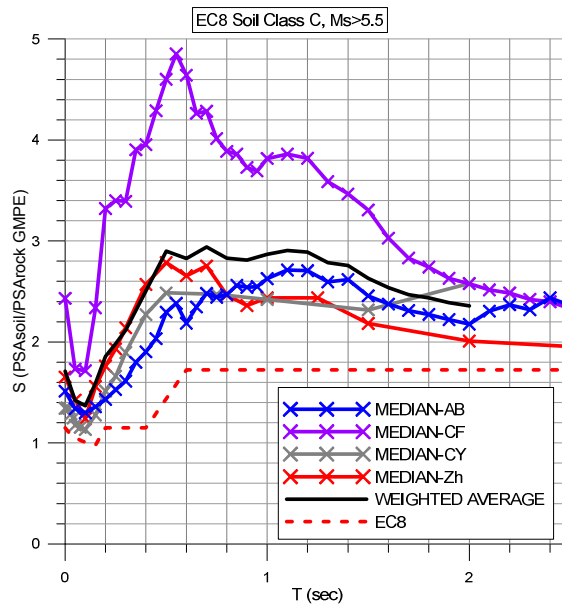


Figure 3.55: SHARE-DS3: Median amplification factors with Approach 1 for soil class C and PSA_{rock} estimated with all GMPEs, for Type 1 seismicity. (different datasets)

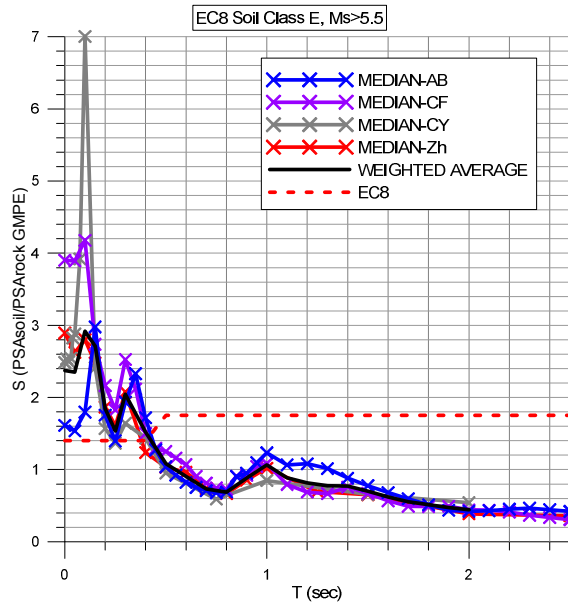


Figure 3.56: SHARE-DS3: Median amplification factors with Approach 1 for soil class E and PSA_{rock} estimated with all GMPEs, for Type 1 seismicity. (different datasets)

The period-dependent amplification factors calculated from Equation (6) are given in detail in Table 3.38. In order to estimate a single period-independent amplification factor for each soil class and each level of magnitude, similar to the S factor proposed in EC8, the weighted average amplification spectra were averaged over a range of periods from $T=0$ to $T=2s$. The resulting amplification factors, divided by the spectral shape ratio SR are presented in Table 3.39.

Table 3.38: SHARE-DS3: Amplification factors for EC8-Type 1 soil classes, estimated with Approach 1. (different datasets)

T	B -Type 1	C -Type 1	E -Type 1
0	1.49	1.71	2.37
0.05	1.29	1.42	2.35
0.1	1.31	1.37	2.92
0.15	1.43	1.59	2.71
0.2	1.60	1.86	1.84
0.25	1.65	1.98	1.54
0.3	1.65	2.12	2.04
0.4	1.73	2.50	1.52
0.5	1.92	2.90	1.08
0.6	2.03	2.83	0.91
0.7	2.07	2.94	0.73
0.8	2.00	2.83	0.69
0.9	2.00	2.81	0.88
1	1.94	2.87	1.06
1.1	1.89	2.91	0.89
1.2	1.76	2.89	0.82
1.3	1.79	2.78	0.78
1.4	1.72	2.76	0.77

1.5	1.72	2.63	0.70
1.6	1.62	2.54	0.62
1.7	1.63	2.47	0.55
1.8	1.61	2.44	0.51
1.9	1.56	2.39	0.48
2	1.53	2.36	0.44

Table 3.39: SHARE-DS3: Soil factors for EC8 soil classes with Approach 1 compared to EC8. (different datasets)

Soil Class	$M_s > 5.5$	
	Approach 1	EC8
B	1.50	1.20
C	1.95	1.15
D	-	1.35
E	0.93	1.40

Comparing the soil factors for soil classes B and C obtained with Approach 1 using on the one hand the common dataset and on the other hand the different datasets, we observe that the differences are rather small (soil class C) or even insignificant (soil class B) (Table 3.40).

For both soil classes the period independent amplification factors are larger than the corresponding EC8 factors.

Table 3.40: SHARE-DS3: Soil factors for EC8 soil classes B and C with Approach 1 obtained from common dataset compared to those obtained from the different datasets.

Soil Class	$M_s > 5.5$	
	Approach 1 (common dataset)	Approach 1 (different datasets)
B	1.49	1.50
C	1.82	1.95

Approach 2

Figures 3.57 to 3.59 illustrate the log average of distance-normalized response spectra for EC8 soil classes B, C and E with respect to soil class A, for the different magnitude intervals of Type 1 seismicity. Due to lack of sufficient data, Approach 2 could not be applied to soil class D.

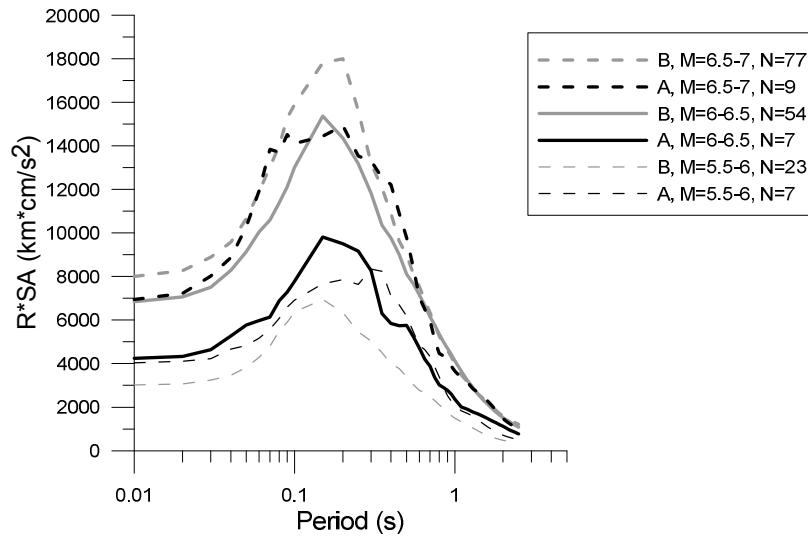


Figure 3.57: SHARE-DS3: Log-average, distance-normalized acceleration response spectra for Type 1 magnitude intervals for sites of soil class B (grey lines) and rock sites (black lines).

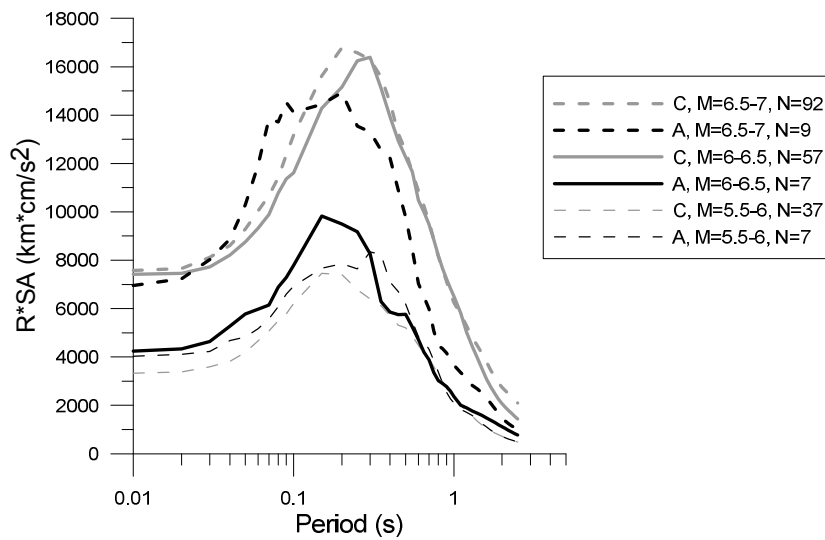


Figure 3.58: SHARE-DS3: Log-average, distance-normalized acceleration response spectra for Type 1 magnitude intervals for sites of soil class C (grey lines) and rock sites (black lines).

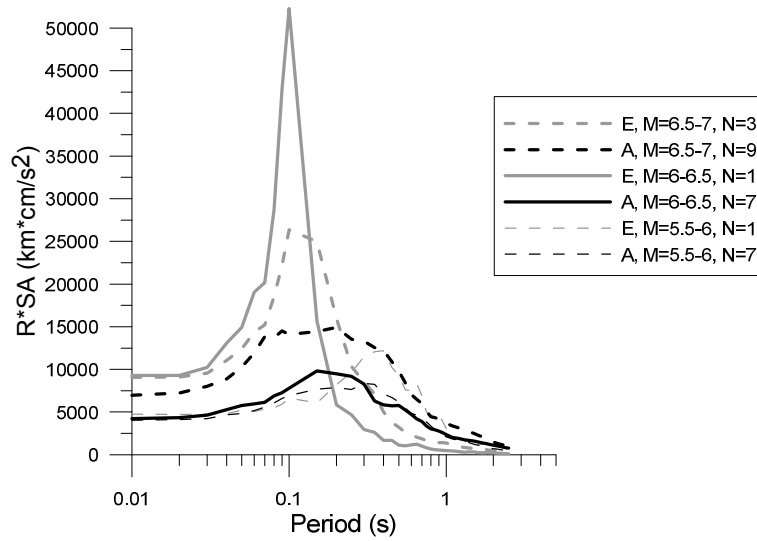


Figure 3.59: SHARE-DS3: Log-average, distance-normalized acceleration response spectra for Type 1 magnitude intervals for sites of soil class E (grey lines) and rock sites (black lines).

I_{soil}/I_A ratios for all Type 1 magnitude intervals and for soil classes B, C and E are presented in Tables 3.41 to 3.43. PGA range for each soil class and magnitude interval is also provided, with the number in the parenthesis representing the median PGA value for each case.

Table 3.41: SHARE-DS3: I_{soil}/I_A ratios for EC8 soil class B-Type 1 and all magnitude intervals.

$M_s > 5.5$			
M_s	I_B/I_A	$n(B)/n(A)$	PGA (cm/s^2)
5.5-6.0	0.67	23/7	≤ 936 (229)
6.0-6.5	1.56	54/7	≤ 953 (264)
6.5-7.0	1.05	77/9	≤ 1207 (286)

Table 3.42: SHARE-DS3: I_{soil}/I_A ratios for EC8 soil class C-Type 1 and all magnitude intervals.

$M_s > 5.5$			
M_s	I_C/I_A	$n(C)/n(A)$	PGA (cm/s^2)
5.5-6.0	0.91	37/7	≤ 630 (238)
6.0-6.5	2.11	57/7	≤ 560 (201)
6.5-7.0	1.41	92/9	≤ 1302 (277)

Table 3.43: SHARE-DS3: I_{soil}/I_A ratios for EC8 soil class E-Type 1 and all magnitude intervals.

$M_s > 5.5$			
M_s	I_E/I_A	$n(E)/n(A)$	PGA (cm/s^2)
5.5-6.0	1.34	1/7	152
6.0-6.5	0.73	1/7	177
6.5-7.0	0.62	3/9	≤ 414 (192)

Table 3.44 gives the I_{soil}/I_A ratios for soil classes B, C and E for Type 1 seismicity. I_{soil}/I_A coefficients of Table 3.44 were calculated as the mean values of the coefficients from all magnitude intervals (M.I.). However, the rather small amount of available records for soil class A in all M.I. (less than 10 records in each M.I.) may affect the uncertainties associated to the estimated amplification factors. The amplification factors S, derived by equation (4), are given in Table 3.45, along with the corresponding soil factors proposed by EC8.

Table 3.44: SHARE-DS3: I_{soil}/I_A ratios for EC8 soil classes and both seismicity contexts

Soil Class	$M_s > 5.5$	
	Selected M.I.	I_{soil}/I_A
B	5.5-6.0, 6.0-6.5, 6.5-7.0	1.09
C	5.5-6.0, 6.0-6.5, 6.5-7.0	1.48
D	-	-
E	5.5-6.0, 6.0-6.5, 6.5-7.0	0.90

Table 3.45: SHARE-DS3: Soil factors with Approach 2 compared to EC8

Soil Class	$M_s > 5.5$	
	Approach 2	EC8
B	0.94	1.20
C	1.15	1.15
D	-	1.35
E	0.78	1.40

SHARE-DS3 Summary

EC8 soil factors S obtained with the two different approaches using SHARE-DS3 dataset are summarized in Table 3.46.

Table 3.46: SHARE-DS3: Approaches 1, 2 and weighted average soil amplification factors for EC8 soil classes using common and different datasets, for $M_s > 5.5$.

Soil Class	$M_s > 5.5$					
	Approach 1		Approach 2	Weighted Average		EC8
	Common dataset	Different datasets		Common dataset	Different datasets	
B	1.49	1.50	0.94	1.22	1.22	1.20
C	1.82	1.95	1.15	1.48	1.55	1.15
D	-	-	-	-	-	1.35
E	-	0.93	0.78	-	0.85	1.40

3.2.3 Summary for EC8 soil classes

Tables 3.47 and 3.48 summarize the soil factors obtained for EC8 soil classes applying different approaches and datasets. In the case of Approach 1 the final amplification factors for soil classes B and C are derived using the common dataset; for soil classes D and E, the amplification factors are obtained from the different datasets, as it has been extensively explained.

Table 3.47: Soil factors obtained with the different approaches and datasets for Type 2 seismicity and corresponding EC8 factors.

Soil Class	$M_s \leq 5.5$									EC8
	SHARE-DS1			SHARE-DS2			SHARE-DS3			
	Ap.1	Ap. 2	W.A.	Ap.1	Ap. 2	W.A.	Ap.1	Ap. 2	W.A.	
B	0.90	1.55	1.23	1.51	1.37	1.44	-	-	-	1.35
C	1.93	2.54	2.23	2.19	2.12	2.16	-	-	-	1.50
D	3.36	3.07	3.22	2.92	2.00	2.46	-	-	-	1.80
E	0.98	1.79	1.39	1.30	1.96	1.63	-	-	-	1.60

Table 3.48: Soil factors obtained with the different approaches and datasets for Type 1 seismicity and corresponding EC8 factors.

Soil Class	$M_s > 5.5$									EC8
	SHARE-DS1			SHARE-DS2			SHARE-DS3			
	Ap.1	Ap. 2	W.A.	Ap.1	Ap. 2	W.A.	Ap.1	Ap. 2	W.A.	
B	1.47	1.34	1.41	1.53	1.08	1.31	1.49	0.94	1.22	1.20
C	2.09	2.24	2.16	2.06	1.46	1.76	1.82	1.15	1.48	1.15
D	1.74	1.42	1.58	1.56	0.92	1.24	-	-		1.35
E	0.91	1.07	0.99	0.97	0.83	0.90	0.93	0.78	0.85	1.40

Comparing the S factors estimated with the different approaches and the different datasets, the following main observations can be made:

- The use of SHARE-DS1, which contains all records regardless of PGA, generally leads to higher S factors, compared to SHARE-DS2 dataset where only the records with $PGA \geq 20 \text{ cm/s}^2$ have been used.
- The use of weak strong motion records in the dataset leads generally to smaller S factors when Approach 1 is used. On the contrary the computed S factors are higher applying Approach 2.
- The dataset of records with $PGA > 150 \text{ cm/s}^2$ (SHARE-DS3) gives smaller S factors, compared to SHARE-DS1 or SHARE-DS2 datasets.
- The S factors estimated for soil class B and both seismicity Types are in general close to the present soil factors in EC8, regardless of method or dataset. For soil class C, however, the values adopted in EC8 are clearly smaller.

- For soil class D-Type 2, the estimated soil factors are much higher than the ones proposed in EC8. However, as they have been derived from a limited number of records the uncertainties may be quite high. There is clearly a need for more soil class D data.
- For soil class E-Type 2, the obtained S factors are close to the soil factors proposed in EC8, while for Type 1, the obtained S factors are much lower, and close to unity regardless of dataset. This is clearly due to the averaging process that both methods use, in order to compute a period-independent S factor, which can be applied to the whole spectrum. This is evident when looking at the soil amplification factors obtained from Approach 1 (Figures 3.25, 3.41 and 3.56), where we observe that amplification peaks at very low periods (around 0.1-0.2) reaching at very high values, and then decreases abruptly, reaching values close to or less than unity for a long spectral period range.

In general the range of PGA values of SHARE-DS2 dataset can be considered as more representative of the seismicity context expressed in seismic regulations. For Type 1 seismicity, SHARE-DS3 could perhaps be considered as more appropriate. However, the soil factors obtained from SHARE-DS2 are more conservative than the ones obtained from SHARE-DS3. That is why it was decided to consider the soil factors derived by SHARE-DS2 as more appropriate for EC8.

This decision was not followed for soil class D, where the lack of sufficient number of records obliged us to adjust the calculated values combining the results from the present analysis with engineering judgment and results from theoretical studies.

For soil class E, it was decided to finally propose the soil amplification factors estimated from Kik-Net surface and bedrock strong-motion records (see paragraph 4.3.3).

The selected soil factors S for EC8 soil classes are given in Table 3.49.

Table 3.49: Soil factors for EC8 soil classes

Soil Class	Type 2 ($M_s \leq 5.5$)		Type 1 ($M_s > 5.5$)	
	Proposed	EC8	Proposed	EC8
B	1.40	1.35	1.30	1.20
C	2.10	1.50	1.70	1.15
D	2.20*	1.80	1.60*	1.35
E	1.80**	1.60	1.40**	1.40

* limited data

** estimated from Kik-Net surface and bedrock strong-motion records

4. New classification system

4.1 Proposed soil classes

The main parameter used in modern code provisions concerning site classification, is $V_{s,30}$, which is computed by dividing a distance of 30 meters by the travel time from the ground surface to a depth of 30m. This parameter was proposed in Borchardt and Glassmoyer (1992), followed by Borchardt (1994). The depth of 30m was basically selected since it is a typical depth of geotechnical sampling borings and, thus, of site characterization. It is also believed that in most cases the main amplification is due to the trapping waves on the surface layers. EC8 uses $V_{s,30}$ as the main soil categorization parameter, along with N_{SPT} blow count and undrained strength C_u . However, we know that there are also other factors affecting seismic ground response, such as the impedance ratio between surface and underlying deposits, the soil type detailing and the stratigraphy, the soil non-linearity and inelasticity varying with the intensity of the ground motion, without referring to other important parameters like source, azimuth, valley-basin and topographic effects, which should be taken into account in a future site classification system.

A new, more detailed, soil classification system that includes soil type, stratigraphy, depth, soil stiffness, fundamental period of soil deposit and average shear wave velocity of the entire soil deposit, as key parameters, was presented by Pitilakis et al. (2004, 2006), based exclusively on theoretical ground response analyses of various representative models of realistic site conditions. The classification system proposed herein, using exclusively experimental data (records) from the **SHARE-AUTH database**, is inspired and based on this initial classification scheme. The classification scheme proposed in Pitilakis et al. (2004, 2006) has been used with some improvements mainly to the limits of values of the parameters describing each soil class.

The proposed classification system, which is described in detail in Table 4.1, is in general compatible with EC8, introducing at the same time some extra subclasses, which allow to take into consideration the influence of the depth of bedrock. *It should be stressed however, that there is no complete correspondence between the proposed soil classes and the main EC8 soil classes.* For instance, a site which is classified as C1, with the new classification, may be a B site according to EC8.

Figure 4.1 summarizes in a simplified way the soil classes proposed in EC8 and the new classification system.

The new improved soil classification system given in Table 4.1 is more convenient and practical from geotechnical point of view. At the same time it introduces as main classification parameter the predominant period of the site (T_0), which is a fundamental factor for site amplification.

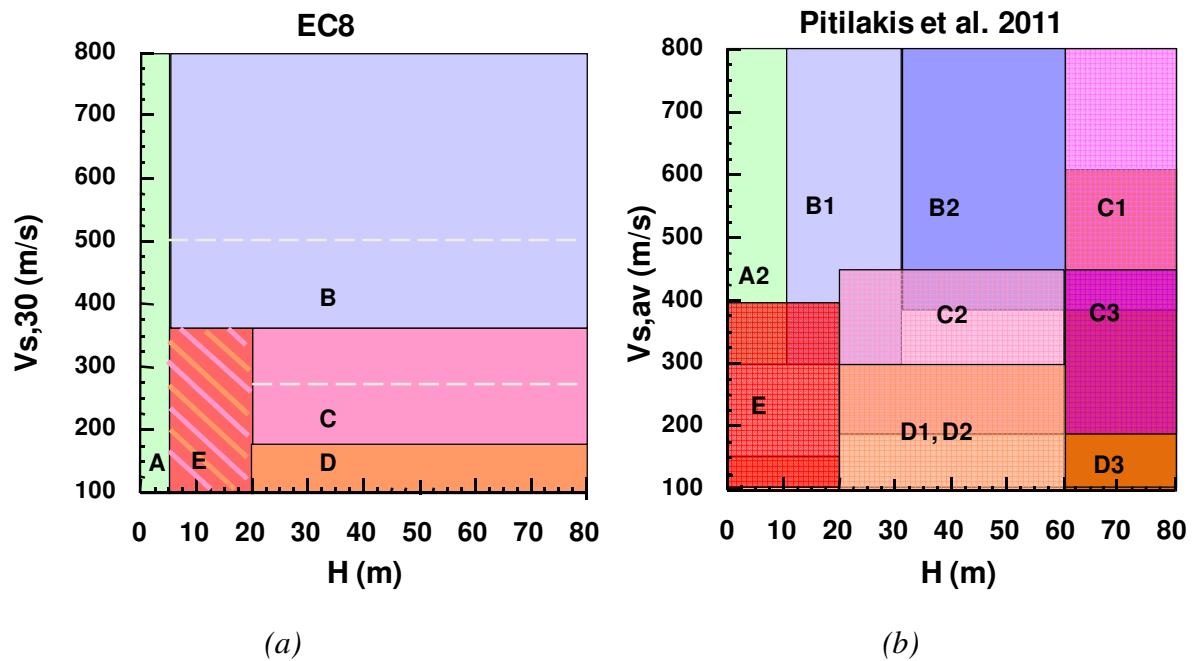


Figure 4.1: Simplified illustration of ground types according to (a) EC8 and (b) the proposed new classification system

The 536 sites of the SHARE-AUTH database were classified according to the new classification scheme (Figure 4.2). Due to the insufficient number of data for the classification of D sites to subclasses D1, D2 and D3, the three subclasses were for the moment unified to one single class (D).

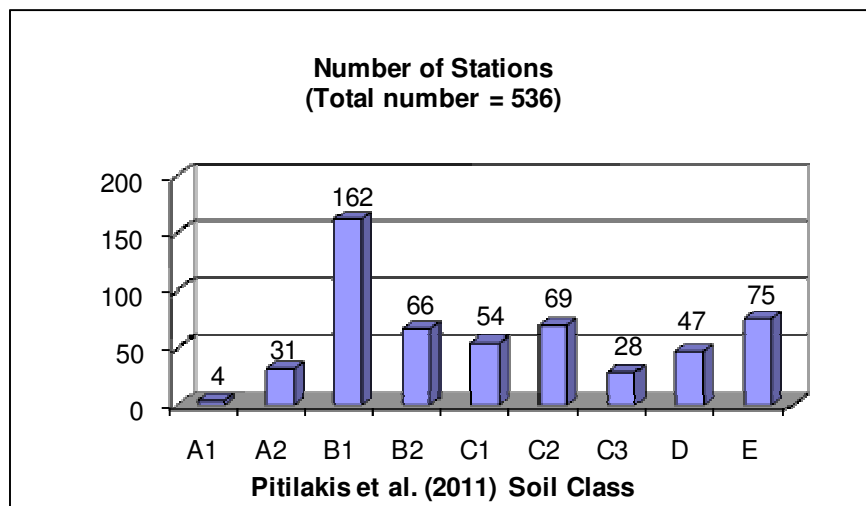


Figure 4.2: Classification of sites according to the new soil classification scheme

Table 4.1: Proposed Soil and Site Characterization Scheme

Soil Class	Description	T ₀ (sec)	Remarks
A1	Rock formations		V _s ≥ 1500 m/s
A2	Slightly weathered / segmented rock formations (thickness of weathered layer < 5.0m)	≤ 0.2	Surface weathered layer: V _s ≥ 200 m/sec Rock Formations: V _s ≥ 800 m/sec
	Geologic formations resembling rock formations in their mechanical properties and their composition (e.g. conglomerates)		V _s ≥ 800 m/sec
B1	Highly weathered rock formations whose weathered layer has a considerable thickness (5.0m - 30.0m)	≤ 0.5	Weathered layer: V _s ≥ 300 m/sec
	Soft rock formations of great thickness or formations which resemble these in their mechanical properties (e.g. stiff marls)		V _s : 400-800 m/sec N-SPT > 50, Su > 200 KPa
	Soil formations of very dense sand – sand gravel and/or very stiff/ to hard clay, of homogenous nature and small thickness (up to 30.0m)		V _s : 400-800 m/sec N-SPT > 50, Su > 200 KPa
B2	Soil formations of very dense sand – sand gravel and/or very stiff/ to hard clay, of homogenous nature and medium thickness (30.0 - 60.0m), whose mechanical properties increase with depth	≤ 0.8	V _s : 400-800 m/sec N-SPT > 50, Su > 200 KPa
C1	Soil formations of dense to very dense sand – sand gravel and/or stiff to very stiff clay, of great thickness (> 60.0m), whose mechanical properties and strength are constant and/or increase with depth	≤ 1.5	V _s : 400-800 m/sec N-SPT > 50, Su > 200 KPa
C2	Soil formations of medium dense sand – sand gravel and/or medium stiffness clay (PI > 15, fines percentage > 30%) of medium thickness (20.0 – 60.0m)	≤ 1.5	V _s : 200-450 m/sec N-SPT > 20, Su > 70 KPa
C3	Category C2 soil formations of great thickness (> 60.0 m), homogenous or stratified that are not interrupted by any other soil formation with a thickness of more than 5.0m and of lower strength and V _s velocity	≤ 1.8	V _s : 200-450 m/sec N-SPT > 20, Su > 70 KPa
D1	Recent soil deposits of substantial thickness (up to 60m), with the prevailing formations being soft clays of high plasticity index (PI > 40), high water content and low values of strength parameters	≤ 2.0	V _s ≤ 300 m/sec N-SPT < 25, Su < 70 KPa
D2	Recent soil deposits of substantial thickness (up to 60m), with prevailing fairly loose sandy to sandy-silty formations with a substantial fines percentage (not to be considered susceptible to liquefaction)	≤ 2.0	V _s ≤ 300 m/sec N-SPT < 25
D3	Soil formations of great overall thickness (> 60.0m), interrupted by layers of category D1 or D2 soils of a small thickness (5 – 15m), up to the depth of ~40m, within soils (sandy and/or clayey, category C) of evidently greater strength, with V _s ≥ 300 m/sec	≤ 3.0	V _s : 150-600 m/sec
E	Surface soil formations of small thickness (5 - 20m), small strength and stiffness, likely to be classified as category C and D according to its geotechnical properties, which overlie category A formations (V _s ≥ 800 m/sec)	≤ 0.7	Surface soil layers: V _s ≤ 400 m/sec
X	-Loose fine sandy-silty soils beneath the water table, susceptible to liquefaction (unless a special study proves no such danger, or if the soil's mechanical properties are improved). -Soils near obvious tectonic faults. -Steep slopes covered with loose lateral deposits. -Loose granular or soft silty-clayey soils, provided they have been proven to be hazardous in terms of dynamic compaction or loss of strength. Recent loose landfills. -Soils with a very high percentage in organic material -Soils requiring site-specific evaluations		

4.2 Normalized acceleration response spectra

It has been decided to keep two levels of earthquake intensity, the same as those proposed in EC8, i.e. Type 1 for $M_s > 5.5$ and Type 2 for $M_s \leq 5.5$. Moreover, based on the observations made in the previous chapter, we decided to use only the strong-motion records of the SHARE-AUTH database with $PGA > 20 \text{ cm/sec}^2$ (SHARE-AUTH-DS2). For the two levels of earthquake intensity we derived normalized acceleration response spectra for each soil class applying the following procedure:

- For all soil classes proposed in Table 4.1 and the two seismicity types, 5% damped normalized acceleration spectral values were plotted for spectral periods ranging from 0 to 2.5sec.
- Then the median normalized acceleration spectra, together with the 16th and 84th percentiles were calculated. The specific percentiles were selected as they correspond to the average minus one standard deviation and average plus one standard deviation respectively, as for the case of a normal distribution.
- The proposed normalized acceleration spectra resulted applying the same equations for each branch as in EC8. However, we observed that EC8 curves do not follow a unique approach regarding the position of the selected curve within the median (+-one standard deviation) spectrum of values. After several trials we decided to apply the general spectral functions to be closer to the 84th percentile. It is an important conceptual decision, which is adopted in order to increase the confidence limits, compared to the median curve, which is not conservative enough for all soil classes. Moreover, it was considered important that normalized acceleration response spectra should be derived based on a common rationale for all soil classes, which is not the case for the normalized response spectra of Eurocode 8.

Figures 4.3 to 4.10 illustrate for the different soil classes the range of the computed normalized acceleration spectra between 16% and 84% percentiles and the proposed design normalized acceleration spectra. The equations defining the proposed acceleration spectra (normalized acceleration response spectra of figures 4.3 to 4.10, multiplied by peak ground acceleration) are given in paragraph 4.4.

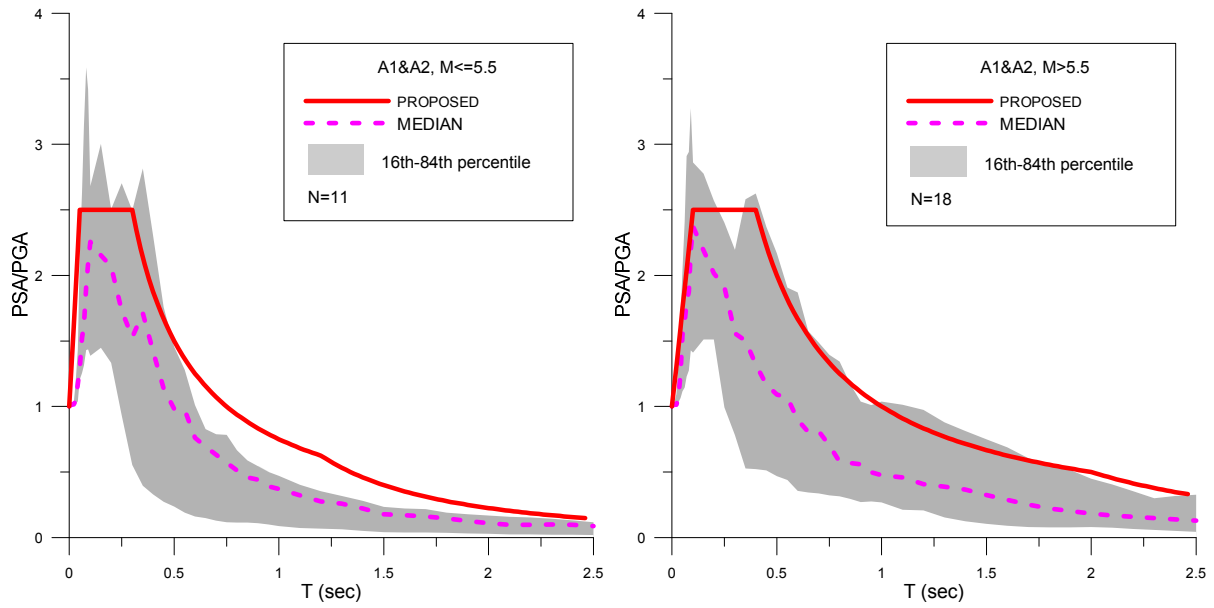


Figure 4.3: SHARE-AUTH-DS2: Normalized elastic acceleration response spectra for soil class A (A1+A2) of the proposed classification system for Type 2 seismicity (left) and Type 1 seismicity (right).

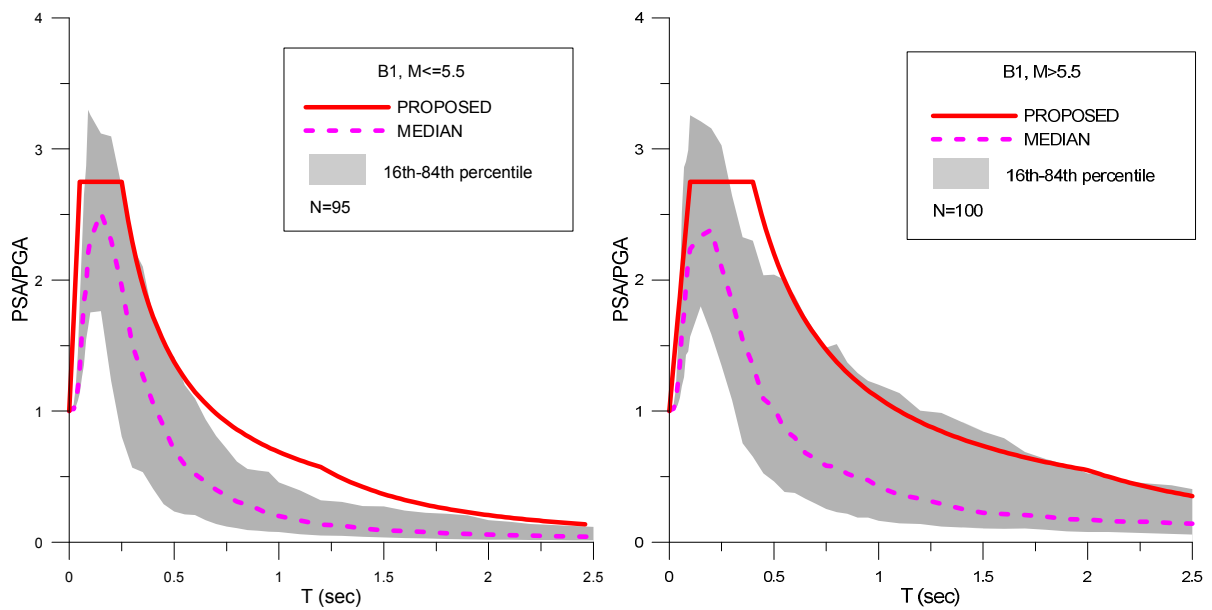


Figure 4.4: SHARE-AUTH-DS2: Normalized elastic acceleration response spectra for soil class B1 of the proposed classification system for Type 2 seismicity (left) and Type 1 seismicity (right).

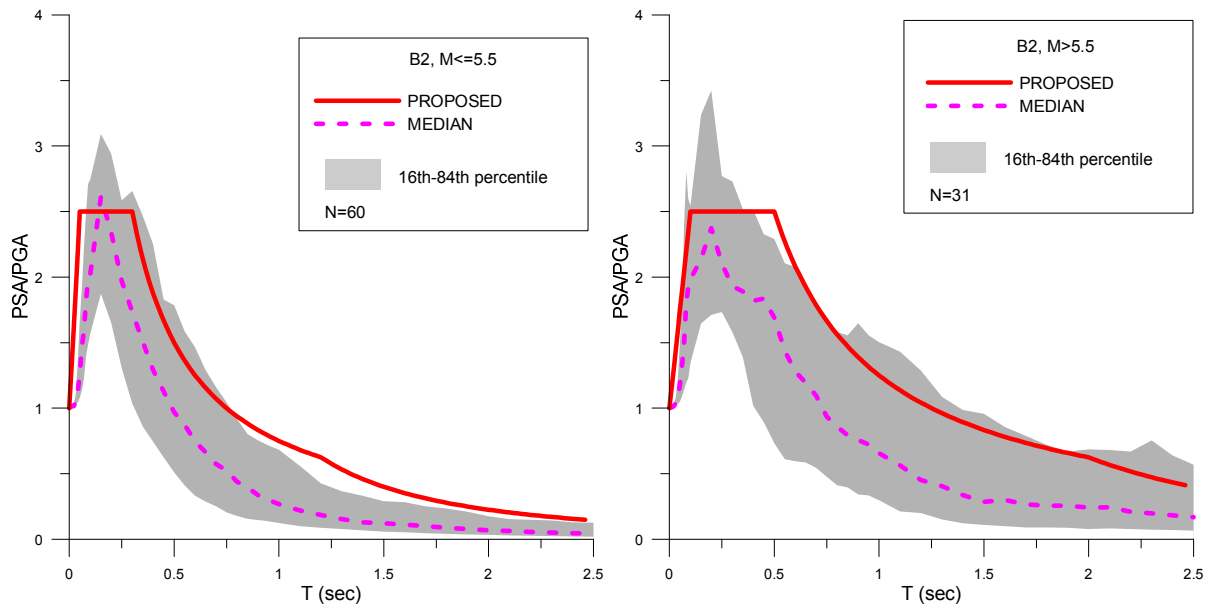


Figure 4.5: SHARE-AUTH-DS2: Normalized elastic acceleration response spectra for soil class B2 of the proposed classification system for Type 2 seismicity (left) and Type 1 seismicity (right).

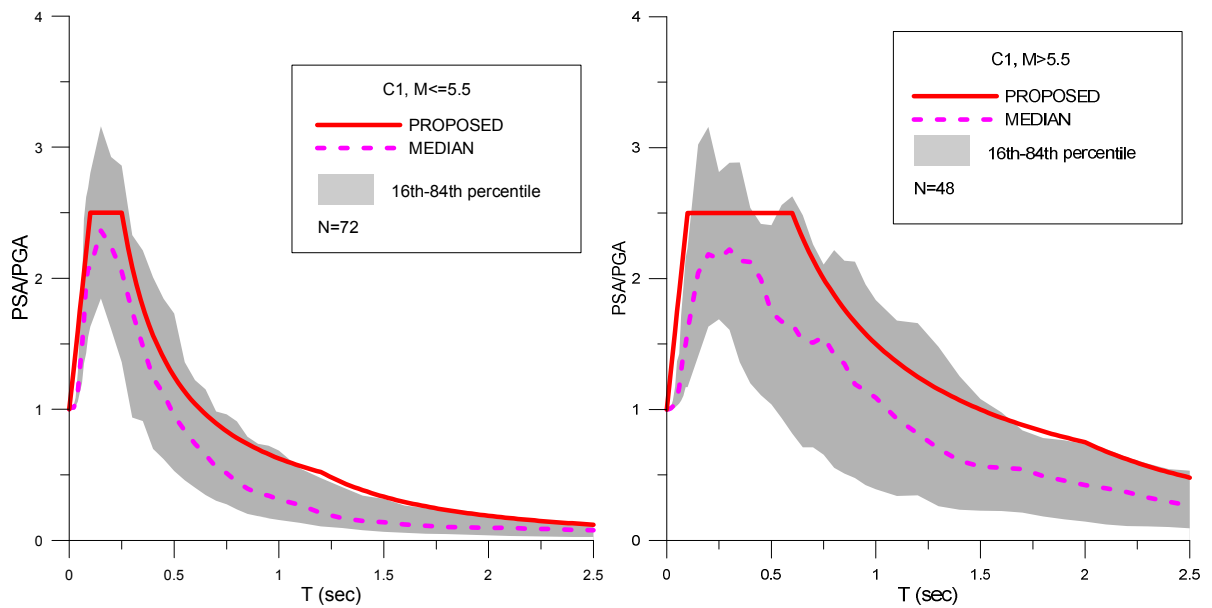


Figure 4.6: SHARE-AUTH-DS2: Normalized elastic acceleration response spectra for soil class C1 of the proposed classification system for Type 2 seismicity (left) and Type 1 seismicity (right).

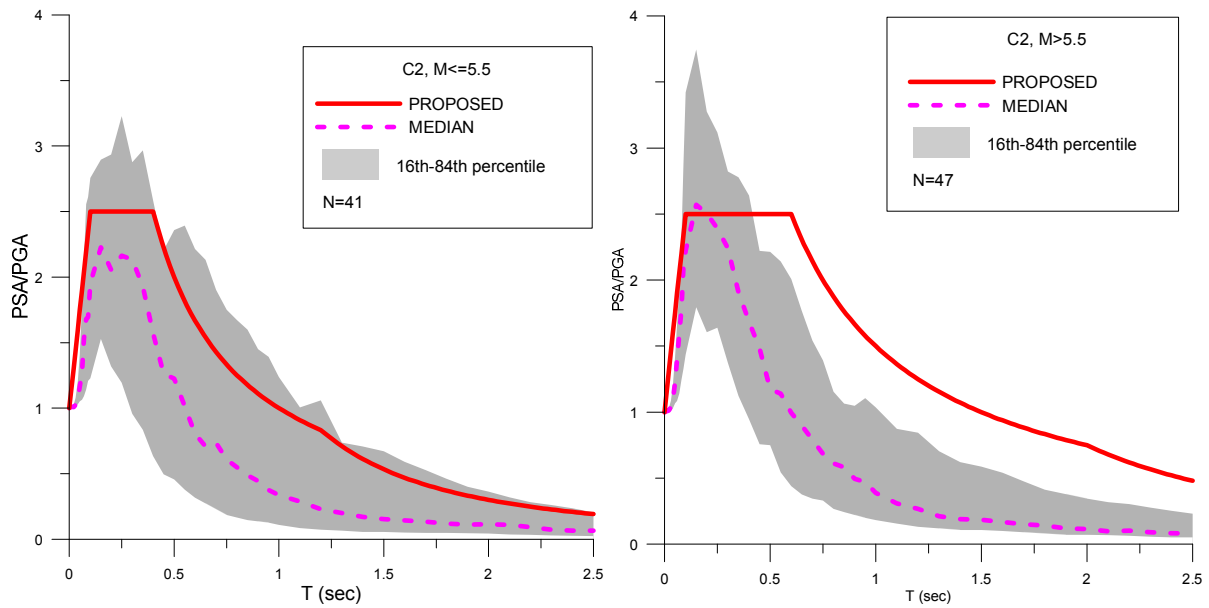


Figure 4.7: SHARE-AUTH-DS2: Normalized elastic acceleration response spectra for soil class C2 of the proposed classification system for Type 2 seismicity (left) and Type 1 seismicity (right).

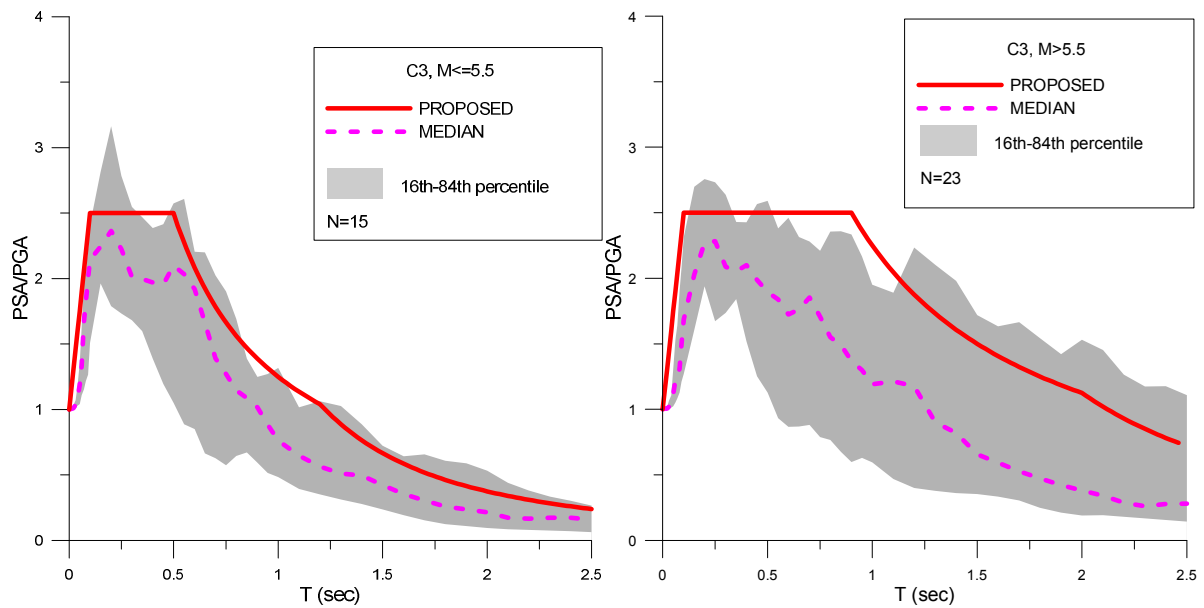


Figure 4.8: SHARE-AUTH-DS2: Normalized elastic acceleration response spectra for soil class C3 of the proposed classification system for Type 2 seismicity (left) and Type 1 seismicity (right).

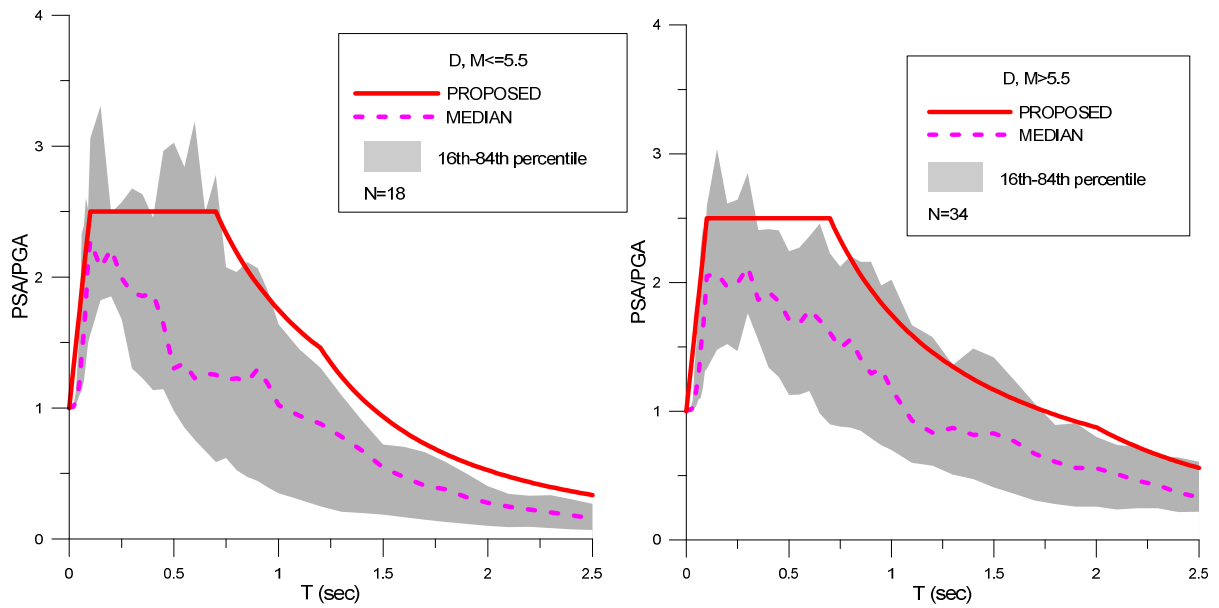


Figure 4.9: SHARE-AUTH-DS2: Normalized elastic acceleration response spectra for soil class D (D1, D2 and D3) of the proposed classification system for Type 2 seismicity (left) and Type 1 seismicity (right).

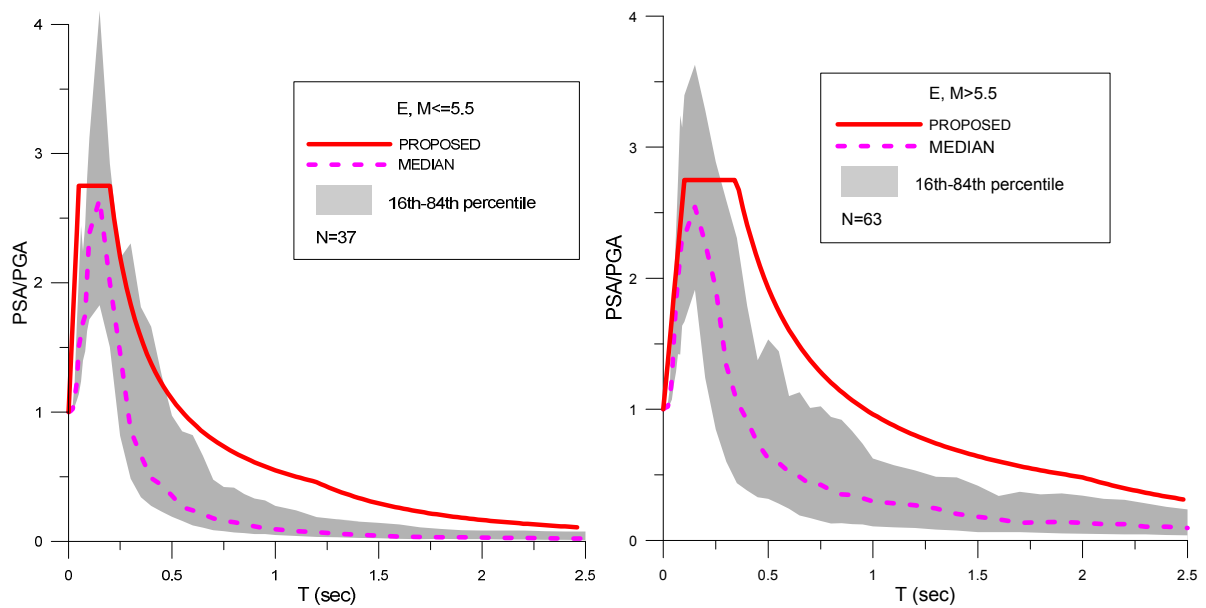


Figure 4.10: SHARE-AUTH-DS2: Normalized elastic acceleration response spectra for soil class E of the proposed classification system for Type 2 seismicity (left) and Type 1 seismicity (right).

Spectral shape ratios SR for the new classification scheme are given in Table 4.2.

Table 4.2: Spectral shape ratios SR for the new classification scheme.

Soil Class	$M_s \leq 5.5$	$M_s > 5.5$
B1	0.97	1.10
B2	1.00	1.16
C1	0.87	1.29
C2	1.20	1.29
C3	1.38	1.62
D	1.67	1.41
E	0.82	1.00

4.3 Soil amplification factors

Soil amplification factors for the soil classes in the new classification system and for two types of earthquake intensity (Type 1 – $M_s > 5.5$ and Type 2 $M_s \leq 5.5$) were estimated using the same procedure and logic tree approach that was used for the estimation of amplification factors for EC8 soil classes.

4.3.1 Approach 1

Following the procedure that was described in detail in paragraph 3.2.1, period-dependent amplification factors were estimated for the new classification system. As it has already been mentioned, the computation of amplification factors using equation (1) requires that reference spectral acceleration at period T can be estimated with all four GMPEs. This restriction unfortunately limits the dataset significantly. For this reason, and following the same rationale as in Chapter 3, soil amplification factors were calculated with Equations (1) and (3) using the common dataset, which includes the strong motion records for which the implementation of all GMPEs was feasible (Table 4.3), and with Equation (6) using the different datasets for each GMPE (Table 4.4).

Table 4.3: SHARE-AUTH-DS2: Number of strong motion records for which reference spectral acceleration could be estimated with all GMPEs. (common dataset)

Soil Class	Type 2 ($4 \leq M_s \leq 5.5$)	Type 1 ($M_s > 5.5$)
B1	33	41
B2	29	9
C1	5	18
C2	15	9
C3	5	10
D	1	7
E	-	4

Table 4.4: SHARE-AUTH-DS2: Number of strong motion records for which each GMPE could be implemented. (different datasets)

Soil Class	A&B		C&F		Zh		C&Y	
	$M_s \leq 5.5$	$M_s > 5.5$						
B1	52	49	76	96	76	96	41	52
B2	41	14	41	25	41	25	31	14
C1	11	20	21	44	21	44	5	27
C2	17	12	26	38	26	38	17	11
C3	11	12	14	20	14	20	15	11
D	7	10	17	34	17	34	1	8
E	8	4	25	46	25	46	-	13

Common dataset for all GMPEs

Figures 4.11 to 4.17 summarize the period-dependent amplification factors calculated with equation (1) for all soil classes of the proposed classification system, using the weighted average $(GM_r)_{ij}$ derived from equation (3) as reference spectral acceleration. The median values of the amplification factors for each spectral period, along with the 16th and 84th percentiles are also depicted in the figures and are given in detail in Tables 4.5 to 4.7.

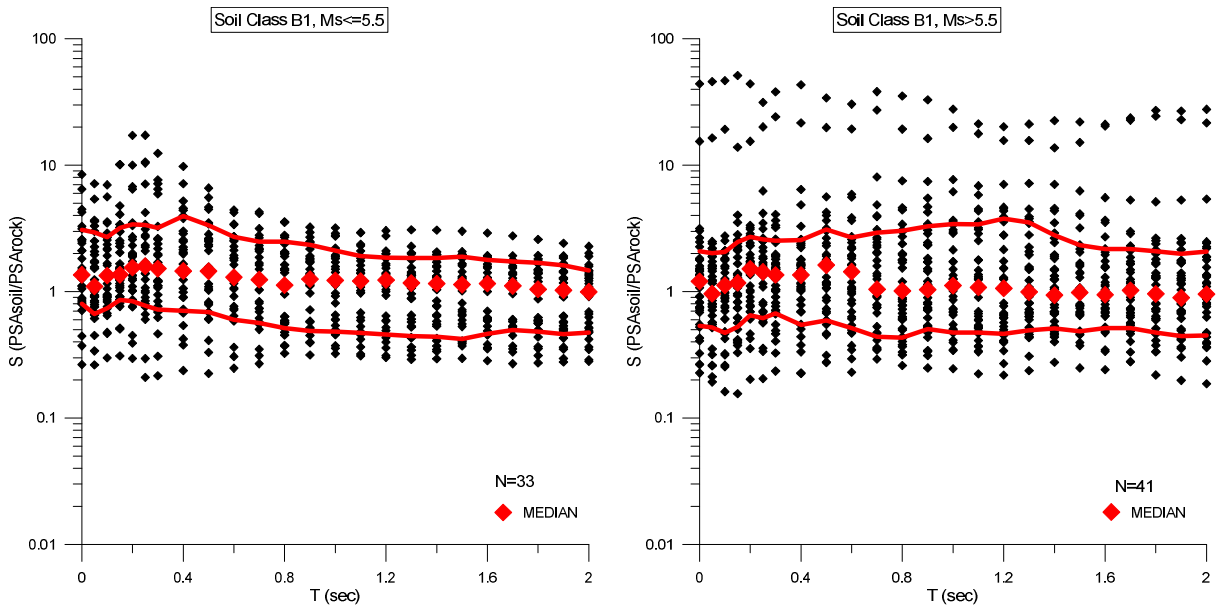


Figure 4.11: SHARE-AUTH-DS2: Amplification factors estimated with Approach 1 for soil class B1, for Type 2 seismicity (left) and Type 1 seismicity (right). The red lines represent the 16th and 84th percentiles. (common dataset)

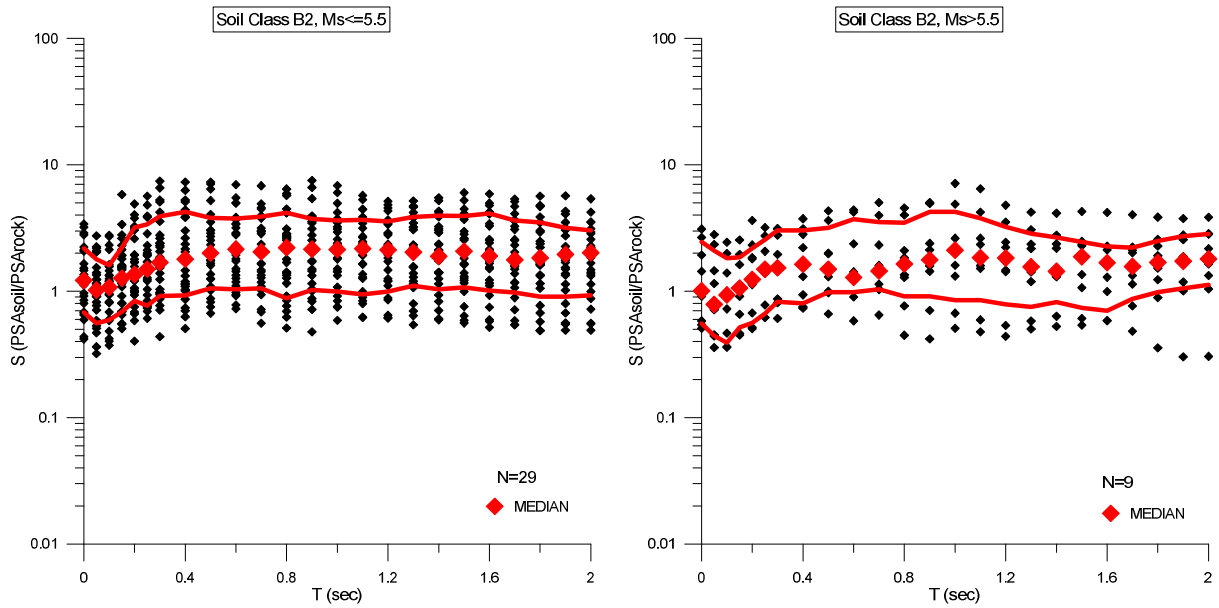


Figure 4.12: SHARE-AUTH-DS2: Amplification factors estimated with Approach 1 for soil class B2, for Type 2 seismicity (left) and Type 1 seismicity (right). The red lines represent the 16th and 84th percentiles. (common dataset)

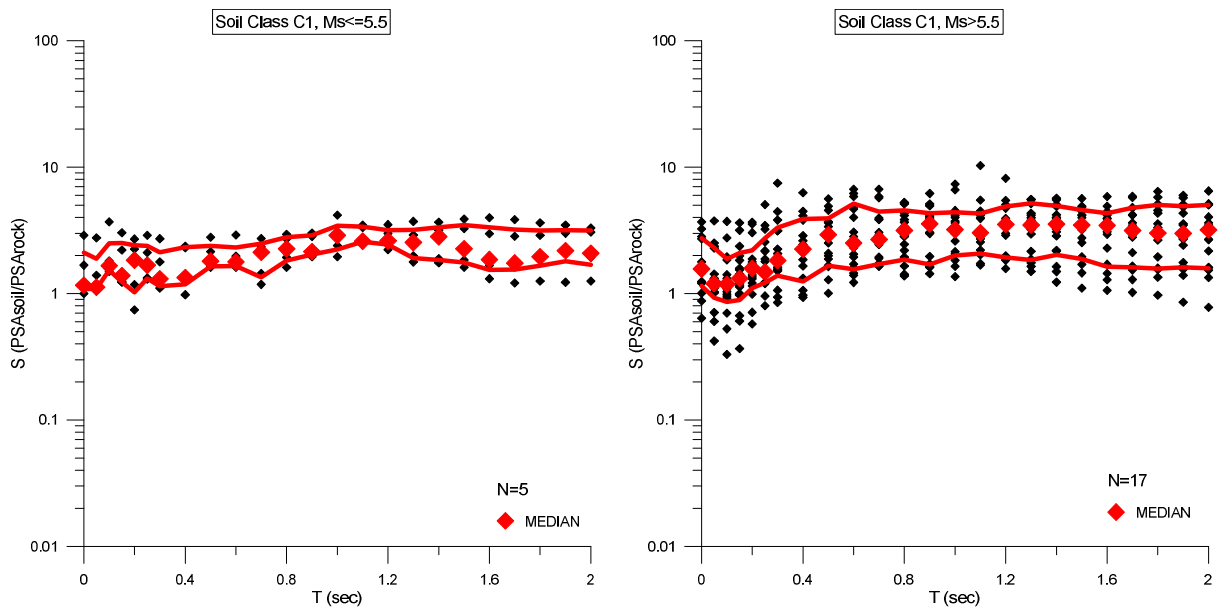


Figure 4.13: SHARE-AUTH-DS2: Amplification factors estimated with Approach 1 for soil class C1, for Type 2 seismicity (left) and Type 1 seismicity (right). The red lines represent the 16th and 84th percentiles. (common dataset)

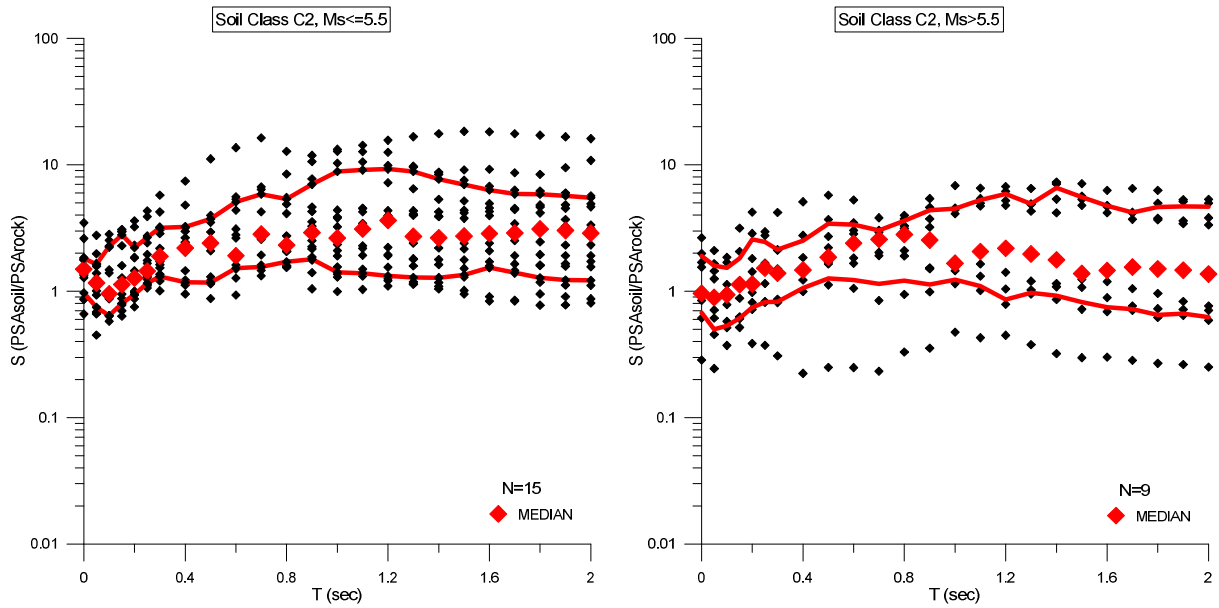


Figure 4.14: SHARE-AUTH-DS2: Amplification factors estimated with Approach 1 for soil class C2, for Type 2 seismicity (left) and Type 1 seismicity (right). The red lines represent the 16th and 84th percentiles. (common dataset)

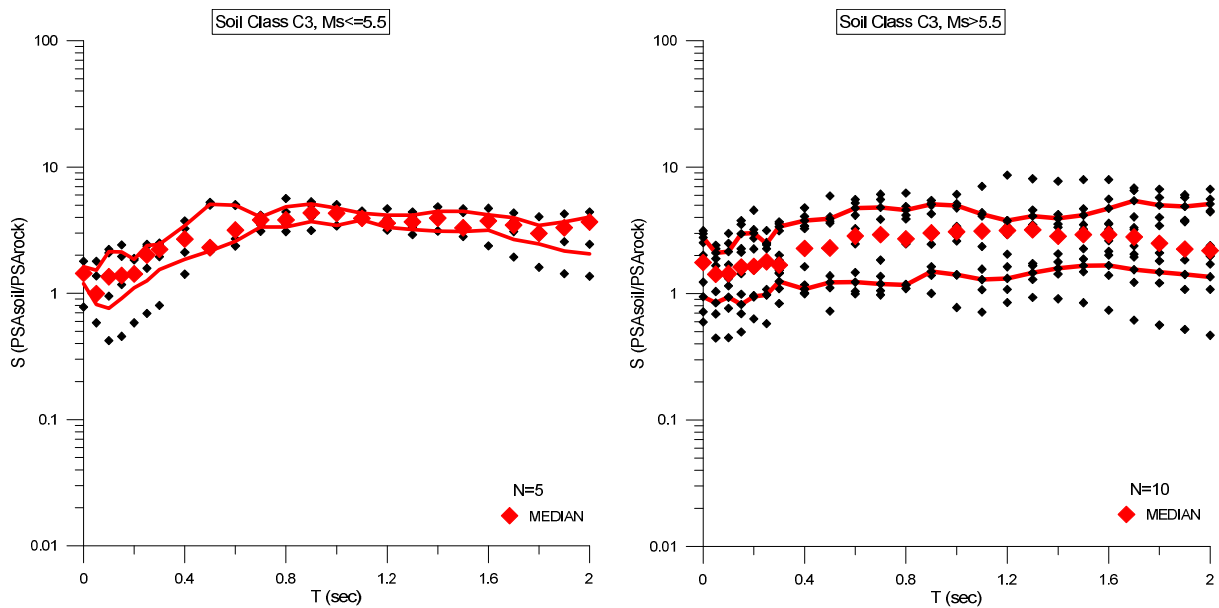


Figure 4.15: SHARE-AUTH-DS2: Amplification factors estimated with Approach 1 for soil class C3, for Type 2 seismicity (left) and Type 1 seismicity (right). The red lines represent the 16th and 84th percentiles. (common dataset)

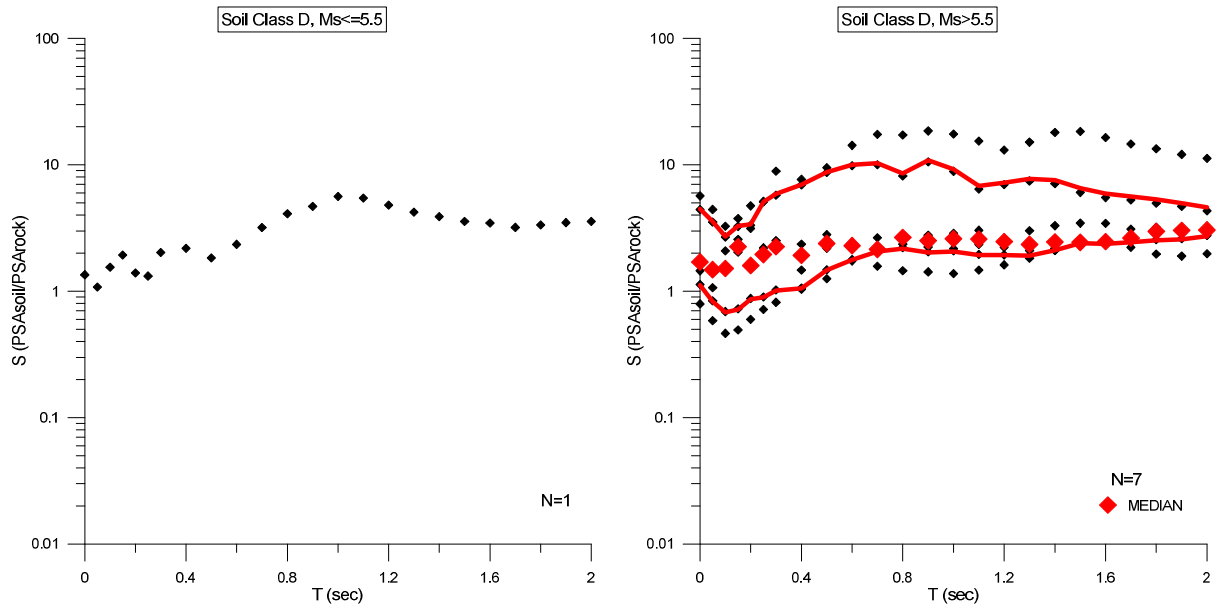


Figure 4.16: SHARE-AUTH-DS2: Amplification factors estimated with Approach 1 for soil class D (D1+D2+D3), for Type 2 seismicity (left) and Type 1 seismicity (right). The red lines represent the 16th and 84th percentiles. (common dataset)

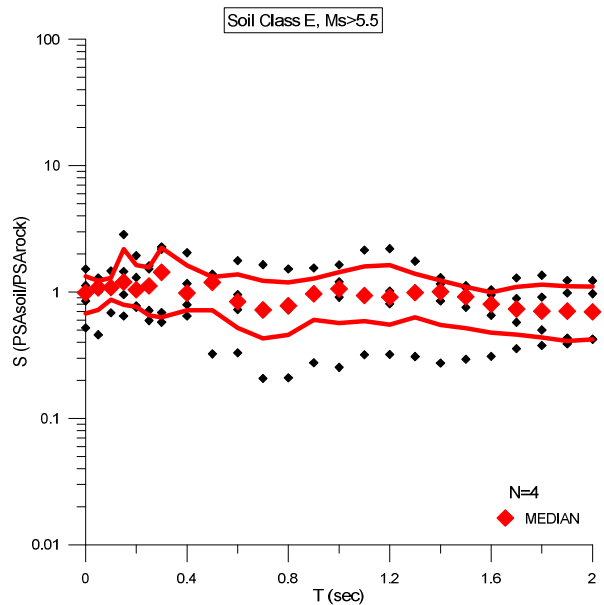


Figure 4.17: SHARE-AUTH-DS2: Amplification factors estimated with Approach 1 for soil class E, for Type 1 seismicity (right). The red lines represent the 16th and 84th percentiles. (common dataset)

Table 4.5: SHARE-AUTH-DS2: Median amplification factors, 16th and 84th percentiles, estimated with Approach 1 for soil classes B1 & B2. (common dataset)

T	B1-Type2			B1-Type1			B2-Type2			B2-Type1		
	Median	16th	84th									
0	1.36	0.80	3.08	1.21	0.54	2.09	1.22	0.68	2.19	1.01	0.55	2.46
0.05	1.10	0.67	2.95	0.96	0.52	2.01	1.02	0.56	1.80	0.79	0.45	2.09
0.1	1.34	0.74	2.69	1.12	0.47	2.06	1.08	0.59	1.60	0.94	0.39	1.83
0.15	1.36	0.86	3.19	1.17	0.53	2.47	1.27	0.69	2.22	1.06	0.52	1.86
0.2	1.55	0.84	3.41	1.51	0.65	2.71	1.36	0.84	3.19	1.24	0.56	2.19
0.25	1.59	0.78	3.37	1.43	0.62	2.59	1.50	0.77	3.38	1.49	0.67	2.55
0.3	1.52	0.72	3.20	1.36	0.67	2.54	1.69	0.92	3.91	1.53	0.83	3.03
0.4	1.46	0.71	3.96	1.35	0.55	2.56	1.80	0.93	4.25	1.64	0.80	3.03
0.5	1.45	0.69	3.35	1.62	0.59	3.11	2.00	1.05	3.80	1.50	0.98	3.18
0.6	1.30	0.60	2.71	1.44	0.51	2.67	2.15	1.04	3.76	1.29	0.99	3.72
0.7	1.24	0.56	2.48	1.05	0.44	2.93	2.05	1.06	3.89	1.45	1.04	3.52
0.8	1.12	0.52	2.49	1.01	0.43	3.03	2.22	0.88	4.18	1.64	0.91	3.48
0.9	1.26	0.49	2.34	1.04	0.51	3.29	2.15	1.02	3.75	1.77	0.91	4.24
1	1.23	0.48	2.12	1.11	0.47	3.43	2.14	1.00	3.63	2.11	0.85	4.26
1.1	1.21	0.47	1.92	1.08	0.47	3.41	2.17	0.94	3.67	1.85	0.85	3.78
1.2	1.23	0.46	1.86	1.06	0.46	3.78	2.12	0.99	3.56	1.83	0.79	3.23
1.3	1.17	0.45	1.84	0.99	0.49	3.53	2.04	1.11	3.87	1.56	0.75	2.86
1.4	1.16	0.44	1.84	0.94	0.51	2.80	1.89	1.04	3.96	1.44	0.82	2.66
1.5	1.14	0.42	1.89	0.99	0.48	2.34	2.07	1.08	3.94	1.88	0.74	2.45
1.6	1.16	0.46	1.78	0.94	0.51	2.17	1.91	1.01	4.13	1.68	0.70	2.27
1.7	1.11	0.50	1.73	1.02	0.51	2.18	1.77	0.98	3.63	1.57	0.87	2.21
1.8	1.04	0.48	1.70	0.96	0.47	2.09	1.84	0.91	3.51	1.69	0.99	2.50
1.9	1.03	0.46	1.62	0.89	0.45	2.00	1.96	0.90	3.17	1.73	1.06	2.72
2	1.00	0.48	1.47	0.96	0.45	2.08	2.02	0.93	3.04	1.80	1.12	2.85

Table 4.6: SHARE-AUTH-DS2: Median amplification factors, 16th and 84th percentiles, estimated with Approach 1 for soil classes C1 & C2. (common dataset)

T	C1-Type2			C1-Type1			C2-Type2			C2-Type1		
	Median	16th	84th									
0	1.16	1.09	2.11	1.57	1.15	2.75	1.49	0.97	1.83	0.96	0.68	1.90
0.05	1.12	1.09	1.89	1.20	0.93	2.31	1.16	0.75	1.64	0.89	0.50	1.59
0.1	1.66	1.53	2.49	1.19	0.86	1.88	0.96	0.64	2.27	0.94	0.53	1.53
0.15	1.39	1.24	2.51	1.32	0.89	2.09	1.13	0.80	2.80	1.13	0.61	1.82
0.2	1.84	1.02	2.41	1.58	1.11	2.20	1.27	0.94	2.21	1.14	0.74	2.57
0.25	1.68	1.32	2.39	1.48	1.22	2.75	1.45	1.16	2.67	1.53	0.82	2.46
0.3	1.31	1.14	2.12	1.83	1.39	3.33	1.89	1.31	3.18	1.39	0.83	2.13
0.4	1.34	1.18	2.33	2.24	1.25	3.90	2.19	1.18	3.23	1.47	1.06	2.51
0.5	1.81	1.64	2.38	2.92	1.66	3.94	2.40	1.17	3.74	1.86	1.27	3.42
0.6	1.78	1.65	2.31	2.51	1.56	5.14	1.91	1.53	5.10	2.40	1.23	3.36
0.7	2.13	1.35	2.49	2.69	1.71	4.45	2.83	1.56	5.87	2.57	1.14	3.02
0.8	2.26	1.82	2.80	3.16	1.86	4.57	2.32	1.71	5.37	2.81	1.21	3.61

0.9	2.15	2.03	2.90	3.56	1.70	4.34	2.91	1.79	7.00	2.54	1.13	4.37
1	2.89	2.24	3.45	3.21	2.00	4.39	2.64	1.41	8.87	1.67	1.23	4.51
1.1	2.60	2.57	3.38	3.03	2.07	4.30	3.11	1.39	9.11	2.06	1.10	5.29
1.2	2.61	2.44	3.18	3.53	1.93	4.89	3.64	1.33	9.26	2.18	0.86	5.90
1.3	2.54	1.91	3.20	3.50	1.84	5.17	2.72	1.28	8.86	1.97	0.97	4.90
1.4	2.82	1.84	3.35	3.54	2.02	4.95	2.65	1.28	7.69	1.77	0.92	6.57
1.5	2.26	1.76	3.49	3.49	1.88	4.59	2.73	1.35	6.98	1.38	0.82	5.56
1.6	1.86	1.54	3.34	3.46	1.63	4.33	2.86	1.54	6.32	1.46	0.75	4.74
1.7	1.75	1.55	3.21	3.15	1.62	4.77	2.89	1.41	5.88	1.55	0.72	4.20
1.8	1.96	1.66	3.16	3.01	1.58	5.04	3.11	1.28	5.87	1.50	0.65	4.64
1.9	2.19	1.81	3.18	2.99	1.62	4.90	3.02	1.23	5.70	1.47	0.67	4.70
2	2.09	1.69	3.15	3.19	1.59	5.04	2.88	1.22	5.51	1.37	0.62	4.66

Table 4.7: SHARE-AUTH-DS2: Median amplification factors, 16th and 84th percentiles, estimated with Approach 1 for soil classes C3, D & E. (common dataset)

T	C3-Type2			C3-Type1			D-Type2	D-Type1			E-Type1		
	Median	16th	84th	Median	16th	84th	Median	Median	16th	84th	Median	16th	84th
0	1.44	1.20	1.62	1.76	0.94	2.78	1.35	1.70	1.12	4.47	0.99	0.68	1.33
0.05	0.99	0.81	1.52	1.42	0.84	2.10	1.08	1.48	0.83	3.56	1.08	0.72	1.23
0.1	1.35	0.76	2.14	1.44	0.94	2.15	1.55	1.51	0.68	2.71	1.09	0.87	1.29
0.15	1.38	0.91	2.12	1.62	0.82	2.98	1.93	2.25	0.72	3.28	1.20	0.79	2.18
0.2	1.42	1.10	1.86	1.64	0.95	3.01	1.40	1.60	0.87	3.38	1.04	0.77	1.64
0.25	2.00	1.26	2.39	1.79	0.98	2.49	1.32	1.95	0.90	5.10	1.12	0.65	1.57
0.3	2.22	1.54	2.44	1.68	1.25	3.38	2.03	2.25	1.02	5.88	1.43	0.63	2.23
0.4	2.69	1.86	3.43	2.28	1.08	3.79	2.19	1.92	1.06	6.97	0.98	0.72	1.62
0.5	2.30	2.17	5.08	2.29	1.23	3.91	1.84	2.39	1.47	8.74	1.19	0.72	1.32
0.6	3.17	2.58	4.98	2.85	1.23	4.76	2.35	2.29	1.78	10.02	0.84	0.52	1.38
0.7	3.80	3.35	4.02	2.93	1.19	4.81	3.19	2.15	2.07	10.30	0.72	0.43	1.23
0.8	3.82	3.35	4.85	2.71	1.17	4.58	4.10	2.67	2.18	8.53	0.78	0.46	1.19
0.9	4.34	3.70	5.10	3.02	1.50	5.08	4.69	2.51	2.03	10.87	0.97	0.60	1.28
1	4.30	3.44	4.73	3.09	1.41	4.97	5.62	2.60	2.06	9.23	1.06	0.57	1.43
1.1	3.92	3.81	4.30	3.12	1.29	4.26	5.45	2.59	1.94	6.80	0.94	0.59	1.60
1.2	3.60	3.34	4.17	3.16	1.32	3.78	4.80	2.47	1.93	7.22	0.91	0.55	1.63
1.3	3.68	3.20	4.15	3.19	1.46	4.11	4.23	2.35	1.91	7.77	0.99	0.63	1.39
1.4	3.94	3.11	4.47	2.84	1.58	3.93	3.90	2.45	2.11	7.55	1.01	0.55	1.23
1.5	3.30	3.09	4.47	2.93	1.66	4.17	3.57	2.44	2.40	6.54	0.92	0.52	1.10
1.6	3.74	3.17	4.19	2.93	1.67	4.72	3.47	2.47	2.37	5.95	0.80	0.48	1.00
1.7	3.46	2.67	3.97	2.81	1.55	5.44	3.20	2.64	2.45	5.64	0.73	0.46	1.10
1.8	2.99	2.47	3.45	2.50	1.48	5.00	3.34	2.97	2.54	5.32	0.71	0.44	1.14
1.9	3.31	2.16	3.68	2.25	1.42	4.90	3.49	3.03	2.58	4.99	0.71	0.41	1.11
2	3.67	2.06	4.03	2.19	1.36	5.12	3.56	3.05	2.73	4.61	0.70	0.42	1.11

In order to estimate a single period-independent amplification factor for each soil class and each level of magnitude, similar to the S factor proposed in the previous chapter for EC8, the

weighted average amplification spectra were averaged over a range of periods from $T=0$ to $T=2s$. The resulting amplification factors, divided by the spectral shape ratio SR (which represents the amplification due to the change in shape of PGA-normalized response), are presented in Table 4.8.

Table 4.8: SHARE-AUTH-DS2: Soil factors for the new soil classes with Approach 1. (common dataset)

Soil Class	$M_s \leq 5.5$	$M_s > 5.5$
	Approach 1	Approach 1
B1	1.28	1.03
B2	1.89	1.36
C1	2.36	2.19
C2	2.08	1.35
C3	2.29	1.57
D	1.98	1.69
E	-	0.93

Different dataset for each GMPE

Figures 4.18 to 4.24 summarize the medians of the amplification factors estimated from the strong motion records of Table 4.4, using the four GMPEs separately, as well as the weighted average amplification factors calculated with equation (6). For the case where the Chiou and Youngs (2006) GMPE could not be implemented, the weight of this GMPE (equal to 0.20) was equally distributed to the remaining three GMPEs, whose weights were as a result increased by the value of $0.20/3$.

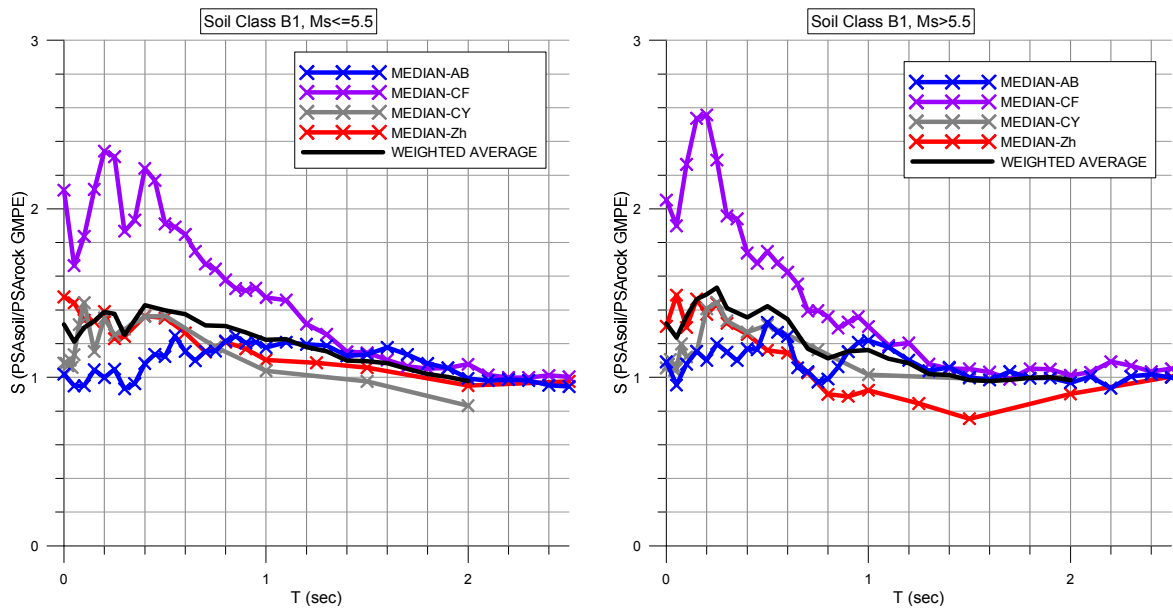


Figure 4.18: SHARE-AUTH-DS2: Median amplification factors with Approach 1 for soil class B1 and PSA_{rock} estimated with all GMPEs, for Type 2 seismicity (left) and Type 1 seismicity (right). (different datasets)

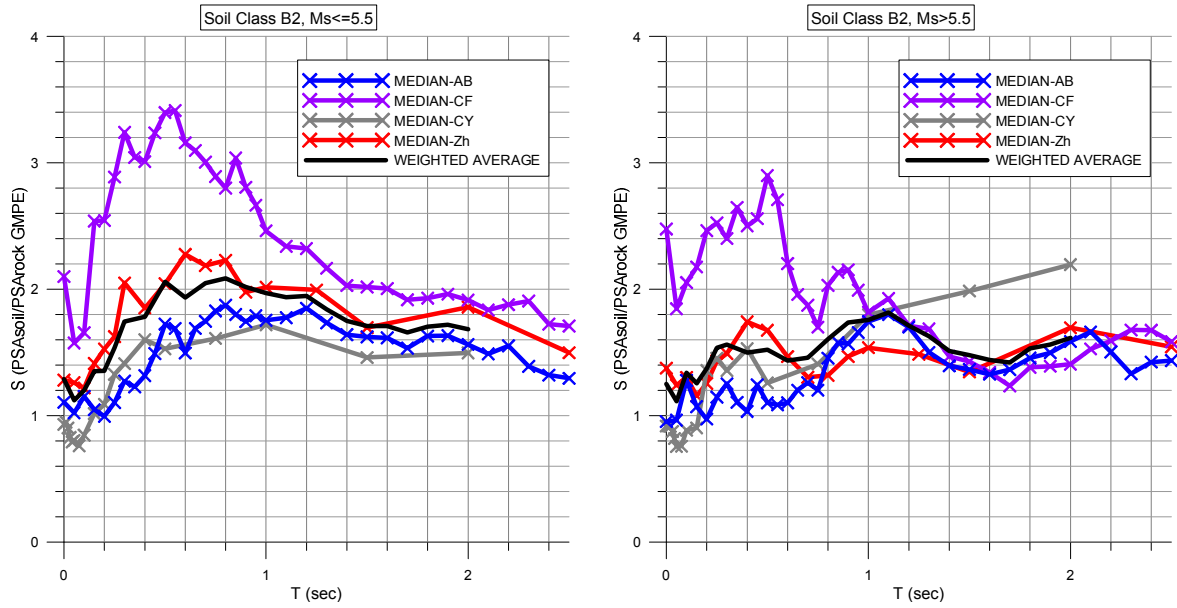


Figure 4.19: SHARE-AUTH-DS2: Median amplification factors with Approach 1 for soil class B2 and PSA_{rock} estimated with all GMPEs, for Type 2 seismicity (left) and Type 1 seismicity (right). (different datasets)

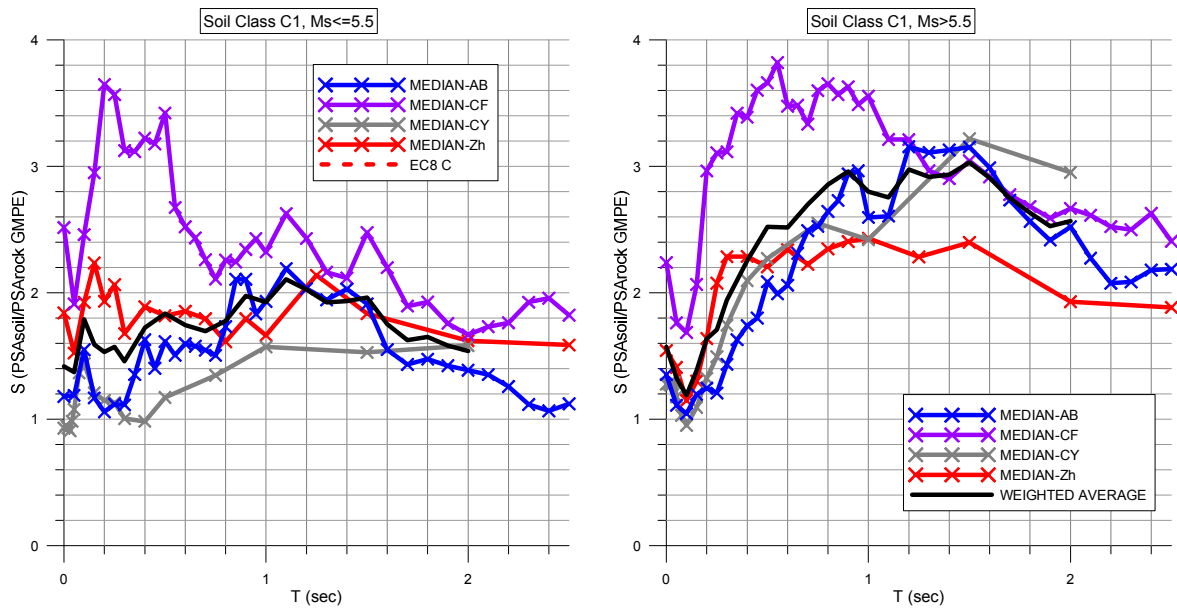


Figure 4.20: SHARE-AUTH-DS2: Median amplification factors with Approach 1 for soil class C1 and PSA_{rock} estimated with all GMPEs, for Type 2 seismicity (left) and Type 1 seismicity (right). (different datasets)

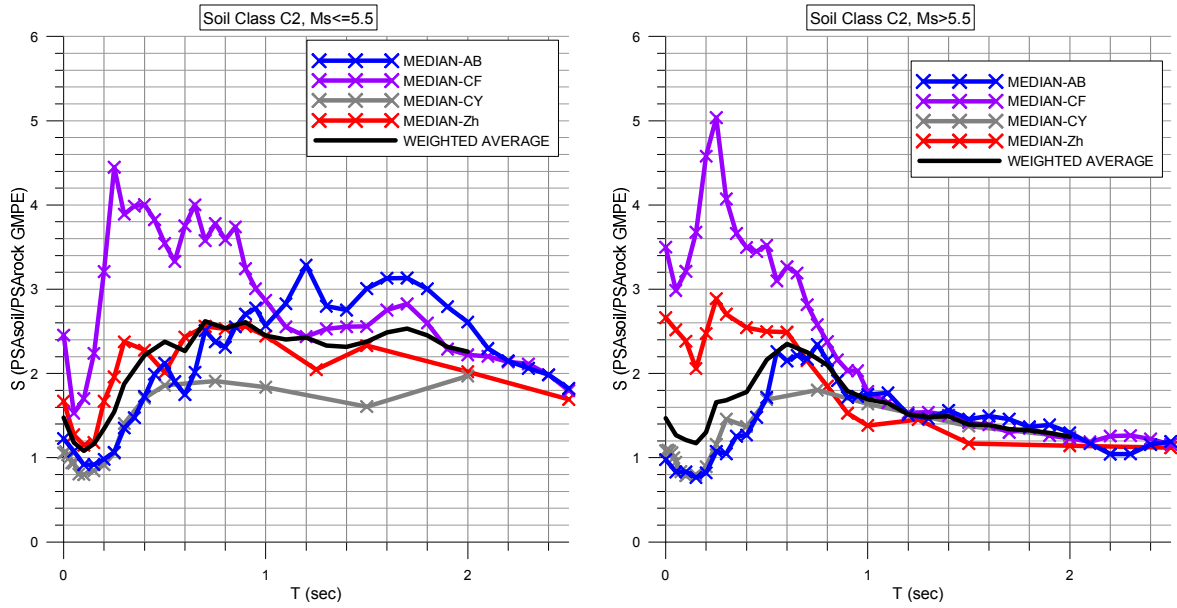


Figure 4.21: SHARE-AUTH-DS2: Median amplification factors with Approach 1 for soil class C2 and PSA_{rock} estimated with all GMPEs, for Type 2 seismicity (left) and Type 1 seismicity (right). (different datasets)

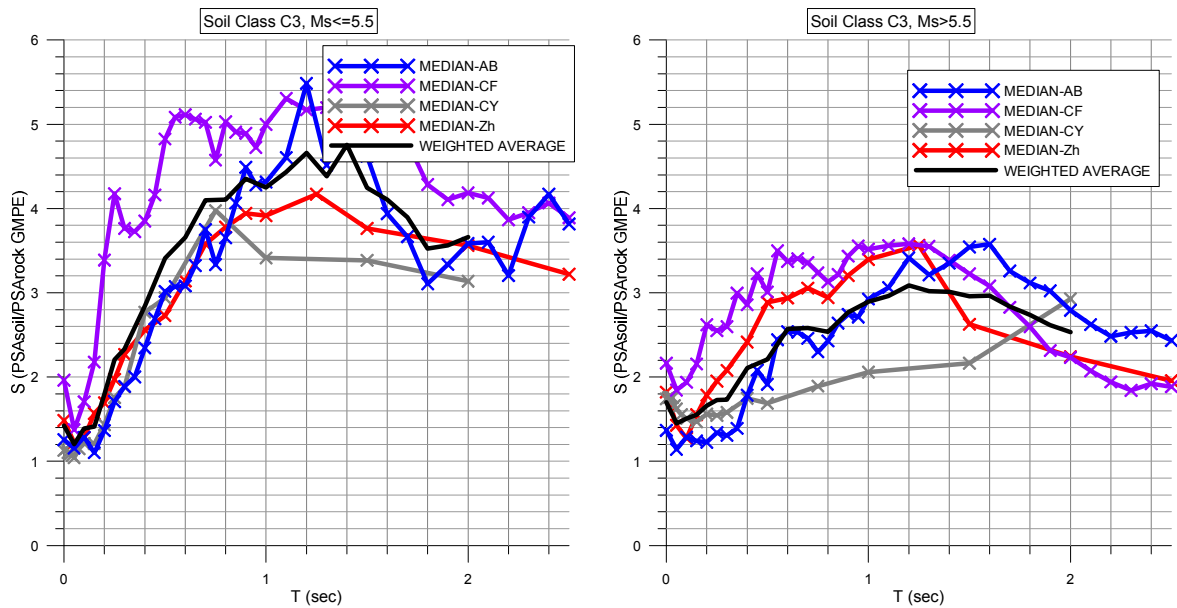


Figure 4.22: SHARE-AUTH-DS2: Median amplification factors with Approach 1 for soil class C3 and PSA_{rock} estimated with all GMPEs, for Type 2 seismicity (left) and Type 1 seismicity (right). (different datasets)

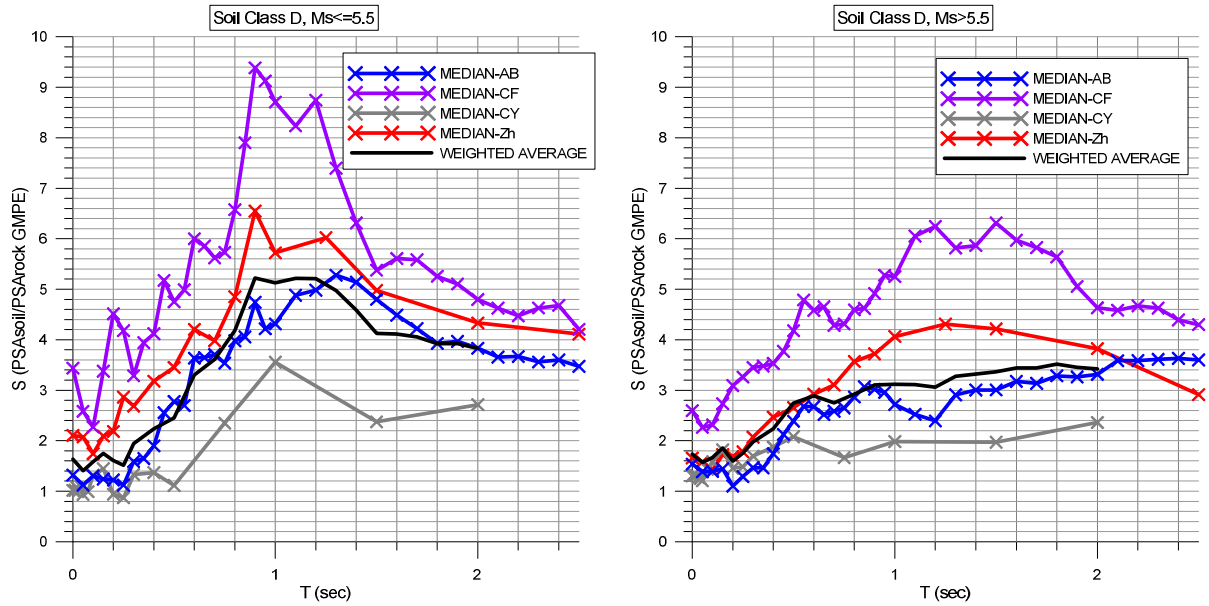


Figure 4.23: SHARE-AUTH-DS2: Median amplification factors with Approach 1 for soil class D (D1+D2+D3) and PSA_{rock} estimated with all GMPEs, for Type 2 seismicity (left) and Type 1 seismicity (right). (different datasets)

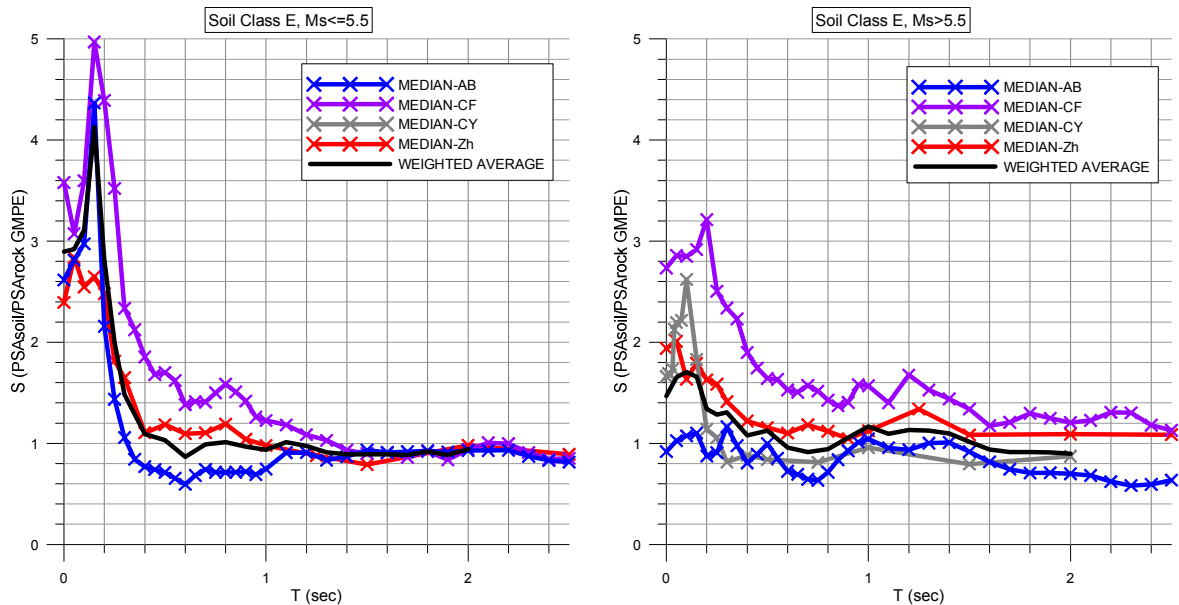


Figure 4.24: SHARE-AUTH-DS2: Median amplification factors with Approach 1 for soil class E and PSA_{rock} estimated with all GMPEs, for Type 2 seismicity (left) and Type 1 seismicity (right). (different datasets)

The period-dependent amplification factors calculated from Equation (6) are given in detail in Tables 4.9 and 4.10. In order to estimate a single period-independent amplification factor for each soil class and each level of magnitude, similar to the S factor proposed in EC8, the weighted average amplification spectra were averaged over a range of periods from $T=0$ to $T=2s$. The resulting amplification factors, divided by the spectral shape ratio SR are presented in Table 4.11.

Table 4.9: SHARE-AUTH-DS2: Amplification factors, estimated with Approach 1 for new soil classes B1, B2, D and E. (different datasets)

T	B1 - Type 2	B1 - Type 1	B2 - Type 2	B2 - Type 1	D - Type 2	D - Type 1	E - Type 2	E - Type 1
0	1.31	1.32	1.29	1.25	1.64	1.74	2.90	1.47
0.05	1.21	1.24	1.12	1.11	1.41	1.57	2.92	1.66
0.1	1.30	1.36	1.20	1.34	1.58	1.67	3.11	1.71
0.15	1.33	1.46	1.35	1.26	1.75	1.86	4.13	1.66
0.2	1.39	1.49	1.35	1.37	1.61	1.59	2.82	1.34
0.25	1.38	1.53	1.54	1.54	1.51	1.75	2.00	1.29
0.3	1.25	1.41	1.74	1.56	1.94	1.97	1.48	1.31
0.4	1.43	1.36	1.78	1.50	2.24	2.23	1.09	1.08
0.5	1.40	1.42	2.06	1.52	2.45	2.74	1.03	1.13
0.6	1.38	1.34	1.93	1.44	3.30	2.89	0.87	0.96
0.7	1.31	1.17	2.05	1.46	3.61	2.75	0.99	0.91
0.8	1.31	1.11	2.09	1.60	4.18	2.92	1.01	0.94
0.9	1.27	1.15	2.02	1.74	5.22	3.11	0.97	1.06
1	1.22	1.16	1.97	1.76	5.13	3.11	0.94	1.17
1.1	1.23	1.11	1.94	1.81	5.22	3.11	1.01	1.09
1.2	1.18	1.08	1.95	1.71	5.21	3.06	0.97	1.13
1.3	1.16	1.02	1.84	1.63	4.97	3.28	0.91	1.13
1.4	1.10	1.01	1.75	1.51	4.59	3.32	0.89	1.10
1.5	1.09	0.98	1.71	1.48	4.13	3.37	0.89	1.01
1.6	1.08	0.98	1.71	1.44	4.12	3.44	0.89	0.94
1.7	1.05	0.98	1.66	1.42	4.06	3.44	0.89	0.91
1.8	1.02	1.00	1.70	1.53	3.92	3.52	0.92	0.91
1.9	1.00	1.00	1.72	1.56	3.92	3.45	0.88	0.91
2	0.98	0.98	1.68	1.61	3.83	3.42	0.94	0.90

Table 4.10: SHARE-AUTH-DS2: Amplification factors, estimated with Approach 1 for new soil classes C1, C2 and C3. (different datasets)

T	C1 - Type 2	C1 - Type 1	C2 - Type 2	C2 - Type 1	C3 - Type 2	C3 - Type 1
0	1.42	1.57	1.48	1.47	1.43	1.70
0.05	1.37	1.32	1.18	1.27	1.20	1.45
0.1	1.79	1.19	1.08	1.21	1.39	1.51
0.15	1.59	1.39	1.17	1.17	1.41	1.55
0.2	1.53	1.64	1.34	1.30	1.79	1.66
0.25	1.57	1.71	1.54	1.66	2.21	1.73
0.3	1.46	1.94	1.88	1.68	2.33	1.73
0.4	1.72	2.25	2.22	1.78	2.85	2.11
0.5	1.84	2.52	2.38	2.17	3.41	2.21
0.6	1.75	2.52	2.27	2.35	3.66	2.57
0.7	1.70	2.70	2.62	2.25	4.10	2.58
0.8	1.78	2.86	2.54	2.10	4.11	2.54
0.9	1.98	2.96	2.61	1.79	4.35	2.77

1	1.93	2.80	2.45	1.69	4.25	2.89
1.1	2.11	2.76	2.40	1.65	4.43	2.96
1.2	2.02	2.98	2.43	1.52	4.66	3.09
1.3	1.93	2.92	2.33	1.49	4.38	3.02
1.4	1.93	2.93	2.32	1.49	4.75	3.01
1.5	1.96	3.03	2.38	1.39	4.24	2.96
1.6	1.75	2.91	2.49	1.39	4.11	2.97
1.7	1.63	2.75	2.53	1.34	3.90	2.84
1.8	1.65	2.63	2.45	1.32	3.53	2.74
1.9	1.58	2.53	2.32	1.29	3.56	2.62
2	1.54	2.57	2.26	1.25	3.66	2.53

Table 4.11: SHARE-AUTH-DS2: Soil factors for the new soil classes with Approach 1 (different datasets)

Soil Class	$M_s \leq 5.5$	$M_s > 5.5$
	Approach 1	Approach 1
B1	1.25	1.05
B2	1.77	1.33
C1	2.02	1.95
C2	1.86	1.26
C3	2.59	1.56
D	2.19	2.03
E	1.54	1.10

Table 4.12 summarizes the soil factors obtained for the new soil classes with Approach 1, using on the one hand the common dataset and on the other hand the different datasets. Soil factors values for classes with sufficient strong motion data in the common dataset (e.g. B1 and B2) obtained from the different datasets are very close to the ones obtained from the common dataset. This justifies the decision to use the different datasets for the cases where there were only few or even no available strong motion data in the common dataset.

Table 4.12: SHARE-AUTH-DS2: Soil factors for the new soil classes with Approach 1 obtained from common dataset compared to those obtained from the different datasets.

Soil Class	$M_s \leq 5.5$		$M_s > 5.5$	
	Approach 1 (common dataset)	Approach 1 (different datasets)	Approach 1 (common dataset)	Approach 1 (different datasets)
B1	1.28	1.25	1.03	1.05
B2	1.89	1.77	1.36	1.33
C1	2.36	2.02	2.19	1.95
C2	2.08	1.86	1.35	1.26
C3	2.29	2.59	1.57	1.56
D	1.98	2.19	1.69	2.03
E	-	1.54	0.93	1.10

4.3.2 Approach 2

Following the procedure that was described in detail in paragraph 3.2.1, period-independent amplification factors were estimated for the new soil classification system. Figures 4.25 to 4.38 illustrate the log average of distance-normalized response spectra for the different soil classes of the new classification system with respect to soil class A (A1+A2), for the different magnitude intervals.

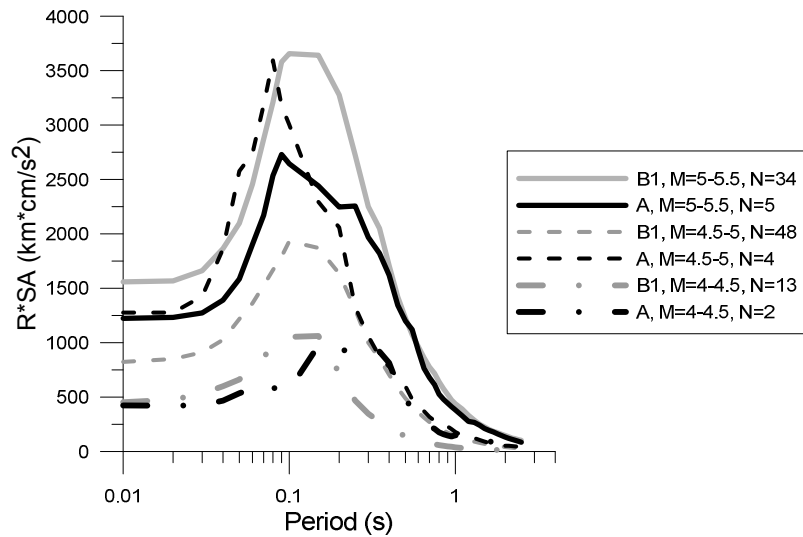


Figure 4.25: SHARE-AUTH-DS2: Log-average, distance-normalized acceleration response spectra for Type 2 magnitude intervals, for sites of soil class B1 (grey lines) and rock sites (black lines).

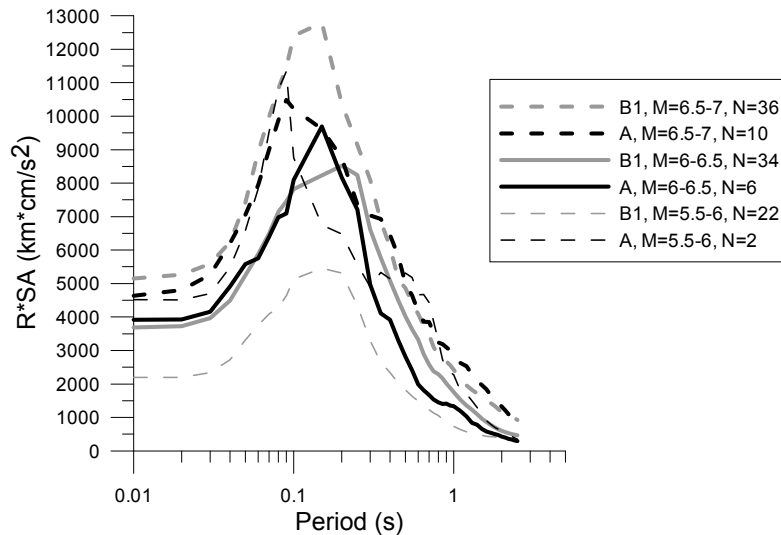


Figure 4.26: SHARE-AUTH-DS2: Log-average, distance-normalized acceleration response spectra for Type 1 magnitude intervals for sites of soil class B1 (grey lines) and rock sites (black lines).

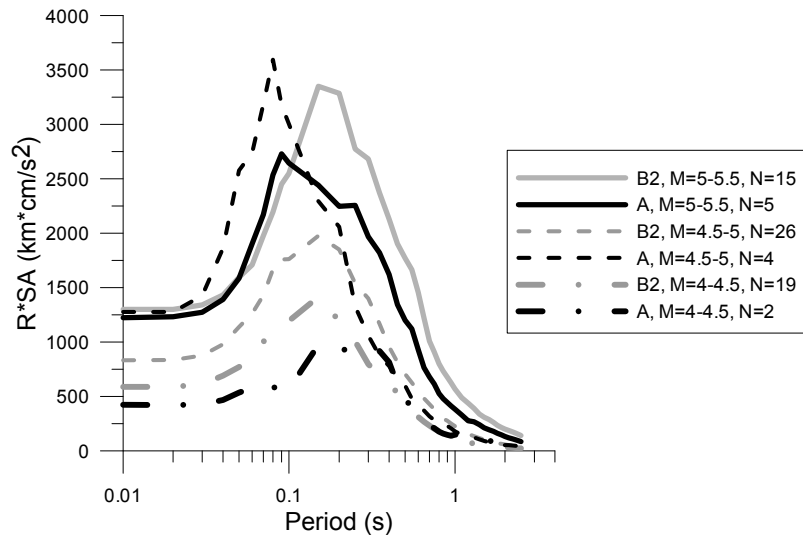


Figure 4.27: SHARE-AUTH-DS2: Log-average, distance-normalized acceleration response spectra for Type 2 magnitude intervals, for sites of soil class B2 (grey lines) and rock sites (black lines).

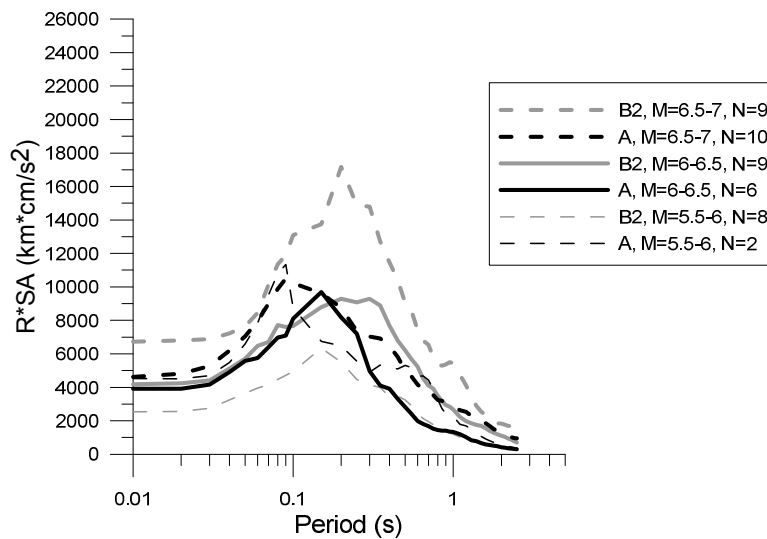


Figure 4.28: SHARE-AUTH-DS2: Log-average, distance-normalized acceleration response spectra for Type 1 magnitude intervals for sites of soil class B2 (grey lines) and rock sites (black lines).

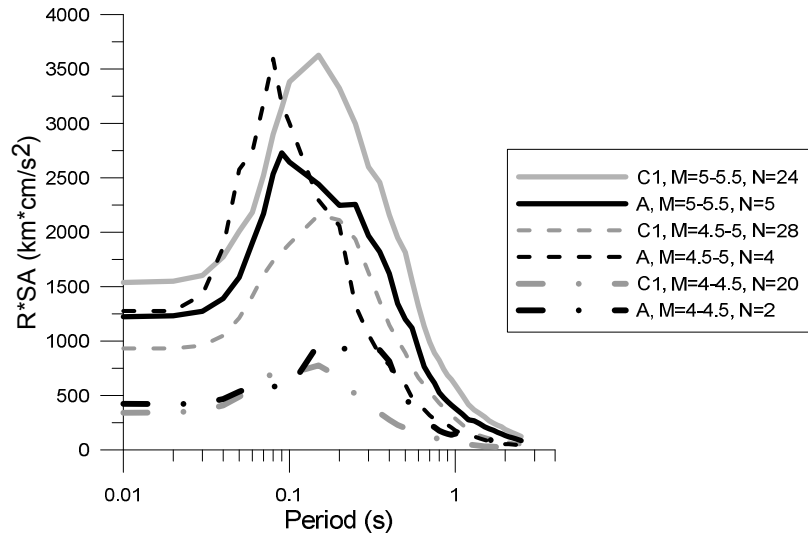


Figure 4.29: SHARE-AUTH-DS2: Log-average, distance-normalized acceleration response spectra for Type 2 magnitude intervals for sites of soil class C1 (grey lines) and rock sites (black lines).

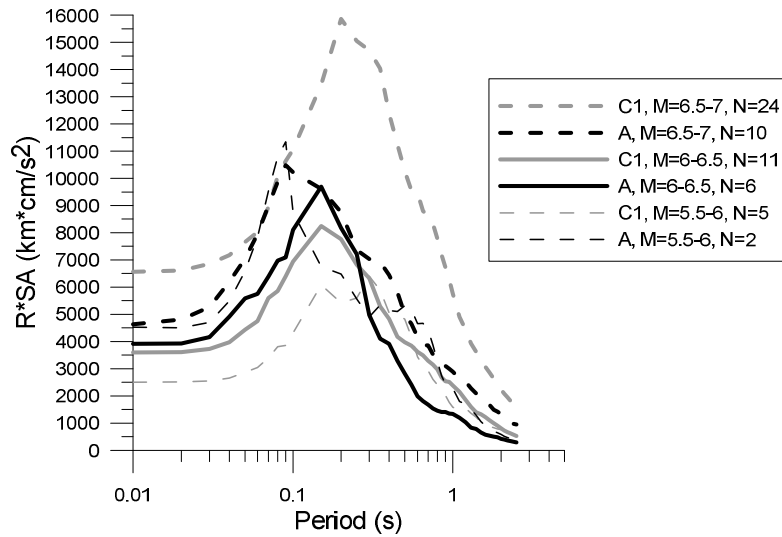


Figure 4.30: SHARE-AUTH-DS2: Log-average, distance-normalized acceleration response spectra for Type 1 magnitude intervals for sites of soil class C1 (grey lines) and rock sites (black lines).

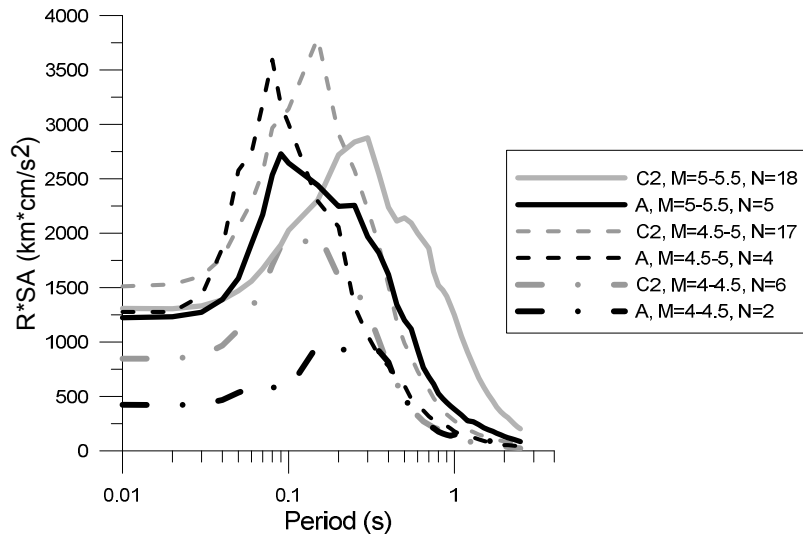


Figure 4.31: SHARE-AUTH-DS2: Log-average, distance-normalized acceleration response spectra for Type 2 magnitude intervals for sites of soil class C2 (grey lines) and rock sites (black lines).

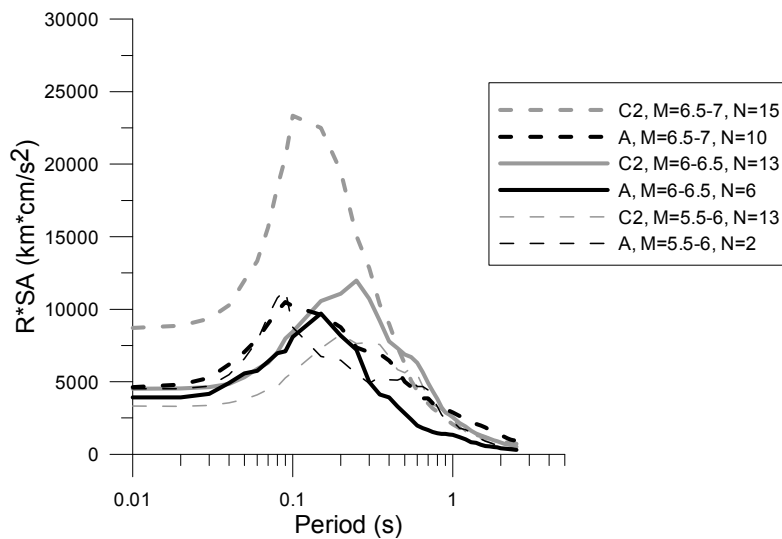


Figure 4.32: SHARE-AUTH-DS2: Log-average, distance-normalized acceleration response spectra for Type 1 magnitude intervals for sites of soil class C2 (grey lines) and rock sites (black lines).

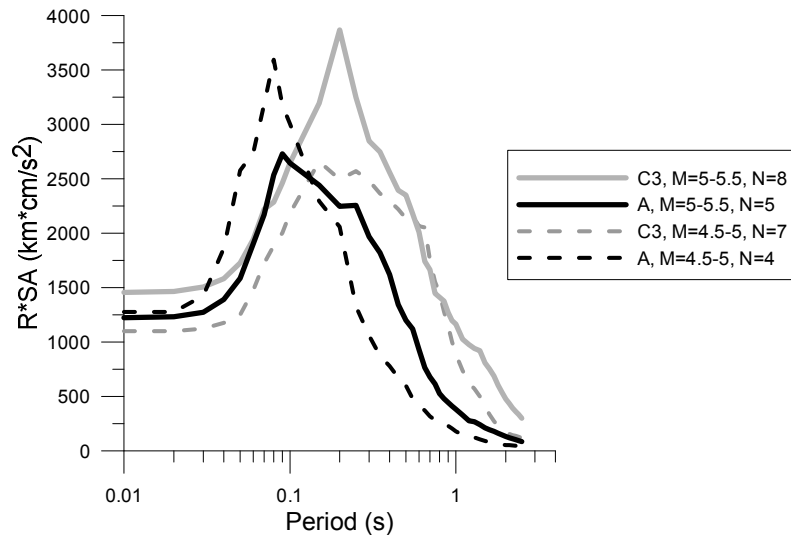


Figure 4.33: SHARE-AUTH-DS2: Log-average, distance-normalized acceleration response spectra for Type 2 magnitude intervals for sites of soil class C3 (grey lines) and rock sites (black lines).

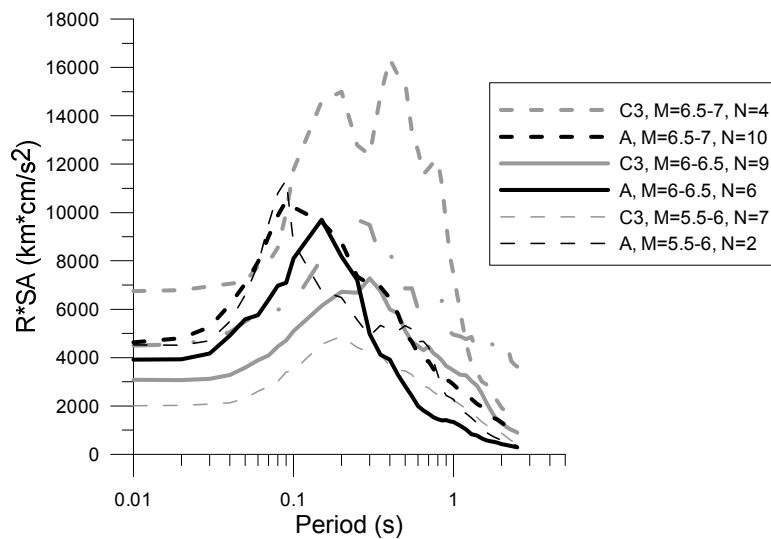


Figure 4.34: SHARE-AUTH-DS2: Log-average, distance-normalized acceleration response spectra for Type 1 magnitude intervals for sites of soil class C3 (grey lines) and rock sites (black lines).

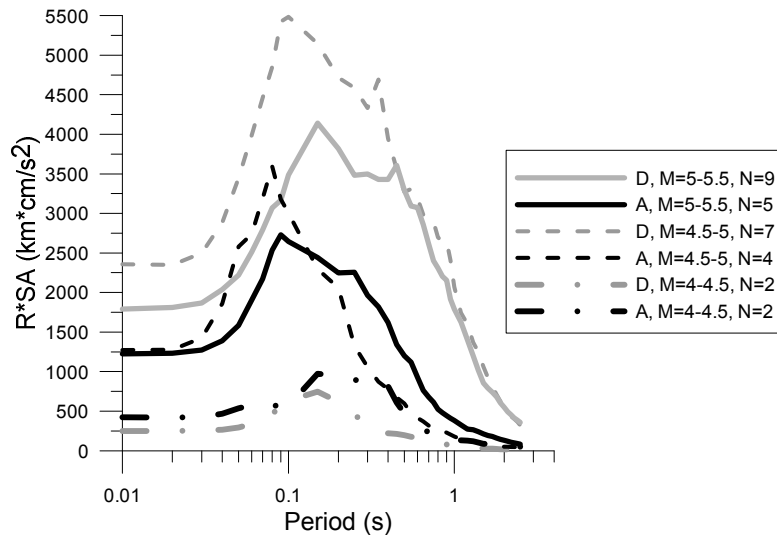


Figure 4.35: SHARE-AUTH-DS2: Log-average, distance-normalized acceleration response spectra for Type 2 magnitude intervals for sites of soil class D (grey lines) and rock sites (black lines).

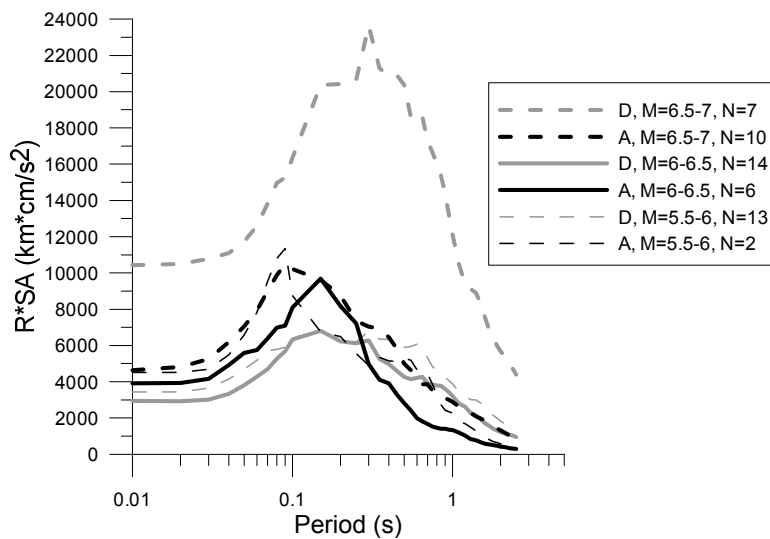


Figure 4.36: SHARE-AUTH-DS2: Log-average, distance-normalized acceleration response spectra for Type 1 magnitude intervals for sites of soil class D (grey lines) and rock sites (black lines).

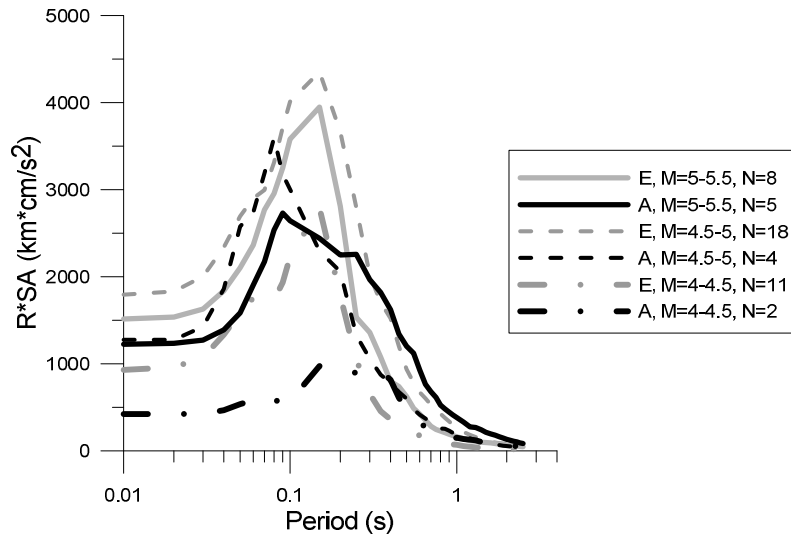


Figure 4.37: SHARE-AUTH-DS2: Log-average, distance-normalized acceleration response spectra for Type 2 magnitude intervals for sites of soil class E (grey lines) and rock sites (black lines).

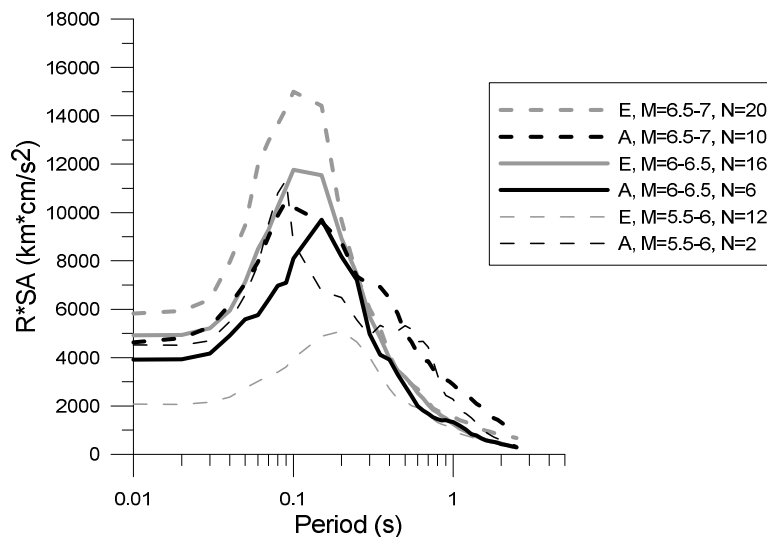


Figure 4.38: SHARE-AUTH-DS2: Log-average, distance-normalized acceleration response spectra for Type 1 magnitude intervals for sites of soil class E (grey lines) and rock sites (black lines).

I_{soil}/I_A ratios for all magnitude intervals and all soil classes are presented in Tables 4.13 to 4.19. The tables also contain the number of available strong motion records for each case. Again it is observed that the sample is not always sufficient for all magnitude intervals, especially for soil class A. The magnitude intervals (M.I.) with a satisfactory number of available strong motion records for both soil and rock are depicted in bold. The PGA range for each soil class and magnitude interval is also provided, with the number in the parenthesis representing the median PGA value for each case.

Table 4.13: SHARE-AUTH-DS2: I_{soil}/I_A ratio for soil class B1 and all magnitude intervals.

$M_s \leq 5.5$				$M_s > 5.5$			
M_s	I_{B1}/I_A	$n(B1)/n(A)$	PGA (cm/s ²)	M_s	I_{B1}/I_A	$n(B1)/n(A)$	PGA (cm/s ²)
4.0-4.5	0.49	13/2	≤ 94 (48)	5.5-6.0	0.48	22/2	≤ 411 (41)
4.5-5.0	0.78	48/4	≤ 261 (38)	6.0-6.5	1.25	34/6	≤ 480 (85)
5.0-5.5	1.20	34/5	≤ 363 (46)	6.5-7.0	0.99	36/10	≤ 545 (79)

Table 4.14: SHARE-AUTH-DS2: I_{soil}/I_A ratio for soil class B2 and all magnitude intervals.

$M_s \leq 5.5$				$M_s > 5.5$			
M_s	I_{B2}/I_A	$n(B2)/n(A)$	PGA (cm/s ²)	M_s	I_{B2}/I_A	$n(B2)/n(A)$	PGA (cm/s ²)
4.0-4.5	0.98	19/2	≤ 157 (38)	5.5-6.0	0.64	8/2	≤ 203 (33)
4.5-5.0	0.98	26/4	≤ 226 (46)	6.0-6.5	1.76	9/6	≤ 590 (145)
5.0-5.5	1.37	15/5	≤ 261 (32)	6.5-7.0	1.64	9/10	≤ 415 (77)

Table 4.15: SHARE-AUTH-DS2: I_{soil}/I_A ratio for soil class C1 and all magnitude intervals.

$M_s \leq 5.5$				$M_s > 5.5$			
M_s	I_{C1}/I_A	$n(C1)/n(A)$	PGA (cm/s ²)	M_s	I_{C1}/I_A	$n(C1)/n(A)$	PGA (cm/s ²)
4.0-4.5	0.53	20/2	≤ 69 (29)	5.5-6.0	0.86	5/2	≤ 251 (84)
4.5-5.0	1.16	28/4	≤ 215 (55)	6.0-6.5	1.36	11/6	≤ 445 (114)
5.0-5.5	1.40	24/5	≤ 332 (80)	6.5-7.0	1.84	24/10	≤ 1302 (377)

Table 4.16: SHARE-AUTH-DS2: I_{soil}/I_A ratio for soil class C2 and all magnitude intervals.

$M_s \leq 5.5$				$M_s > 5.5$			
M_s	I_{C2}/I_A	$n(C2)/n(A)$	PGA (cm/s ²)	M_s	I_{C2}/I_A	$n(C2)/n(A)$	PGA (cm/s ²)
4.0-4.5	1.29	6/2	≤ 151 (40)	5.5-6.0	1.06	13/2	≤ 198 (46)
4.5-5.0	1.52	17/4	≤ 188 (42)	6.0-6.5	1.83	13/6	≤ 243 (40)
5.0-5.5	1.79	18/5	≤ 246 (42)	6.5-7.0	1.26	15/10	≤ 661 (79)

Table 4.17: SHARE-AUTH-DS2: I_{soil}/I_A ratio for soil class C3 and all magnitude intervals.

$M_s \leq 5.5$				$M_s > 5.5$			
M_s	I_{C3}/I_A	$n(C3)/n(A)$	PGA (cm/s ²)	M_s	I_{C3}/I_A	$n(C3)/n(A)$	PGA (cm/s ²)
4.0-4.5	0.00	0/2		5.5-6.0	0.80	7/2	≤ 335 (116)
4.5-5.0	2.41	7/4	≤ 169 (79)	6.0-6.5	1.75	9/6	≤ 217 (61)
5.0-5.5	2.04	8/5	≤ 66 (35)	6.5-7.0	2.08	4/10	≤ 448 (140)

Table 4.18: SHARE-AUTH-DS2: I_{soil}/I_A ratio for soil class D and all magnitude intervals.

$M_s \leq 5.5$				$M_s > 5.5$			
M_s	I_D/I_A	$n(D)/n(A)$	PGA (cm/s ²)	M_s	I_D/I_A	$n(D)/n(A)$	PGA (cm/s ²)
4.0-4.5	0.47	2/2	≤ 135 (80)	5.5-6.0	1.46	13/2	≤ 424 (53)
4.5-5.0	4.87	7/4	≤ 159 (67)	6.0-6.5	1.57	14/6	≤ 221 (55)
5.0-5.5	2.69	9/5	≤ 245 (57)	6.5-7.0	3.59	7/10	≤ 443 (274)

Table 4.19: SHARE-AUTH-DS2: I_{soil}/I_A ratio for soil class E and all magnitude intervals.

$M_s \leq 5.5$				$M_s > 5.5$			
M_s	I_E/I_A	$n(E)/n(A)$	PGA (cm/s ²)	M_s	I_E/I_A	$n(E)/n(A)$	PGA (cm/s ²)
4.0-4.5	1.04	11/2	≤ 126 (42)	5.5-6.0	0.54	12/2	≤ 152 (41)
4.5-5.0	1.60	18/4	≤ 403 (40)	6.0-6.5	1.13	16/6	≤ 242 (74)
5.0-5.5	0.75	8/5	≤ 322 (77)	6.5-7.0	0.78	20/10	≤ 414 (77)

Table 4.20 gives the I_{soil}/I_A ratios for the soil classes of the new classification scheme and for the two seismicity contexts. I_{soil}/I_A coefficients of Table 4.20 were calculated as the mean values of the coefficients from the magnitude intervals considered as more reliable (in bold). The actual amplification factors S, as derived by equation (4) are given in Table 4.21.

Table 4.20: SHARE-AUTH-DS2: I_{soil}/I_A ratios for the new soil classes and both seismicity contexts

Soil Class	$M_s \leq 5.5$		$M_s > 5.5$	
	Selected M.I.	I_{soil}/I_A	Selected M.I.	I_{soil}/I_A
B1	4.5-5.0, 5.0-5.5	0.99	6.0-6.5, 6.5-7.0	1.12
B2	4.5-5.0, 5.0-5.5	1.17	6.0-6.5, 6.5-7.0	1.70
C1	4.5-5.0, 5.0-5.5	1.28	6.0-6.5, 6.5-7.0	1.60
C2	4.5-5.0, 5.0-5.5	1.66	6.0-6.5, 6.5-7.0	1.55
C3	4.5-5.0, 5.0-5.5	2.22	6.0-6.5, 6.5-7.0	1.91
D	4.5-5.0, 5.0-5.5	3.78	6.0-6.5, 6.5-7.0	2.58
E	4.5-5.0, 5.0-5.5	1.18	6.0-6.5, 6.5-7.0	0.96

Table 4.21: SHARE-AUTH-DS2: Soil factors for the new soil classes with Approach 2

Soil Class	$M_s \leq 5.5$	$M_s > 5.5$
	Approach 2	Approach 2
B1	1.02	1.02
B2	1.17	1.47
C1	1.47	1.24
C2	1.38	1.20
C3	1.61	1.18
D	2.26	1.83
E	1.44	0.96

Summary

The values of the soil factors for the new classification system obtained with the two different approaches are summarized in Tables 4.22 and 4.23. As far as Approach 1 is concerned, the results from the analyses with both the common and the different datasets are presented. For the cases where there were only few available strong motion data in the common dataset, the results obtained from the different datasets were considered as more reliable. Since both approaches were assigned a weighting factor equal to 0.5, the weighted average values are the mean of the values obtained with the two approaches considered. The weighted average soil factors considered as more reliable for each soil class and seismicity type, based on the dataset used for Approach 1 (common or different datasets), are depicted in bold.

Table 4.22: SHARE-AUTH-DS2: Soil factors for the new classification system obtained with Approaches 1 and 2, and weighted average for $M_s \leq 5.5$.

Soil Class	$M_s \leq 5.5$				
	Approach 1		Approach 2	Weighted Average	
	Common dataset	Different datasets		Common dataset	Different datasets
B1	1.28	1.25	1.02	1.15	1.13
B2	1.89	1.77	1.17	1.53	1.47
C1	2.36	2.02	1.47	1.91	1.75
C2	2.08	1.86	1.38	1.73	1.62
C3	2.29	2.59	1.61	1.95	2.10
D	1.98	2.19	2.26	2.12	2.23
E	-	1.54	1.44	-	1.49

Table 4.23: SHARE-AUTH-DS2: Soil factors for the new classification system obtained with Approaches 1 and 2, and weighted average for $M_s > 5.5$.

Soil Class	$M_s > 5.5$				
	Approach 1		Approach 2	Weighted Average	
	Common dataset	Different datasets		Common dataset	Different datasets
B1	1.03	1.05	1.02	1.02	1.04
B2	1.36	1.33	1.47	1.41	1.40
C1	2.19	1.95	1.24	1.72	1.60
C2	1.35	1.26	1.20	1.28	1.23
C3	1.57	1.56	1.18	1.38	1.37
D	1.69	2.03	1.83	1.76	1.93
E	0.93	1.10	0.96	0.95	1.03

4.3.3 Amplification factors for soil class E with Kik-net records

We observe that for soil class E-Type 1, the calculated S factors are very close to, or even below unity, regardless of the method used, as was the case for Eurocode 8 soil class E. This is due on one hand to the averaging process that both methods use, which was already commented on in Chapter 3, and on the other hand the poor number of available records.

The seismological documentation of soil class E stations of the database is also quite poor, since parameters such as R_{jb} or R_{up} are unknown in most of the cases. As a result, for Approach 1, the C&Y GMPE could not be applied for events with $M_s \leq 5.5$, while the A&B GMPE could be applied for only 8 events with $M_s \leq 5.5$ and 4 events with $M_s > 5.5$. It was therefore decided to apply a complementary approach in addition to the previous two, by estimating amplification directly from surface and bedrock records from Kik-net stations, which are accurately classified as soil class E.

20 pairs of surface and bedrock records from 10 Kik-Net stations were carefully selected (see Appendix II), classified as soil class E. The procedure that was applied to estimate the amplification factors is the following:

- Surface and bedrock acceleration response spectra were first calculated for each pair of records.
- Then for each pair of acceleration response spectra we calculated the spectrum intensities $I_{surface}$ and $I_{bedrock}$, originally defined by Housner (1952) for spectral velocities and here adapted for spectral accelerations, using the following equation:

$$I = \int_{0.05}^{2.5} S_A(T) dt \quad (7)$$

Figure 4.39 illustrates an example of the calculated acceleration response spectra for station HYGH08.

- Soil amplification factors for each pair of records were calculated using the following equation as:

$$S = \frac{I_{surface}}{2 \cdot I_{bedrock}} \quad (8)$$

where 2 is a coefficient used to rough-estimate the free-surface effect, ignoring at this first stage the downgoing waves.

- Finally the calculated amplification factors were grouped in two magnitude categories ($M_s \leq 5.5$ and $M_s > 5.5$), and median amplification factors were estimated for each category. The calculated amplification factors are given in Table 4.24. These factors are clearly more realistic reflecting the theoretical background and physics of the amplification ground motion related to soil category E.

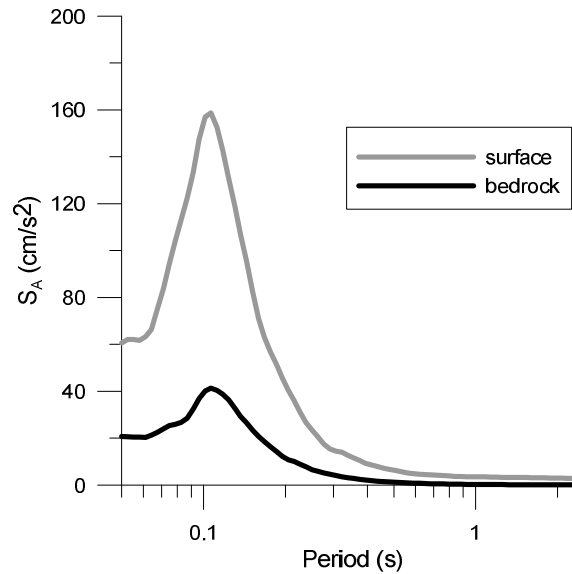


Figure 4.39: Surface and Bedrock acceleration response spectra for an $M_s=4.2$ event recorded at Kik-Net station HYGH08.

Table 4.24: Soil amplification factors for selected Kik-Net soil class E stations

$M_s \leq 5.5$			$M_s > 5.5$		
Site code	M_s	S	Site code	M_s	S
EHHM02	4.34	1.46	EHHM02	6.09	1.34
EHHM02	3.50	2.64	EHHM07	6.09	1.09
HYGH08	4.23	2.31	NARH05	6.67	2.87
NARH05	5.03	3.94	SIGH01	7.45	0.88
NARH05	3.50	6.36	SMNH04	7.31	1.21
SIGH01	4.23	1.30	SMNH04	6.09	1.32
SIGH01	4.13	1.24	TKSH02	6.09	2.85
SIGH02	4.23	1.15	WKYH02	7.45	1.67
TKSH02	4.02	4.11	WKYH02	6.67	1.58
WKYH06	4.13	1.28	WKYH06	6.67	0.87
<i>Median:</i>		1.89	<i>Median:</i>		1.33

4.3.4 Proposed amplification factors

The finally proposed S factors for the soil classes of the new classification scheme were determined by approximating and rounding (usually to slightly higher values) the weighted average of the values obtained from the two approaches, applying the logic tree approach which was presented in Figure 3.17. In case of excessively or “unrealistically” high values (i.e. for soil class D, Type 2 earthquakes) the proposed factor is lowered to more realistic values.

For soil class E the proposed amplification factors are calculated from the analyses of records selected from Kik-Net (see paragraph 4.3.3). The final proposed S factors for the new soil classification system are given in Table 4.25.

Table 4.25: SHARE-AUTH-DS2: Weighted average soil factors for the new classification system and proposed values

Soil Class	$M_s \leq 5.5$			$M_s > 5.5$		
	Weighted Average		Proposed	Weighted Average		Proposed
	Common dataset	Different datasets		Common dataset	Different datasets	
B1	1.15	1.13	1.2	1.02	1.04	1.1
B2	1.53	1.47	1.5	1.41	1.40	1.4
C1	1.91	1.75	1.8	1.72	1.60	1.7
C2	1.73	1.62	1.7	1.28	1.23	1.3
C3	1.95	2.10	2.1	1.38	1.37	1.4
D	2.12	2.23	2.0	1.76	1.93	1.8
E	-	1.49	1.8**	0.95	1.03	1.4**

** estimated from Kik-Net surface and bedrock strong-motion records

4.3.5 Validation with theoretical analyses

In order to validate the results of this study and the new classification system with the corresponding amplification factors and normalized response spectra, which was based entirely on experimental data (records), the estimated soil amplification factors were compared to soil amplification factors estimated from theoretical analyses of various representative models of realistic site conditions. This is not really a “strict” validation, as a-priori the experimental results should be considered more accurate compared to the theoretical ones. However it is made as a crosscheck of the “realism” of the proposed classification system and amplification factors following common engineering practice, as well as numerous results of the literature which have shown that dynamic soil models in general reproduce observed behavior.

The soil profiles that were selected in this validation analysis cover an important range of different realistic soil conditions and all the soil classes of the new proposed soil classification system. The soil models used in the analysis are selected from an extended database (AUTH) of high quality geotechnical and geophysical data of representative soil profiles and well-documented Strong Motion sites found worldwide. It comprises homogeneous clayey and sandy, as well as, ‘mixed soil’ models with various physical and mechanical properties and non-homogeneous models having at different depths a ‘lower stiffness’ layer of variable thickness, laying in bedrock with shear wave velocity from 750m/s to 2000m/s. The range of the main parameters of the theoretical soil models that were used in the analyses, as well as the number of sites and analyses for each soil class are described in Table 4.26.

Table 4.26. Range of parameters of soil models used in the theoretical analyses, number of sites and number of analyses for each soil class

Soil Class	H_{bedrock} (m)	T_0 (s)	$V_{s,av}$ (m/s)	Number of sites		Number of analyses	
				Type 2	Type 1	Type 2	Type 1
B1	20-32	0.189-0.250	423-528	4	2	15	8
B2	40-60	0.341-0.796	325-525	4	3	24	25
C1	80-110	0.457-0.978	500-700	20	19	96	128
C2	20-40	0.360-0.607	225-275	2	2	10	12
C3	80	1.067	300	2	2	10	14
D	20-100	0.573-1.533	100-418	30	30	54	132
E	10-20	0.2-0.55	130-250	12	12	72	72

For the selected soil profiles, 1D equivalent linear (EQL) site response analyses were performed using CYBERQUAKE computer code (Modaressi and Foerster, 2000). It should be also acknowledged that this analysis is not always very reliable especially for very deep profiles and shallow high impedance profiles. In particular it is known that in case of deep profiles or in case of shallow profiles with high impedance contrast and/or high seismically induced shear strain levels, the theoretical 1D analyses have the tendency to overestimate or underestimate the ground response amplification in certain frequencies, and hence the results may not be always reliable.

Twelve real accelerograms were considered in the analyses, with PGA values ranging from 0.1g to 0.7g. The normalized response spectra of the selected accelerograms are presented in Figure 4.40. More than 650 analyses were performed with the various selected representative soil models to generate acceleration time history and the corresponding response spectrum with 5% damping ratio at ground surface. Period dependent amplification factors were then determined in terms of surface to input motion (bedrock) for two levels of expected seismic intensity at rock site (Type 1 – $PGA_{\text{rock}} > 0.20g$, Type 2 – $PGA_{\text{rock}} < 0.20g$). The boundary of 0.20g for PGA_{rock} was considered as equivalent to the boundary of 5.5 for M_s , which is used in EC8 and was also adopted in the present study.

Figures 4.41 to 4.47 illustrate the median amplification factors resulting from the theoretical analyses described above, along with the 16th and 84th percentiles, for Type 1 and Type 2 expected intensity in rock site (Type 1 – $PGA_{\text{rock}} > 0.20g$, Type 2 – $PGA_{\text{rock}} < 0.20g$). The theoretical amplification factors are compared to the period-dependent amplification factors derived in Approach 1, as well as to the proposed acceleration spectra for each soil class, normalized by the proposed acceleration spectrum for soil class A.

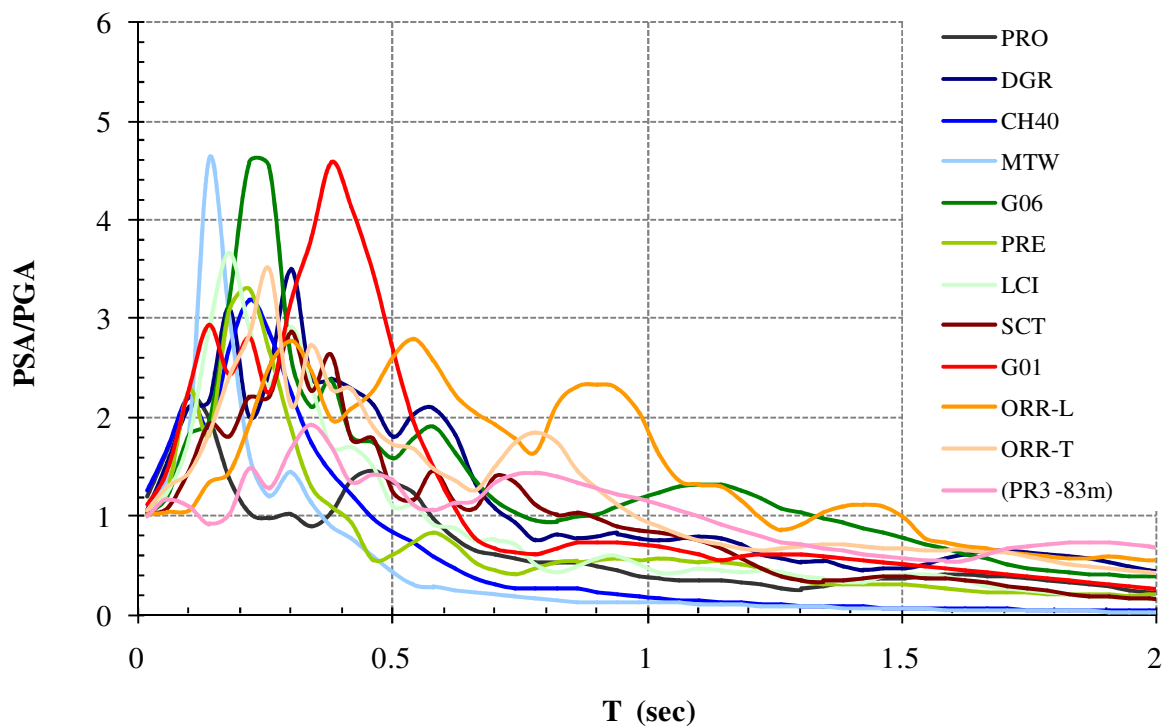


Figure 4.40: Normalized acceleration response spectra of the twelve accelerograms used for the theoretical analyses.

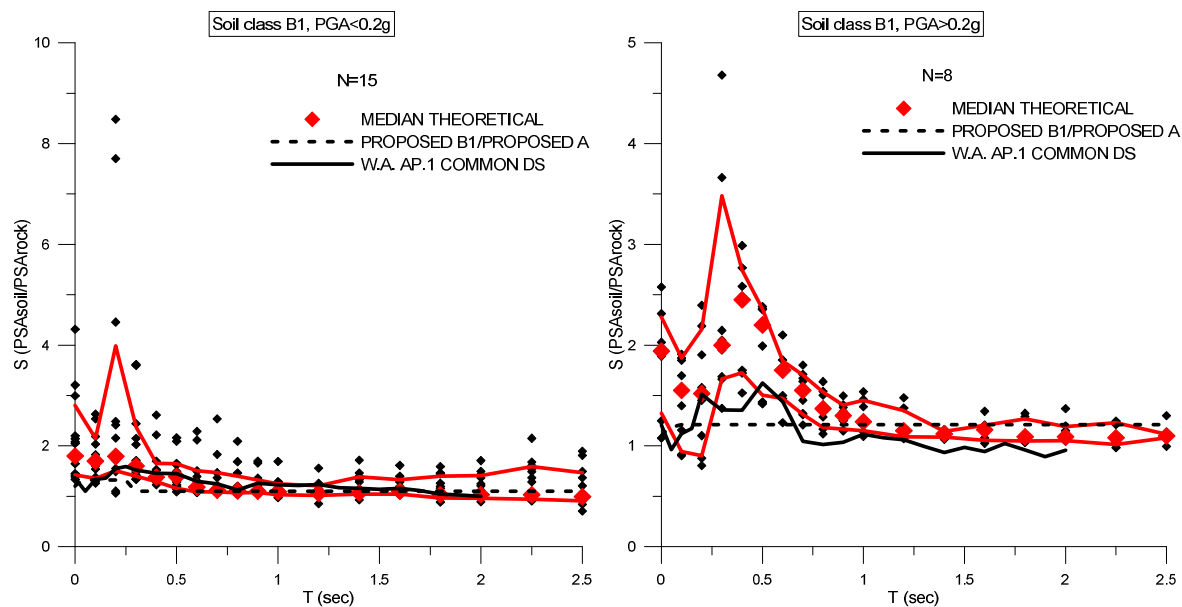


Figure 4.41: Amplification factors estimated from theoretical analyses for soil class B1, for Type 2 seismicity (left) and Type 1 seismicity (right). The red lines represent the 16th and 84th percentiles of the theoretical factors.

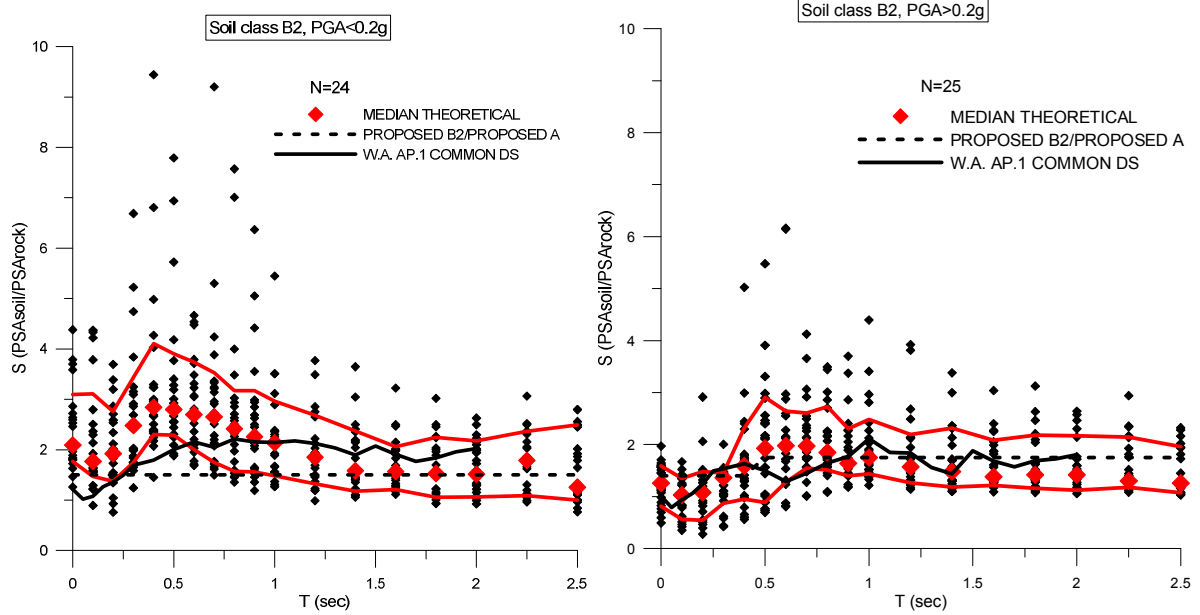


Figure 4.42: Amplification factors estimated from theoretical analyses for soil class B2, for Type 2 seismicity (left) and Type 1 seismicity (right). The red lines represent the 16th and 84th percentiles of the theoretical factors.

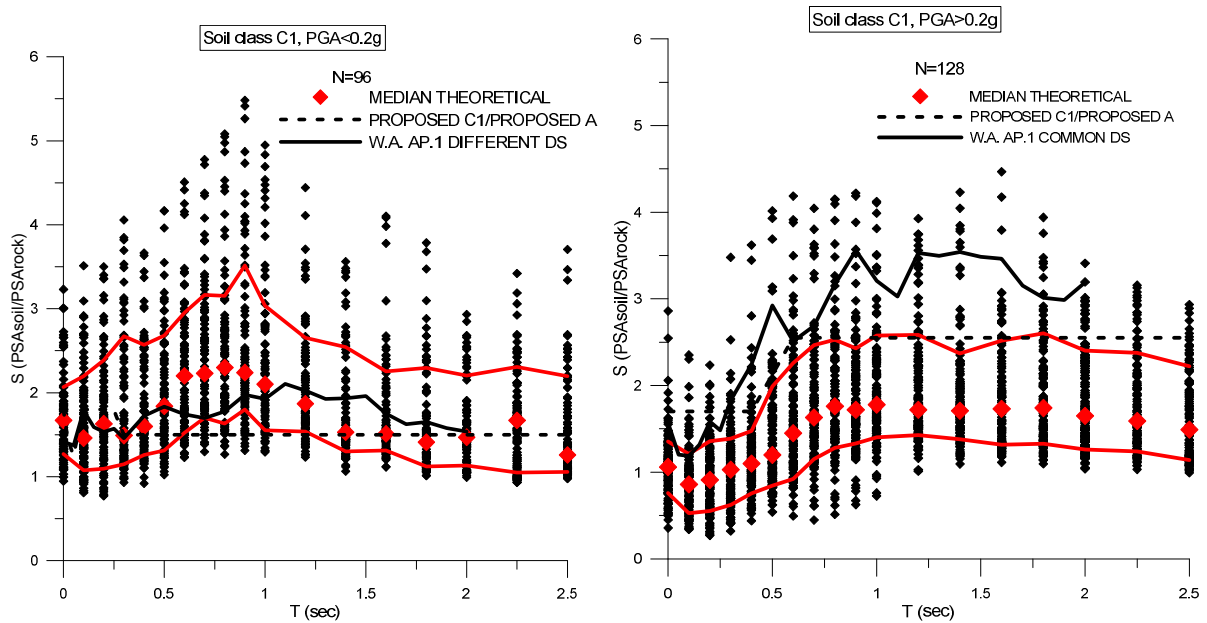


Figure 4.43: Amplification factors estimated from theoretical analyses for soil class C1, for Type 2 seismicity (left) and Type 1 seismicity (right). The red lines represent the 16th and 84th percentiles of the theoretical factors.

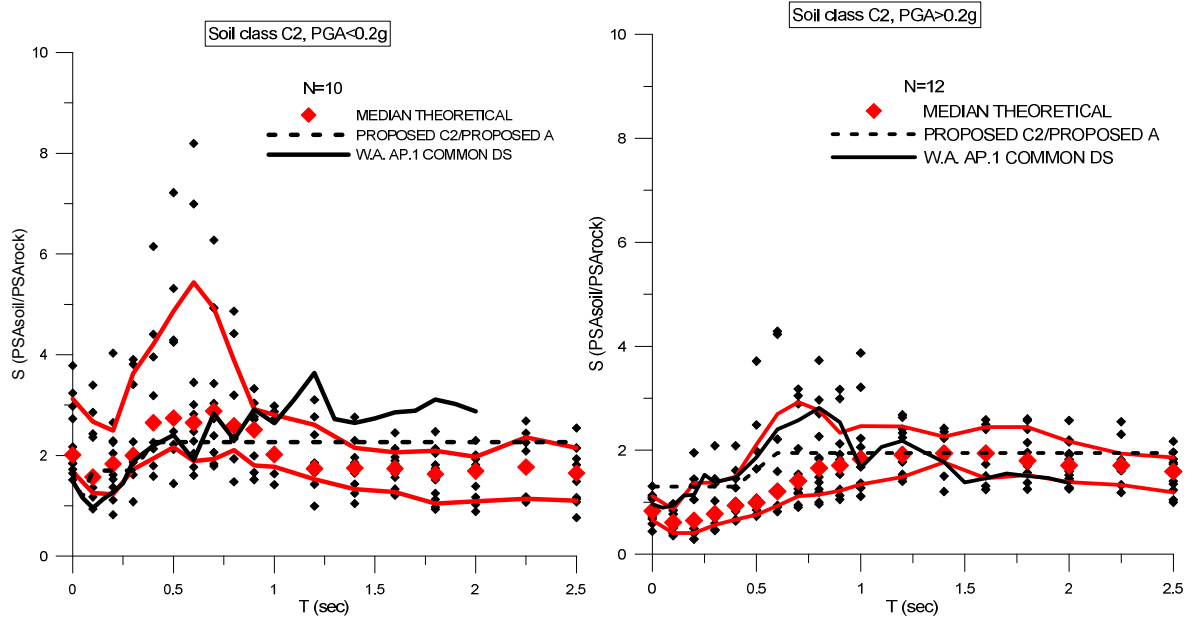


Figure 4.44: Amplification factors estimated from theoretical analyses for soil class C2, for Type 2 seismicity (left) and Type 1 seismicity (right). The red lines represent the 16th and 84th percentiles of the theoretical factors.

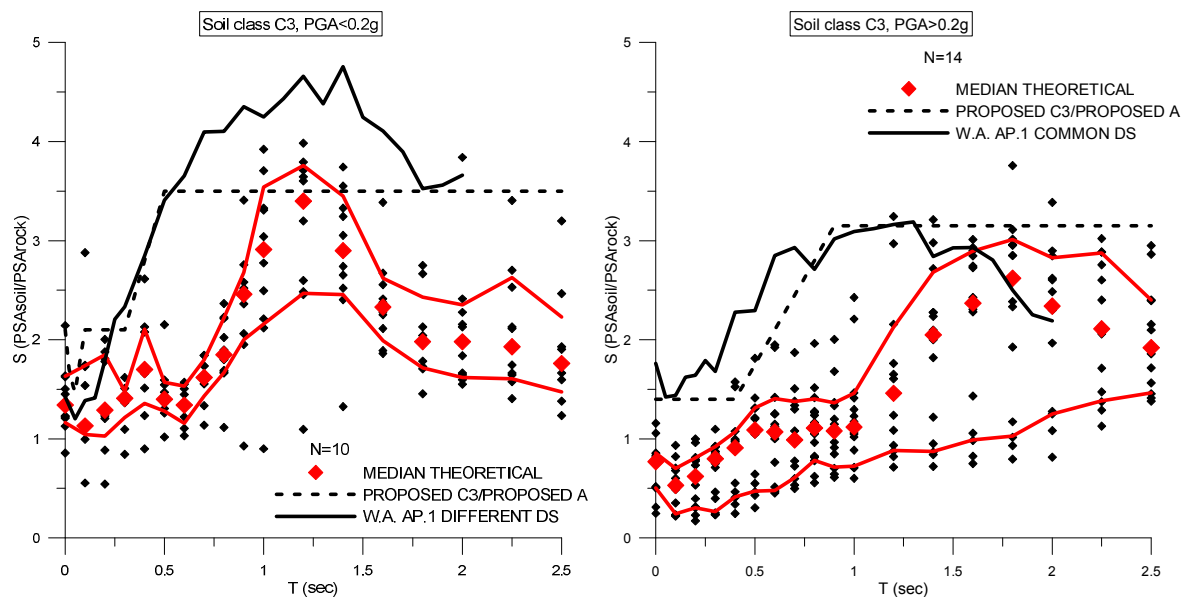


Figure 4.45: Amplification factors estimated from theoretical analyses for soil class C3, for Type 2 seismicity (left) and Type 1 seismicity (right). The red lines represent the 16th and 84th percentiles of the theoretical factors.

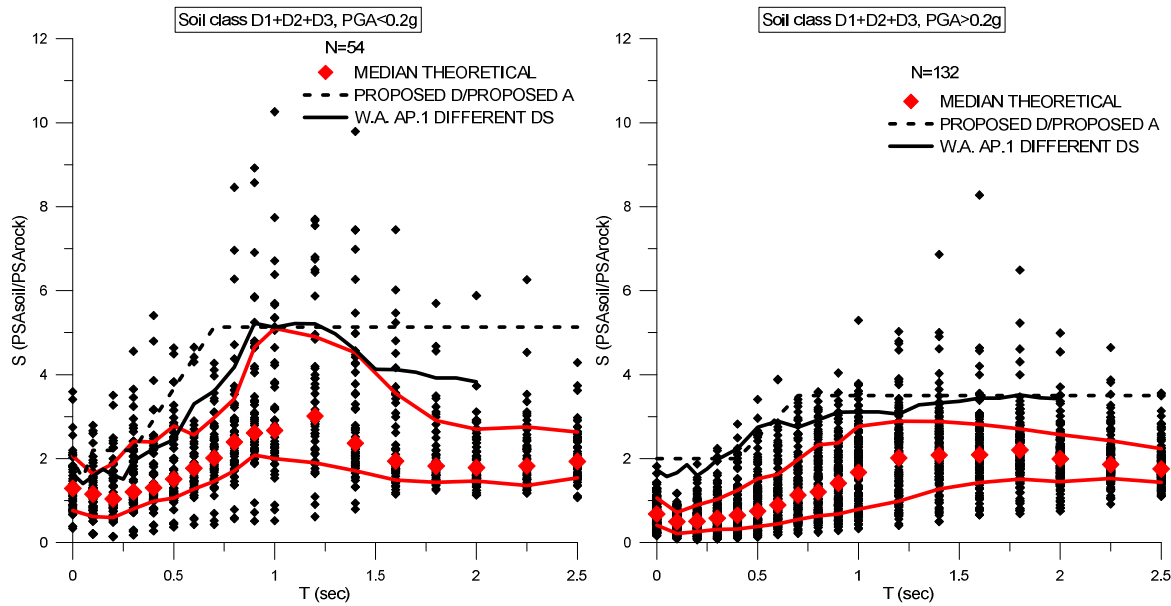


Figure 4.46: Amplification factors estimated from theoretical analyses for soil class D, for Type 2 seismicity (left) and Type 1 seismicity (right). The red lines represent the 16th and 84th percentiles of the theoretical factors.

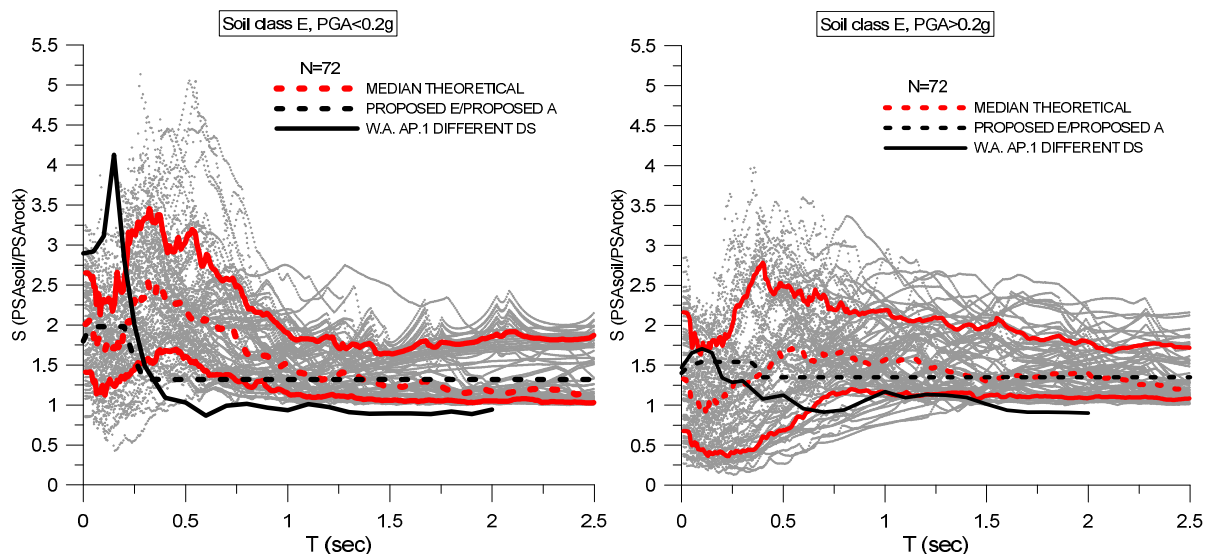


Figure 4.47: Amplification factors estimated from theoretical analyses for soil class E, for Type 2 seismicity (left) and Type 1 seismicity (right). The red lines represent the 16th and 84th percentiles of the theoretical factors.

In general the comparison is satisfactory. In most cases, the new amplification factors lie close to the median or 84th percentile of the theoretical amplification factors. The calculated site coefficients for sites of class B1 and B2 exhibit maximum (median) values ranging from 1.9 to 2.5 for periods of 0.1-0.5s and from 2.0-3.0 for periods 0.2-0.8s, respectively. The observed differences and the resulted scatter of amplification values are mainly attributed to the coincidence of predominant period of input motion (0.1 to 0.4s) and predominant period of soil profile (0.19 to 0.8s), which results in ‘high’ calculated values of site coefficients for low periods and ‘low’ site coefficients for higher periods. The theoretically derived site

coefficients for sites C1 and C2 exhibit maximum (median) values which fit reasonably well with the proposed amplification factors especially in the case of Type 2 seismicity. The expected problems mentioned above concerning the accuracy and the applicability of theoretical 1D analyses are, however, evident in case of low soil stiffness models and deep profiles (Figures 4.45 and 4.46 - soil classes C3 and D according to the new classification system), where the theoretical 1D EQL analyses tend to underestimate amplification for a wide range of periods, compared to the experimental results of Approach 1.

4.4 Proposed acceleration response spectra and amplification factors for the new soil classes

The equations describing the proposed elastic acceleration spectra for 5% viscous damping are the following:

$$0 \leq T \leq T_B : \frac{S_a(T)}{a_g} = S \cdot \left[1 + \frac{T}{T_B} \cdot (\beta - 1) \right] \quad (9)$$

$$T_B \leq T \leq T_C : \frac{S_a(T)}{a_g} = S \cdot \beta \quad (10)$$

$$T_C \leq T \leq T_D : \frac{S_a(T)}{a_g} = S \cdot \beta \cdot \frac{T_C}{T} \quad (11)$$

$$T_D \leq T : \frac{S_a(T)}{a_g} = S \cdot \beta \cdot T_C \cdot \left(\frac{T_D}{T^2} \right) \quad (12)$$

where a_g is the design ground acceleration at rock-site conditions, T_B and T_C are the limits of the constant spectral acceleration branch, T_D is the value defining the beginning of the change of the slope branch and the beginning of the constant spectral displacement range of the spectrum, β is the spectral amplification parameter and S is the soil amplification factor. Table 4.27 presents the proposed parameters (control periods T_B , T_C , T_D , spectral amplification parameter β and soil amplification factor S) for each site category of Table 4.1 and the two levels of earthquake intensity ($M_s \leq 5.5$ and $M_s > 5.5$). Table 4.28 shows the values of S and β parameters of the new classification system compared to the corresponding values of EC8 soil classes.

Table 4.27: Parameters of proposed acceleration response spectra

Soil Class	Type 2 ($M_s \leq 5.5$)					Type 1 ($M_s > 5.5$)				
	T_B (sec)	T_C (sec)	T_D (sec)	S	β	T_B (sec)	T_C (sec)	T_D (sec)	S	β
A	0.05	0.3	1.2	1.0	2.5	0.1	0.4	2	1.0	2.5
B1	0.05	0.25	1.2	1.2	2.75	0.1	0.4	2	1.1	2.75
B2	0.05	0.3	1.2	1.5	2.5	0.1	0.5	2	1.4	2.5
C1	0.1	0.25	1.2	1.8	2.5	0.1	0.6	2	1.7	2.5
C2	0.1	0.4	1.2	1.7	2.5	0.1	0.6	2	1.3	2.5
C3	0.1	0.5	1.2	2.1	2.5	0.1	0.9	2	1.4	2.5
D	0.1	0.7	1.2	2.0	2.5	0.1	0.7	2	1.8	2.5
E	0.05	0.2	1.2	1.8	2.75	0.1	0.35	2	1.4	2.75

Table 4.28: Comparison of parameters S and β of the proposed soil classification system with EC8

Soil Category		Type 2 ($M \leq 5.5$)				Type 1 ($M > 5.5$)			
Proposed	EC8	S	S (EC8)	β	β (EC8)	S	S (EC8)	β	β (EC8)
A	A	1	1.0	2.5	2.5	1.0	1.0	2.5	2.5
B1	B	1.2	1.35	2.75	2.5	1.1	1.2	2.75	2.5
B2		1.5		2.5		1.4		2.5	
C1	C	1.8	1.5	2.5	2.5	1.7	1.15	2.5	2.5
C2		1.7		2.5		1.3		2.5	
C3		2.1		2.5		1.4		2.5	
D (D1&D2&D3)	D	2.0	1.8	2.5	2.5	1.8	1.35	2.5	2.5
E	E	1.8	1.6	2.75	2.5	1.4	1.4	2.75	2.5

The elastic acceleration response spectra for Type 2 and Type 1 seismicity, normalized by design ground acceleration at rock-site conditions a_g , are illustrated in Figures 4.48 and 4.49 respectively.

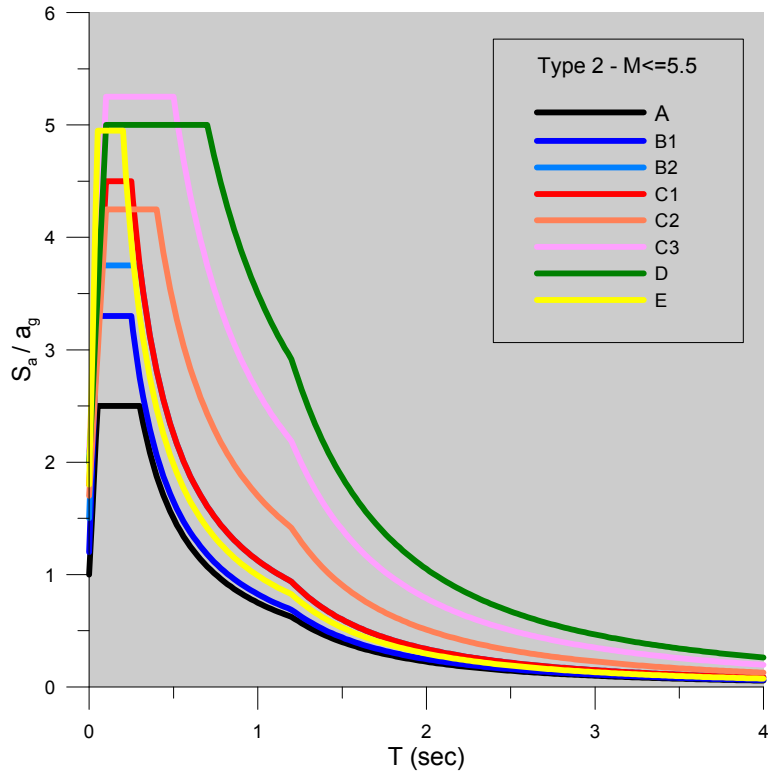


Figure 4.48: Type 2 elastic acceleration response spectra for the new soil classes

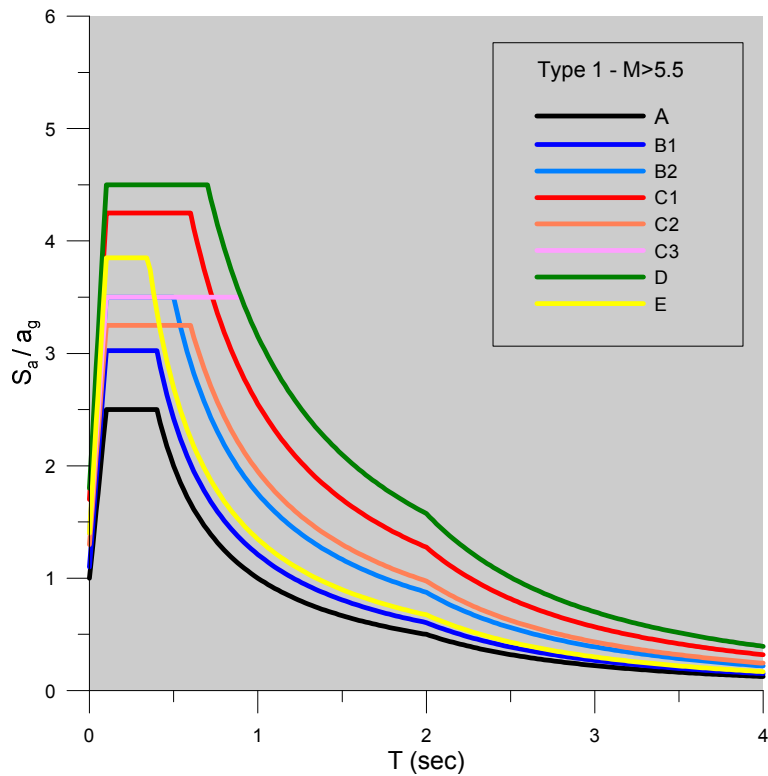


Figure 4.49: Type 1 elastic acceleration response spectra for the new soil classes

4.5 Comparison of the performance of the proposed classification system and EC8 classification system

The performance of the proposed soil classification system is examined and compared to the performance of EC8 soil classification system in terms of an inter-category error term (Stewart et al., 2003). This error term represents the average dispersion of data within all categories of a given classification scheme. In this way, the ability of each classification scheme to capture site-to-site variations of spectral acceleration can be quantified. The inter-category error term is calculated with the following equation:

$$\sigma_R = \sqrt{\frac{\sum_{i=1}^{M_c} \sum_{j=1}^{N_i} (\varepsilon_{ij} - \varepsilon_i)^2}{\left(\sum_{i=1}^{M_c} N_i\right) - df}} \quad (13)$$

where M_c is the number of categories in the scheme and df is the total number of degrees-of-freedom.

Residuals ε_{ij} , which have a mean value ε_i are calculated between the amplification prediction, which is derived from least-square regression analyses, and the actual amplification, as was calculated from Approach 1. It is reminded that in Approach 1, period-dependent amplification factors for ground motion j within site class i , S_{ij} , were evaluated for each strong-motion record, by dividing the geometric mean of 5% damped acceleration response spectra for the two horizontal components of shaking with the reference ground motion, which was estimated using the weighted average of the four GMPEs (see paragraph 3.2.1 for a more detailed description of the methodology).

Soil amplification factors calculated for the common dataset of SHARE-AUTH-DS2 were sorted into the site categories defined by both the EC8 and the proposed classification scheme. A total amount of 191 strong motion records was used. For each scheme, regression analyses were performed to relate amplification factors S_{ij} at a certain period with a parameter G_{ij} which represents the amplitude of reference ground motion as follows:

$$\ln(S_{ij}) = a_i + b_i \ln(G_{ij}) + \varepsilon_{ij} \quad (14)$$

where a_i and b_i are the regression coefficients. Peak reference ground acceleration (PGA_r) was selected as G_{ij} , as in Stewart et al. (2003).

The residuals ε_{ij} are calculated with the following equation:

$$\varepsilon_{ij} = \ln(S_{ij})_{data} - \ln(S_{ij})_{model} \quad (15)$$

Example results for EC8 classification scheme are given in Figure 4.50, which illustrates the amplification factors at three selected periods (PGA , $T=0.3s$ and $T=1s$) for soil classes B and C. Results of regression analyses performed according to Equation (14) (solid lines), as well as median regression \pm standard error (dashed lines) are also plotted. The regression coefficients and standard error terms are listed in Table 4.29.

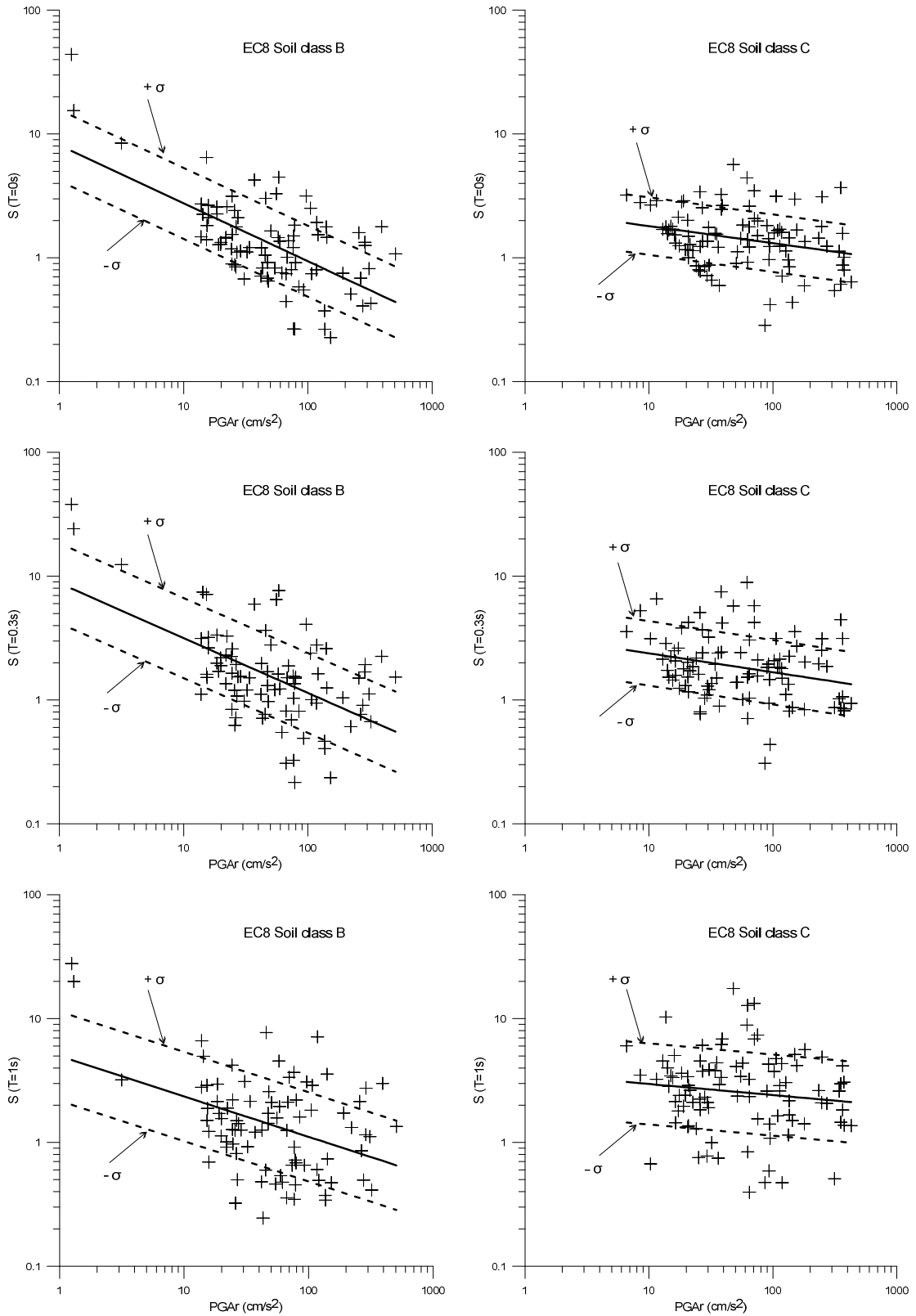


Figure 4.50: Regression results for EC8 soil classes B and C.

Table 4.29: Regression Coefficients for EC8 soil classes B and C.

Soil Class	Period	a	b	σ
B	PGA	2.090	-0.468	0.660
	0.3s	2.171	-0.443	0.744
	1.0s	1.606	-0.326	0.830
C	PGA	0.907	-0.138	0.534
	0.3s	1.218	-0.152	0.599
	1.0s	1.294	-0.090	0.754

Example results for the proposed classification scheme are given in Figures 4.51 (soil classes B1 and B2) and 4.52 (soil classes C1, C2 and C3), which illustrate the amplification factors at three selected periods (PGA, T=0.3s and T=1s). Results of regression analyses performed according to Equation (14) (solid lines), as well as median regression \pm standard error (dashed lines) are also plotted. The regression coefficients and standard error terms are listed in Table 4.30.

Table 4.30: Regression Coefficients for new soil classes B1, B2, C1, C2 and C3

Soil Class	Period	a	b	σ
B1	PGA	2.272	-0.508	0.674
	0.3s	2.143	-0.444	0.776
	1.0s	1.566	-0.353	0.830
B2	PGA	1.280	-0.296	0.515
	0.3s	1.801	-0.337	0.607
	1.0s	1.110	-0.113	0.678
C1	PGA	0.991	-0.123	0.422
	0.3s	0.966	-0.071	0.530
	1.0s	1.540	-0.094	0.413
C2	PGA	1.022	-0.199	0.532
	0.3s	1.871	-0.347	0.573
	1.0s	1.944	-0.248	0.830
C3	PGA	0.471	-0.013	0.507
	0.3s	0.518	0.025	0.492
	1.0s	1.515	-0.103	0.588

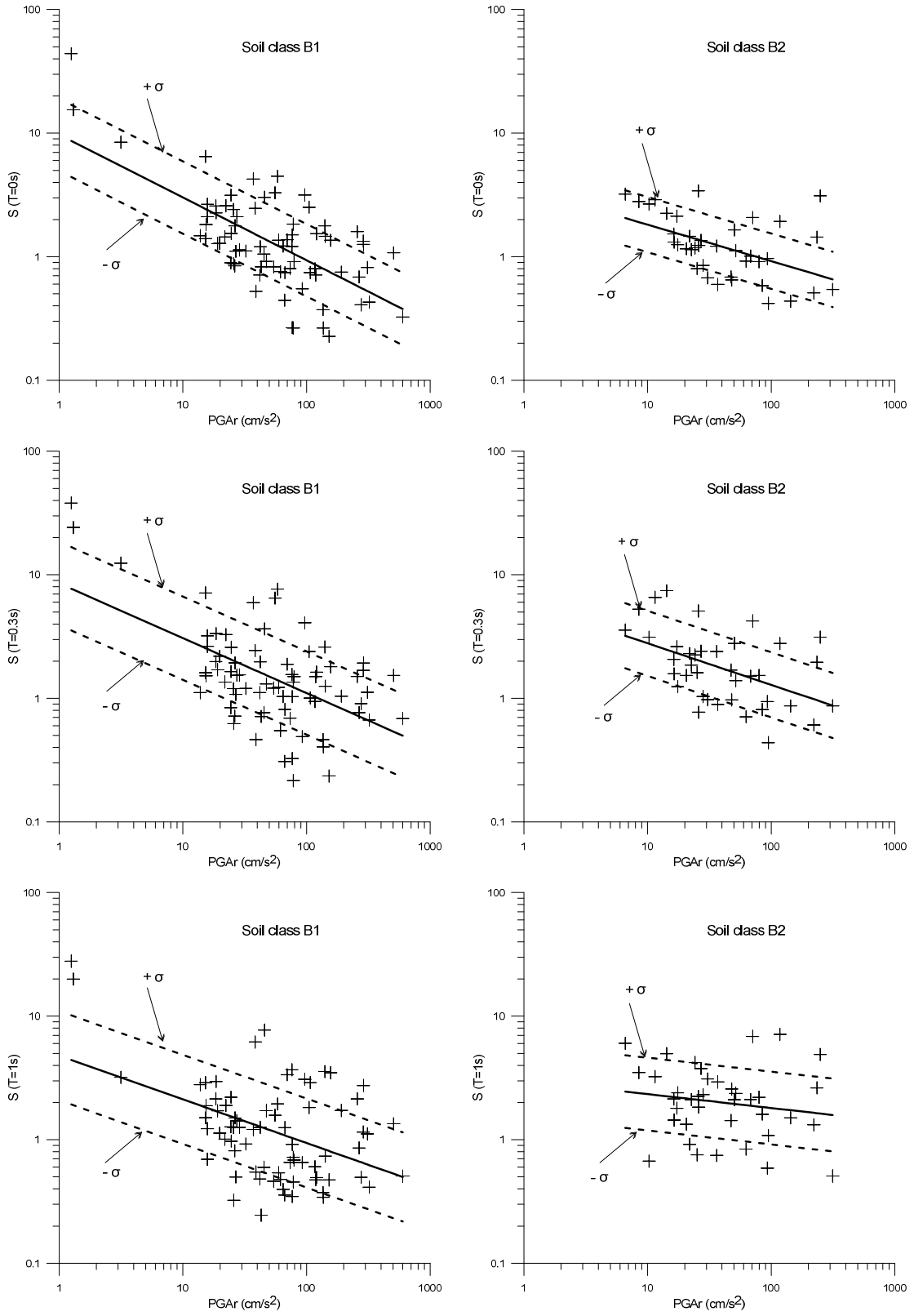


Figure 4.51: Regression results for new soil classes B1 and B2

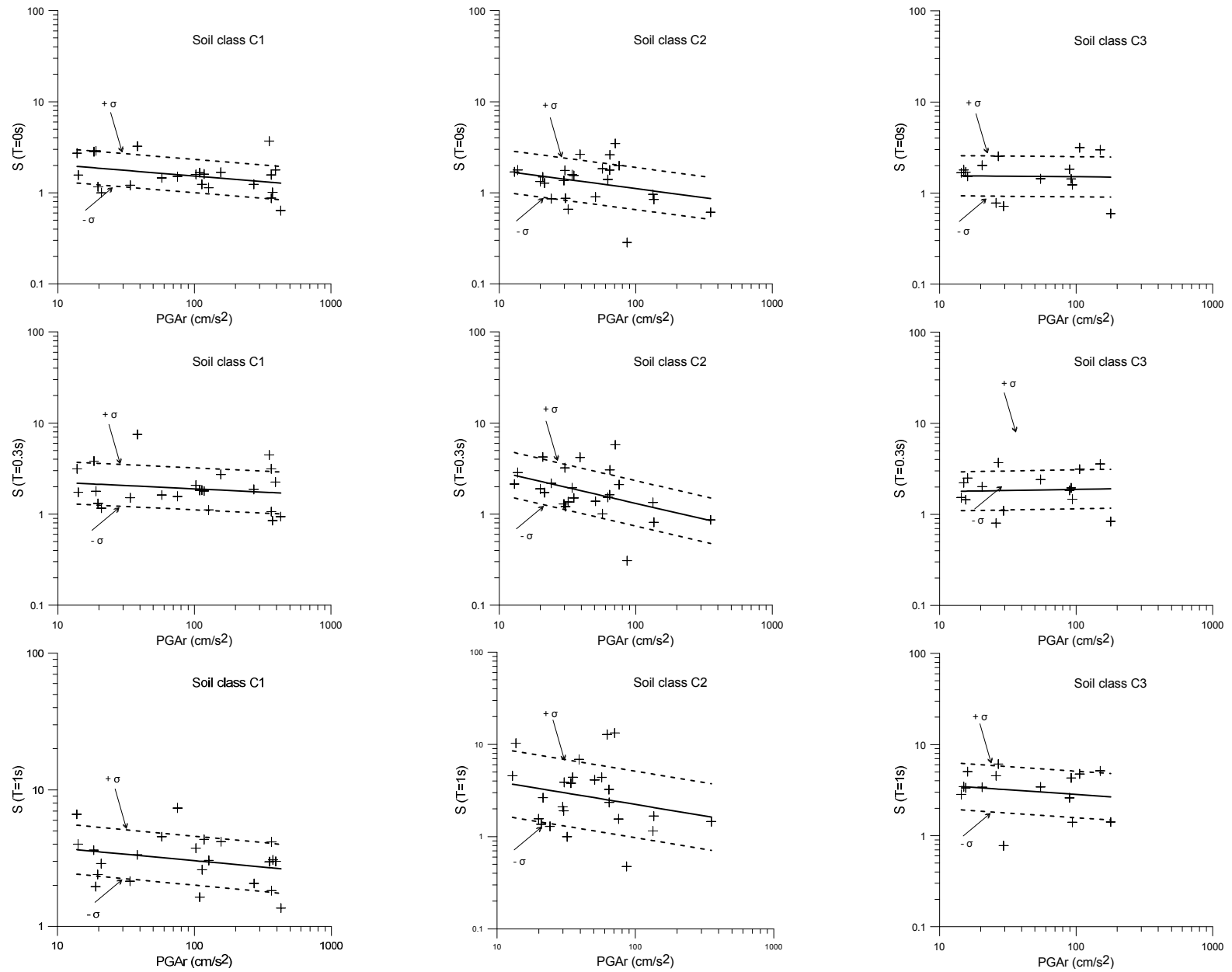


Figure 4.52: Regression results for new soil classes C1, C2 and C3

Inter-category error terms σ_R for the two classification systems were calculated with Equation (13) and are plotted as a function of period in Figure 4.53. We observe that for the new classification system, σ_R error terms at all periods are lower than the error terms for EC8 classification system. The differences are amplified for longer periods ($T > 0.4$ sec).

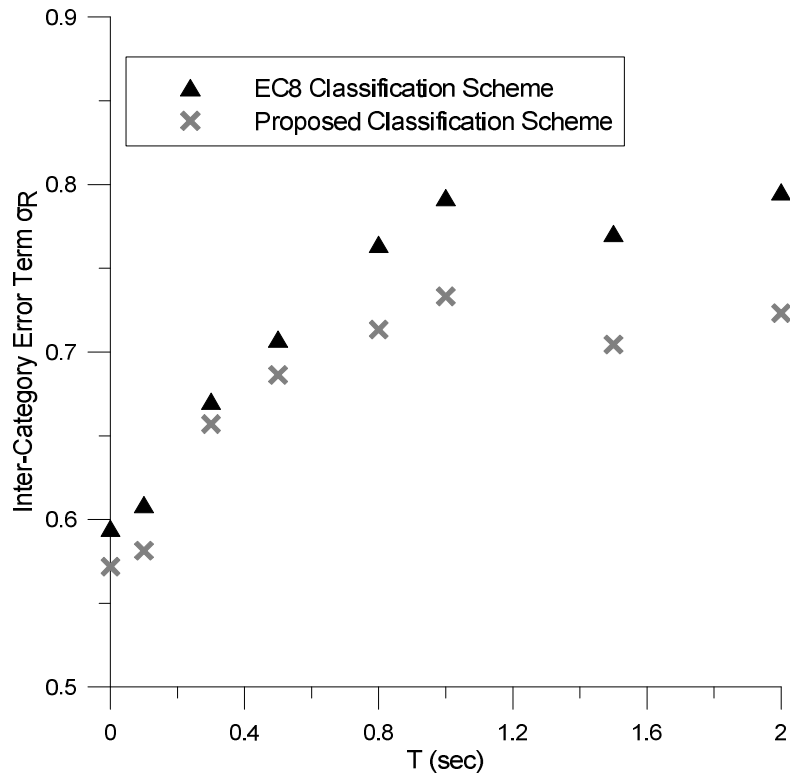


Figure 4.53: Comparison of Inter-category error term (σ_R) for the EC8 and the Proposed classification system as a function of period.

5. Executive Summary

The main outcome of this study, which is on the one hand the new S factors for EC8 classification scheme, and on the other hand the parameters defining the elastic acceleration response spectra for the new classification scheme, are summarized in Tables 5.1 and 5.2.

Table 5.1: Soil factors S for EC8 soil classes.

Soil Class	Type 2 ($M_s \leq 5.5$)		Type 1 ($M_s > 5.5$)	
	Proposed	EC8	Proposed	EC8
B	1.40	1.35	1.30	1.20
C	2.10	1.50	1.70	1.15
D	2.20*	1.80	1.60*	1.35
E	1.80**	1.60	1.40**	1.40

*limited data

**estimated from Kik-Net surface and bedrock strong-motion records

Table 5.2: Parameters of proposed acceleration response spectra for the new classification scheme

Soil Class	Type 2 ($M_s \leq 5.5$)					Type 1 ($M_s > 5.5$)				
	T_B (sec)	T_C (sec)	T_D (sec)	S	β	T_B (sec)	T_C (sec)	T_D (sec)	S	β
A	0.05	0.3	1.2	1.00	2.5	0.1	0.4	2	1.00	2.5
B1	0.05	0.25	1.2	1.20	2.75	0.1	0.4	2	1.10	2.75
B2	0.05	0.3	1.2	1.50	2.5	0.1	0.5	2	1.40	2.5
C1	0.1	0.25	1.2	1.80	2.5	0.1	0.6	2	1.70	2.5
C2	0.1	0.4	1.2	1.70	2.5	0.1	0.6	2	1.30	2.5
C3	0.1	0.5	1.2	2.10	2.5	0.1	0.9	2	1.40	2.5
D	0.1	0.7	1.2	2.00	2.5	0.1	0.7	2	1.80	2.5
E	0.05	0.2	1.2	1.80**	2.75	0.1	0.35	2	1.40**	2.75

**estimated from Kik-Net surface and bedrock strong-motion records

The design spectra for the soil classes of the new classification system, normalized by design ground acceleration at surface, are illustrated in Figures 5.1 and 5.2 for Type 2 and Type 1 seismicity respectively. No changes were proposed for the normalized design spectra of EC8 soil classes.

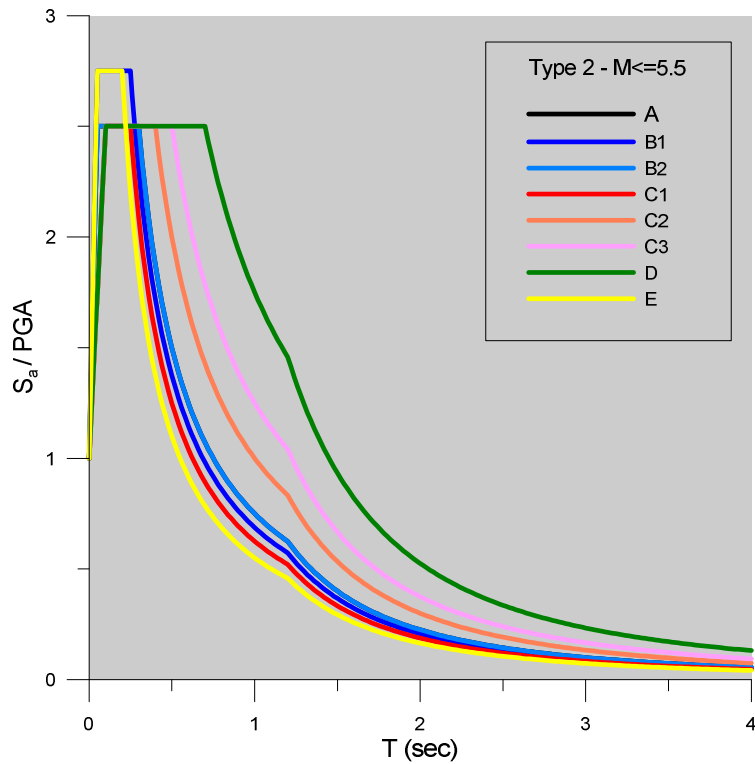


Figure 5.1: Type 2 normalized design spectra for the new soil classes

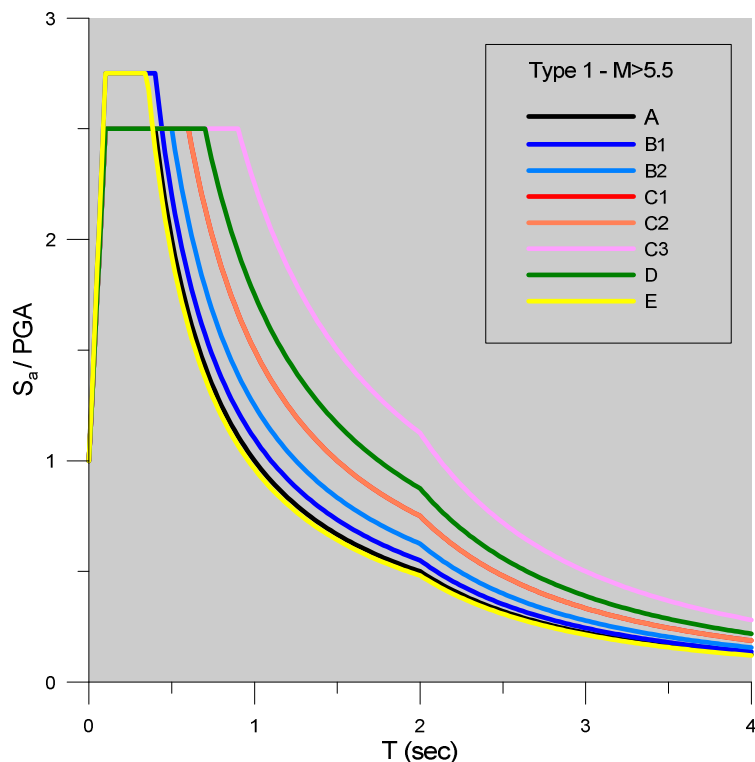


Figure 5.2: Type 1 normalized design spectra for the new soil classes

References

- Akkar, S., and J.J. Bommer (2010), Empirical equations for the prediction of PGA, PGV and spectral accelerations in Europe, the Mediterranean region and the Middle East, *Seismological Research Letters*, 81(2), 195-206, DOI: 10.1785/gssrl.81.2.195.
- Bommer, J.J., and S.G. Scott (2000), The feasibility of using real accelerograms for seismic design, in *Implications of Recent Earthquakes on Seismic Risk*, Series of Innovation in Structures and Construction, vol. 2, edited by A.S. Elnashai and S. Antoniou, pp. 115–126, Imperial College Press.
- Boore, D.M. (2004). Estimating $V_s(30)$ (or NEHRP Site Classes) from shallow velocity models (Depths<30 m), *Bulletin of the Seismological Society of America*, 94(2), 591–597.
- Borcherdt, R.D., and G. Glassmoyer (1992), On the characteristics of local geology and their influence on ground motions generated by the Loma Prieta earthquake in the San Francisco Bay region, California, *Bulletin of the Seismological Society of America*, 82(2), 603-641.
- Borcherdt, R.D. (1994), Estimates of site-dependent response spectra for design (methodology and justification), *Earthquake Spectra*, 10, 617-653, doi :10.1193/1.1585791.
- Cauzzi, C., and E. Faccioli (2008), Broadband (0.05 to 20 s) prediction of displacement response spectra based on worldwide digital records, *Journal of Seismology*, 12(4), 453–475, DOI: 10.1007/s10950-008-9098-y.
- CEN (European Committee for Standardization), (2004), Eurocode 8: Design of structures for earthquake resistance - Part 1: General rules, seismic actions and rules for buildings, EN 1998-1:2004, Brussels, Belgium.
- Chiou, B. S.-J., and R.R Youngs (2008), An NGA model for the average horizontal component of peak ground motion and response spectra, *Earthquake Spectra*, 24(1), 173–215, doi:10.1193/1.2894832.
- Choi, Y., and J.P. Stewart (2005), Nonlinear site amplification as function of 30 m shear wave velocity, *Earthquake Spectra*, 21(1), 1-30, doi:10.1193/1.1856535.
- Delavaud, E, F. Cotton, S. Akkar, F. Scherbaum, L. Danciu, C. Beauval, S. Drouet, J. Douglas, R. Basili, M.A. Sandikkaya, M. Segou, E. Faccioli, and N. Theodoulidis, Toward a Ground-Motion Logic Tree for Probabilistic Seismic Hazard Assessment in Europe, *Journal of Seismology* (submitted).
- Housner, G.W. (1952), Spectrum intensities of strong-motion earthquakes, in *Proceedings of the Symposium on Earthquakes and Blast Effects on Structures*, Earthquake Engineering Research Institute.
- Kaklamanos, J., L.G. Baise, and D.M. Boore (2011), Estimating unknown input parameters when implementing the NGA ground-motion prediction equations in engineering practice, *Earthquake Spectra*, 27(4), in press.
- Lermo J., and F.J. Chávez-García (1993), Site effects evaluation using spectral ratios with only one station, *Bulletin of the Seismological Society of America*, 83, 1574 – 1594.

- Modaressi, H, and E. Foerster, CyberQuake. User's manual, BRGM, France, 2000.
- Molas, G.L., and F. Yamazaki (1995), Attenuation of earthquake ground motion in Japan including deep focus events, *Bulletin of the Seismological Society of America*, 85(5), 1343–1358.
- Pitilakis, K., C. Gazepis, and A. Anastasiadis (2004), Design response spectra and soil classification for seismic code provisions, presented at 13th World Conference on Earthquake Engineering, Vancouver, B.C., Canada, Paper No. 2904.
- Pitilakis, K., C. Gazepis, and A. Anastasiadis (2006), Design response spectra and soil classification for seismic code provisions, in *Proceedings of geotechnical evaluation and application of the seismic Eurocode EC8 2003-2006, ETC-12 Workshop*, pp. 37-52, NTUA Athens.
- Rey, J., E. Faccioli, and J.J. Bommer (2002), Derivation of design soil coefficients (S) and response spectral shapes for Eurocode 8 using the European Strong-Motion Database, *Journal of Seismology*, 6(4), 547-555, DOI: 10.1023/A: 1021169715992.
- Scordilis, E.M. (2006), Empirical global relations converting M_S and m_b to moment magnitude, *Journal of Seismology*, 10(2), 225-236, DOI: 10.1007/s10950-006-9012-4.
- Stewart, J.P., A.H. Liu, and Y. Choi (2003), Amplification factors for spectral acceleration in tectonically active regions, *Bulletin of the Seismological Society of America*, 93(1), 332–352, DOI: 10.1785/0120020049.
- Yenier, E., M.A. Sandikkaya, and S. Akkar (2010), Report on the fundamental features of the extended strong motion databank prepared for the SHARE project (v1.0).
- Zhao, J.X., J. Zhang, A. Asano, Y. Ohno, T. Oouchi, T. Takahashi, H. Ogawa, K. Irikura, H.K. Thio, P.G. Somerville, Y. Fukushima, and Y. Fukushima (2006), Attenuation relations of strong ground motion in Japan using site classification based on predominant period, *Bulletin of the Seismological Society of America*, 96(3), 898–913, DOI: 10.1785/0120050122.

Appendix I

Table I. Stations included in SHARE-AUTH database

ID	Station Name	Country	H bedrock (m)	Vs,30 (m/s)	Vs,av (m/s)	New Site Class	EC8 Site Class	Number of records	Mw	PGA (cm/s ²)
3	Tolmezzo Base Diga	Italy	5	1030	706	A2	A	15	4.1-6.4	9-324
8	Forgaria-Cornio	Italy	28	454	440	B1	B	23	4.1-5.9	16-334
9	Buia	Italy	45	254	321	C2	C	7	4.1-5.9	25-156
11	Tarcento	Italy	4	901	383	A2	A	6	4.1-5.9	17-185
15	Izmir Guzelyali Meteoroloji Mudurlugu	Turkey	17.6	771	654	B1	B	12	4.4-5.6	0.1-225
16	Dursunbey-Kandilli Gozlem Istasyonu	Turkey	34.82	496	522	B1	B	1	5.3	243
19	Bevagna	Italy	>150	162	~300	D	D	9	4.8-6	27-74
20	Brienza	Italy	78	402	623	C1	B	5	4.8-6.9	3-193
21	Auletta	Italy	4	1149	530	A2	A	3	6.2-6.9	20-56
22	Tricarico	Italy	60	467	600	B2	B	4	5.1-6.9	20-40
23	Mercato San Severino	Italy	72	483	570	C1	B	2	6.2-6.9	42-120
25	Bagnoli Irpino	Italy	30	498	498	B1	B	3	6.2-6.9	32-152
26	Calitri	Italy	28	495	480	B1	B	3	5.8-6.9	30-163
27	Rionero In Vulture	Italy	28	539	525	B1	B	5	4.8-6.9	22-96
28	Bisaccia	Italy	3	976	372	A2	A	2	6.2-6.9	72-88
29	Sturno	Italy	30	382	382	B1	B	5	4.9-6.9	15-261
30	Arienzo	Italy	8	578	200	E	E	4	4.9-6.9	27-47
31	Benevento	Italy	9	744	424	B1	B	1	6.9	41
32	Bovino	Italy	19	364	285	C2	B	2	6.2-6.9	24-46
42	Horasan-Meteoroloji Mudurlugu	Turkey	44.77	316	386	B2	C	2	5.3-6.6	0.1-119
44	Garigliano-Centrale Nucleare 1	Italy	>100	192	~400	D	C	2	5.9-6.9	34-60
54	Kalamata-Ote Building	Greece	>50	411	496	C1	B	9	3.9-6.6	13-251
55	Kalamata-Prefecture	Greece	35	517	534	B2	B	10	4.1-6	12-240
56	Edessa-Prefecture	Greece	19.2	408	370	C2	B	5	5.3-6.6	24-96
65	Refahiye-Kaymakamlik Binasi	Turkey	31.6	433	443	B2	B	1	6.6	73
94	Kozani-Prefecture	Greece	26	510	520	B1	B	12	3-6.6	10-172
100	Chromio-Community Building	Greece	35	623	722	B2	B	9	4.2-5.3	9-142
105	Denizli Merkez Bayindirlik Ve Iskan Mudurlugu	Turkey	47.31	356	430	B2	C	35	3.7-7.6	0.3-58
106	Burdur-Meteoroloji Mudurgulu	Turkey	86.72	335	472	C1	C	1	6.4	37
108	Dinar-Meteoroloji Mudurlugu	Turkey	72.26	196	320	C3	C	7	4.2-6.4	0.3-296
114	Kusadasi-Meteoroloji Mudurlugu	Turkey	50.87	369	449	B2	B	18	4.1-6	0.1-76
117	Rieti	Italy	200	176	409	D	D	7	4.7-6	4-28
118	Norcia	Italy	10	681	474	B1	B	18	4.9-5.6	14-185

ID	Station Name	Country	H bedrock (m)	Vs,30 (m/s)	Vs,av (m/s)	New Site Class	EC8 Site Class	Number of records	Mw	PGA (cm/s ²)
120	Colfiorito	Italy	54	143	156	D	D	19	4.2-6	14-307
122	Nocera Umbra	Italy	9	555	272	E	E	30	4.2-6	23-452
124	Gubbio-Piana	Italy	>60	219	~300	C3	C	11	4.3-6	8-94
129	Sellano Ovest	Italy	83	518	568	C1	B	10	4.4-5.3	6-186
131	Nocera Umbra 2	Italy	9	534	272	E	E	27	4.2-5.6	15-403
133	Aydin Merkez Tarim Ve Koy Isleri Bakanligi Hayvan Sagligi Sube Mudurlugu	Turkey	56.21	310	399	C2	C	11	4.2-7.6	1-14
134	Izmir Bornova Ege Universitesi Ziraat Fakultesi	Turkey	56.95	270	362	C2	C	61	3.8-7.6	1-54
135	Manisa-Bayindirlik Mudurlugu	Turkey	47.72	340	416	B2	C	8	4.4-7.6	2-18
136	Usak Merkez Meteoroloji Istasyon Mudurlugu	Turkey	64.43	286	401	C2	C	12	4.9-7.6	1-13
137	Afyon-Bayindirlik Ve Iskan Mudurlugu	Turkey	49.66	226	307	C2	C	10	3.7-7.6	1-103
138	Kutahya Merkez Sivil Savunma Mudurlugu	Turkey	57.95	243	336	C2	C	23	3.9-7.6	1-55
139	Balikesir Merkez Balikesir Huzurevi	Turkey	17.8	662	549	B1	B	31	4.2-7.6	1-18
140	Bursa Merkez Sivil Savunma Mudurlugu	Turkey	38.3	457	496	B2	B	13	4-7.6	1-49
141	Tokat Merkez Devlet Su Isleri 72. Sube Mudurlugu	Turkey	51.13	324	407	B2	C	3	4.5-7.6	1-5
142	Goynuk-Devlet Hastanesi	Turkey	45.98	348	419	C2	C	2	7.1-7.6	25-129
143	Izmit-Karayollari Sefligi Muracaati	Turkey	73.1	197	320	C3	C	5	4.5-7.6	1-107
144	Gebze-Tubitak Marmara Arastirma Merkezi	Turkey	17	701	567	B1	B	3	5.6-7.6	0.1-183
145	Izmit-Meteoroloji Istasyonu	Turkey	10.9	827	532	B1	A	3	5.8-7.6	20-195
146	Duzce-Meteoroloji Mudurlugu	Turkey	58.09	283	386	B2	C	23	3.7-7.6	2-457
147	Tekirdag Merkez Valilik Binasi	Turkey	34.05	408	432	B1	B	27	3.9-7.6	1-41
148	Cekmece-Kucuk	Turkey	46.98	283	357	C2	C	10	4.1-7.6	3-150
149	Istanbul-Bayindirlik Ve Iskan Mudurlugu	Turkey	18.6	596	483	B1	B	36	3.9-7.6	1-51
150	Kastamonu Tosya Meteoroloji Istasyon Mudurlugu	Turkey	43	362	421	B2	B	16	3.7-7.6	1-32
153	Canakkale Merkez Meteoroloji Istasyon Mudurlugu	Turkey	87.08	192	332	C3	C	42	4.1-7.6	0.5-26
155	Sakarya Merkez Bayindirlik Ve Iskan Mudurlugu	Turkey	34.48	412	439	B1	B	67	2.8-7.6	0.8-408
165	Adana Ceyhan Ptt Mudurlugu	Turkey	61.49	223	319	C2	C	1	5.4	10
168	Eregli-Kaymakamlik Binasi	Turkey	43.24	326	390	B1	C	1	7.6	95
181	Ldeo Station No. C0362 Ch	Turkey	26.8	455	430	B1	B	31	3.9-7.1	0.3-51

ID	Station Name	Country	H bedrock (m)	Vs,30 (m/s)	Vs,av (m/s)	New Site Class	EC8 Site Class	Number of records	Mw	PGA (cm/s ²)
182	Sakarya Karadere Koyu	Turkey	33.52	448	468	B1	B	41	3.7-7.1	0.3-138
183	Sakarya Karadere Koyu	Turkey	32	456	468	B1	B	50	3.7-7.1	0.5-113
184	Ldeo Station No. C1062 Fi	Turkey	55.56	316	394	B2	C	41	3.7-7.1	0.4-171
187	Sakarya Karadere Koyu	Turkey	25.4	482	445	B1	B	47	3.7-7.1	1.3-655
188	Bolu Merkez Bayindirlik Ve Iskan Mudurlugu	Turkey	52.4	294	380	B2	C	37	3.7-7.1	1.2-775
189	Ldeo Station No. C1058 Bv	Turkey	19.6	719	631	B1	B	44	3.7-7.1	0.3-88
190	Ldeo Station No. C1060 Bu	Turkey	17.7	616	488	B1	B	31	3.9-7.1	0.2-36
193	Mudurnu-Kaymakamlik Binasi	Turkey	32	355	368	B1	C	1	7.1	85
194	Ldeo Station No. C1059 Fp	Turkey	24.9	441	403	B1	B	40	3.7-7.1	1-158
226	Balikesir Bandirma Meteoroloji Mudurlugu	Turkey	50.78	321	406	B2	C	12	3.9-6.5	0.6-5
227	Sakarya Akyazi Orman Isletme Mudurlugu	Turkey	50.39	271	356	C2	C	12	3.8-5.3	2.5-87
228	Karabuk Merkez Karabuk Anadolu Lisesi	Turkey	15.5	703	561	B1	B	5	4.7-6	0.6-6
229	Bingol Merkez Bayindirlik Ve Iskan Mudurlugu	Turkey	23.4	528	480	B1	B	65	3.7-6.3	0.5-385
231	Elazig Merkez Bayindirlik Ve Iskan Mudurlugu	Turkey	36.89	407	445	B1	B	12	4.5-6.3	1.3-55
232	Erzincan Merkez Bayindirlik Ve Iskan Mudurlugu	Turkey	54.14	315	401	B2	C	9	3.8-6.3	3-43
233	Erzincan Tercan Ptt Binasi	Turkey	55	417	498	B2	B	10	4.6-6.3	0.9-8
242	Almiros Volos-Town Hall	Greece	100	467	503	C1	B	4	4.4-5.3	27-113
255	Anza - Pinyon Flat	USA	7.5	725	278	E	E	4	4.9-7.1	30-290
269	Joshua Tree	USA	78	346	456	C1	C	5	4.9-7.3	7-274
274	Wrightwood Post Office	USA	14	486	339	B1	B	3	4.5-7.1	12-47
296	La - 116Th St School	USA	151	317	459	C3	C	7	5.3-7.3	24-335
319	Arleta - Nordhoff Fire Sta	USA	138	302	544	C1	C	5	5.3-7.1	22-319
321	Jensen Filter Plant Generator	USA	89.5	526	642	C1	B	4	5.1-7.1	38-750
324	Newhall - Fire Sta	USA	105.2	269	487	C1	C	6	5.2-7.1	18-575
330	Palmdale Fire Station	USA	17	453	337	B1	B	3	4.9-7.1	7-133
336	Apeel 2 - Redwood City	USA	100	134	249	D	D	2	5-6.9	8-241
364	Tenryu	Japan	10	456	263	E	B	2	5.3-5.5	2-3
378	Mamba	Japan	27	460	440	B1	B	3	5.3-6.6	3-30
388	Sakamoto	Japan	10	652	354	B1	B	1	5.3	3
390	Ueda	Japan	9	545	359	B1	B	2	5.3-6.3	6-11

ID	Station Name	Country	H bedrock (m)	Vs,30 (m/s)	Vs,av (m/s)	New Site Class	EC8 Site Class	Number of records	Mw	PGA (cm/s ²)
404	SIGH01	Japan	14	563	350	E	E	15	3.6-7.5	2-23
405	HYGH11	Japan	50	271	364	C2	C	17	3.6-7.5	2.8-64
420	Shiramine	Japan	16	479	360	B1	B	1	5.8	19
436	Hachijoh	Japan	13	615	393	B1	B	6	5.2-6.4	3-71
437	Kamitsuki	Japan	90	406	507	C1	B	13	5.2-6.4	3-157
440	Minamiizu	Japan	7	538	213	E	E	7	5.5-6.4	2-26
442	Habuminato	Japan	197	294	316	D	C	12	5.2-6.4	3-62
443	Haibara	Japan	106	343	382	C3	C	3	5.6-6.2	7-22
444	Matsuzaki	Japan	60	209	219	C2	C	6	5.5-6.2	5-38
445	Okada	Japan	20	458	377	B1	B	11	5.2-6.4	3-71
447	Higashiizu	Japan	40	187	192	C2	C	11	5.2-6.4	6-109
448	Yaidu	Japan	211	219	253	D	C	4	5.6-6.2	2-25
450	Shirahama	Japan	3	600	245	A2	B	5	5.5-6.2	3-14
451	Toi	Japan	107	455	557	C1	B	4	5.5-6.2	5-16
455	Itoh	Japan	21	336	269	E	C	4	5.5-6.2	6-156
456	Numadu	Japan	127	350	422	C1	C	5	5.5-6.2	2-16
457	Atami	Japan	19	437	346	B1	B	4	5.5-6.2	2-82
458	Katsuura	Japan	12	378	194	E	E	4	5.5-6.2	3-5
462	Odawara	Japan	166	104	200	D	D	4	5.5-6.2	7-63
464	Kisaradu	Japan	208	174	375	D	D	3	5.5-6.2	6-10
472	Shuzenji	Japan	10	554	343	B1	B	3	5.5-6	5-73
474	Yokosuka	Japan	5	489	177	E	B	2	6-6.4	4-7
475	Misaki	Japan	162	162	195	D	D	3	5.5-6	4-5
477	Kamakura	Japan	12	443	283	B1	B	6	5.5-6	3-35
484	Hachiohji	Japan	89	311	389	C3	C	3	5.5-6	6.6-7
485	Urayasu	Japan	85	128	126	D	D	3	5.5-6	3-5
493	Seto	Japan	8	1052	413	A2	A	7	4.3-7.5	1-30
494	OKYH07	Japan	13.5	940	671	B1	A	13	3.2-6.6	1-151
498	KOCH04	Japan	4	1184	400	B1	A	2	4.2-6.6	1-5
509	EHHM06	Japan	18	717	495	B1	B	2	4.2-6.6	5-35
515	FKOH05	Japan	3	777	140	E	E	1	6.6	2
517	KOCH01	Japan	27	363	336	C2	B	6	3.8-7.5	3-11
518	WKYH04	Japan	4	550	121	E	E	11	3.3-7.5	1-53
519	FKOH03	Japan	25	504	438	B1	B	1	6.6	2
521	WKYH07	Japan	27	316	291	C2	C	15	3.5-7.5	2-95
522	WKYH06	Japan	5	756	290	E	E	11	3.3-7.5	2-78
523	FKOH02	Japan	40	273	333	C2	C	1	6.6	3
524	KOCH02	Japan	8	394	136	E	E	5	3.4-6.6	3-34
525	EHHM05	Japan	29	364	356	C2	B	1	6.6	9
527	WKYH10	Japan	18	466	314	C2	B	20	3.1-7.5	1-61
529	TKSH03	Japan	7.5	404	143	E	E	8	3.5-7.5	4-37
530	FKOH01	Japan	13	588	303	E	E	1	6.6	5
531	EHHM04	Japan	196	260	559	C1	C	6	3.4-6.6	2-23

ID	Station Name	Country	H bedrock (m)	Vs,30 (m/s)	Vs,av (m/s)	New Site Class	EC8 Site Class	Number of records	Mw	PGA (cm/s ²)
532	EHHM03	Japan	10	802	457	B1	A	6	3.4-7.5	5-57
533	NARH01	Japan	26	338	301	C2	C	17	3.4-7.5	4-117
534	WKYH01	Japan	10	463	204	E	E	17	3.1-7.5	4-137
535	YMGH06	Japan	Rock	>800	>1500	A1	A	1	6.6	5
536	TKSH02	Japan	14	349	205	E	E	8	3.5-7.5	5-54
537	YMGH04	Japan	20	659	492	B1	B	1	6.6	15
539	YMGH01	Japan	Rock	>800	>1500	A1	A	2	3.4-6.6	5-6
541	YMGH02	Japan	20	398	287	C2	B	1	6.6	7
542	YMGH07	Japan	20	351	265	C2	C	1	6.6	5
543	YMGH08	Japan	16	342	212	E	E	1	6.6	7
544	WKYH02	Japan	16	369	225	E	E	20	3.4-7.5	2-81
545	YMGH03	Japan	23.5	536	460	B1	B	1	6.6	19
546	YMGH05	Japan	23	450	369	C2	B	1	6.6	21
547	YMGH11	Japan	16	711	509	B1	B	2	3.4-6.6	12-15
549	KGWH01	Japan	35	255	282	C2	C	5	4.3-7.5	7-80
553	WKYH09	Japan	76	349	511	C1	C	17	3.2-7.5	1-23
554	HRSH07	Japan	52	462	500	B2	B	2	5.1-6.6	8-80
555	NARH03	Japan	11.5	497	229	E	E	8	3.6-7.5	2-54
556	HYGH01	Japan	100	344	470	C1	C	15	3.3-7.5	1-22
557	NARH04	Japan	22.5	592	483	B1	B	11	3.4-7.5	2-85
558	WKYH08	Japan	90	344	561	C1	C	15	3.4-7.5	1-36
563	HRSH01	Japan	28	403	383	C2	B	4	4.2-6.6	12-164
564	HRSH04	Japan	15.5	458	280	E	E	4	4.5-6.6	2-28
566	HRSH08	Japan	12	781	548	B1	B	1	6.6	31
568	Higashihiroshima	Japan	24	332	290	B1	C	3	5.1-6.6	6-79
569	NARH05	Japan	18	398	275	E	E	11	3.3-7.5	5-177
571	YMGH10	Japan	18	526	366	C2	B	2	3.4-6.6	17-19
572	OKYH01	Japan	44	238	271	C2	C	6	4.2-7.5	11-133
573	HRSH03	Japan	20	487	370	C2	B	5	4.4-6.6	16-277
574	OSKH03	Japan	23.5	408	346	C2	B	12	3.2-7.5	2-190
577	HRSH02	Japan	12	391	197	E	E	5	4.2-6.6	6-98
578	HRSH05	Japan	56	382	489	B2	B	5	4.4-6.6	5-124
581	YMGH09	Japan	38	304	351	C2	C	2	3.4-6.6	34-67
582	NARH06	Japan	14	370	214	E	E	8	3.3-7.2	4-51
583	OKYH04	Japan	10	360	151	E	E	8	4.2-6.6	1-32
584	OKYH06	Japan	42	555	615	B2	B	6	4.2-6.6	6-77
585	SMNH07	Japan	60	318	419	C1	C	2	5.1-6.6	8-43
586	HRSH09	Japan	30	496	496	B1	B	7	3.4-6.6	1-58
589	OSKH04	Japan	15	529	345	B1	B	18	3.4-7.5	1-20
592	OKYH03	Japan	20	317	227	C2	C	5	4.3-6.6	8-108
593	Takahashi	Japan	10	393	202	E	B	2	5.1-6.6	12-97
594	HYGH06	Japan	32	369	378	C2	B	6	3.6-7.5	3-49
595	HYGH10	Japan	82	224	316	C3	C	15	3.4-7.5	2-46

ID	Station Name	Country	H bedrock (m)	Vs,30 (m/s)	Vs,av (m/s)	New Site Class	EC8 Site Class	Number of records	Mw	PGA (cm/s ²)
597	SIGH03	Japan	37.5	393	414	B2	B	12	3.4-7.5	3-57
598	OKYH05	Japan	18	620	469	B1	B	7	4.3-6.6	3-127
599	SMNH05	Japan	14	711	420	B1	B	9	3.1-6.6	3-102
601	SMNH06	Japan	62	293	436	C1	C	5	3.1-6.6	1-81
603	HYGH05	Japan	13	533	289	E	E	9	3.4-6.6	3-77
604	HYGH09	Japan	52	365	469	B2	B	11	3.6-7.5	5-55
605	OKYH08	Japan	22	694	587	B1	B	23	3.4-6.6	4-232
606	HRS06	Japan	51	279	371	C2	C	16	3.1-6.6	2-211
607	Yoshii	Japan	8	421	193	E	B	2	5.1-6.6	8-114
608	HYGH12	Japan	20	677	532	B1	B	12	3.6-7.5	2-71
611	SIGH04	Japan	36	483	494	B2	B	9	3.7-7.5	2-24
613	Kohduki	Japan	5	440	147	E	B	1	6.6	77
617	HYGH07	Japan	26.5	506	457	B1	B	12	3.6-7.5	2-227
619	HYGH02	Japan	14	612	378	B1	B	16	3.4-7.5	1-23
621	HYGH04	Japan	22	476	381	C2	B	18	3.4-7.5	3-60
622	OKYH11	Japan	20	543	420	B1	B	5	4.4-6.6	4-122
623	SMNH04	Japan	11	285	131	E	E	8	3.1-6.6	1-80
624	OKYH12	Japan	11	757	380	B1	B	16	3.4-7.5	3-77
629	OKYH09	Japan	21	601	474	B1	B	19	3.4-6.6	3-227
632	HYGH03	Japan	18	528	356	C2	B	11	3.4-7.5	3-79
633	SMNH02	Japan	63.5	510	675	C1	B	22	3.1-6.6	2-421
634	SMNH03	Japan	78	440	651	C1	B	15	3.1-6.6	3-155
635	TTRH02	Japan	100	310	522	C1	C	34	3.3-6.6	2-836
636	SIGH02	Japan	6	569	260	E	E	18	3.1-7.5	2-101
637	TTRH01	Japan	31	437	442	B1	B	19	3.4-6.6	1-39
642	OKYH10	Japan	8	504	250	E	E	21	3.4-6.6	3-192
644	SMNH01	Japan	22	464	380	C2	B	38	3.2-6.6	4-661
652	Muraoka	Japan	3	699	361	A2	B	1	6.6	19
665	Sadamitsu	Japan	15	336	213	E	C	1	5.1	2
676	Kasaoka	Japan	8	495	256	E	B	1	5.1	8
683	HRS10	Japan	42	265	306	C2	C	4	3.1-5.1	5-10
688	Hamada	Japan	7	613	347	B1	B	1	5.1	2
699	Iitate	Japan	26	314	287	B1	C	3	5.3-5.9	7-16
703	Yonezawa	Japan	83	136	150	D	D	3	5.3-6.6	4-44
704	Shimoyachi	Japan	6	401	148	E	E	4	5.3-6.1	2-20
711	Iwanuma	Japan	204	231	368	D	C	4	5.3-6.1	12-67
715	Sendai	Japan	150	273	392	C3	C	4	5.3-6.1	8-104
716	Shiogama	Japan	6	452	154	E	E	5	5.3-6.1	7-211
717	Sakunami	Japan	34	370	385	B1	B	4	5.3-6.1	19-86
721	Ishinomaki	Japan	209	262	294	D	C	3	5.5-6.1	13-221
731	Tohwa	Japan	10	515	301	B1	B	5	5.3-6.1	7-130
733	Shinjoh	Japan	41	388	432	B1	B	3	5.3-5.7	7-129
735	Naruko	Japan	276	337	366	D	C	3	5.3-5.9	18-424

ID	Station Name	Country	H bedrock (m)	Vs,30 (m/s)	Vs,av (m/s)	New Site Class	EC8 Site Class	Number of records	Mw	PGA (cm/s ²)
744	Tsubakidai	Japan	10	606	354	B1	B	4	5.3-6.1	3-15
758	Momma	Japan	22	459	398	B1	B	4	5.3-6.1	7-32
798	Shiroishi	Japan	265	420	531	D	B	3	5.3-6.1	7-33
803	Murakami	Japan	20	336	261	B1	C	3	5.7-6.1	6-13
805	Oshika	Japan	1	1433	220	A1	A	2	5.3-6.1	51-289
806	Higashine	Japan	105	281	294	C3	C	4	5.3-6.1	8-37
807	Taiwa	Japan	7	537	278	E	B	4	5.3-6.1	5-173
809	Kitakami	Japan	35	245	254	C2	C	3	5.3-6.1	9-112
810	Toyosato	Japan	11	231	107	E	C	2	5.3-6.1	54-189
811	Tsukidate	Japan	106	430	510	C1	B	3	5.3-6.1	62-334
812	Kesenuma	Japan	26	462	433	B1	B	4	5.3-6.1	18-82
813	Ichinoseki	Japan	4	668	430	B1	B	4	5.3-6.1	13-61
814	Daitoh	Japan	6	580	226	E	E	3	5.3-6.1	27-143
816	Ohfunato	Japan	6	1086	573	B1	A	2	5.7-6.1	6-27
817	Mizusawa	Japan	208	250	250	D	C	4	5.3-6.1	7-37
821	Yamada	Japan	19	232	164	E	E	3	5.3-6.1	16-68
822	Ishidoriya	Japan	116	273	326	C3	C	3	5.3-6.1	10-48
824	Kawai	Japan	16	440	326	B1	B	4	5.3-6.1	5-28
827	Morioka	Japan	20	390	310	B1	B	3	5.3-6.1	4-35
847	Hijiori	Japan	56	136	142	D	D	4	5.3-5.9	9-108
850	Ohshida	Japan	20	336	261	B1	C	4	5.3-5.9	3-71
893	Koumi	Japan	18	330	244	E	C	1	6.6	11
909	Kuzuu	Japan	8	508	213	E	E	1	6.6	15
925	Minakami	Japan	6	461	195	E	B	2	6.3-6.6	242-309
939	Hinoemata	Japan	7	492	174	E	E	2	6.3-6.6	177-192
943	Takinohara	Japan	5	603	344	E	B	2	6.3-6.6	76-85
946	NIGH11	Japan	205	375	547	C1	B	27	3.4-6.6	1-517
947	NIGH12	Japan	110	553	694	C1	B	23	3.5-6.6	1-445
964	Chichibu	Japan	4	656	187	A2	B	1	6.3	32
966	Shimonita	Japan	4	709	347	A2	B	1	6.3	21
981	Iwayaguchi	Japan	2	683	130	A2	B	1	6.3	63
1001	Idyllwild - Keenwild Fire Sta.	USA	10	845	475	B1	A	2	4.9-5.2	36-45
1509	Yaku	Japan	3	607	224	B1	B	1	5.7	74
1520	Nishinoomote	Japan	5	814	550	A2	A	1	5.7	42
1523	Tashiro	Japan	43	220	243	C2	C	3	5.4-6.1	5-19
1525	Ei	Japan	58	311	398	B2	C	3	5.4-6	17-72
1530	Uchinoura	Japan	12	352	196	E	C	1	6	8
1534	Ohsaki	Japan	225	274	361	D	C	3	5.4-6.1	10-25
1535	Kushima	Japan	48	341	400	B2	C	3	5.7-6.1	13-31
1538	Hiyoshi	Japan	33	263	269	C2	C	3	5.4-6.1	19-198
1539	Ohsumi	Japan	17	385	267	E	E	3	5.4-6.1	10-23
1540	Kagoshima	Japan	221	223	310	D	C	4	5.4-6.1	4-58
1542	Shimokoshiki	Japan	46	391	423	B2	B	3	5.4-6.1	15-35

ID	Station Name	Country	H bedrock (m)	Vs,30 (m/s)	Vs,av (m/s)	New Site Class	EC8 Site Class	Number of records	Mw	PGA (cm/s ²)
1546	Miyakonojoh	Japan	179	273	287	D	C	3	5.4-6.1	18-53
1548	Kokubu	Japan	106	197	226	D	C	3	5.4-6.1	45-146
1549	Kamoh	Japan	138	309	333	D	C	3	5.4-6.1	51-123
1550	Sendai	Japan	255	197	226	D	C	3	5.4-6.1	149-309
1553	Tano	Japan	139	276	390	C2	C	3	5.4-6.1	4-16
1558	Miyazaki	Japan	98	170	170	D	D	3	5.4-6.1	4-16
1562	Kobayashi	Japan	349	282	307	D	C	3	5.4-6.1	7-21
1563	Akune	Japan	69	204	276	C3	C	3	5.4-6.1	105-196
1568	Ohkuchi	Japan	41	272	296	C2	C	3	5.4-6.1	174-243
1570	Saito	Japan	271	395	435	D	B	3	5.4-6.1	9-24
1573	Ushibuka	Japan	17	325	210	E	E	3	5.4-6.1	29-64
1574	Azuma	Japan	28	392	378	B1	B	3	5.4-6.1	57-118
1575	Hitoyoshi	Japan	18	300	209	E	E	3	5.4-6.1	33-81
1579	Minamata	Japan	13	369	216	E	E	3	5.4-6.1	78-152
1582	Taragi	Japan	354	368	468	D	B	3	5.4-6.1	14-28
1591	Shinwa	Japan	6	555	296	B1	B	3	5.4-6.1	34-51
1592	Tanoura	Japan	57	372	459	B2	B	3	5.4-6.1	19-42
1594	Mangoh	Japan	2	651	330	B1	B	1	6	5
1595	Ryuhgatake	Japan	33	454	466	B1	B	3	5.4-6.1	34-88
1596	Itsuki	Japan	5	817	220	E	E	2	5.4-6	27-48
1598	Hyuhga	Japan	2	891	300	A2	A	1	6.1	3
1604	Kitagoh	Japan	2	632	160	A2	B	1	6	6
1610	Nomozaki	Japan	10	479	294	B1	B	4	5.4-6.1	3-8
1611	Kuchinotsu	Japan	14	234	127	E	E	3	5.4-6.1	25-49
1612	Misumi	Japan	47	193	245	C2	C	3	5.4-6.6	6-18
1613	Tomochi	Japan	32	242	247	C2	C	3	5.4-6.1	15-37
1627	Takachiho	Japan	42	412	425	B1	B	3	5.4-6.1	9-17
1632	Nagasaki	Japan	93	372	450	C1	B	3	5.4-6.1	9-22
1634	Ec Meloland Overpass Ff	USA	281.9	199	381	D	C	1	6.5	299
1635	Kumamoto	Japan	204	238	335	D	C	4	5.4-6.1	4-14
1636	Shimabara	Japan	61	354	367	B2	C	4	5.4-6.6	8-36
1647	Takamori	Japan	15	341	219	E	C	3	5.4-6.1	6-22
1648	El Centro Array #7	USA	181.37	215	380	D	C	5	4.9-6.5	5-388
1651	Isahaya	Japan	242	347	426	D	C	3	5.4-6.1	6-7
1659	Ohmura	Japan	13	327	179	E	E	2	6-6.1	6-11
1660	Kinkai	Japan	36	469	482	B1	B	5	5.4-6.6	4-39
1663	Konagai	Japan	4	750	340	E	B	4	5.4-6.6	3-30
1667	Tamana	Japan	44	281	316	C2	C	3	6-6.6	9-51
1671	Superstition Mtn Camera	USA	31.5	373	365	B1	B	3	5.9-6.5	89-766
1676	Yamaga	Japan	151	356	546	C1	C	3	5.4-6.6	10-66
1677	Higashisonogi	Japan	170	400	544	C1	B	4	5.4-6.6	2-46
1679	EHHM01	Japan	10	743	420	B1	B	2	3.6-4.2	11-19

ID	Station Name	Country	H bedrock (m)	Vs,30 (m/s)	Vs,av (m/s)	New Site Class	EC8 Site Class	Number of records	Mw	PGA (cm/s ²)
1680	Inukai	Japan	6	696	235	E	E	1	5.4	23
1681	Naoiri	Japan	7	521	213	E	E	1	5.4	3
1685	Oguni	Japan	7	431	170	E	E	3	5.4-6.1	4-10
1688	Yabe	Japan	6	723	305	B1	E	1	5.4	11
1693	Sasebo	Japan	45	384	451	B1	B	3	5.4-6.6	3-58
1697	Yame	Japan	139	380	558	C1	B	3	5.4-6.1	5-47
1699	Amagase	Japan	13	569	366	B1	B	1	5.4	15
1704	KOCH03	Japan	30.5	677	679	B1	B	1	4.2	2
1719	Kitsuki	Japan	19	389	303	B1	B	2	5.4-6.6	13-29
1725	Yabakei	Japan	5	662	328	A2	B	3	5.4-6.6	23-134
1732	Chikushino	Japan	306	342	551	D	C	3	5.4-6.6	23-115
1734	Chinzei	Japan	4	820	360	A2	A	2	5.4-6.6	30-197
1748	WKYH05	Japan	16	591	367	C3	B	5	3.6-7.5	1-25
1754	Iiduka	Japan	41	281	329	C2	C	3	5.4-6.6	37-216
1773	Rancho Palos Verdes - Luconia	USA	Rock	>800	>800	A2	A	1	6.0	21
1786	TKSH01	Japan	16	515	327	E	E	6	3.5-7.5	1-28
1801	Nakama	Japan	18	168	109	E	E	3	5.4-6.6	32-110
1803	Kitakyushu	Japan	17	298	204	E	C	1	6.6	75
1805	Kaminoseki	Japan	1	1373	250	A2	A	1	5.8	19
1814	EHMH02	Japan	16	489	291	E	E	5	3.4-4.5	7-27
1850	NARH02	Japan	12	450	226	E	E	6	3.4-4.1	4-17
1858	Ube	Japan	Rock	>800	>800	A2	A	3	5-6.6	1-20
1866	La - Baldwin Hills	USA	167.4	293	470	D	C	5	5.3-6.7	57-196
1884	La - Saturn St	USA	135.17	296	441	C3	C	2	6-6.7	116-448
1886	Garvey Res. - Control Bldg	USA	25	468	432	B1	B	1	6.0	411
1888	Houfu	Japan	Rock	>800	>1500	A2	A	3	5-6.6	0.5-13
1931	La - Wonderland Ave	USA	3	1274	380	A2	A	3	5.3-6.7	42-136
1934	La - Griffith Park Observatory	USA	7	971	612	B1	A	2	5.3-6.7	41-213
1938	WKYH03	Japan	8	547	184	E	E	12	3.2-7.5	1-20
1958	Pasadena - Old Seismo Lab	USA	5.7	969	381	B1	A	1	6.6	131
1964	Tarzana - Cedar Hill	USA	82.5	302	405	C1	C	3	5.3-7.3	52-527
1965	Tarzana - Cedar Hill A	USA	82.5	302	405	C1	C	5	5.2-6.7	31-1302
1976	KGWH02	Japan	55	185	243	C2	C	2	4.5-7.5	14-102
1982	Canoga Park - Topanga Can	USA	124.65	267	417	C1	C	2	6-6.7	124-379
1988	Santa Susana Ground	USA	12	715	430	B1	B	1	6.7	254
1993	La - Sepulveda Va Hospital	USA	152	386	572	C1	B	1	6.7	820
1995	Simi Valley - Katherine Rd	USA	12.8	557	326	E	E	2	5.3-6.7	82-735
2000	Cedar Springs, Allen Ranch	USA	14	814	502	B1	A	2	5.3-6.6	17-59
2001	Rinaldi Receiving Sta	USA	73.3	333	426	C1	C	2	5.3-6.7	519-622
2006	La Dam	USA	42.5	629	652	B2	B	1	6.7	415

ID	Station Name	Country	H bedrock (m)	Vs,30 (m/s)	Vs,av (m/s)	New Site Class	EC8 Site Class	Number of records	Mw	PGA (cm/s ²)
2010	Sylmar - Converter Sta	USA	97.58	251	403	C1	C	2	5.3-6.7	250-727
2011	Jensen Filter Plant	USA	103.4	377	529	C1	B	3	5.1-6.7	47-750
2013	Sylmar - Olive View Med Ff	USA	80	441	523	C1	B	2	6-6.7	58-700
2014	Pacoima Dam (Downstr)	USA	Rock	>800	>1500	A1	A	1	6.7	417
2018	Wrightwood - 6074 Park Dr	USA	14	486	339	B1	B	2	5.3-6.6	51-177
2025	Newhall - W Pico Canyon Rd.	USA	78	282	465	C1	C	2	6-6.7	68-377
2027	Toyotama	Japan	8	503	283	B1	B	1	5.4	25
2044	Pearblossom Pump	USA	18	529	411	B1	B	1	6.6	115
2048	Lake Hughes #12	USA	10	602	317	B1	B	1	6.6	316
2049	Lake Hughes #12A	USA	10	602	317	B1	B	3	5.3-6.7	13-208
2061	Lake Hughes #9	USA	9	659	323	B1	B	2	6.6-6.7	142-186
2066	Kamitsushima	Japan	3	894	382	A2	A	2	5.4-6.6	20-69
2089	Fort Tejon	USA	20	398	305	E	E	1	6.6	23
2093	Yermo Fire Station	USA	145.79	353	500	C1	C	3	4.5-7.3	17-189
2094	Tehachapi Pump	USA	7	670	385	B1	B	1	6.6	36
2105	HYGH08	Japan	23.5	288	239	E	E	15	3.6-7.5	2-38
2106	Kyonan	Japan	76	141	152	D	D	4	5.5-5.6	6-23
2118	TTRH03	Japan	74	189	329	C3	C	9	3.2-5.1	2-169
2147	Temblor Pre-1969	USA	27.7	528	514	B1	B	1	6.2	306
2174	Hannoh	Japan	15	713	565	B1	B	1	5.5	2
2193	Parkfield - Vineyard Cany 3W	USA	140	297	501	C1	C	1	6.4	114
2205	Hatay Samandag Meteoroloji Istasyon Mudurlugu	Turkey	58.42	210	302	C2	C	1	4.2	10
2206	Hatay Altinozu Tarim Mudurlugu Bahcesi	Turkey	48.12	344	420	B2	C	2	4.2-5	2-3
2222	Hatay Merkez Koy Hizmetleri Mudurlugu Bahcesi	Turkey	39.8	469	514	B1	B	2	4.2-5	1-3
2240	Antalya Finike Meteoroloji Istasyon Mudurlugu	Turkey	49.05	300	379	C2	C	3	5.2-5.8	8-24
2248	Hatay Serinyol Orman Fidanlik Mudurlugu Bahcesi	Turkey	50.73	338	419	B2	C	3	4.7-5.7	1-4
2258	Hatay Kirikhan Guzelce Koyu Saglikevi Bahcesi	Turkey	56.59	271	370	C2	C	3	4.2	1-2
2262	Mugla Fethiye Meteoroloji Istasyon Mudurlugu	Turkey	55.54	248	340	C2	C	19	4.1-5.3	0.1-13
2268	Bear Valley #5, Callens Ranch	USA	35	391	418	B2	B	1	6.9	69
2269	Hatay Hassa Aktepe Saglik Ocagi Bahcesi	Turkey	30	688	688	B1	B	1	4.2	2
2274	Mersin Merkez Meteoroloji Istasyon Mudurlugu	Turkey	38.27	367	411	B2	B	1	6.2	122
2277	Hatay Hassa Merkez Saglik Ocagi Bahcesi	Turkey	26.5	619	592	B1	B	1	4.7	2

ID	Station Name	Country	H bedrock (m)	Vs,30 (m/s)	Vs,av (m/s)	New Site Class	EC8 Site Class	Number of records	Mw	PGA (cm/s ²)
2281	Marmaris-Meteorological Station	Turkey	45.39	392	461	B2	B	8	4.1-5.7	2-32
2304	Gilroy Array #1	USA	3	1428	569	A2	A	4	5.1-6.9	81-433
2307	Gilroy Array #2	USA	160	297	489	C1	C	3	5.7-6.9	182-338
2308	Gilroy Array #3	USA	188.5	282	561	D	C	4	4.9-6.9	135-443
2311	Usc Lick Observatory	USA	8	737	305	E	E	2	6.2-6.9	53-414
2315	Gaziantep Islahiye Meteoroloji Istasyon Mudurlugu	Turkey	38.56	421	464	B1	B	2	4.7-5.7	1
2316	Gilroy Array #6	USA	27.5	663	654	B1	B	4	4.9-6.9	94-363
2317	Adana Ceyhan Tarim Ilce Mudurlugu	Turkey	57.55	263	356	C2	C	1	6.2	246
2322	Mugla Bodrum Meteoroloji Istasyon Mudurlugu	Turkey	12.6	746	530	B1	B	51	3.7-6.2	1-40
2325	Corralitos	USA	37.5	463	498	B1	B	2	6.2-6.9	92-545
2329	Denizli Cameli Orman Isletme Mudurlugu	Turkey	45.71	344	415	B2	C	1	5.3	40
2331	Osmaniye Merkez Dsi Isletme Bas Muhendisligi	Turkey	44.51	350	417	B2	C	1	4.2	2
2343	Gaziantep Nurdagi Merkez Saglik Ocagi Bahcesi	Turkey	25	599	562	B1	B	2	4.7	2
2346	Mugla Merkez Tarim Il Mudurlugu	Turkey	Rock	1024	>800	A2	A	3	4.1-5.3	0.3-1
2348	Kyparrisia-Agriculture Bank	Greece	12	778	643	B1	B	10	4.6-6.6	10-86
2356	Halls Valley	USA	48	308	354	C2	C	4	5.6-6.9	43-217
2360	Kahramanmaraş Turkoglu Dr. Kemal Beyazit Fizik Tedavi Ve Rehabilitasyon Merkezi Bahcesi	Turkey	43.28	390	450	B1	B	1	4.1	31
2361	Kahramanmaraş Narli Cukobirlik Kooperatifi Bahcesi	Turkey	32	485	507	B1	B	1	4.1	2
2366	Palo Alto - Slac Lab	USA	50	425	492	B2	B	1	6.9	228
2368	Woodside	USA	30	454	454	B1	B	1	6.9	80
2381	Kahramanmaraş Pazarcik 1 Nolu Saglik Ocagi	Turkey	12.2	672	437	B1	B	1	5.7	1
2388	Kahramanmaraş Merkez Dsi 20. Bolge Mudurlugu Bahcesi	Turkey	44.81	345	410	B2	C	1	4.7	1
2390	Mcgee Creek - Surface	USA	30	359	359	B1	C	2	5.8-6.2	79-104
2397	Kahramanmaraş Andirin Tufan Pasa Ilkogretim Okulu	Turkey	13.4	613	418	B1	B	12	4.1-5.4	1-62
2399	Kahramanmaraş Merkez Bayindirlik Ve Iskan Mudurlugu	Turkey	31.3	465	474	B1	B	4	4.2-6.2	6-13
2406	Sunol - Forest Fire Station	USA	35	401	419	B2	B	2	4.9-6.9	11-73
2413	Sf Intern. Airport	USA	151	225	415	D	C	2	6.2-6.9	47-274
2421	Apeel 3E Hayward	USA	8	523	261	E	E	3	5.4-6.9	38-79

ID	Station Name	Country	H bedrock (m)	Vs,30 (m/s)	Vs,av (m/s)	New Site Class	EC8 Site Class	Number of records	Mw	PGA (cm/s ²)
	Csuh									
2424	Pyrgos-Agriculture Bank	Greece	85	277	526	C1	C	21	4.1-6.6	10-239
2427	Hayward City Hall - North	USA	13	735	569	B1	B	1	6.9	50
2430	Burdur Merkez Bayindirlik Ve Iskan Mudurlugu	Turkey	47.45	294	371	B2	C	14	3.9-6.5	0.2-24
2442	Zakynthos-Ote Building	Greece	80	235	414	C1	C	24	3.6-6.6	4-146
2446	Sf - Presidio	USA	17.5	595	482	B1	B	1	6.9	138
2450	Yerba Buena Island	USA	15	572	404	B1	B	1	6.9	43
2451	Oakland - Outer Harbor Wharf	USA	155	249	342	D	C	1	6.9	273
2457	Emeryville - 6363 Christie	USA	151	198	390	D	C	1	6.9	232
2458	Aydin Merkez Devlet Su Isleri 6. Bolge Mudurlugu	Turkey	70.65	271	396	C3	C	3	3.7-4.3	2-8
2459	Kosk Saglik Ocagi	Turkey	43.8	366	428	B2	B	15	4.9-5.8	1-13
2462	Sultanhisar Meteoroloji Mudurlugu	Turkey	47.28	355	432	B1	C	10	4.3-5.7	1-22
2464	Aydin Kuyucak Kuyucak Saglik Ocagi	Turkey	83.72	302	443	C1	C	10	4.1-5.4	1-55
2465	Nazilli Meteoroloji Mudurlugu	Turkey	63.27	267	381	C3	C	14	4.3-5.8	4-27
2466	Saraykoy Jeotermal Lojmanlari	Turkey	58.77	236	339	C2	C	32	4.1-5.8	1-114
2469	Athens 3 (Kallithea District)	Greece	42	513	608	B2	B	3	3.5-6	10-277
2470	Aydin Buharkent Elektrik Dagitim Merkezi	Turkey	42.46	391	431	B1	B	5	4.1-4.9	1-9
2472	Athens 4 (Kipseli District)	Greece	30	934	1079	A2	A	1	6.0	114
2478	Athens 2 (Chalandri District)	Greece	45	672	850	B1	B	1	6.0	130
2488	Malatya Dogansehir Meteoroloji Istasyon Mudurlugu	Turkey	17.4	655	537	B1	B	4	4.3-5.4	1-11
2492	Konya Doganhisar Omer Izgi Devlet Hastanesi	Turkey	41.9	385	439	B2	B	1	4.3	1
2493	Argostoli-Ote Building	Greece	51.5	448	616	B2	B	21	4.1-6.6	9-203
2495	Kahramanmaraş Elbistan Meteoroloji Istasyon Mudurlugu	Turkey	57.06	315	416	B2	C	4	4.5-5.4	1-4
2498	Patra-San Dimitrios Church	Greece	85	371	429	C1	B	8	4.2-6.6	9-224
2500	Aigio-Ote Building	Greece	22	474	424	B1	B	5	5.4-5.9	26-150
2503	Malatya Merkez Bayindirlik Ve Iskan Mudurlugu	Turkey	40.11	481	522	B1	B	28	4-5.8	0.1-18
2507	Manisa Salihli Meteoroloji Istasyon Mudurlugu	Turkey	55.77	272	371	C2	C	2	4.4-5.2	1-2
2508	Van Merkez Bayindirlik Ve Iskan Mudurlugu	Turkey	44.4	364	430	B2	B	12	4.1-5.8	1-27

ID	Station Name	Country	H bedrock (m)	Vs,30 (m/s)	Vs,av (m/s)	New Site Class	EC8 Site Class	Number of records	Mw	PGA (cm/s ²)
2509	Afyon Sultandagi Merkez Saglik Ocagi	Turkey	42.46	368	427	B2	B	5	4.3-5.7	0.1-20
2514	Mus Merkez Bayindirlik Ve Iskan Mudurlugu	Turkey	54	314	409	B2	C	6	4.4-4.8	0.1-5
2517	Lefkada-Hospital	Greece	60	258	348	C2	C	22	3.7-6.9	5-151
2522	Manisa Akhisar Meteoroloji Istasyon Mudurlugu	Turkey	52.26	292	382	C2	C	2	-	1-5
2526	Bingol Solhan Ogretmen Evi	Turkey	28.3	485	472	B1	B	4	4.4-5.6	6-23
2529	Kutahya Gediz Meteoroloji Istasyon Mudurlugu	Turkey	43.9	343	409	B2	C	3	3.9-5.2	0.3-3
2530	Manisa Demirci Meteoroloji Istasyon Mudurlugu	Turkey	53.07	336	419	B2	C	6	3.9-5.2	1-8
2532	Izmir Dikili Meteoroloji Istasyon Mudurlugu	Turkey	70.05	193	311	C3	C	8	4.3-5.2	0.2-7
2534	Kutahya Simav Meteoroloji Istasyon Mudurlugu	Turkey	76	259	319	C3	C	3	4.4-5.2	1-6
2540	Bingol Karliova Belediye Garaji	Turkey	123.31	356	512	C1	C	11	4.2-5.3	0.1-145
2542	Balikesir Ayvalik Meteoroloji Istasyon Mudurlugu	Turkey	32	387	400	B1	B	8	4.4-5.2	0.4-8
2543	Kawajiri	Japan	10	571	363	B1	B	3	5.7-5.9	5-24
2553	Kutahya Merkez Bayindirlik Ve Iskan Mudurlugu	Turkey	59	266	371	B2	C	3	4.4-5.2	1-5
2568	Eskisehir Kaymaz Belediye Garaji	Turkey	26.7	482	454	B1	B	2	5.6-5.7	0.5-1
2571	Agri Dogubeyazit Meteoroloji Istasyon Mudurlugu	Turkey	60.64	271	375	C2	C	2	4.3-4.4	1-3
2575	Balikesir Dursunbey Meteoroloji Istasyon Mudurlugu	Turkey	19.8	562	460	B1	B	4	4.4-5.2	0.3-3
2576	Balikesir Edremit Meteoroloji Istasyon Mudurlugu	Turkey	59.25	223	326	B2	C	2	5.2-6.1	3-22
2577	Kakunodate	Japan	10	490	276	E	E	2	5.7-5.9	3-21
2579	Balikesir Merkez Bayindirlik Ve Iskan Mudurlugu	Turkey	43.1	460	523	B1	B	6	3.9-5.2	0.2-2
2581	Agri Merkez Bayindirlik Ve Iskan Mudurlugu	Turkey	56.21	295	385	C2	C	2	5.1-5.3	1-3
2584	Eskisehir Merkez Turk Silahli Kuvvetleri Hava Hastanesi	Turkey	58.39	249	348	C2	C	1	5.2	3
2585	Eskisehir Merkez Anadolu Universitesi Yunus Emre Kampusu	Turkey	44.78	328	398	B2	C	2	5.1-5.2	1-2
2586	Eskisehir Merkez Anadolu Universitesi Iki Eylul Kampusu	Turkey	74	223	346	C3	C	4	5.1-5.7	1-4
2588	Eskisehir Inonu Orman Isletme	Turkey	49.54	279	361	C2	C	6	3.9-5.7	0.1-2

ID	Station Name	Country	H bedrock (m)	Vs,30 (m/s)	Vs,av (m/s)	New Site Class	EC8 Site Class	Number of records	Mw	PGA (cm/s ²)
	Mudurlugu									
2589	Eskisehir Merkez Anadolu Universitesi Borabey Kampusu	Turkey	26.7	631	607	B1	B	1	4.3	0.1
2591	Erzurum Merkez Bayindirlik Ve Iskan Mudurlugu	Turkey	42.42	375	433	B2	B	32	4-6.6	1-31
2592	Bilecik Bozoyuk Meteoroloji Mudurlugu	Turkey	32.9	401	426	B1	B	3	5.1-5.2	1-3
2594	Bursa Keles Meteoroloji Mudurlugu	Turkey	40.1	411	472	B2	B	7	3.9-5.2	0.3-8
2599	Kentro-Town Hall	Greece	100	318	467	C1	C	2	4.2-4.8	21-112
2603	Bursa M. Kemal Pasa Orman Isletme Mudurlugu	Turkey	54.2	264	354	C3	C	3	4.9-5.2	1-4
2606	Knidi-Forest Inspection Building	Greece	20	629	707	B1	B	3	4.2-4.8	21-69
2607	Gonen-Meteoroloji Mudurlugu	Turkey	41.84	397	453	B1	B	7	3.9-6.1	0.2-46
2608	Bilecik Merkez Meteoroloji Mudurlugu	Turkey	Rock	929	>800	A2	A	6	3.9-5.7	0.2-2
2610	Bursa Merkez Ulastirma Bolge Mudurlugu (Koy Hiz. 17. Bol. Mud. Nun Eski Arazisi)	Turkey	38.3	457	496	B2	B	4	3.9-5.2	1-32
2611	Bursa-Emergency Management Centre	Turkey	53.67	249	338	C2	C	15	3.9-5.8	1-53
2616	Demirtas-Kirantepe	Turkey	46	496	565	B2	B	3	4.6-4.9	3-5
2624	Balikesir Bandirma Bolge Trafik Denetleme Mudurlugu	Turkey	46.68	417	488	B2	B	5	4.2-5.7	2-29
2625	Edincik-Kandilli Gozlem Istasyonu	Turkey	32	516	528	B1	B	1	6.1	49
2627	Kurtul-Garden Of The Mosque	Turkey	33.58	301	322	C2	C	14	3.9-5.8	1-169
2629	Gemlik-Military Veterinary Training Command	Turkey	75.83	176	300	C3	D	11	3.9-5.7	1-190
2632	Umurbey-Celal Bayar Medical High School	Turkey	43.6	366	410	B2	B	7	3.9-5.7	1-83
2633	Cargill Agricultural Industries Factory	Turkey	57.63	349	436	B2	C	5	4.6-5.7	1-37
2635	Gemlik-Industrial Crafts Vocational School	Turkey	101.75	229	378	C3	C	19	3.9-5.8	1-79
2636	Bursa Iznik Hukümet Konagi	Turkey	73.48	251	379	C3	C	1	4.6	4
2638	Bursa Orhangazi Gedelek Saglik Ocagi	Turkey	22.4	572	499	B1	B	3	4.2-4.6	1-6
2647	Yalova Merkez Sugoren Dogus Et Sut Urunleri Fabrikasi	Turkey	29.7	388	386	C2	B	3	4.6-5.2	9-27
2652	Fortuna - Fortuna Blvd	USA	55	457	517	B2	B	1	7.0	113
2653	Yalova Merkez Sogucak Koyu Kardelen Ilkogretim Okulu	Turkey	32.8	358	370	C2	C	2	4.9-5.2	1-31

ID	Station Name	Country	H bedrock (m)	Vs,30 (m/s)	Vs,av (m/s)	New Site Class	EC8 Site Class	Number of records	Mw	PGA (cm/s ²)
2657	Thessaloniki-City Hotel	Greece	140	230	593	C1	C	3	4.8-6.3	9-141
2661	Amasya Merkez Bayindirlik Ve Iskan Mudurlugu	Turkey	43	444	494	B1	B	8	3.7-5.8	9-54
2665	Cankiri Cerkes Meteoroloji Istasyon Mudurlugu	Turkey	51.59	349	429	B2	C	31	3.8-6	1-63
2690	Borgo-Ottomila 2	Italy	310	90	250	D	D	3	5.6-6	7-10
2797	Minatomachi	Japan	7	563	335	A2	B	1	5.7	778
2821	Maiano-Piano Terra	Italy	>50	344	~370	C3	C	7	4.2-4.7	6-15
2822	Maiano-Prato	Italy	>50	344	~370	C3	C	6	4.2+4.7	8-20
2912	Muradiye-Meteoroloji Mudurlugu	Turkey	57.35	292	394	C2	C	1	5.3	41
2925	Bucak-Kandilli Gozlem Istasyonu	Turkey	24.1	713	662	B1	B	1	5.9	14
2936	San Severo	Italy	>100	393	~500	C1	B	3	5.7-6.9	21-52
2937	Vieste	Italy	20	444	460	B1	B	2	6-3-6.9	2-32
2953	Pescasseroli	Italy	Rock	1000	>800	A2	A	14	4.5-5.6	1-42
2987	Valle Aterno-Colle Dei Grilli	Italy	25	685	646	B1	B	12	4.2-6.3	5-480
3011	Lauria-Galdo	Italy	24	603	542	B1	B	3	5.6-6.9	15-233
3017	Novellara	Italy	>180	190	~330	D	C	4	4.7-5.4	25-159
3020	Sannicandro Garganico	Italy	Rock	965	>800	A2	A	3	5.2-5.7	35-111
3021	Catania-Piana	Italy	>100	159	>325	D	D	5	4.2-5.6	0.5-224
3027	Pachino	Italy	14.9	593	459	B1	B	1	5.6	53
3134	Korinthos-Town Hall	Greece	81	345	476	C1	C	3	4.5-5.9	24-64
3604	Garigliano-Centrale Nucleare 2	Italy	>100	192	~400	D	C	2	5.9-6.9	36-58
3609	L. Aquila - V. Aterno - F. Aterno	Italy	18	552	358	B1	B	7	4.1-6.3	4-415
3612	L. Aquila - V. Aterno - M. Pettino	Italy	7	836	500	B1	A	8	4.1-5.6	4-159
3614	L. Aquila - V. Aterno - Centro Valle	Italy	48	474	517	B2	B	13	4.1-6.3	13-590
3620	Avezzano	Italy	160	200	376	C3	C	12	4.4-6.3	1-61
3626	Bagnone	Italy	19	640	502	B1	B	1	4.8	42
3629	Bojano (Nuova)	Italy	334	306	656	D	C	4	5-6.3	1-14
3633	Bazzano	Italy	23	679	640	B1	B	8	4.1-5.6	7-60
3645	Caltagirone	Italy	30.4	374	375	B1	B	1	5.9	5
3657	Capestrano	Italy	19	732	633	B1	B	3	4.5-5	0.2-0.4
3658	Cesena	Italy	25	541	503	B1	B	1	4.2	46
3661	Cattolica	Italy	74	207	297	C3	C	2	5.6-6.3	3-4
3663	Faenza (Nuova)	Italy	284	292	466	D	C	2	4.6-5.3	8-45
3666	Forli (Nuova)	Italy	44	296	288	C2	C	2	4.2-6.3	2-26
3669	Firenzuola l	Italy	76	311	458	C1	C	1	5.4	2
3670	Fivizzano	Italy	12	509	278	E	E	2	4.9-5.4	3-8
3676	Genova	Italy	3	1048	366	A2	A	2	4.9-5.4	1-3
3678	Grumento Nova	Italy	192	283	462	D	C	3	5.1-5.8	26-37
3679	Gran Sasso (Lab. Infn	Italy	40	488	512	B2	B	11	4.1-6.3	1-261

ID	Station Name	Country	H bedrock (m)	Vs,30 (m/s)	Vs,av (m/s)	New Site Class	EC8 Site Class	Number of records	Mw	PGA (cm/s ²)
	Assergi)									
3692	Modena	Italy	>150	213	~400	D	C	2	4.9-5.4	5-9
3697	MI03	Italy	80	378	518	C1	B	6	4.1-5.6	12-123
3705	Mormanno	Italy	Rock	1400	>800	A2	A	1	-	2
3707	Marsico Vetere	Italy	17	686	590	B1	B	3	4.4	1-2
3733	Pieve Santo Stefano	Italy	22.5	613	545	B1	B	1	4.7	180
3734	Piazza Al Serchio	Italy	14	490	350	B1	B	2	4.9-5.4	4-8
3743	Scanno	Italy	20	839	750	B1	A	4	5-5.6	2-17
3750	Sellano Est	Italy	19.5	469	379	B1	B	7	4.8-5.3	6-86
3754	S. Giuliano Di Puglia B	Italy	47	357	398	B2	C	1	4.6	32
3769	Sansepolcro	Italy	69	323	395	C1	C	2	5.6-6.3	3-4
3774	Spezzano Della Sila (Camigl.)	Italy	29	318	310	C2	C	2	4.9	1-3
3777	S.Severo	Italy	130	393	519	C1	B	1	6.3	5
3779	Satriano Di Lucania	Italy	53.5	395	504	B2	B	3	6.3	1-16
3783	Tolmezzo - Base Diga	Italy	5	1030	706	A2	A	1	4.6	5
3787	Tortorici	Italy	17.5	527	369	B1	B	1	5.9	5
3789	Tortona	Italy	24	442	388	E	B	1	4.8	59
3809	Hikimi	Japan	7	630	252	E	E	3	5.1-6.6	3-58
3812	Sata	Japan	13	342	203	E	C	2	5.7-6	8-22

Appendix II

Table II. Kik-Net waveforms used for estimation of amplification for soil class E

Waveform ID	Station	M_w	M_s	Depth	R_{epi}	$V_{s,30}$	$V_{s,av}$	$V_{s,bedrock}$	S
1	EHHM02	6.15	6.09	51	53	489	291	2195	1.34
2	EHHM02	4.98	4.34	49	51	489	291	2195	1.46
3	EHHM02	4.41	3.50	48	58	489	291	2195	2.64
4	EHHM07	6.15	6.09	51	69	391	281	1853	1.09
5	HYGH08	4.90	4.23	12	6	288	239	1076	2.31
6	NARH05	6.67	6.67	38	170	275	398	1193	2.87
7	NARH05	5.44	5.03	44	32	275	398	1193	3.94
8	NARH05	4.41	3.50	44	17	275	398	1193	6.36
9	SIGH01	4.90	4.23	12	39	563	350	1200	1.30
10	SIGH01	7.45	7.45	44	243	563	350	1200	0.88
11	SIGH01	4.83	4.13	12	77	563	350	1200	1.24
12	SIGH02	4.90	4.23	12	6	569	260	810	1.15
13	SMNH04	7.31	7.31	11	77	285	131	850	1.21
14	SMNH04	6.15	6.09	51	109	285	131	850	1.32
15	TKSH02	6.15	6.09	51	129	349	205	918	2.85
16	TKSH02	4.76	4.02	42	36	349	205	918	4.11
17	WKYH02	7.45	7.45	44	185	369	225	1200	1.67
18	WKYH02	6.67	6.67	38	169	369	225	1200	1.58
19	WKYH06	4.83	4.13	46	21	756	290	970	1.28
20	WKYH06	6.67	6.67	38	134	756	290	970	0.87